PULSING AND SELF-ORGANIZATION

By

DAESEOK KANG

A DISSERTATION PRESENTED TO THE GRADUATE SCHOOL
OF THE UNIVERSITY OF FLORIDA IN PARTIAL FULFILLMENT
OF THE REQUIREMENTS FOR THE DEGREE OF
DOCTOR OF PHILOSOPHY

UNIVERSITY OF FLORIDA

1998

ACKNOWLEDGMENTS

I am grateful to have had the opportunity to work with my committee chair, Dr. H.T. Odum. His holistic views and deep insights into general systems led me to view the world around me from systems perspectives. Thanks are extended to other members of my committee for their contributions: Dr. M.T. Brown, Dr. C.L. Montague, Dr. P.A. Mueller, and Dr. D.A. Denslow.

Guy McGrane provided valuable input to my work and shared some of his research. Other students in systems ecology provided many challenging ideas during systems seminars. Thanks also go to Joan Breeze for improving my English.

This work was aided by funding from a contract between Space Biospheres Ventures (Biosphere 2) and the University of Florida, H.T. Odum, principal investigator. The College of Engineering provided a graduate assistantship in 1998.

I am indebted to my parents and mother-in-law for their love and unconditional support during my study. Finally, I would like to acknowledge my wife, Kyung Bok, and son, Minwon, for providing joy and purpose for completing this dissertation.

TABLE OF CONTENTS

ACKNOWLEDGMENTS ii

LIST OF TABLES vi

LIST OF FIGURES viii

ABSTRACT xviii

CHAPTERS

1 INTRODUCTION 1

- Concepts and Theory 2
  - General Systems Principles 2
  - Generalizing Concepts with Energy Systems Language 14
  - Theory of Pulsing Paradigm 15
- Previous Studies of Pulsing 24
  - Pulses in Chemical Reactions 24
  - Aquatic Ecosystems 27
  - Terrestrial Ecosystems 37
  - Weather and Climate Pulses 40
  - Geologic Episodes 41
  - Economic Fluctuations 42
  - Pulses of Organic Evolution 43
- Previous Simulation Studies of Pulsing 46
  - Energy Systems Models 47
  - Other Models 54
- Study Plan 77

2 METHODS 81

- Energy Systems Diagramming 81
  - Detailed Diagram 81
  - Aggregated Diagram 86
- Simulation 86
  - Labeled Diagram with Difference Equations 86
  - Model Calibration 88
  - Computer Program 92

Base Run of the Model 97
Validation 97
What-Ifs 99
Analysis of Published Pulsing Data 99

3 RESULTS 103

Pulsing Patterns in Observed Data 103
Production Function and Power Inflow 110
Basic Pulse Model 132
Base Run 132
Variation in Energy Input 137
Efficiency of Primary Production 140
Changes in Consumption Efficiency 143
Level of Depreciation of Consumer Storage 150
Steady Model 150
Pulse Model with Consumer Feedback 155
Detritus Model 165
Layered Pulse Model 170
Two Module Pulse Model 185
Three Module Pulse Model 194
Characteristics of Simulation Pulses 194

4 DISCUSSION 202

Attributes of the Pulse Mechanism 202
Production Function and Maximum Power 203
Comparison of Pulsing and Steady States 204
Internal and External Pulses 205
Pulsing and Complex Webs 205
Emergy and Transformity Characteristics of Pulses 207
Pulse Intensity and Transformity 207
Transformity and Hierarchy 207
Comparison of Observed Pulses with Simulation Pulses 208
Adaptation to the Edge of Chaos 209
Information and Pulsing 210
Adaptive Cooperative Oscillator Theory 210
Pulsing Hierarchy and Episodic Events 211
Pulsing Cycles in Economy 212
Sampling Frequency and Systems Dynamics 213
Implications of Pulsing Concepts for Ecosystem Management 214
Management of Deltaic Systems 214
Diversity Management 215
Fisheries Management and Hierarchy of Pulsing 216
Summary 216

Conclusion 219

APPENDICES

A ORIGINAL FIGURES USED TO FIND PULSING PATTERNS IN THE OBSERVED DATA 221

B CALIBRATION TABLES OF THE MODELS 230

C LISTINGS OF THE SIMULATION PROGRAMS 241

LIST OF REFERENCES 267

BIOGRAPHICAL SKETCH 283

LIST OF TABLES

Table page

1-1. Definitions of terms and concepts used in the energy systems language relevant to this study (Odum, 1996). 3

2-1. Calibration of the pathway coefficients for the computer simulation of the basic pulse model with a flow limited energy source in Figure 2-4........ 91

2-2. BASIC program listing of the basic pulse model in Figure 2-4. 93

B-1. Calibration of the pathway coefficients for the computer simulation of the simple two storage model with a flow limited energy source in Figure 3-4. 230

B-2. Calibration of the pathway coefficients for the computer simulation of the steady model in Figure 3-25. 231

B-3. Calibration of the pathway coefficients for the computer simulation of the pulse model with consumer feedback on primary production in Figure 3-28. 232

B-4. Calibration of the pathway coefficients for the computer simulation of the pulse model with a detritus storage in Figure 3-36. 233

B-5. Calibration of the pathway coefficients for the computer simulation of the layered pulse model in Figure 3-41. 234

B-6. Calibration of the pathway coefficients for the computer simulation of the two module pulse model in Figure 3-50. 236

B-7. Calibration of the pathway coefficients for the computer simulation of the three module pulse model in Figure 3-57. 238

C-1. Program listing of the simple two storage model in Figure 3-4. 241

C-2. Program listing of the simple two storage model with a pulsing recycle pathway in Figure 3-5........ 243

C-3. Program listing of the steady model in Figure 3-25. 245

C-4. Program listing of the pulse model with consumer feedback on primary production in Figure 3-28........ 248

C-5. Program listing of the pulse model with a detritus storage in Figure 3-36. 251

C-6. Program listing of the layered pulse model in Figure 3-41. 254

C-7. Program listing of the two module pulse model in Figure 3-50. 258

C-8. Program listing of the three module pulse model in Figure 3-57. 262

LIST OF FIGURES

Figure page

1-1. Common design features found in many systems 6

1-2. Energy transformation network and hierarchy. a) Spatial pattern of units and their territories; b) Network of energy transformation; c) Aggregation of the network in b) into an energy chain; d) Energy flows in each hierarchy; e) Solar transformities in each hierarchy (Odum, 1988 and 1996). 9

1-3. Symbols and definitions of the energy systems language (Odum, 1983)............ 16

1-4. Two different views of systems development over time. a) Steady state concept in which systems components level off after growth; b) Pulsing dynamics with alternations of slow production and fast consumption. 17

1-5. Frequency of pulses as a function of position in the energy hierarchy; pulses smaller than the system of concern are considered as noise, and larger pulses of systems larger than that of concern are regarded as catastrophes. a) Energy transformation spectrum; b) Pulse period as a function of transformity; c) Energy systems diagram of production and consumption with pulse frequencies appropriate to sources and hierarchical position (Odum, 1983). 20

1-6. Pulsing minimodel of many kinds of systems alternating slow accumulation of production followed by frenzied consumption and recycle. The model provides three different pathways of consumption which operate during different periods of systems development 23

1-7. Energy systems language translation of the Oregonator model of the Belouzov-Zhabotinskii reaction by Field and Noyes (1974), where A = BrO_2^-, P = HOBr, Y = Br^-, Z = 2Ce(IV), X = $HOBr_2$, and f = stoichiometric factor. Bromate ion (A) was considered as constant in this model and hypobromous acid (P) as a dead-end product of the reaction. Author's original equations are shown below the diagram............ 26

1-8. Energy systems language translation of the diffusion model of phytoplankton bloom by Kierstad and Slobodkin (1953). Dashed are inferred elements from the original equations. Author's original equations are shown below the diagram. 35

1-9. Order-disorder model of environmental catastrophes with self-organized pulses (redrawn after Alexander, 1978). Author's original equations are shown below the diagram. 48

1-10. Pulsing production minimodel with the quadratic consumption of stored production (redrawn after Richardson and Odum, 1981). Author's original equations are shown below the diagram. 50

1-11. Production-consumption minimodel of the modern civilization supported by fossil fuels with quadratic pulsing mechanisms (redrawn after Odum, 1982 and 1987). Author's original equations are shown below the diagram. 51

1-12. Energy systems language translation of the three species food chain model by Hastings and Powell (1991). Dashed are inferred elements from the original equations. Author's original equations were used in this translation, instead of their nondimensionalized forms. 56

1-13. Energy systems language translation of the food chain model without omnivory of an arthropod-dominated lotic community by Camilo and Willig (1995). Dashed lines are inferred elements. Author's original equations are shown below the diagram. 58

1-14. Energy systems language translation of the boreal rodents' cycle model of Hanski et al. (1993) and Hanski and Korpimaki (1995). Dashed are inferred components from the original equations by the authors. Author's equations are shown below. 60

1-15. Energy systems language translation of the microbial food web model by Eldridge and Sieracki (1993). Dashed lines are components inferred from the original equations and the description of the model. Author's original equations are shown below. 63

1-16. Energy systems language translation of the models by Rowe (1996) on systems in food limited environments. Original equations are the same as the equations from the systems diagram in which long names for the coefficients and storages are replaced by more abbreviated ones. 66

1-17. Energy systems language translation of the size-based plankton ecosystem model by Moloney and Field (1991). Dashed are inferred elements from the original model. Author's original equations are shown below. PI = Picophytoplankton, NA = Nanophytoplankton, NE = Netphytoplankton, B = Bacterioplankton, HN = Heterotrophic nanoflagellates, MI =

Microzooplankton, ME = Mesozooplankton, DOC = Dissolved Organic Carbon, DON = Dissolved Organic Nitrogen. 70

1-18. Energy systems language translation of the spatial plankton pulse model of Dubois (1975). Dashed are inferred elements from the original equations. Author's original equations are shown below the diagram. 72

1-19. Energy systems language translation of the model of spruce budworm oscillation by Ludwig et al. (1978). Dashed are inferred elements from the original equations. Author's equations are shown below. 74

1-20. Energy systems language translation of Sepkoski's (1984) three phase kinetic model for the diversification of marine fauna during the Phanerozoic. Dashed are inferred elements from the model. Author's equations are shown below. 79

2-1. A flow chart summarizing the overall procedure in the energy systems simulation methodology. 82

2-2. Detailed overview diagram of the upper part of an open ocean ecosystem. POM = Particulate Organic Material. 85

2-3. Aggregated diagram of the upper open ocean ecosystem in Figure 2-2. 87

2-4. Systems diagram of the basic pulse model as in Figure 1-6, with labels for sources, storages and pathways, and difference equations derived from the model. MT = Total material in the system; f1 and f2 = Material fraction of producer (P) and consumer (H) storages, respectively. 89

2-5. Systems diagram of the basic pulse model in Figure 2-4 with flow and storage values for calibration. 90

2-6. Equations for simulating emergy and transformity of storages and flows. 96

2-7. Simulation results of the basic pulse model in Figures 2-4 and 2-5, calibrated in Table 2-1, with the program listing in Table 2-2. 98

2-8. A what-if run of the basic pulse model in Figure 2-4. A. 50% decrease in the energy input (J). B. The base run in Figure 2-7. 100

2-9. Illustration of the method used to analyze pulsing patterns in time series graphs found in literature. 101

3-1. Relationship between pulse interval and amplitude in the observed data. 105

3-2. Relationship between pulse interval and percent of time in pulse in the observed data. 112

3-3. Relationship between pulse amplitude and frequency in the observed data. 118

3-4. Systems diagram of the simple two storage model with a flow limited energy source and the linear recycle pathway (k3), to investigate characteristics of the production function in relation to power inflow. Calibration values are given in steady state. MT = Total material inside the system; f = Material fraction of the activated storage (Q). 123

3-5. Systems diagram of the simple two storage model as in Figure 3-4, but with an additional recycle pathway (k4) by an internal pulsing mechanism. Pulsing is given as a step function which turns on the additional material recycle at a given time interval. MT = Total material inside the system; f = Material fraction of the activated storage (Q). 124

3-6. Simulation results of the pulse model in Figure 3-5 (a) and the steady model in Figure 3-4 (b), when material fraction (f) of the activated storage (Q) is 0.15 127

3-7. Simulation results of the pulse model in Figure 3-5 (a) and the steady model in Figure 3-4 (b), when material fraction (f) of the activated storage (Q) is 0.05 128

3-8. Power inflow as a function of the dispersed material (M). a) Simulation results of the models in Figures 3-4 and 3-5. Dispersed material is given as the percentage of the total material; b) Equations of the power inflow (J1) as a function of the dispersed material. 130

3-9. Effects of variations in pulse amplitude (a) and pulse interval (b) on the total power inflow in the pulse model in Figure 3-5. In each case, two different material fractions of the activated storage (Q) were compared with those in the steady model in Figure 3-4. 131

3-10. Effects of change in the material fraction (f) of the activated storage (Q) which was used to calibrate the model in Figures 3-4 and 3-5, on the total power inflow. Pulse interval and amplitude for the base case in Figure 3-5 were used in this simulation: pulse interval (X) = 100 and amplitude (P) = 20. 133

3-11. Emergy (a) and transformity (b) simulation of the basic pulse model in Figure 2-4. 134

3-12. Changes in primary production (J2) and the percent power use (a) and the turnover time of producer and consumer (b) in the base run of the basic pulse model in Figure 2-4. Percent power use is the percentage of power inflow (J1) used in primary production (J2). Turnover time of each storage is the amount of stored quantity divided by the sum of the inflows to each storage. 136

3-13. Simulation results of the basic pulse model for varied energy input from the source (J). c) is the base case shown in Figure 2-7. 138

3-14. Emergy and transformity simulation of the basic pulse model in Figure 2-4, for varied energy input from the source (J). c) is the base case shown in Figure 3-11. 139

3-15. Simulation results of the basic pulse model in Figure 2-4, for varied production efficiency of producer (P). Production efficiency = (k2/k1)*100. Production efficiency was varied by changing the coefficient k2. c) is the base case shown in Figure 2-7. 141

3-16. Emergy and transformity simulation of the basic pulse model in Figure 2-4, for varied production efficiency of producer (P). Production efficiency = (k2/k1)*100. Efficiency was varied by changing the coefficient k2. c) is the base case shown in Figure 2-8 142

3-17. Simulation results of the basic pulse model in Figure 2-4, for varied efficiency of energy transfer from producer (P) to consumer (H) through the linear pathway. Efficiency, e = (k4/k3)*100. Efficiency was varied by changing the coefficient k4. b) is the base case shown in Figure 2-7. 144

3-18. Emergy and transformity simulation of the basic pulse model in Figure 2-4, for varied efficiency of energy transfer from producer (P) to consumer (H) through the linear pathway (from k3 to k4). b) is the base case shown in Figure 3-11. 145

3-19. Simulation results of the basic pulse model in Figure 2-4, for varied efficiency of energy transfer from producer(P) to consumer (H) through the autocatalytic pathway (from k5 to k6). c) is the base case shown in Figure 2-7. 146

3-20. Emergy and transformity simulation of the basic pulse model in Figure 2-4, for varied efficiency of energy transfer from producer (P) to consumer (H) through the autocatalytic pathway (from k5 to k6). c) is the base case shown in Figure 3-11 147

3-21. Simulation results of the basic pulse model in Figure 2-4, for varied efficiency of energy transfer from producer (P) to consumer (H) through the quadratic autocatalytic pathway (from k7 to k8). c) is the base case shown in Figure 2-7. 148

3-22. Emergy and transformity simulation of the basic pulse model in Figure 2-4, for varied efficiency of energy transfer from producer (P) to consumer (H) through the quadratic autocatalytic pathway (from k7 to k8). c) is the base case shown in Figure 3-11. 149

3-23. Simulation results of the basic pulse model in Figure 2-4, for varied depreciation coefficient (k10) of the consumer unit (H). b) is the base case shown in Figure 2-7. 151

3-24. Emergy and transformity simulation of the basic pulse model in Figure 2-4, for varied depreciation coefficient (k10) of the consumer unit (H). b) is the base case shown in Figure 3-11. 152

3-25. Systems diagram of the steady model without the quadratic autocatalytic pathway. Other configurations are the same as the basic pulse model in Figure 2-4. 153

3-26. Calibration diagram of the steady model in Figure 3-25. Flow values on the autocatalytic pathway were obtained by adding those of the autocatalytic and quadratic autocatalytic pathways in Figure 2-5. 154

3-27. Simulation results of the steady model in Figure 3-25, with coefficients calibrated as in Appendix Table B-2. a) Energy simulation and b) emergy and transformity simulation. 156

3-28. Pulse model with direct consumer feedback on primary production. The producer has two different production processes: a process based on its own feedback and available material (k4) and the other with feedback from the consumer unit (H) (k4). MT = Total material inside the system; f1 and f2 = Material fraction of the producer and consumer storages, respectively.......... 157

3-29. Calibration diagram of the pulse model with consumer feedback on primary production in Figure 3-28.......... 158

3-30. Simulation results of the pulse model with consumer feedback on primary production in Figure 3-28, with coefficients as calibrated in Appendix Table B-3. a) Storage of producer and consumer; b) Material storage and primary production; c) Transformity of producer and consumer; d) Energy and emergy of feedback flow (k13). 159

3-31. Simulation results of the pulse model with consumer feedback on primary production in Figure 3-28, for varied feedback flow (k13). b) is the base case shown in Figure 3-30.......... 162

3-32. Transformity simulation of the pulse model with consumer feedback on primary production in Figure 3-28, for varied feedback flow (k13). b) is the base case shown in Figure 3-30.......... 163

3-33. Energy and emergy of the feedback flow (k13) in the pulse model with consumer feedback on primary production in Figure 3-28, for varied coefficient k13. b) is the base case shown in Figure 3-30. 164

3-34. Simulation results of the pulse model with consumer feedback on primary production in Figure 3-28, for varied efficiency of primary production with consumer feedback (k2). c) is the base run in Figure 3-30. 166

3-35. Simulation results of the pulse model with consumer feedback on primary production in Figure 3-28, for varied efficiency of primary production without consumer feedback (k4). c) is the base run in Figure 3-30. 167

3-36. Pulse model with a detritus storage. Detritus is supplied through three different pathways: directly from the producer (k9) and consumer (k10), and through messy feeding of the consumer (k16). The consumer unit feeds on both producer and detritus. MT = Total material in the system; f1, f2, and f3 = Material fraction of the producer (P), consumer (H), and detritus (D), respectively. 168

3-37. Calibration diagram of the pulse model with a detritus storage in Figure 3-36. 169

3-38. Simulation results of the pulse model with a detritus storage in Figure 3-36, with coefficients as calibrated in Appendix Table B-4. a) Simulation of energy storages and b) transformity simulation. 171

3-39. Simulation results of the pulse model with a detritus storage for varied production efficiency of the producer (P). c) is the base case shown in Figure 3-38. 172

3-40. Transformity simulation of the pulse model with a detritus storage in Figure 3-36, for varied production efficiency of the producer (P). c) is the base case shown in Figure 3-38. 173

3-41. Layered pulse model with the pulsing pair in the basic pulse model in Figure 2-4 arranged in parallel. The pulsing pairs compete for the available energy and material, and connected through the autocatalytic pathway from the upper pair to the lower pair. MT = Total material inside the system; f1, f2, f3, and f4 = Material fraction of producer 1, consumer 1, producer 2, and consumer 2 storage, respectively. 175

3-42. Calibration diagram of the layered pulse model in Figure 3-41. 176

3-43. Simulation results of the layered model in Figure 3-41, with coefficients as calibrated in Appendix Table B-5. a) Upper pulsing pair of producer 1 (P1) and consumer 1 (H1); b) Lower pulsing pair of producer 2 (P2) and consumer 2 (H2); c) Total producer and consumer in the system. 177

3-44. Emergy (a) and transformity (b and c) simulation of the layered model in Figure 3-41, with coefficients as calibrated in Appendix Table B-5. 178

3-45. Simulation results of the layered model in Figure 3-41, for varied energy input from the source (J). b) is the base case shown in Figure 3-43. 179

3-46. Simulation results of the layered model in Figure 3-41 when the production efficiency, e, of producer 1 (P1) was varied. c) is the base case shown in Figure 3-43. 181

3-47. Simulation results of the layered model in Figure 3-41 when the production efficiency, e, of producer 2 (P2) was varied. c) is the base case shown in Figure 3-43. 182

3-48. Simulation results of the layered model in Figure 3-41 when the efficiency, e, of energy transfer from the consumer 1 (H1) to the consumer 2 (H2) was varied. Pulse frequency of both producers and consumers increased, and pulse amplitude decreased as the efficiency increased. b) is the base case shown in Figure 3-43. 183

3-49. Transformity simulation results of the layered model in Figure 3-41 when the efficiency, e, of energy transfer from the consumer 1 (H1) to the consumer 2 (H2) was varied. Variability of the transformity of both producer 2 and consumer 2 decreased as the efficiency increased, and the average transformities of storages also decreased. b) is the base case shown in Figure 3-44. 184

3-50. Two module pulse model with two pulsing pairs connected in series. Two pulsing pairs are connected through two different pathways: linear and autocatalytic. MT = Total material conserved in the system; f1, f2, f3, and f4 = Material fraction of the producer (P), herbivore (H), 1st carnivore (C), and 2nd carnivore (D), respectively. 186

3-51. Calibration diagram of the two module pulse model in Figure 3-50. MT = Total material conserved in the system. 187

3-52. Simulation results of the two module pulse model in Figure 3-50, with coefficients as calibrated in Appendix Table B-6. a) Simulation of energy storages and b) transformity simulation. 188

3-53. Simulation results of the two module pulse model in Figure 3-50, for varied level of energy input (J) to the system. c) is the base case shown in Figure 3-52. 190

3-54. Transformity simulation of the two module pulse model in Figure 3-50, for varied level of energy input (J) to the system. c) is the base case shown in Figure 3-52. 191

3-55. Simulation results of the two module pulse model in Figure 3-50, for varied efficiency of primary production of the producer (P). c) is the base case shown in Figure 3-52 192

3-56. Transformity simulation of the two module pulse model in Figure 3-50, for varied efficiency of primary production of the producer (P). c) is the base case shown in Figure 3-52. 193

3-57. Three module pulse model in which three pulsing pairs are connected in series. Each pulsing pair is connected through two different pathways: linear and autocatalytic. MT = Total material conserved in the system; f1, f2, f3, f4, f5, and f6 = Material fraction of the producer (P), herbivore (H), 1st carnivore (C), 2nd carnivore (D), 3rd carnivore (K), and top predator (L), respectively. 195

3-58. Calibration diagram of the three module pulse model in Figure 3-57. MT = Total material conserved in the system. 196

3-59. Simulation results of the three module pulse model in Figure 3-57, with coefficients calibrated as in Appendix Table B-7. a) Simulation of energy storages and b) transformity simulation 197

3-60. Characteristics of pulses in the simulation results of the basic pulse model in Figure 2-4. a) Relationship between pulse interval and intensity; b) Maximum transformity over the simulation period as a function of pulse interval; c) Relationship between pulse intensity and transformity. 198

3-61. Quantity-quality diagram on a log-log plot, using the simulation results of the two module pulse model in Figure 3-50 (a) and the three module pulse model in Figure 3-57 (b) 200

3-62. Pulsing patterns in the simulation results of the three module pulse model in Figure 3-57. a) Relationship between pulse interval and amplitude; b) Relationship between pulse interval and percent of time in pulse; c) Relationship between pulse amplitude and frequency. 201

A-1. Fluctuations in chlorophyll-a levels at three sampling stations of Lake Okeechobee, Florida (Philips et al., 1993) 221

A-2. Time series of chlorophyll-a (a), total phytoplankton (b), and total zooplankton and total Daphnia (c) in Lake Mendota, Wisconsin during 1976-1989 (Lathrop and Carpenter, 1992a and 1992b) 222

A-3. Trends of total phosphorus (·····) and chlorophyll-a (—) (a) and biomass (as cell volume) of total phytoplankton (—) and blue-green algae (·····) (b) in the upper 20m of Lago Maggiore, Italy (de Bernardi et al., 1988) 223

A-4. Time series of algal concentration in a microcosm over 10 years (Kersting, 1985). 224

A-5. Time series of phytoplankton biomass in Lake Kinneret, Israel from 1972 through 1993 (Berman et al., 1995). 224

A-6. Temporal distribution of total phytoplankton and *Aulacoseira granulata* in Trelew station (a) and Rawson station (b) of the Chubut River in Argentina from November 1989 to July 1992 (Sastre et al., 1994). 225

A-7. Daily variation in total phytoplankton abundance (cells/l) and Shannon-Wiener diversity index during the summer of 1978 in the Gulf of Maine (Balch, 1981). 226

A-8. Hourly variation of chlorophyll-a at an anchored station in the Middle Estuary of the St. Lawrence River, Canada (Demers and Legendre, 1981). 226

A-9. Fluctuations in gross production inside Biosphere 2 over a year in 1994 (Kang and Engel, 1996). 227

A-10. Population fluctuations of the prairie vole, *Microtus ochrogaster* (Getz et al., 1997). 227

A-11. 1700-year hindcast series of Pacific sardine and northern anchovy biomasses off California and Baja California obtained by conversion of scale deposition rate data (Baumgartner et al., 1992). 228

Abstract of Dissertation Presented to the Graduate School
of the University of Florida in Partial Fulfillment of the
Requirements for the Degree of Doctor of Philosophy

PULSING AND SELF-ORGANIZATION

By

Daeseok Kang

December, 1998

Chairman: H.T. Odum
Major Department: Environmental Engineering Sciences

This dissertation investigated systems designs to account for the pulsing paradigm, a general systems concept, that states that self-organization increases performance by accumulating storages, which are transferred to a higher consumer level in the energy hierarchy and fed back in sharp repeating pulses. Similar pulsing patterns were found in published data from many fields, and graphical analyses were made of published time series of plankton data of limnology and oceanography. Although the data appeared to be noisy and irregular, pulse amplitude was proportional to the time interval between pulses of similar size. Small-scale pulses were more frequent. Larger scale pulses delivered their effects in shorter time periods relative to their intervals. Such patterns may be explained as the result of simultaneous pulsing on several scales.

After review of simulation models by other investigators, alternative systems designs were simulated including a single simple producer-consumer-recycle model and compound combinations. Designs which generated time series like those observed in many fields were analyzed for their energy characteristics.

Simulation of the emergy (spelled with an “m”; the available energy of one kind required to make a product) flows and storages showed pulses to be high transformity, a hypothetical measure of feedback impact. Whereas the model with a single pulsing pair unit (e.g. consumer-resource unit) did not generate pulsing patterns when energy input was very low or very high, compound designs allowed excess input energy to be routed to the productivity of other pulsing units. The model with two producer-consumer-recycle units connected in parallel pulsed over a wide range of input energy levels and efficiencies. A hierarchy of pulses of different frequency was obtained when producer-consumer-recycle models were connected in series, with more frequent pulses in lower energy levels. The pulsing producer-consumer unit drew more power than a non-pulsing producer-consumer unit with similar calibrations. The theory that self-organization selects pulsing which increases performance of complex systems was compared with other theories for pulsing in various fields including economics and earth science.

The pulsing paradigm explains fluctuations observed in systems as the concurrent dynamic pulsing on many scales.

CHAPTER 1
INTRODUCTION

This dissertation considers general systems hypotheses about pulsing and maximum empower. Data from the literature were used to examine variations in pulsing period and concentration with position in a universal scale of energy hierarchy. Energy and emergy calculations were used to test whether pulsing maximizes systems performance at each level of hierarchy. Systems designs were sought to represent pulsing dynamics, and simulation models were developed using them to investigate the energetics of pulsing systems. From pulsing principles, inferences were made to improve prediction and management.

All systems on the earth and in the universe face continuous change in their components and surrounding environments. Through self-organizing development in time and space, they have developed adaptive strategies to those changes, and the ones that utilized and organized the given resources and components in such a way to maximize systems performance have survived competition.

In the traditional concept of succession, systems reach a steady state after a period of self-organization. Viewed as indefinitely sustainable, the structure and components of the systems do not change appreciably over time. This steady state concept has been the basis of environmental policy and management, and a model for achieving sustainability of the society. In recent years many studies on various systems suggest that natural systems pulse regularly in response to external sources and internal pulsing mechanisms. The concept of pulsing steady state provided a new way of viewing the development of systems in nature and the economy.

Concepts and Theory

General Systems Principles

In nature, there are many different entities, living and nonliving, with a great range of sizes and life spans. These are interconnected through myriad relationships. These connected parts make a system in which they work together for their survival. Systems we see on the earth today are the result of self-organizing development, in time and space, of various systems existing throughout earth history.

General systems theory arises from the observations that vastly different systems share common basic features of energy and matter by which we can generalize about systems dynamics and self-organizing development. Below is given a brief summary of general systems principles that appear to apply to all systems examined.

Table 1-1 shows definitions of important terms and concepts in energy systems language relevant to this study. These terms and concepts will be used throughout this dissertation.

Self-organization

All systems in nature, from molecules to the universe, struggle for existence, under continuously fluctuating environments of energy sources, and system components and processes. They self-organize their components and processes to meet constraints imposed on them for their survival, through competition of separate units and of pathways for reinforcement. Self-organization is a way by which we can explain how systems develop and survive the test of time.

In ecosystems, these are represented in succession of ecosystems, the self-organization process by which ecosystems develop structures, functions, and diversity from available energies and materials. For example, at each stage of forest development,

Table 1-1. Definitions of terms and concepts used in the energy systems language relevant to this study (Odum, 1996).

Available energy	Potential energy capable of doing work and being degraded in the process (units: kilocalories, joules, etc).
Emergy	Available energy of one kind previously required directly and indirectly to make a product or service (units: emjoules).
Empower	Emergy flow per unit time (units: emjoules per unit time).
Energy transformation hierarchy	Energy flows of the universe are organized in an energy transformation hierarchy. The position in the energy hierarchy is measured with transformities.
Energy	May be defined as anything that can be 100% converted into heat.
First energy law	Energy is neither created nor destroyed in circulation and transformations in systems. That energy is conserved is a consequence of its definition above.
Heat	The collective motions of molecules, whose average intensity is the temperature which may be measured by expansion of matter in a thermometer.
Maximum empower principle	Principle that explains that in the competition among self-organizing processes, network designs that maximize empower will prevail.
Maximum power principle	Principle that explains that the system designs that prevail are those that organize to use more energy.
Power	Useful energy flow per unit time.
Pulse intensity	Energy or emergy concentration during a pulse divided by energy or emergy concentration in a complete pulse cycle.

Table 1-1 -- continued

Pulsing	Surge of storage and flow. Gradual build-up of production followed by fast frenzy consumption and material recycle.
Second energy law	Concentrations of available energy are continuously degraded (depreciating). Available energy is degraded in any energy transformation process.
Self-organization	Process by which various parts of a system connect themselves to work together.
Solar emergy	Solar energy required directly and indirectly to make a product or service (units: solar emjoules).
Solar empower	Solar emergy flow per unit time (units: solar emjoules per unit time).
Solar transformity	Solar emergy per unit available energy (units: solar emjoules per joule).
Transformity	emergy per unit available energy (units: emjoule per joule).
Turnover time	Time for a flow to replace a stored quantity. There will be as many turnover times as flows into or out of a storage.
Useful energy	Available energy used to increase system production and efficiency.
Work	An energy transformation process that results in a change in concentration or form of energy.

self-organization results in the combinations of different species and processes so that the forest system can utilize given resources better. Bernard cell convection is a nonliving example of self-organization. When water in a pot receives a steady flow of heat from below, the gradient of heat energy in the water column causes convection of fluid and the development of regular structure in the fluid. Also, our society and culture are the result of self-organization of people throughout human history. Human history is full of examples in which people organized themselves around newly introduced ideas and social structures.

Self-organization seems to produce common patterns and relationships that can be observed in any system because those may provide a competitive edge for better performance of systems and thus survival. Below are some common features which can be found in any self-organizing systems.

Structures and storages

Systems develop structures and storages which are discrete units, such as plankton in oceans, forest biomass, buildings in our cities, and so on (Figure 1-1). They provide forces for pathways and functions within systems which limit the systems performance, unless outside energy sources provide necessary forces. Those structures and storages also enable the systems to operate by supplying energies and materials during periods when inputs from outside are interrupted. Symbols used in Figure 1-1 will be explained in a later section of this chapter.

Feedback reinforcement

Systems and processes within them actively reinvest their energy to draw in more energies and materials, rather than passively waiting for resources to flow in. In Figure 1-1, the storage interacts with the energy source in the production process, pumping more energy into the production process. Increased energy inflow builds more storage. The storage will continue to grow until it reaches the limit imposed on it by energies and

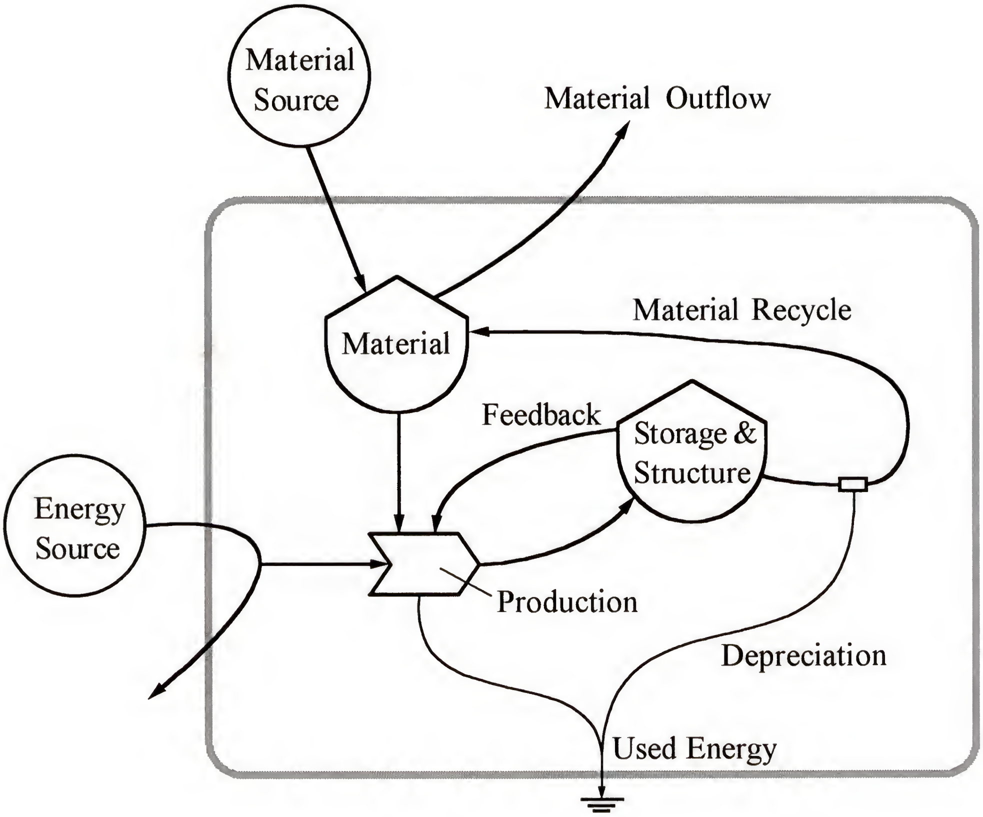

Figure 1-1. Common design features found in many systems.

materials available for the given system. For example, in a forest system, trees use sunlight energy to build trunks and leaves which result in more area for trees to capture more sunlight energy. Their growth is limited by the sunlight energy and nutrients available. This autocatalytic reinforcement may be selected during self-organization because it increases production and efficiency of energy use (i.e., production per unit energy input).

Components in systems deliver some feedback action on other components and processes that increase systems performance (maximize energy flows that reinforce production). For example, grazing by herbivores in terrestrial and aquatic ecosystems controls and changes species composition which affects production and efficiency under the given resource basis during a specific period in time.

Systems also develop feedback reinforcement in the form of material recycle. All systems require materials for their production processes. These materials are supplied by outside sources and/or by internal recycling. The internal recycling processes provide a way by which systems can avoid failure when material inputs from outside are interrupted. For example, zooplankton releases nutrients directly available to phytoplankton which uses them to produce organic materials, again supplying more phytoplankton biomass to be consumed. Most materials are, however, tied up in the storages, and thus systems develop special components and processes of decomposition to recycle materials.

Multiple pathways

Systems seem to show several different pathways for a process performed by a component, and have many parallel components which perform the same process. In other words, webs of components and processes are developed in self-organizing systems. By developing multiple pathways, a system can use different pathways within various environments of energies and materials. Redundancy develops in systems, and these are stored in genetic information and systems organizations. This multiplicity may enable systems to cope with and benefit from fluctuations in their environments.

Energy transformation hierarchy

Any processes in real systems transform energy from one form to another. Many different kinds of energies are involved in this transformation process, such as electromagnetic, kinetic, potential, chemical, thermal, and so on. These energies in different forms are converted into other forms through various mechanisms. For example, electromagnetic energy in sunlight is converted into chemical energy in organic matter through photosynthesis, and kinetic and potential energy in falling water is converted into electrical energy in a water power plant.

These transformation processes are subjected to the universal energy laws. Energy cannot be created or destroyed in these conversion processes. The form of energy is only changed. This is the first energy law of conservation. No real processes transform energies with perfect efficiency, that is, 100% efficiency. Much of the energy going into the transformation process is lost from the process as used energy, no longer capable of doing work. This tendency of energy to be degraded is called the second energy law. In Figure 1-1, energy which goes into the production process is the sum of the energy stored in the storage and the portion of energy lost in the process, which satisfies both energy laws.

The second energy law also applies to the storages and structures which are some form of concentrated energies (Figure 1-1). Thus, continuous energy input is required to maintain the storages and structures. While energy is depreciated, materials associated with it are dispersed in the system, contributing to the production process again.

Any system in nature consists of components and processes with various sizes and time scales. These are organized into a hierarchy in which many small components support a few large units (Figure 1-2a). Smaller units turn over faster with short life spans

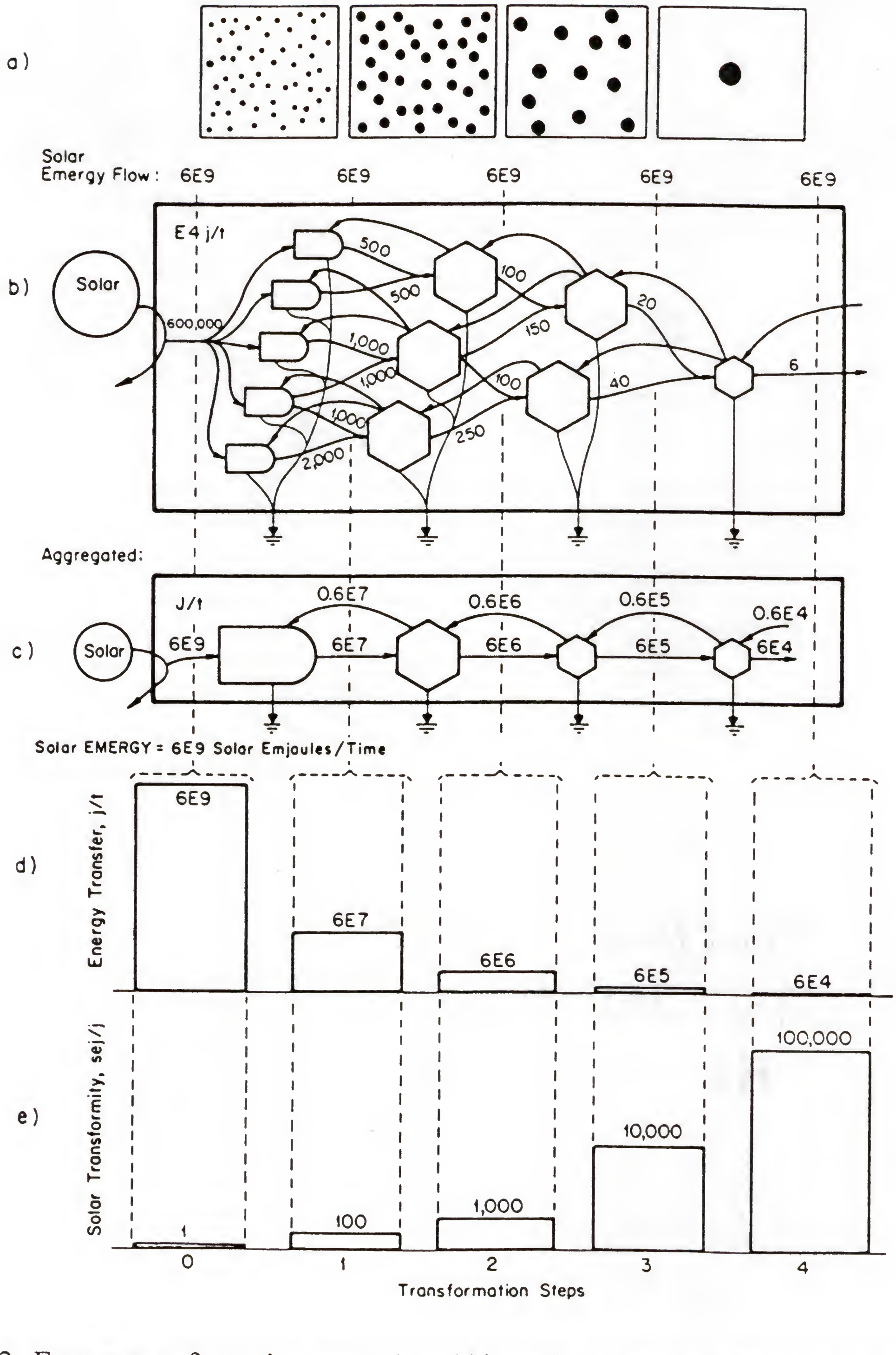

Figure 1-2. Energy transformation network and hierarchy. a) Spatial pattern of units and their territories; b) Network of energy transformation; c) Aggregation of the network in b) into an energy chain; d) Energy flows in each hierarchy; e) Solar transformities in each hierarchy (Odum, 1988 and 1996).

and have smaller territory, and larger units turn over slowly with longer life spans and have larger territory. For example, in marine ecosystems tiny phytoplankton use lots of sunlight energy to grow and reproduce. They become food of zooplankton that are bigger in size but lower in total number and biomass. Much bigger fishes with fewer numbers depend on these small planktonic animals for their food, and they support larger marine mammals. Larger organisms in this hierarchy of marine ecosystems require a larger area to feed. Each level in the hierarchy of systems seems to have structures and functions operating on its own scale.

There is much literature about hierarchical organizations in terrestrial ecosystems (Brokaw, 1982; Delcourt et al., 1983; Kotliar and Wiens, 1990; Wu and Loucks, 1995), in marine ecosystems (Harris, 1980; Horne and Platt, 1984; Ricklefs, 1992), in climate phenomena and related ecosystem and social processes (Clark, 1985), in genealogy and related evolutionary processes (Vrba and Eldredge, 1984), and so on. Military rankings and those of governmental organizations are social hierarchies that we see in our daily lives.

The second energy law says that every energy transformation loses much of the energy involved in the process (Figure 1-1 and 1-2b,c). Thus, successive transformations of energies provide smaller amounts of available energy to subsequent steps, leaving very little energy available after several steps of transformations (Figure 1-2d). This is the energetic basis of the hierarchical organizations observed in the real world. Energy transformations form a hierarchy in which many units at one level converge to fewer units at the next.

Because of their large energy requirement derived from units low in the hierarchy, units in higher levels have to have a positive effect commensurate with their energy consumption to be sustainable. Self-organization appears to develop feedback reinforcement in any energy transformation. In the example of marine ecosystems used above, zooplankton provide feedback actions to phytoplankton through nutrient recycle and control information on species composition and abundance, fishes control biomass, species composition, and distribution of zooplankton, and marine mammals in turn control actions of fishes. Figure 1-2b and c show this energy transformation hierarchy in which energy flows from low to high in hierarchy, and control actions feed back in the opposite direction.

Energy quality and transformity

Energies are upgraded in their quality through transformation processes, in the sense that more energy is required to make the products and these new energies have control effects with small amounts of energy. Energy in fishes can be said to be higher in quality than that of phytoplankton. Energy transformation hierarchy can be called energy quality hierarchy; the higher in hierarchy, the higher in quality. Thus, it is misleading to compare different energies just based on actual contents of energy.

Energies can be compared on the same basis by tracking energy history in producing the products. Emergy is defined as the available energy of one kind previously used up directly and indirectly through transformations to make a product or service (Odum, 1988 and 1996). This quantity provides a measure of value based on what went into a product. In Figure 1-2b and c is given solar emergy that is defined as the available solar energy used up directly and indirectly to make a service or product.

Another quantity, transformity, measures energy quality and position in the universal energy hierarchy. Transformity is defined as the calories of available energy of one kind previously required to make one calorie of another kind (Odum, 1988 and 1996). Figure 1-2e shows that increasingly more solar energy is required to produce a given unit of energy from left to right along the energy hierarchy; that is, higher transformity as going from left to right along the chain. Here, solar transformity is defined as the solar emergy required to make one joule of a service or product, with units of solar emjoule per joule (sej/J) (Odum, 1996). In contrast, actual energy content decreases during successive transformations (Figure 1-2d). Even though the final product in Figure 1-2 carries the smallest amount of actual energy, its transformity is the highest, which represents its position in the hierarchy.

Energy transformation hierarchy is represented as a network of units of various sizes in spatial dimension. Energies from smaller units that turn over fast converge to support larger units with slower turnover time. In turn, controls from the centers spread out to smaller units. Larger territory is required to support units in centers even though they occupy a small portion of the supporting territory. Because available energy decreases through successive energy transformation processes, required by the second energy law, areas to support units increase as they go up the energy hierarchy. There is a hierarchy of territory needed to support units.

Maximum power and empower

Previous sections listed common features that observed in any real system and discussed organization of these features into a hierarchical network of energy transformations. These are the successful systems designs that survived the test of time. Why do those features occur during self-organization? How can we explain why some systems survive and others do not? Why do certain patterns of system organization develop and others do not, and why do successful systems have similar patterns? In all, what describes the direction of systems development during self-organization?

Several goal functions, or design principles, have been suggested for ecosystems and other systems to explain systems development during self-organization. This does not mean that systems have predetermined goals, but rather that self-organization enables systems to meet perturbations by directive reactions (Jorgensen, 1994). Jorgensen (1992) gives an overview of several goal functions proposed for ecosystems during the last 1-2 decades by several systems ecologists; maximum power (Lotka, 1922; Odum and Pinkerton, 1955), minimum entropy (Glansdorff and Prigogine, 1971), maximum biomass

(Margalef, 1968; Straskraba, 1979), maximum ascendency (Ulanowicz, 1980), maximum exergy (Mejer and Jorgensen, 1979), maximum persistent organic matter (Whittaker and Woodwell, 1971; O'Neill et al., 1975), and maximum profits for economic systems. Jorgensen (1994) reviewed and compared several goal functions using lake models and suggested that all the investigated goal functions are highly correlated. Odum (1983, 1994, and 1995) also compared several goal functions and showed that others are special cases of maximum power.

Available energy was the center of Boltzmann (1905)'s struggle for existence. Lotka (1922), quoting Boltzmann, formulated the maximum power principle, to which later Odum (1955, 1971, 1983, and 1996) provided several corollaries and refined the concept. According to the maximum power principle, "during self-organization, systems designs develop and prevail that maximize power intake, energy transformation, and those uses that reinforce production and efficiency" (Odum, 1995). Efficiency of an energy transformation was defined as the quotient of the output energy divided by the flux of input energy. Thus, power provides a criterion of whether a system or system design could survive or be displaced by others, under given energy constraints. Among alternatives, those designs that reinforce to draw in more power and use it with the best efficiency are selected and continue to function. This selection process according to maximizing power continues to work under continuous fluctuations of internal structures and external sources of any given system. Common features of systems discussed in the previous sections are those that survived the test of time.

The power concept that is defined using actual energy content does not reflect the concept of energy quality along the energy transformation hierarchy discussed in the previous section. Thus, maximizing power might imply that self-organizing systems would increase energy flow at lower levels in the hierarchy with more energy but lower transformity. Empower is defined as the flow of emergy per unit time and it places energy of each level of the hierarchy on a common basis. Thus, the maximum power principle can be restated as the maximum empower principle; that is, “prevailing systems are those whose designs maximize empower by reinforcing resource intake at the optimum efficiency” (Odum, 1996).

In marine ecosystems marine organisms often develop until they maximize their utilization of sunlight energy falling on the oceans and other physico-chemical energies operating in the oceans. They develop reinforcing designs, such as nutrient recycle and control actions on biomass and species distribution. Seasonal variation of species participating in production and consumption processes can be viewed as a way of maximizing overall power inflow into marine ecosystems under varying energy inputs with seasons.

In this dissertation, systems designs are considered in relation to maximum power and maximum empower principle as explained in Odum (1983, 1994, and 1995). Power is defined as energy flow per unit time.

Generalizing Concepts with Energy Systems Language

People have used models as simplified pictures of the real world to understand complex systems around them, to test hypotheses about the systems, and to solve problems they are facing. These models can be in the form of verbal language, physical models, or mathematical representation.

Models can be constructed in two different ways: reductionistic or holistic. The reductionistic approach, also called the bottom-up approach, separates a whole system into parts and then tries to investigate the properties of the system by studying the component parts separately. In the sense that a whole system is not just the sum of its parts, the reductionistic approach can not give an understanding of a system until some kind of synthesis recombines the parts to show the collective behavior. In contrast, the holistic, or top-down, approach attempts to investigate mechanisms of the way a system works by studying it as a whole. It starts with simplified overall patterns and relationships rather than detailed mechanisms of component parts. While analysis by the reductionistic approach needs to be synthesized to reveal properties at the system level, the holistic synthesis requires analysis so that it can be corrected and verified.

In this dissertation, systems dynamics and energetics are investigated using energy systems language which is a top-down approach, developed by H.T. Odum (1971 and 1983). Energy systems language uses a set of symbols that have special meanings and mathematical relationships of components and processes of systems, for modeling of all kinds of systems of interest. When drawn in an appropriate way, energy systems diagrams show energetics and kinetics at the same time in a holistic way. Figure 1-3 shows symbols of energy systems language with a brief description of each symbol.

The energy systems language shows systems organization graphically while keeping important energy constraints and systems kinetics so that anyone with a little understanding of the symbols and their meanings can grasp network organizations of systems and their properties easily. In most other modeling conventions, true pictures of nature- energy constraints and network organization are hidden behind ambiguous verbal languages, complex differential equations, or long computer programs. To investigate the systems dynamics, a computer simulation program can easily be written from the energy systems diagram, using the mathematical meanings of the symbols connected in the diagram.

Theory of Pulsing Paradigm

As a way of seeing systems development, the steady-state concept suggested that all systems develop to reach certain levels that are determined by resource available and stay there for long time (Figure 1-4a). In recent years, many studies have shown that fluctuations may be an inherent property of all systems in nature. Even human history

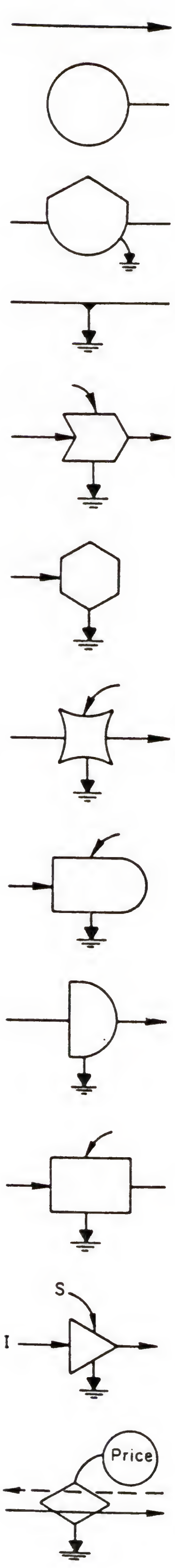

Energy circuit A pathway whose flow is proportional to the quantity in the storage or source upstream.

Source Outside source of energy delivering forces according to a program controlled from outside; a forcing function.

Tank A compartment of energy storage within the system storing a quantity as the balance of inflows and outflows; a state variable.

Heat sink Dispersion of potential energy into heat that accompanies all real transformation processes and storages; loss of potential energy from further use by the system.

Interaction Interactive intersection of two pathways coupled to produce an outflow in proportion to a function of both; control action of one flow on another; limiting factor action; work gate.

Consumer Unit that transforms energy quality, stores it, and feeds it back autocatalytically to improve inflow.

Switching action A symbol that indicates one or more switching actions.

Producer Unit that collects and transforms low-quality energy under control interactions of high-quality flows.

Self-limiting energy receiver A unit that has a self-limiting output when input drives are high because there is a limiting constant quantity of material reacting on a circular pathway within.

Box Miscellaneous symbol to use for whatever unit or function is labeled.

Constant-gain amplifier A unit that delivers an output in proportion to the input *I* but changed by a constant factor as long as the energy source *S* is sufficient.

Transaction A unit that indicates a sale of goods or services (solid line) in exchange for payment of money (dashed). Price is shown as an external source.

Figure 1-3. Symbols and definitions of the energy systems language (Odum, 1983).

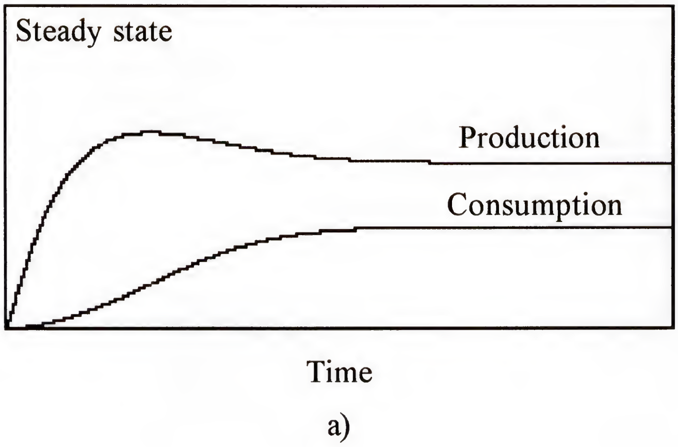

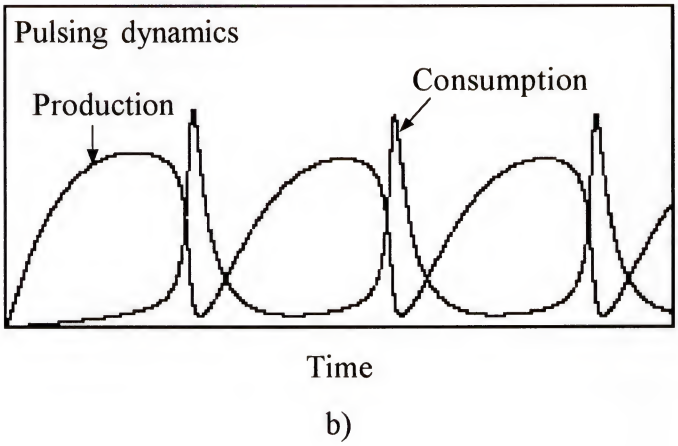

Figure 1-4. Two different views of systems development over time. a) Steady state concept in which system components level off after growth; b) Pulsing dynamics with alternations of slow production and fast consumption.

shows rising and sudden collapse of dominant civilizations in the past. And we always feel in our lifetime the falling and rising of the economy. As a new paradigm (Odum, 1983 and Odum et al., 1995), pulsing dynamics may reveal the true nature of the systems.

Pulsing in time and space

Pulsing, in this dissertation, is defined as alternation of the gradual build-up of production and a short period of frenzied consumption that recycles materials for another cycle of production and consumption (Figure 1-4b). For example, earthquakes result from pulsed consumption of strain in fault boundaries accumulated over time. And harvest from a pine plantation is a consumption process within a short time period on the tree biomass produced over long period of time. There are many other examples of temporal pulsing events that can be seen in our daily lives: seasonal phytoplankton bloom in coastal ecosystems, locust outbreaks, dominant year classes in fish populations, outbreaks of epidemic diseases, stock market crashes, El Nino episodes, extinction of dinosaurs in geologic history, and so on.

Pulsing dynamics can also be observed in the spatial dimension as well as in the temporal scale. Different parts of a system may be in different stages of the production-consumption cycle, forming mosaic patterns. Plotting production and consumption along a spatial transect in those systems may produce a pattern similar to the temporal pulsing in Figure 1-4b. Examples are: moving atmospheric front between two different air masses and oceanic front between two different water masses, spreading out of upwelled water in upwelling systems, patch distribution of plankton in oceans, forest gaps, and so on. In most systems, pulsing dynamics are reflected in both temporal pattern and spatial structure.

Pulsing hierarchy

Pulsing occurs simultaneously on many scales. Each scale in the energy transformation hierarchy seems to have its own characteristic pulsing frequency and amplitude, forming a pulsing hierarchy (Figure 1-5). Smaller scale systems with faster turnover times are characterized by more frequent and smaller pulses. Pulsing amplitude and interval between successive pulses increase from the low energy to the high energy end of the hierarchy. For example, in ocean ecosystems small plankton with fast turnover time show more frequent and smaller pulses than fishes, while fishes turn over faster and pulse more frequently than top predators.

Pulses in each hierarchy can be viewed as combined results of the pulsing characteristics in its own scale and the pulsing patterns in the next scales larger and smaller, because units in one scale are connected to smaller and larger scales through energy transformations. Pulses from the smaller scale with low transformity often appear as random noise in the larger scale systems. On the other hand, larger scale pulses with high transformity can have a catastrophic effect on the smaller scale systems. For example, small scale, frequent pulses in sunlight and nutrient inputs are averaged out in patterns of biomass fluctuations of the whole forest. Volcanoes are catastrophic events that wipe out the whole forest ecosystem, leaving the area for self-organization to start over again. But, these catastrophic pulses may be a part of regular pulsing when viewed in the next larger system.

Large pulses require more time and area for production storage to accumulate (Figure 1-5 c) because less energy is available at higher hierarchy due to energy loss through depreciation along the energy transformation chain. Pulses of smaller sizes converge over space and time to support less frequent, larger pulses. In turn, larger pulses deliver high quality feedback control actions. These pulses spread out in time and space from centers, reinforcing and reorganizing the smaller scale systems.

Pulses from larger scales are sometimes considered as catastrophic and seem to occur randomly from the perspective of small scale systems. In pulsing paradigm, they are generated by internal dynamics of the larger system. Another way of looking at pulses from outside of a system in interest is the use of stochastic shocks. Internal dynamics of

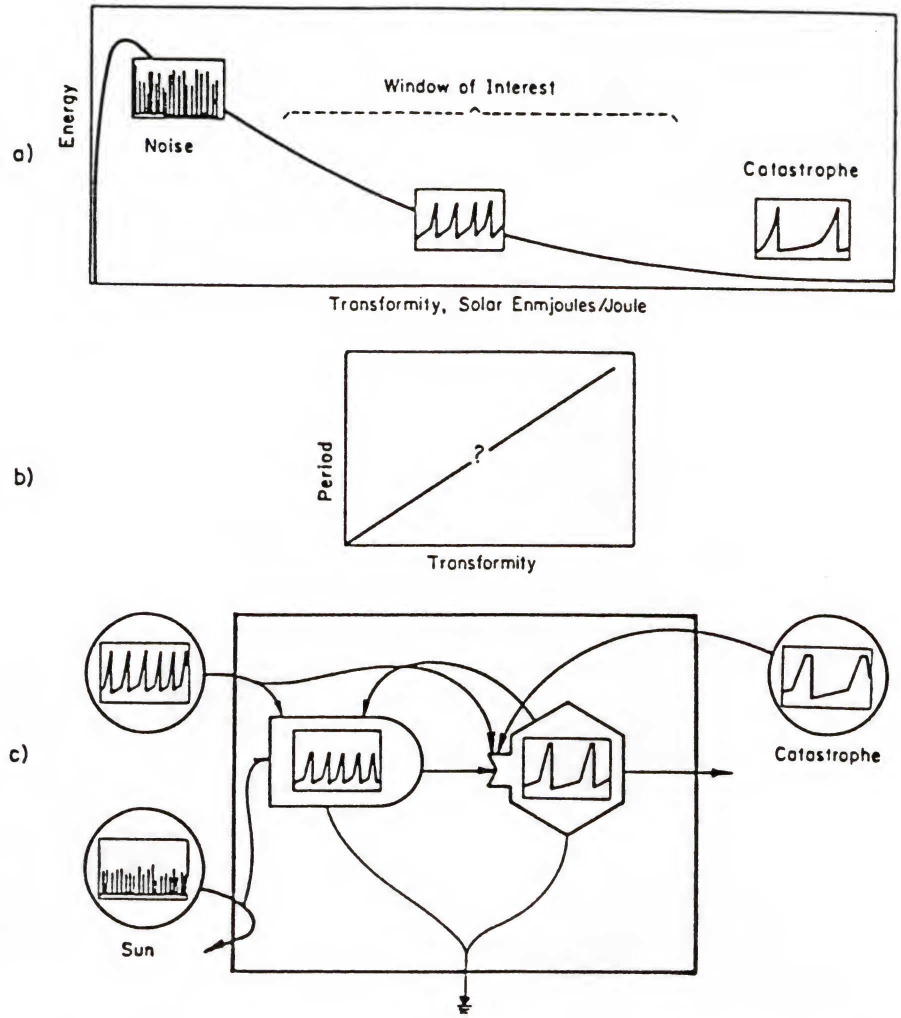

Figure 1-5. Frequency of pulses as a function of position in the energy hierarchy; pulses smaller than the system of concern are considered as noise, and larger pulses of systems larger than that of concern are regarded as catastrophes. a) Energy transformation spectrum; b) Pulse period as a function of transformity; c) Energy systems diagram of production and consumption with pulse frequencies appropriate to sources and hierarchical position (Odum, 1983).

systems are modified by randomly varying outside sources. Using economic systems as examples, Stokey and Lucas (1989) modified dynamic growth equations by multiplying production function by a term representing stochastic variation.

Pulsing and maximum empower

In a previous section, the maximum empower concept was introduced as the design principle of systems development during self-organization. If pulsing is general for all scales, systems that pulse have to draw in more empower than systems that do not. Odum and Odum (1996a) suggested that "pulsing may prevail because more energy is transformed during operations that pulse than during those at steady state". By repeating slow accumulation of production and pulsed consumption, systems may maintain a stronger gradient between energy source and loading of the receiving units, resulting in more energy inflow. Thus pulsing may provide better long run coupling of energy intake for maximum empower than a steady state.

If pulsing maximizes empower, there will be optimum frequency and amplitude for maximum empower. Too frequent pulses do not allow production potential of a system to recover fully. It will take too long for the system to recover its production potential if pulses are too big to be absorbed in the system. Systems can not get better loading if pulses are too infrequent or too small. Systems in the energy transformation hierarchy may need appropriate pulse frequency and amplitude to maximize empower in each scale. Timing and shape of pulses can have an effect on empower in a given system.

Systems may maximize empower when internal pulses of systems match external rhythms. Most pulses have been considered externally controlled, usually by oscillations of the next larger system with longer periods. But, many systems also seem to oscillate due to the interaction of component turnover characteristics. Pulsing in nature may be a result of a combination of internal mechanisms and external factors. Proper matching of external and internal pulsing sources would amplify empower input through a resonance effect.

Thus, systems may pulse regularly to make a pulsing steady state rather than just a steady state that levels off after the initial period. Pulsing dynamics may be a result of systems adaptation to maximize empower in the long run.

Pulsing minimodel for all scales

Figure 1-6 shows a minimodel that can be applied for pulsing in all kinds of systems. It is a simple production-consumption model with material conserved inside the system. This simple model can represent any system because all systems have some kind of production and consumption processes that can be aggregated into the model like Figure 1-6. For example, all green plants in a forest ecosystem can be grouped into producer storage in Figure 1-6, and all other components that use organic material produced by green plants can be grouped into consumer storage.

The producer units synthesize organic material using an outside energy sources and material within the system. Most of the energy is lost in the process. The consumer unit in Figure 1-6 has three different options in consuming organic material from the producer storage. They may represent different phases of consumer growth or various species under different conditions. The linear pathway operates at low energy levels, providing a minimum energy for the consumer persistence.

As the producer storage increases, the autocatalytic pathway takes over and a further increase in the producer storage provides enough energy for the quadratic autocatalytic pathway to activate a pulse. This higher mathematical function provides an internal pulsing mechanism without pulsing controls from outside the system. These pathways with various orders of mathematical functions provide alternative pathways which exist in real systems. Different pathways may be activated at different times that

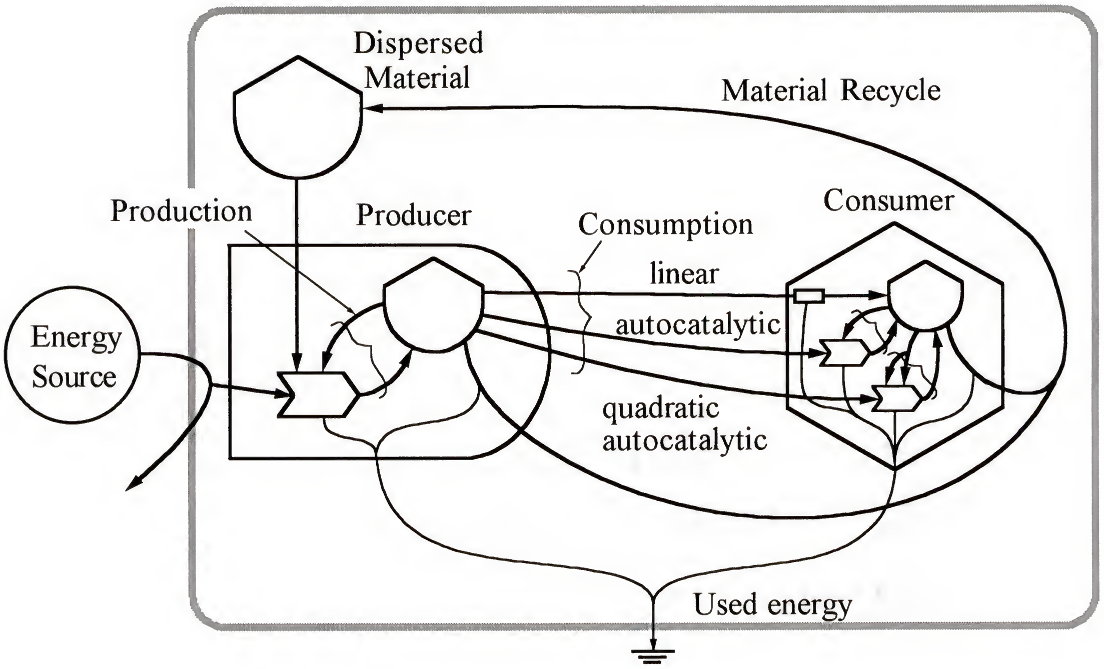

Figure 1-6. Pulsing minimodel of many kinds of systems alternating slow accumulation of production followed by frenzied consumption and recycle. The model provides three different pathways of consumption which operate during different periods of systems development.

have different energy conditions and material flows. Or, different species with similar function may take over when conditions are appropriate.

Previous Studies of Pulsing

Because the steady state concept of system development so prevailed over various fields in the past, most earlier literature on systems dynamics considered fluctuations found in measurements as errors or unusual cases. During recent decades, there has been increasing interest in nonequilibrium dynamics and fluctuations in all systems. Much attention has been devoted to the pulsing dynamics in various systems, from molecules to the universe.

Using observed data, some authors isolated pulses of different frequency using Fourier analysis. For example, Platt (1972 and 1978) applied Fourier spectrum to analysis of spatial structure of phytoplankton in the oceans.

This is a brief review of pulsing phenomena in several different systems. In the following review an energy systems diagram was drawn for each model based on equations and explanations, when possible.

Pulses in Chemical Reactions

Chemical systems have provided good and easily observable examples of systems with pulsing dynamics. They constitute the faster end of pulsing hierarchy, with fast turnover times and frequent pulses. Gray and Scott (1990) and Scott (1991) provide many such systems with their kinetics and models; among those systems are Belousov-Zhabotinskii reaction, catalytic oxidation of carbon dioxide, reaction between hydrogen and oxygen, electrodissolution of metals, and glycolysis. Chemical reactions in controlled environments have provided excellent opportunities for chemists to study pulsing systems. Below are two examples among various chemical systems with pulsing dynamics.

Belousov-Zhabotinsky reaction

The Belousov-Zhabotinskii reaction is the most widely studied and best-understood pulsing chemical system, in which concentrations of the reaction intermediates oscillate. The reaction consists of oxidation of an organic material by bromate ion (BrO_3^-) in a strongly acid, aqueous medium, catalyzed by a metal ion with two oxidation states (Field and Schneider, 1989). The most evident feature of the reaction is the periodic change of color or redox potential due to the change in the oxidation state of the metal-ion catalyst. This reaction has been observed in both batch and flow (or open) reactors.

Field et al. (1972) proposed the mechanism of the oscillating Belousov-Zhabotinskii reaction. From this detailed mechanism, Field and Noyes (1974) derived a reduced, irreversible model, called Oregonator, which described the essential features of the Belousov-Zhabotinskii reaction (Figure 1-7). This model describes the Belousov-Zhabotinskii reaction in batch reactors. In the model, bromate ion (A) was assumed to be constant as each oscillatory cycle consumes only a very small fraction of bromate ion. Hydroboric acid (P) was considered to be a dead-end product in this irreversible model.

Field (1975) expanded the Oregonator to include reversibility of the various steps in the reaction. Recent experiments on the Belousov-Zhabotinskii reaction have revealed a sequence of alternating periodic and chaotic regimes (Turner et al., 1981; Pikovsky, 1981; Strizhak and Menzinger, 1996). Yoshida et al. (1996) synthesized a polymeric gel which generated an autonomic swelling-deswelling oscillation without any external stimuli. Chemical oscillation of the Belousov-Zhabotinsky reaction in the gel induced mechanical oscillation of the polymer network.

Salt-water oscillator

Yoshikawa et al. (1989) observed periodic pulses of water flow in a simple system called the salt-water oscillator. In the system, a fluid of high density salt water above, was connected to lower density pure water below, by a small hole, cylindrical tube, or capillary, between the two fluids. A downward pulse of salt water flow was followed by

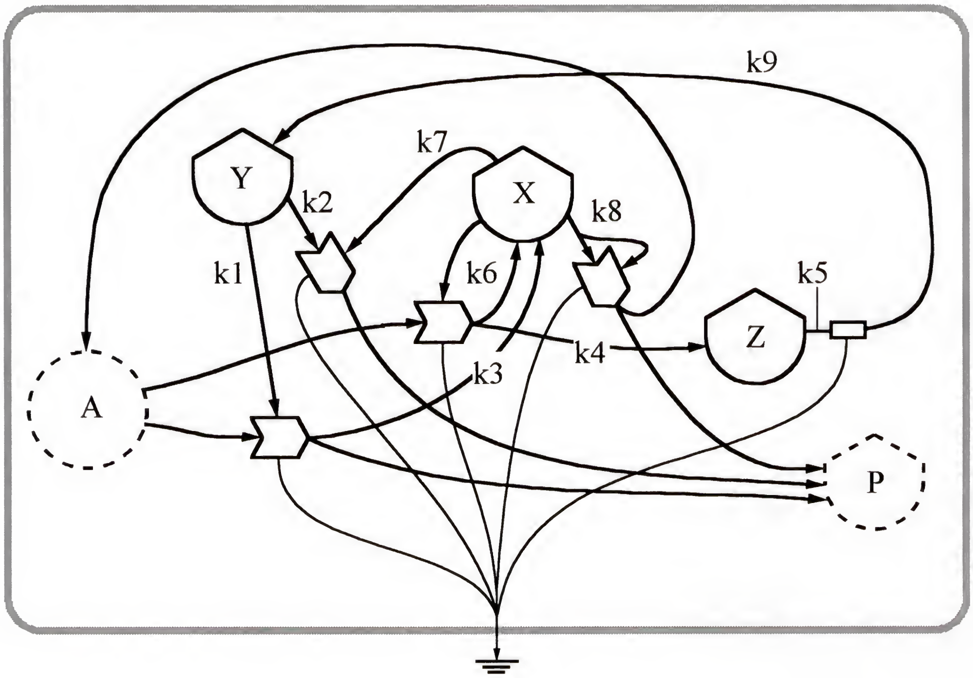

$dX = k3*A*Y + k6*A*X - k7*X*Y - k8*X*X$
$dY = k9*Z - k1*A*Y - k2*X*Y$
$dZ = k4*A*X - k5*Z$

Author's Original Equations:
Process A : $A + Y \longrightarrow X + P$
$X + Y \longrightarrow P + P$
Process B : $A + X \longrightarrow 2X + Z$
$X + X \longrightarrow A + P$
Process C : $Z \longrightarrow fY$
Differential Equations:
$dX/dt = k_{M1}*A*Y - k_{M2}*X*Y + k_{M3}*A*X - 2k_{M4}*X*X$
$dY/dt = -k_{M1}*A*Y - k_{M2}*X*Y + f*k_{M5}*Z$
$dZ/dt = k_{M3}*A*X - k_{M5}*Z$

Figure 1-7. Energy systems language translation of the Oregonator model of the Belousov-Zhabotinskii reaction by Field and Noyes (1974), where $A = BrO_2^-$, $P = HOBr$, $Y = Br^-$, $Z = 2Ce(IV)$, $X = HOBr_2$, and f = stoichiometric factor. Bromate ion (A) was considered as constant in this model and hypobromous acid (P) as a dead-end product of the reaction. Author's original equations are shown below the diagram.

an upward pulse of pure water through the connection. This cycle of water flow continued until the system reached equilibrium with mixing of both fluids. Oscillation lasted longer with greater density difference. The period of the oscillation increased when a narrow capillary was used instead of a cylindrical tube.

Aquatic Ecosystems

Aquatic ecosystems have also provided good time series data because their small components turn over quickly. Many such data show various pulsing frequencies and amplitudes. In particular, plankton data provided time series of sufficient duration to show pulsing hierarchies.

Pulsed supply of resources

Even if light energy is supplied at a constant rate, phytoplankton, the main producer in the water column, experiences pulses of light because of the vertical water motion. Phytoplankton face different durations and intensities of light, depending on the intensity of water motion. Denman and Gargett (1983) estimated time and space scales of vertical cycling of phytoplankton caused by turbulent mixing, internal waves, Langmuir circulations, and double diffusive processes.

Marra (1978) investigated the effect of three different light regimes on photosynthesis of a marine diatom grown in axenic continuous culture: constant, simulated diurnal variation, and fluctuating light environment superimposed on the diurnal regime, over a photoperiod of 11 hours in light and 13 hours in dark condition. Diatom cells utilized light energy most efficiently during photosynthesis with the pulsed fluctuation of light, and they also showed a much higher level of light-saturated photosynthesis under the fluctuating light regime. The pulsed light fluctuations, however, resulted in more average cell yield for the given total daily light in only one of three experiments that compared culture yields under diurnal and fluctuating regimes.

It has long been believed that open ocean ecosystems are very low in productivity due to nutrient limitations. Recent studies suggest higher primary production in those systems. Pulsed input of nutrients from below the euphotic zone was suggested as a mechanism for the high primary productivity (McGowan and Hayward, 1978; Platt and Harrison, 1985), enhanced chlorophyll concentration (Holligan et al., 1985), and transient cyanobacterial bloom (Glover et al., 1988). Vertical mixing of water was caused by internal waves (McGowan and Hayward, 1978; Holligan, 1985) and by mesoscale features such as cyclonic eddies (Jenkins, 1988; Falkowski et al., 1991).

Leichter et al. (1996) observed high frequency variation in temperature, salinity, water velocity, and concentration of chlorophyll-a on a reef ecosystem, and discussed the potential consequences of these variations. They related those variations to pulsed delivery of cold, nutrient rich subthermocline water caused by internal tidal bores linked to a semidiurnal internal tide. Cullen et al. (1983) observed pulses of nitrate input into the surface layer associated with vertical mixing by internal waves on the Southern California Shelf. In freshwater phytoplankton, nutrient pulses had an effect on the community structure and cell size (Suttle et al., 1987).

Pulsed settlement of a temperate reef fish was attributed to phytoplankton production pulses, followed by consumption by microzooplankton, the food sources for the fish larvae (Thresher et al., 1989). Witman et al. (1993) also observed a pulsed supply of phytoplankton to rocky subtidal zones, by internal waves during ebb and flood tides. They related this pulsed supply of food to potential enhancement of secondary productivity of benthic suspension-feeding invertebrate populations.

Upwelling pulses

The upwelling ecosystem is one of the most productive of the world oceans. Pulsed nutrient input during upwelling enhances primary production (Walsh, 1983; Parsons et al., 1984; Verheye et al., 1992). Caused by prevailing winds and the Coriolis effect, upwelling occurs in coastal areas along the western margin of continents and in open oceans and the Southern Ocean. Pulses spread out downstream from the upwelling centers, producing a pulsing hierarchy in space (Walsh, 1983; Pages, 1992; Valiela, 1995).

Jury and Brundrit (1992) suggested an optimum upwelling pulse frequency of 10 days in the southern Benguela ecosystem, after analyzing time series of upwelling events with considerable variations in duration and amplitude. They argued that the productivity residual was depleted by higher trophic levels with too long intervals between upwelling pulses, and the quiescent phase was too short for a phytoplankton bloom to occur when the upwelling pulses were too frequent. They also concluded that at the frequency of 10 days, matching of the free and forced modes of coastal trapped waves produced the greatest amplitude change in environmental variables between active and passive upwelling phases.

Pulses in microcosm

Isolated from outside environments, many microcosms do not show fluctuations in their components after an initial transient period. However, in some cases microcosms also show pulsing patterns in their dynamics. A microcosm that was spatially separated by Ringelberg (1977) and Kersting (1985) into three subsystems of autotrophs, herbivores, and decomposers, but interconnected by a continuous flow system, showed wide fluctuations in its components during 10 years of experiments. Analysis of time series of algal biomass by Ringelberg (1977) revealed an oscillation time of 44 days.

Brockmann et al. (1977) observed a phytoplankton succession in nutrient-poor water in an outdoor plastic tank. During 28 days of experiments, there were three major pulses in phytoplankton biomass dominated by different species. They found intensive nutrient recycling processes due to the phytoplankton pulses in the nutrient-poor water used in the experiment.

Microcosm experiments with freshwater phytoplankton by Robinson and Sandgren (1983) showed different species diversity for three different perturbation periodicities of 1, 7, and 28 days. Shannon-Weaver-Wiener diversity and evenness were highest at the 28-day periodiocity, and the highest species richness occurred under the 7-day periodicity. Discriminant analyses indicated that average perturbation periodicity had more significant influence on the species abundance patterns.

Sommer (1985) investigated how fluctuations in resource levels affect species richness and the competitive performance of species by comparing competition experiments with natural phytoplankton assemblages. Pulsed input of nutrients at weekly intervals allowed more species to coexist than steady input of nutrients. His results also showed more biomass in the pulsed nutrient regime.

Using semicontinuous competition experiments, Gaedeke and Sommer (1986) studied the influence of pulse frequency on the maintenance of phytoplankton. Pulses consisted of dilution events that added fresh nutrients and reduced the population size. The intervals between dilution events varied from 1 to 14 days. Shannon-Weaver-Wiener diversity index was maximum at 7-day intervals between pulses. Pulse intervals greater than the average generation time of phytoplankton allowed more species to coexist than under steady state conditions. They concluded that variation of growth conditions between pulses prevented competitive exclusion and permitted the persistence of species that would have been excluded under steady state conditions.

Plankton pulses

Because of its fast turnover time in days, plankton has provided quite good time series in regard to sampling frequency and study period. There is much literature on the well-known seasonal pulsing of plankton in temperate seas. Observed data in plankton ecosystems show several scales of pulsing patterns, on time scales of hours, days, months, and years.

Demers and Legendre (1981) observed pulsed variation in chlorophyll-a concentration in the St. Lawrence Estuary, over a 7-day period. The time series showed pulses in the scale of several hours, with one major pulse during the period. Hourly observations of phytoplankton and zooplankton biomass at a single station over a period of about 430 days showed pulses of several different frequencies (Ascioti et al., 1993). Both phytoplankton and zooplankton showed clear seasonality, reaching high levels in May-June. Fourier spectra of both data exhibited inertial and tidal peaks at roughly 19, 12, and 24 hours.

Lohrenz et al. (1988) used satellite imagery to examine the synoptic distribution of primary production in the western Mediterranean. They correlated satellite-derived surface pigment concentrations, and shipboard measurements of surface chlorophyll-a and integrated water column primary production, over an 18-day period. They concluded that a significant fraction of regional production was attributable to production pulses associated with a mesoscale circulation feature.

Balch (1981) presented data that showed phytoplankton bloom and succession associated with a lunar tidal cycle. Phytoplankton counts showed three major pulses occurring several days after each major spring tide over three months of observation, with about 20 pulses in total over the period. He argued that variations in vertical mixing during the spring to neap tidal cycles influenced the vertical transport of chlorophyll upwards, causing an increase in the surface cell counts and species number. The Shannon-Weaver-Wiener diversity closely followed the pattern of the total cell abundances.

Production in permanently stratified tropical seas removed from immediate land influence has been believed to be either low or relatively uniform throughout the year. Steven and Glombitza (1972), however, observed pulses of phytoplankton population with a periodicity of between 3 and 4 months in the surface layer of the tropical Western Atlantic.

Plankton records over several years have shown seasonal pulses of both phytoplankton and zooplankton with more frequent pulses embedded in the seasonal pattern (de Bernardi et al., 1988; Philips et al., 1993; Sastre et al., 1994). Longer term observations of plankton show pulses of plankton in the scales of several years as well as seasonal patterns. A long term record over 22 years in Lake Kinneret in Israel showed a multiannual oscillation of 3-6 years in primary production and phytoplankton biomass as well as clear annual variation (Berman et al., 1995). Time series of diatoms and flagellates in the German Bight over 23 years not only shows seasonal pulses and more frequent pulses embedded in the seasonal pattern, but also interannual variations (Radach, 1992). Lathrop and Carpenter (1992a and 1992b) provide phytoplankton and zooplankton data in Lake Mendota, Wisconsin over a 14-year period that show plankton pulses on scales of months, years, and several years.

Margalef (1958) observed pulsed variations of species diversity along the successional stages of coastal phytoplankton in the ria of Vigo, Spain. Species diversity started to increase from the lowest value of the first stage in phytoplankton succession. It reached maximum at the third stage and then rapidly declined, indicating completion of one cycle of ecological succession. He recognized three to four complete successions in a year, and suggested that intense exchange of water between the ria and the open sea is necessary to end and start a new sequence of succession. Travers (1971) also found the same relationship between stages of ecological succession and fluctuations in species diversity in microplankton populations.

Connell (1978) and Huston (1979) proposed a hypothesis that species diversity in a local area would be highest at an intermediate level of disturbance, such as fire, windstorms, insect outbreaks, predation, and the like. Species diversity in communities is the result of variations in frequency and intensity of disturbances and area perturbed (Connell, 1978) or variations in the dynamic equilibrium between the rate of competitive displacement among species and the frequency (and intensity) of disturbance (Huston, 1979). They started from the notion that under continually changing environments natural communities seldom or never reach an equilibrium state.

Townsend and Scarsbrook (1997) found the highest species richness in stream beds which were subjected to intermediate intensities and frequencies of disturbance in the form of bed movement pulses caused by flood episodes.

Natural populations live in variable environments and often fluctuate dramatically in abundance. External factors (environmental variability) have been suggested as a major responsible mechanism for those observed pulsing patterns. However, populations living in constant environments also display large fluctuations, which suggests that internal mechanisms play an important role in pulsing dynamics. Based on experiments with replicate Daphnia and algal populations, McCauley (1993) concluded that periodic fluctuations of populations of Daphnia and their algal prey in lakes and ponds could be internally generated by the predator-prey interaction between them rather than external environmental variability. He found significant correlations between replicates started at the same time, but no significant correlations between those staggered in time.

Spinning wheel hypothesis

Goldman (1984a and 1984b) proposed the spinning wheel-aggregate hypothesis to explain the possibility of very rapid growth of phytoplankton in oligotrophic oceanic waters. He suggested that there are small amorphous aggregates of organic matter in the water column with resident populations of bacteria, autotrophs, and microflagellates. In these aggregates, the microbial food chain of bacteria, autotrophs, and microflagellates operates as a rapidly spinning wheel with both the grazing and regeneration of nutrients keeping pace with the growth of autotrophs. Microaggregates might serve as sites of intense nutrient recycling compared to the nutrient-poor surrounding environments so that phytoplankton would grow at a fast rate.

Goldman (1984a) suggested a prey-predator type oscillation for variations of biomass of autotroph and grazer and dissolved nutrients, on time scales of hours to days. In the model, autotrophs grow using nutrients in the aggregates, followed by pulsed consumption of autotrophs by grazers, which returns nutrients for the cycle to repeat.

Patches of phytoplankton were a result of balance between reproduction and diffusion in a model (Figure 1-8) by Kierstad and Slobodkin (1953). For a phytoplankton bloom to develop in a finite region, reproduction (K) should be greater than loss through diffusion by turbulent energy (D). They derived a minimum critical size for the water mass below which no increase in phytoplankton concentration can occur. Patches smaller than this size are dispersed into the surrounding area unsuitable for the survival of the population, and blooms can not develop.

Ocean bottoms

Strong interannual variability was also evident in time series of macrobenthic abundance in Chesapeake Bay, which showed clear seasonal pulses, mainly due to difference in the amplitude of recruitment pulses (Holland, 1985). Sousa (1979) investigated the effects of disturbance on local species diversity in an algal-dominated, intertidal boulder fields. Intermediate-sized boulders that were subjected to intermediate frequencies of overturning pulses by waves supported the most diverse communities.

It has long been believed that the deep-sea bottom has a constant environment at spatial and temporal scales. Recent studies with better sampling programs have revealed that the deep sea environments also show much spatial and temporal variations. Pulses of organic inputs from the surface layer are believed to be the major cause of the observed temporal variations (Tyler, 1996), which are reflected in periodic reproduction (Tyler, 1988) and pulsed growth (Gooday et al., 1993). Gooday et al. (1993) observed periodic growth of xenophyophores with 2-3 days of growth pulses followed by about two months of inactivity, at 4944 m on the Madeira Abyssal Plain.

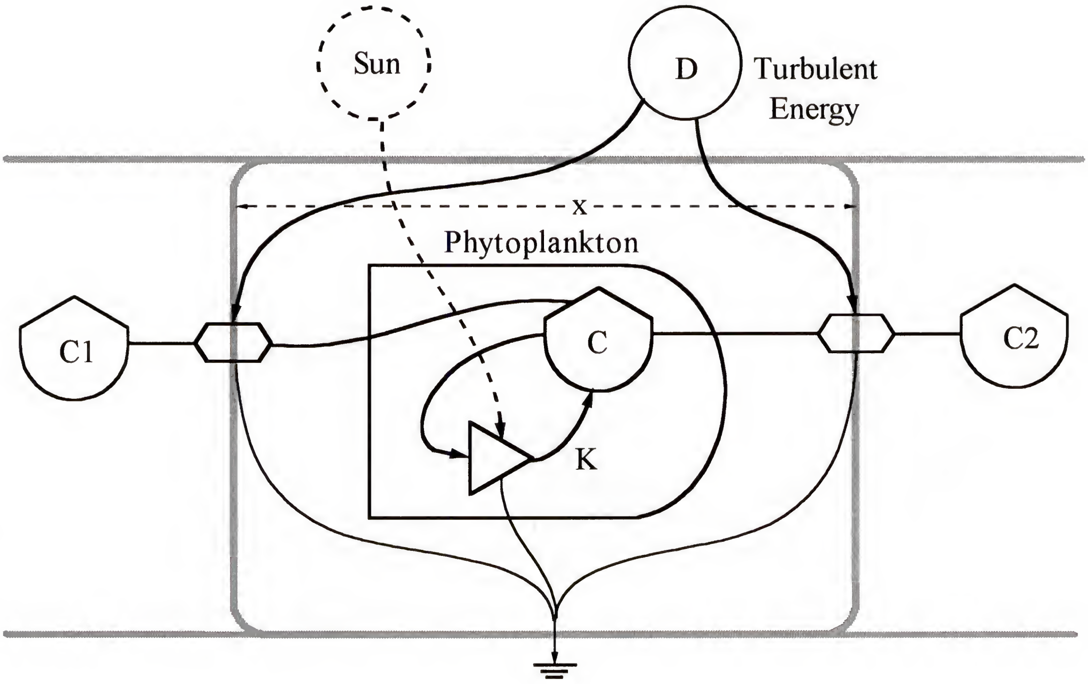

Author's Original Equations:

$\partial C/\partial t = D * (\partial^2 C / \partial x^2) + K*C$

where, C = phytoplankton population

D = eddy diffusivity

K = rate of growth per unit population

Figure 1-8. Energy systems language translation of the diffusion model of phytoplankton bloom by Kierstad and Slobodkin (1953). Dashed are inferred elements from the original equations. Author's original equations are shown below the diagram.

Gardner and Sullivan (1981) measured light scattering at 20 meters above the deep ocean bottom in the western North Atlantic and estimated concentrations of suspended particulate matter. Time series for 2.5 months showed rapid, pulsed variations in light scattering, indicating a high degree of activity near the sea floor. They interpreted two large peaks in their data as local benthic storms which punctuated variations in light scattering due to passage of a distally resuspended cloud of sediment, and related them to passing atmospheric storms.

Fishes and fisheries

Variations in fish populations have caught lots of attention and been recorded well, especially for commercially important species, because of economic activities associated with them. Much literature is devoted to variability in fish populations and fisheries (Gulland, 1977; Cushing, 1981 and 1982; Rothschild, 1986; Glantz, 1992). Time series graphs included in that literature shows pulses in fish stocks, recruitment, catches, and landings, with various frequencies and amplitudes. Rothschild (1986) discussed variability of fish-stock abundance and theories about fluctuations in fish abundance. Cushing (1982) and papers in Glantz (1992) discussed relationships between changes in fish populations and climate variability. Glantz (1992) also discussed potential implications for fisheries and societies of the regional impacts of a global warming of the atmosphere.

Russell (1973) summarized records of the occurrence of planktonic stages of fish off Plymouth, UK during the period of 1924-1972. Sustained low abundance of fish larvae after a sharp decrease in the 1930s was broken by a pulsed increase in the number of fish larvae since 1965. He suggested that higher survival of young fishes was due to the larger amount of zooplankton available as food.

Baumgartner et al. (1992) estimated biomass of Pacific sardines and northern anchovies from fish-scale deposited in sediments of the Santa Barbara Basin off southern California, over the past 1700 years. Time series of estimated biomass showed several different pulse frequencies and amplitudes. Spectral analysis of the scale deposition rate showed pulses at periods of 60, 100, and 680 years for anchovies, and at periods of 60 and 480 years for sardines.

Terrestrial Ecosystems

Organisms in terrestrial environments generally turn over slowly compared to their counterparts in aquatic environments, producing pulses with greater amplitude and longer intervals. Insect outbreaks and forest fires are examples that affect our daily lives. Even though observations in terrestrial ecosystems do not provide rich pulsing data as in long term plankton records, there have been plenty of records of pulsing dynamics in terrestrial ecosystems.

Pulsing in tropical environments

Bigger (1976) analyzed time series of tropical insect populations in tropical tree crops. He found strong annual oscillations in abundance with shorter or longer cycles superimposed, contrary to the long-believed constancy of tropical environments. Hemiptera showed fluctuations with a periodicity of 1 year and 9.2 weeks, cocoa mirids with 1 year and longer, and coffee leaf-miners with 1 and 2 years. He argued against the idea that stability produced by the great complexity of tropical ecosystems would damp out oscillations in populations.

Hydrologic pulses in wetlands

Hydroperiod, the seasonal pattern of the water level of a wetland, is a pulsing event that is a major determinant of wetland structure and function (Mitsch and Gosselink, 1993). In tidal wetlands such as salt marshes, pulses occur in daily or semi-daily scale by tides and in seasonal scale. Nontidal wetlands, such as inland marshes, floodplain, and swamp forests, experience seasonal and periodic pulses in hydroperiod.

Many studies have shown that there is an optimum hydrologic pulse to which wetland ecosystems adapt for maximum productivity. Productivity was highest when flooding was moderate in forested cypress swamps (Mitsch and Ewel, 1979; Conner and Day, 1982) and in coastal salt marshes (Odum et al., 1995). Mitsch et al. (1991) compared productivity of five forested wetland with different hydrologic regimes. Wetlands with pulsing hydroperiods showed highest productivity.

Fire pulses

Fire is an important ecological factor in forest and grassland regions of temperate zones and in tropical areas with a dry season (Odum, 1971). Once thought of as bad, fire pulses are an important limiting factor for productivity and species composition of those systems.

Species richness was maximum in areas which were burned approximately every 2 years in prescribed burning experiments over 20 years on oak forest and oak savanna (Tester, 1989). Intervals between fires ranged from 1 to 12 years. He suggested that the fire frequency of every 2 years would allow typical forest trees to persist and would increase prairie species.

Leach and Givnish (1996) found that prairie remnants in Wisconsin lost 6-26 % of the original plant species over a 32-52 year period after comparing census data in the 1980s with those in the 1940s and 1950s. They proposed fire suppression caused by landscape fragmentation as a mechanism for the pattern of species loss in those prairies.

Swetnam and Betancourt (1990) analyzed fire scars recorded in tree rings in the southwestern United States over 300 years from 1700 to 1900. Time series of the percentage of trees scarred showed a hierarchical distribution of fire intensity with more frequent small fires and less frequent big fires. They correlated their data with variation in the phase of the Southern Oscillation. They also concluded that climate would force fire regimes on a subcontinental scale, based on synchrony of fire-free and severe fire years across diverse forests.

Fir waves

In high-altitude fir forests, pulses of tree death induced by wind occur as crescent-shaped bands of standing dead trees, moving through the forests like waves (Sprugel and Bormann, 1981; Marchand, 1995). The waves move in the general direction of the prevailing wind and follow each other at intervals of about 60 years. A moving wave through the forests creates a gradient in forest development, in which mature forest precedes the wave, followed by a zone of dead trees with seedlings underneath, an area of very dense saplings, and a progressively older stand leading back to mature forest. Continuous bands of the gradients look like spatial representation of temporal pulsing in Figure 1-4b.

Sprugel and Bormann (1981) divided the gradient into three zones of death and regeneration, young and intermediate firs, and mature firs, and compared several ecosystem parameters between different zones. Soil nitrate showed the highest concentration in the zone of death and regeneration due to the increased decomposition rate. Living biomass increased as the forest developed to mature forest, while aboveground net primary productivity and living biomass accumulation were maximum in the zone of young and intermediate zones. Species richness and equitability were greatest in the zone of death and regeneration and were lowest in the zone of young and intermediate firs.

Spruce-budworm outbreaks

The spruce budworm ecosystem is one of the best-recorded terrestrial studies (see Morris, 1963). The spruce budworm is a defoliating lepidopteran insect that undergoes population outbreaks recurring at 30-70 year intervals and lasting from 12-15 years in any given area (Clark et al., 1978).

Swetnam and Lynch (1993) reconstructed the long-term history of western spruce budworm outbreaks in northern New Mexico, using tree ring chronologies. They found variable periodicity of 20 to 33 years in the regional outbreak record during the past three centuries. They hypothesized that the complex dynamics of budworms is the result of a combination of time lagged responses to external forces and inherent structural characterization of the forest-budworm system.

Terrestrial animals

Many published papers report pulsing oscillations in populations of animals – mammals, birds, insects, and so on. - on land. Oscillation of the snowshoe hare and the lynx is a classic example with a 9- to 10-year cycle (MacLulich, 1937; Elton and Nicholson, 1942). Elton and Nicholson's data showed several different frequencies and amplitudes in lynx fur returns. Also well-documented are the cycles of the lemming, arctic fox, and the snowy owl in the tundra (Elton, 1942). Populations of lemmings pulsed every 3 or 4 years, and foxes and owls followed the pattern of their prey, the lemmings.

Weather and Climate Pulses

There are pulsed transformations of energy in weather phenomena on several scales, such as thunderstorms, tornadoes, tropical storms, hurricanes, and El Nino. These may be disasters to smaller scale units in a forest, a town, or city. But, from a larger systems view, these pulses appear to be a necessary part of systems organization. For example, hurricanes redistribute solar energy absorbed by earth, from tropics to polar regions. El Nino pulses once every 2 to 10 years reflect global weather changes.

Simpson and Riehl (1981) related recurrence interval and strength of hurricanes in which stronger hurricanes were less frequent. Wiegel (1964) plotted frequency of high water at the Hook of Holland that showed a decrease in frequency with increase in storm water level.

Climate pulses in geologic history

Climatic records preserved in ice and sediments have shown a hierarchy of climatic pulses in the past. Glacial cycles which have time scales of $10^4 - 10^5$ years have been attributed to periodic changes in solar irradiation caused by variation of the earth's orbital parameters (Hays, et al., 1976; Berger, 1988; Imbrie et al., 1993; Thompson et al., 1997).

Climatic pulses on the time scale of 10^3 years have also been found in ice cores (Dansgaard et al., 1982) and in sediment cores (Behl and Kenett, 1996; Bond et al., 1997; Heusser and Sirocko, 1997). Fluctuations in climate on this time scale are too frequent to be explained by the earth's orbital variation. Broecker et al. (1990) and Broecker (1997) suggested reorganization of the ocean's large-scale thermohaline circulation as a mechanism for pulses on the millenial time scale.

After reviewing climate proxy data, Stocker and Mysak (1992) found century-scale climatic pulses (50-400 years), and suggested that those pulses reflect natural variability in the ocean's thermohaline circulation. Thompson et al. (1997) found pulses in oxygen isotopes, dust, NH_4^+, and NO_3^- levels in ice cores from China with an average period of 200 years and others of 19,000 years.

Geologic Episodes

Volcanoes, and earthquakes with their destructive sea waves have been recorded in human history as major disasters. Even though these are disasters from the human perspective of scales, these phenomena may be the way for larger systems to circulate materials and energy in a geochemical aspect, globally or regionally.

Earthquakes result from pulsed release of strain accumulated along faults (Press, 1975; Press and Siever, 1994). Steady motion of plates along faults slowly accumulates strain over time. Friction between plates prevents slip until strain builds up to some critical level, after which strain is suddenly released, causing earthquakes. There is a cycle of slow accumulation of strain and its pulsed release in earthquakes.

Denham (1979) plotted magnitude of earthquakes in California and Australia as a function of return interval. The graph showed that more time is required between bigger earthquakes. Johnston (1981), Okamoto (1984), and McClelland et al. (1989) showed that the bigger the earthquakes the less frequent they are, by plotting number of earthquakes as a function of magnitude of earthquakes. Wiegel (1964) plotted the probability of tsunami at Hilo, Hawaii finding the typical relationship of pulse amplitude and frequency.

Raleigh et al (1982) proposed an idealized model for the cycle of repeating earthquakes along a plate boundary. Over most of the 50- to 500-year interval between great earthquakes, there is slow buildup of strain and little seismic activity. Frequent moderate-sized earthquakes occur just before great earthquakes that release the accumulated shear stress. Declining aftershocks follow for several years.

Periodic volcanic eruptions consume molten rock stored in magma chambers. McClelland et al. (1989) plotted frequency of volcanic eruptions as a function of volcanic explosivity. The number of eruptions decreased as volcanic explosivity increased.

Economic Fluctuations

Stock market indices fluctuate rapidly. Historical records of the Dow Jones averages show stock market pulses ranging from daily fluctuations to major stock market crashes such as those in 1929 and 1987. The Dow Jones averages have been increasing over time (Pierce, 1991).

Economic fluctuations, also called business cycles, have been observed in all economies. A business cycle includes a period of declining aggregate economic activity (a recession) followed by a period of rising economic activity (a boom) (Abel and Bernanke, 1995). Economic expansion is periodically interrupted by episodes of declining production, income, spending and rising unemployment. Abel and Bernanke define that the business cycle is not periodic, implying that it does not occur at regular, predictable intervals and does not last for a fixed or predetermined length of time. Business oscillations are irregular, but recurrent. Frequently, the major industrial economies undergo recessions and expansions at about the same time, indicating coupling on a large scale.

Economic activities also have regular seasonal patterns which fluctuate more frequently (Franses, 1996; Miron, 1996). Seasonal cycles can be considered as noise when viewed from the scale of business cycles. Fluctuations in economic activities with longer periods than the business cycles are called long waves (Kondratief cycles), alternating phases of rapid expansion and stagnation in the world economy, with about fifty years per cycle (Goldstein, 1988; Berry, 1991). Slow accumulation of infrastructure and its replacement produce Kondratief cycles. Modelski (1987) related long waves to cycles of war and world leadership. In summary, economic studies show economic systems pulsing on many scales.

Pulses of Organic Evolution

Current patterns of life, such as the number of species and their distributions on earth, are results of evolutionary events that have occurred throughout earth history. Organisms that survived those events have shaped the surface of earth. Geologic records have shown pulses of appearances and disappearances of organisms.

Extinction

Simpson (1952) estimated that up to 4 billion species of plants and animals have lived at some time in the geologic past, most of these in the last 600 million years. Only a few million species are living today on earth (Raup, 1986). This indicates that extinction has been an ongoing process of organic evolution. Small and large extinction events were used by 19th century geologists to define the geologic time scale.

Climate change (Crowley and North, 1988), change in sea level (Hallam, 1987a), global volcanism (Hallam, 1987b), and extraterrestrial impact (Alvarez et al., 1980) have been suggested as causes of the extinction events. Raup (1991 and 1994) viewed extinction events as a major restructuring mechanism of the biosphere, providing space for evolutionary innovations. He also discussed randomness and selectivity of extinctions.

Raup (1986) argued that "extinction may be episodic at all scales with relatively long periods of stability alternating with short lived extinction events," based on the survivorship curves of marine animals. Raup (1991) showed the hierarchy in extinction pulses using a cumulative distribution of extinction frequency (or kill curve) and a histogram of extinction intensity for fossil genera; that is, the larger the event, the rarer it is. Raup and Sepkoski (1984 and 1986) proposed 26-million-year periodicity in major extinctions over the last 250 million years of the earth history, based on the analysis of variation in extinction intensity for fossil families and genera of marine animals.

Speciation

Punctuated equilibrium proposed by Eldredge and Gould (1972) has provided another way to look at the fossil records. In a Darwinian perspective, new species arise from the slow and steady transformation of entire populations, referred to as phyletic gradualism by Eldredge and Gould. Pulses in the fossil records had been ascribed to the imperfection of those records. In punctuated equilibrium, Eldredge and Gould argued that species tend to persist unchanged for millions of years before abruptly giving rise to new species, instead of evolving gradually. They suggested that the geographic isolation of a small population of one species for tens or hundreds of thousands of years could produce geologically instantaneous speciation when the isolation broke down and the new species spread into the rest of the world.

Elena et al. (1996) observed a punctuated pattern in the evolution of bacterial cell size in their experiment with Escherichia coli. They found that bacterial cells stayed at one average size for many generations and suddenly increased in their average size within a few generations. They argued that this punctuated pattern in change in the cell size was caused by natural selection of rare, beneficial mutations sweeping successively through the evolving population.

From the perspective of population genetics, Carson (1975 and 1982) proposed more frequent pulses of speciation. He argued that even the shortest punctuation in Gould and Eldridge (1977) would be sufficient for a speciation cycle to occur. Carson suggested two different systems of genetic variability in diploid species. The open system consists of genes which recombine freely without major viability effects, and may vary within species. The closed system consists of blocks of genes which form coadapted and internally balanced gene complexes. The closed system varies between but not within species.

Carson's speciation hypothesis requires some type of destructive events, such as a flush-crash cycle in a population, to disorganize the closed system of genetic variability. The disorganizing events could be accomplished in a relatively small number of generations. Natural selection operating on the perturbed genetic system may result in a new species with a new coadapted closed system.

Vrba (1985, 1993, and 1995) extended Gould and Eldredge's punctuated equilibrium and proposed the turnover pulse hypothesis. Vrba used turnover to refer to the actual appearances and disappearances of taxa from particular areas in the real world through speciation, extinction, and migration. The hypothesis holds that species tend to remain stable until the physical environments change. Pulsed changes in the physical environments, such as global climatic and tectonic changes, trigger pulses in lineage turnover, varying from minute to massive in scale across disparate groups of organisms. She suggested bovids and hominids as a testing ground for the turnover pulse hypothesis. Vrba (1995) also emphasized the importance of biotic interactions in influencing the nature of turnover. She suggested a hierarchically nested pattern of turnover pulses which reflects the pattern in the physical environments.

A similar idea to Vrba's turnover pulse hypothesis was introduced by Brett and Baird (1992) as coordinated stasis. They used coordinated stasis to represent an empirical pattern found in the fossil record showing apparent evolutionary and ecological stability separated by abrupt pulses of faunal change. Stable periods which lasted several million years were characterized by a high degree of persistence in taxonomic composition, morphology, and ecological structure. These extended periods of stability were punctuated by rapid and synchronous turnover of a large proportion of the fauna, resulting from high rates of speciation, extinction, and immigration, within a small fraction (10% or less) of stable periods. Brett et al. (1996) gave an overview of coordinated stasis. Ivany (1996) classified and discussed potential mechanisms, intrinsic and extrinsic, which could generate the pattern of coordinated stasis.

Previous Simulation Studies of Pulsing

This section summarizes some models which showed pulsing patterns in their simulation results, concentrating mainly on ecological models. Recent interest in non-equilibrium dynamics and improvement in computing power have produced many simulation models with pulsing patterns in their results, whether modelers had those in mind or not. The review is separated into two parts; review on models developed using energy systems language and review on those that were not constructed using the language. Models in the energy systems language provided the basic configuration of pulsing models which will be developed in this dissertation. Models not in the energy systems language were translated into energy systems diagrams using original equations and descriptions on the models, to clearly show kinetics and energetics of the models, where possible.

Energy Systems Models

In his study of order-disorder by environmental catastrophes, Alexander (1978) found that a producer-consumer model with linear and nonlinear consumption pathways could pulse by a self-induced mechanism without requiring any outside pulsing sources or switches. Simulation results showed the same frequency for both storages of producer and consumer. In his model (Figure 1-9), the producer builds up slowly into an ordered state using an unlimited energy source and dispersed material in a disordered state. The consumer grows slowly by a linear pathway until the producer storage reaches a critical point, which triggers a shift in consumption to a nonlinear autocatalytic pathway. Self-induced pulsing recycles material for the system to start the cycle again. Materials are conserved in this system.

Based on the simulation results of his basic order-disorder model, Alexander (1978) also suggested that pulsing could maximize power by recycling the material stored in the system to stimulate regrowth again. His simulation results showed more integrated production over the simulation time period for the pulsed order-disorder model. But, this result could be different depending on the calibration conditions.

Alexander (1978) constructed a simple two-storage model of production and recycle to test whether pulsing dynamics would maximize power inflow to systems. In his model, there was no limit in external energy supply. The pulsing mechanism in the model reset the activated storage to the predetermined low level at a given time interval, returning material to the dispersed material storage. Integrated production over time, as a measure of power inflow to the system, was greater in the pulsed model than in the model without pulse.

Kemp and Mitsch (1979) developed a model to investigate the effect of physical turbulence in an aquatic ecosystem on the coexistence of phytoplankton species competing for the same resources. Their simulation showed that more species coexisted with the

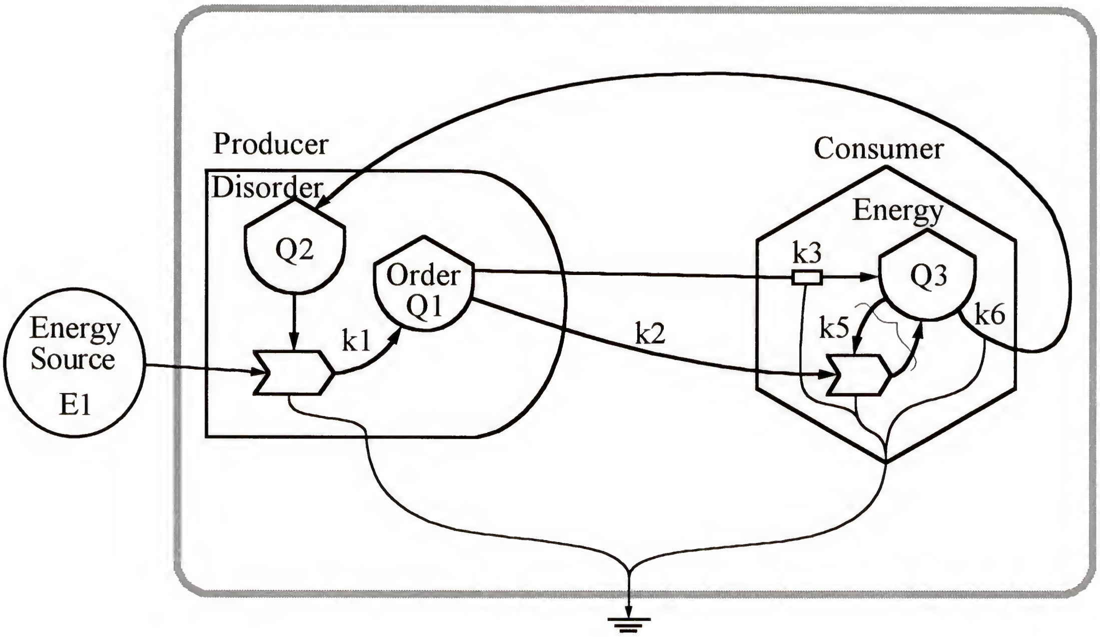

dQ1 = k1*E1*Q2 - k2*Q1*Q3 - k3*Q1
dQ2 = Qt - Q1
dQ3 = k5*Q1*Q3 + k3*Q1 - k6*Q3

Figure 1-9. Order-Disorder model of environmental catastrophes with self-generated pulses (redrawn after Alexander, 1978). Author's original equations are shown below the diagram.

addition of a random turbulent component to the model. All species coexisted when the frequency of turbulence approached the metabolic turnover rates of phytoplankton in the model.

Richardson and Odum (1981) studied the energetic properties of the pulsing model similar to Alexander (1978) (Figure 1-10). The energy source of their model was flow limited, which is appropriate for sources like sunlight. They included one more storage of stored production between producer and consumer which is used by the consumer with linear and quadratic autocatalytic consumption pathways. Material was also conserved in this model.

Richardson and Odum (1981) found that pulsing dynamics occurs in the intermediate range of energy input and material concentration in the system. Their simulation also showed an optimum frequency for maximum power over a part of the range of coefficients. Model behaviors were controlled by energy level, material concentration, and turnover times of components in the model. When calibrated with biomass, soils, and woods, this model pulsed with a frequency of 200 – 300 years.

Odum (1982 and 1987) used a variation of Alexander's model (1978) in which the autocatalytic consumption pathway was replaced by quadratic autocatalytic consumption, to simulate world production and pulsing consumption (Figure 1-11). The simulation resulted in a pulsing pattern with a frequency of about one million years when it was calibrated for world fuel reserves and economic assets. The model generated more frequent pulses with calibration for soil and wood biomass storages of the landscape. He proposed that the model with more frequent pulses is appropriate for human civilizations, such as Mayan culture, mainly supported by photosynthetic products. He also provided pulsing models with external threshold control of pulsing (Odum, 1982) and with an internal threshold switch (Odum, 1987).

Campbell (1984) used wave filter concepts to investigate how ecosystems organize their structure and function to absorb external energy inputs to the system. He found that

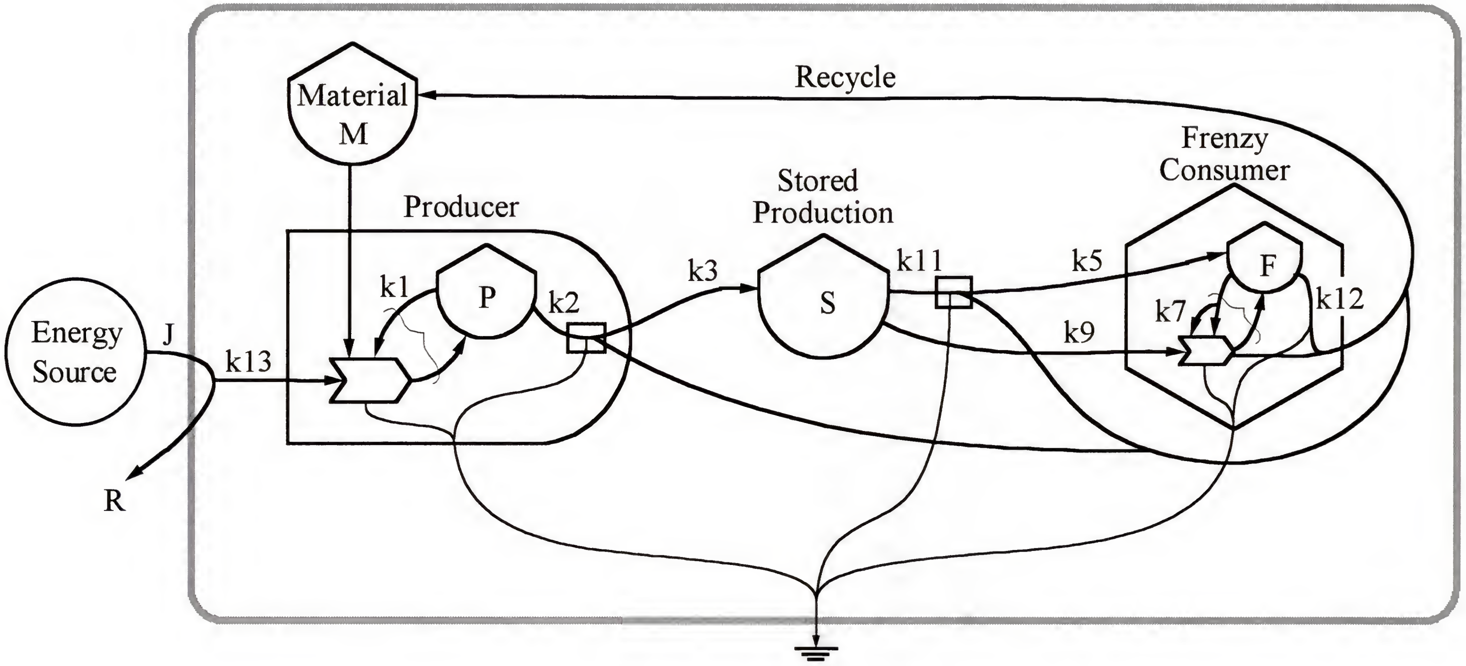

$R = J - k13*M*P*R$

$dP = k1*M*P*R - k2*P$

$dF = k5*S + k7*S*F*F - k12*F$

$M = T - P - S$

$dS = k3*P - k11*S - k9*S*F*F$

Figure 1-10. Pulsing production minimodel with the quadratic consumption of stored production (redrawn after Richardson and Odum, 1981). Author's original equations are shown below the diagram.

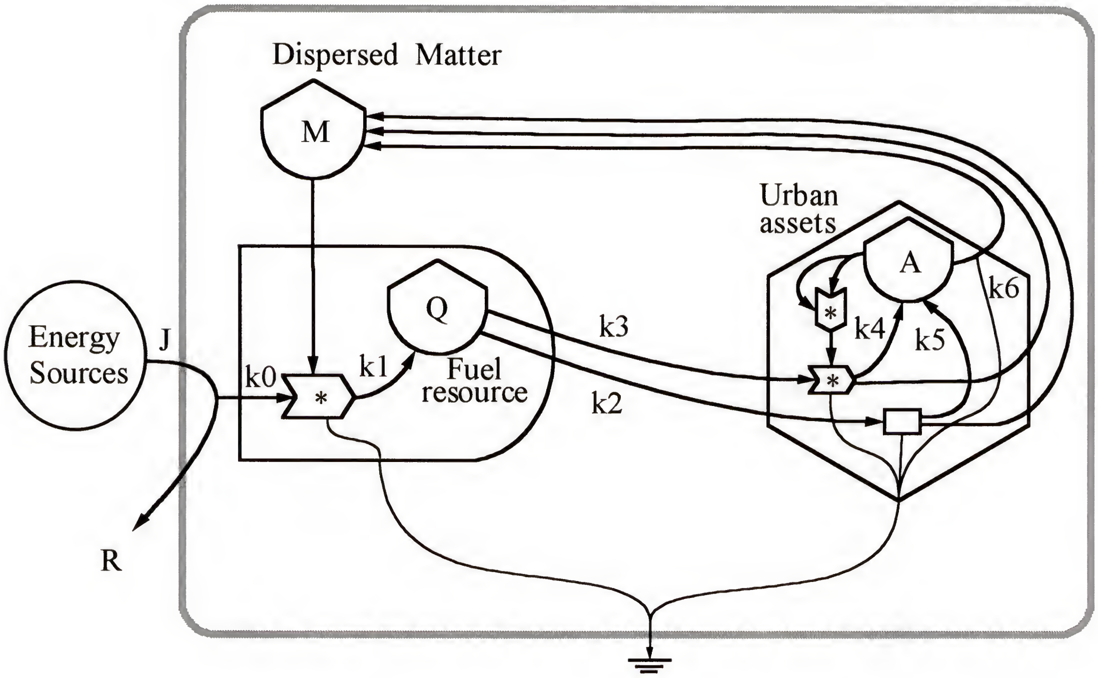

R = J / (1 + k0*M)
M = K - k7*Q
dQ = k1*R*M - k2*Q - k3*Q*A*A
dA = k4*Q*A*A + k5*Q - k6*A

Figure 1-11. Production-consumption minimodel of the modern civilization supported by fossil fuels with quadratic pulsing mechanisms (redrawn after Odum, 1982 and 1987). Author's original equations are shown below the diagram.

systems used the most power when the turnover of the receiving components in the system was matched with the input frequencies of the external energy. Power production and use were greatest when the input frequencies were similar to the frequencies of natural oscillation of the system produced by the interaction of components.

Zwick (1985) studied ecosystem configurations with inertial elements and oscillators using general systems models. Energy selectivity produced by inertial oscillators increased competitive ability of components in the system and system diversity, and maximized system power by allocating input energy among various subsystems. The greatest power input and transfer was obtained when the frequency of internal oscillations by autocatalytic inertial oscillators was the same as that of the primary energy source, as in Campbell (1984).

Energetic properties of the pulsing model by Odum and Richardson (1981) were further investigated by Richardson (1988). Material storage was simulated with its own rate equations, compared to that in Richardson and Odum (1981) which was the difference between total material in the system and material tied up in the producer and consumer storages. Calibrated with data from a tropical forest ecosystem, the model pulsed at a frequency of about 325 years. As in the previous model (Richardson and Odum, 1981), there was a medium range of energy level which produced pulsing dynamics, and within this range pulsing frequency increased with increase in energy level. A push-pull model of physical energy pulses by Odum et al. (1995) also showed that optimum levels of pulsed physical energy increased gross production and made net production greater than removal.

The model also pulsed more frequently, with the amplitude decreasing as the turnover time of the consumer increased within some range. Using this result, he argued that there is a window of size of the consumer for the system to pulse. After adding one more consumer with linear and quadratic autocatalytic pathways, Richardson (1988) investigated the effect of turnover time of the added higher level consumer. Percent power used by the system was decreased as the turnover time of the higher consumer increased. Because of higher level consumption, lower level consumption was less and nutrients were tied up in stored production.

Richardson (1988) used his pulsing model to simulate spatial pattern formation in ecosystems, and found various spatial pulsing patterns depending on input energy patterns, connectivity between individual cells, and the level of hierarchy of intercell connections.

Odum and Munroe (1993) simulated variations in animal populations and ecosystem processes in a tropical lagoon in southwestern Puerto Rico. Both aggregated and complex models showed pulsing oscillations of production and consumption. Even though their models included several outside inputs, internal prey-predator type oscillations between animal consumers controlled the overall pulsing dynamics of the system. In this situation, pulsing frequencies were determined by turnover times of prey-predator pairs.

By connecting two prey-predator oscillators with different turnover times, Beyers and Odum (1993) obtained a chaotic pulsing pattern. Pulsing oscillations of the prey-predator pair at a lower level were controlled by the slower oscillating pair higher in the hierarchy.

Odum (1997) constructed a pulsing simulation model of global diversity. In the model, the production units were divided into pioneer and support units. Both production units were used through the linear pathway to support information and diversity, and the support units provided energy for the quadratic autocatalytic transformation. By increasing efficiency of diversity generation by the quadratic autocatalytic pathway, he obtained pulsing dynamics for the global diversity model.

Using a flow limited energy source, McGrane (1998) further investigated the production-recycle model by Alexander (1978). He showed that power inflow to the system depended on the level of the activated storage. Maximum power inflow was achieved when 50% of total material was in the activated storage and the remaining 50%

in the dispersed material storage. The effect of pulsing on the system depended on the pre-pulse value of the activated storage. When the pre-pulse value of the storage was greater than 50% of total material, pulsing increased power inflow. Pulsing decreased power inflow when the pre-pulse of the storage was less than 50% of total material. Based on this finding, he suggested that any mechanism that makes the system operate closer to 50% of material in the activated storage would maximize power inflow. His simulation results showed that the effects of pulsing on power inflow depended on the value of the activated storage at steady state.

Other Models

Chaotic dynamics

Hastings and Powell (1991) investigated dynamics of a theoretical three species food chain model (Figure 1-12). They used nonlinear, Holling type-II functional response to represent the interaction between prey and predator species, in which the consumption rate of the predator species saturates when the prey abundance is high. Using biologically reasonable parameters, they obtained chaotic dynamic results which can not be seen in two species time models. Based on the results, they argued that chaotic dynamics might be common in natural food webs. The simulation result of Hastings and Powell (1991) showed two different pulsing frequencies. The pair of the first two species oscillated at two frequencies. More frequent pulses were generated by the prey-predator pair, and these were controlled by the slower pulsing pair of the second and third trophic levels.

In the energy systems diagram of Hastings and Powell's model (Figure 1-12), three species were connected through two pairs of prey-predator relationships. They used a logistic growth equation for the first level producer species and type-II saturating functional response for both consumer species. An unlimited energy source was implicit in their model and included in the energy systems diagram.

Figure 1-12. Energy systems language translation of the three species food chain model by Hastings and Powell (1991). Dashed are inferred elements from the original equations. Author's original equaitons were used in this translation, instead of their nondimensionalized forms.

Author's original equations:

$$\begin{aligned}
dX/dT &= R_oX(1 - X/K_o) - c_1F_1(X)Y \\
dY/dT &= F_1(X)Y - F_2(Y)Z - D_1Y \\
dZ/dT &= c_2F_2(Y)Z - D_2Z
\end{aligned}$$

where, $F_i(U) = A_i{*}U/(B_i + U)$

R_o = intrinsic growth rate of species X

K_o = carrying capacity of species X

c_1^{-1} and c_2 = conversion rates of prey to predator for species Y and Z, respectively

A_i = maximum predation rate per unit prey

B_i = prey population level where the predation rate per unit prey is half its maximum

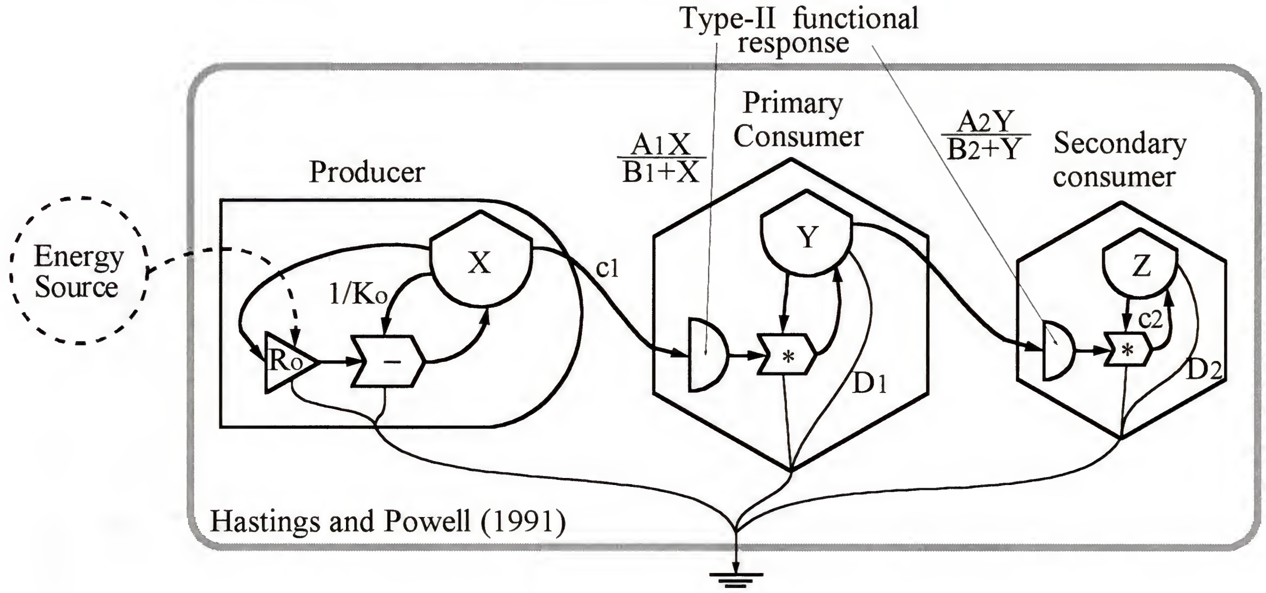
Type-II functional response
Energy Source
Producer
1/Ko
Ro
–
X
c1
A1X / B1+X
Primary Consumer
Y
*
D1
A2Y / B2+Y
Secondary consumer
Z
c2
*
D2
Hastings and Powell (1991)

Abrams and Roth (1994) further investigated the Hastings and Powell model with different parameterization of both consumer species. The simulation showed that the mean density of top trophic level species increases with increase in carrying capacity of the bottom level species (i.e. increase in energy input to the system), but eventually decreases as carrying capacity is further increased. Their results showed two different pulsing frequencies for some parameter values. Top level species went extinct in some cases when carrying capacity of the bottom species was sufficiently increased. The model system showed more complex dynamics, including chaos, at intermediate carrying capacities of the bottom level species. Using these results, they argued that nutrient enrichment of a system could endanger the existence of the top level species.

Camilo and Willig (1995) also obtained pulsing with the same type of three species food chain model (Figure 1-13) used by Hastings and Powell (1991). They modified the equations to reflect the observed food chains of an arthropod-dominated lotic community. They made two models to investigate the effects of omnivory on the dynamics of each trophic level and on the stability and persistence of food chains. Without omnivory, primary and secondary consumers showed typical prey-predator type oscillations. The oscillation pattern was modified by the tertiary consumer with a somewhat different pulsing frequency.

The diagram (Figure 1-13) shows somewhat strange dynamics of consumer growth in the original equations in which type-II functional response of each consumer is a function of each consumer itself, not a function of prey.

Hanski et al. (1993) and Hanski and Korpimaki (1995) used a prey-predator model (Figure 1-14) to investigate hypotheses on the microtine rodents' cycle in boreal and arctic regions. They analyzed real data using nonlinear time series analysis and compared them with the simulation results. In their model, both rodents and their mustelid predators have logistic growth form, and a type-II functional response was used to model interaction

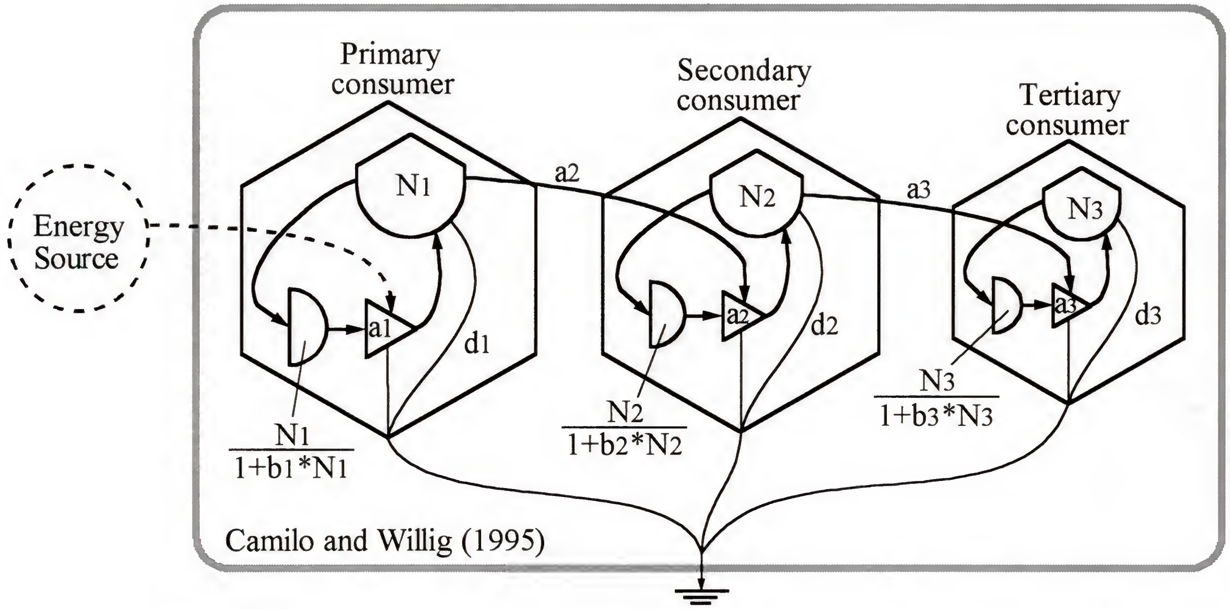

Original Equations:

$dN_i/dt = a_iN_i/(1 + b_iN_i) - a_{i+1}N_{i+1}/(1 + b_{i+1}N_{i+1}) - d_iN_i$

where, N_i = relative density

a_i = consumption rate of a species at i-th consumer trophic level (i = 1,3)

b_i = growth rate; d_i = death rate

Figure 1-13. Energy systems language translation of the food chain model without omnivory of an arthropod-dominated lotic community by Camilo and Willig (1995). Dashed lines are inferred elements. Author's original equations are shown below the diagram.

Figure 1-14. Energy systems language translation of the boreal rodents' cycle model of Hanski et al. (1993) and Hanski and Korpimaki (1995). Dashed are inferred components from the original equations by the authors. Author's equations are shown below.

1) Summer season
Prey: $dN/dt = rN(1 - N/K) - cPN/(N+D)$
Predator: $N > Ncrit$, $dP/dt = vP(1- qP/N)$
$N < Ncrit$, $dP/dt = -d_{high}*P$

2) Winter season
Prey: $dN/dt = r'N(1 - N/K') - cPN/(D+N)$
Predator: $N > Ncrit$, $dP/dt = -d_{low}*P$
$N < Ncrit$, $dP/dt = -d_{high}*P$

N = prey density (number of individuals / ha)
Ncrit = critical minimum prey density for predator reproduction
P = predator density (number of individuals / ha)
r and K = intrinsic growth rate and carrying capacity of prey in summer
r' and K' = intrinsic growth rate and carrying capacity of prey in winter
v and N/q = intrinsic growth rate and carrying capacity of predator
c = maximum per capita predation rate
D = predation half-saturation constant
d = death rate of predator
q = equilibrium prey/predator ratio

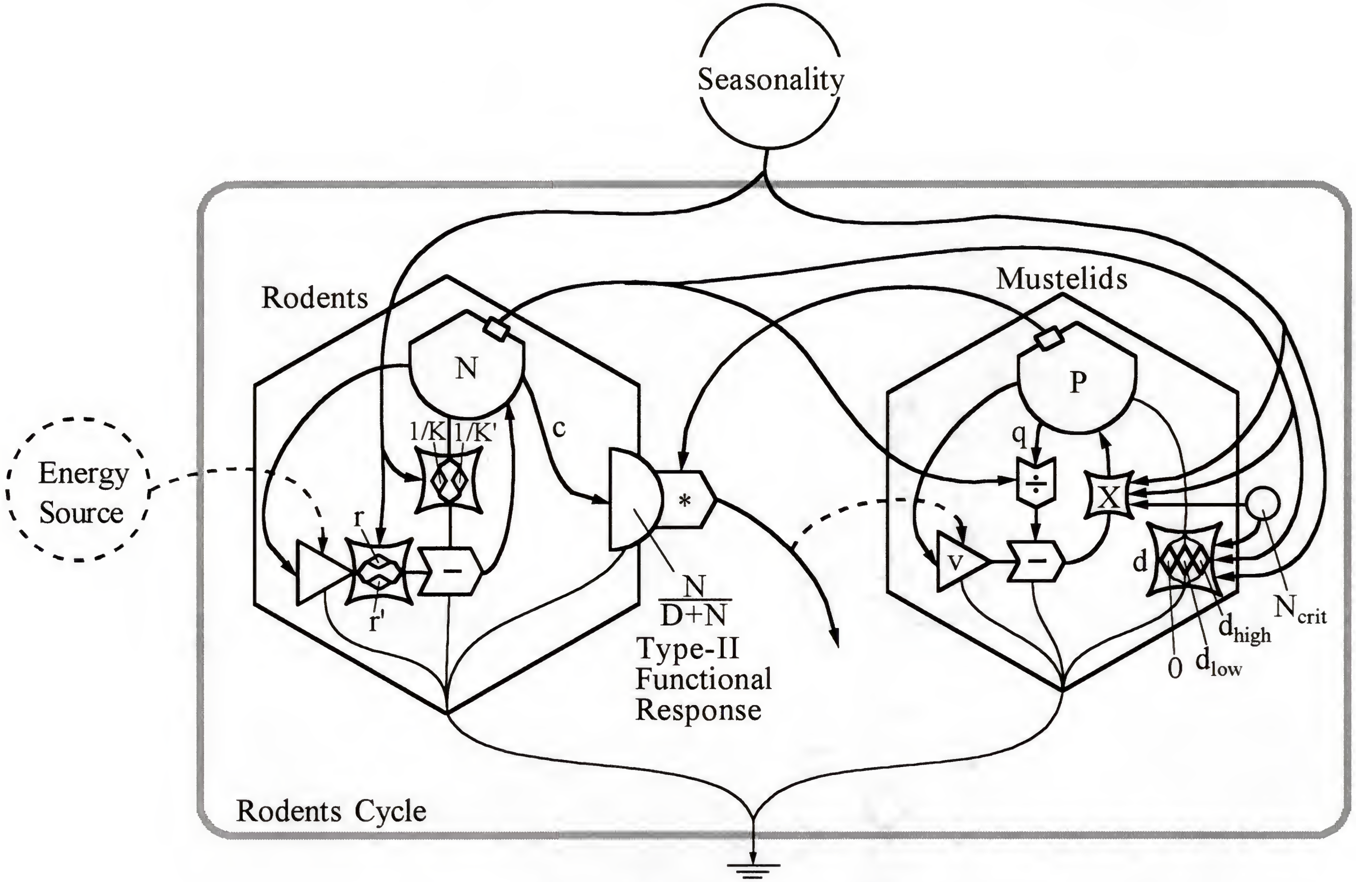

$$dN = r*N*(1-1/K*N) - c*P*N/(D+N)$$
$$dP = X*v*P*(1-q/N*P) - d*P$$

between prey and predator. They included seasonality in the model to reflect a strong influence of seasons on the dynamics of mammals in boreal and arctic regions.

Calibrated with field data, simulation reproduced the observed dynamics of rodents and mustelids, which were chaotic. The results also showed seasonal frequencies in rodent oscillations as well as multiannual oscillations. They suggested that the multiannual oscillations of rodents are due to delayed density dependence imposed by their mustelid predators.

An unlimited outside energy source was implied. The original equations did not represent constraining energy limits. Growth of the mustelid predator was not a function of the amount of prey consumed which was modeled using type-II functional response. Rather the growth rate of the predator was determined by the carrying capacity (N/q) proportional to the number of prey (N) present in the model.

Microbial food web

Many studies in last decades have proved that phototrophic and heterotrophic microorganisms play a major role in material cycling and energy transfer of plankton ecosystems (Azam et al., 1983; Azam and Cho, 1987; Fenchel, 1988).

Eldridge and Sieracki (1993) simulated the dynamics of the microbial food web in a periodically mixed estuary (Figure 1-15). The stratification and destratification cycle induced by spring-neap tide was a major forcing function in their model. Stratification affected light availability to primary producers in the surface mixed layer by changing the mixed layer depth during the cycle. The model included feedback functions and prey preference terms. Two different feedbacks by resources (fb_{ij}) and their recipients (fb_{j}) controlled material and energy flows between resource-recipient pairs. Using a sine wave representing the stratification and destratification cycle, the simulation results represented the 28 days of pulsing periodicity in the observed data of cyanobacteria and heterotrophic bacteria.

Figure 1-15. Energy systems language translation of the microbial food web model by Eldridge and Sieracki (1993). Dashed lines are components inferred from the original equations and the description of the model. Author's original equations are shown below.

$\delta s = 5*\sin(2\pi t/28)$; $h = \exp(3.0666 - 0.6064*\delta s^{0.6528})$; $D_i = (m - h')*(X_i - Xb_i)/h,\ h' > 0$
$fb_{ij} = 1 - (X_i - G_{ij})/(A_{ij} - G_{ij})$; $fb_j = (X_j - A_j)/(G_j - A_j)$; $TF_{ij} = 1 - (1 - fb_{ij})*[1 - fb_j*(1 - C_j)]$
$I_m = I_o*[1 - \exp(-kh)]/kh$; $P_2 = \mu max_2*X2*(1 - TF_{12})$
$p'_{i4} = p_{i4}*(1 - fb_{i4})/[p_{24}*(1 - fb_{24}) + p_{34}*(1 - fb_{34})]$

$dX1/dt = te_3*X3 + 10*te_3*X3 + Ex_4(?) - \mu max_2*X2*(1 - TF_{12})$
$dX2/dt = P_2 - (tr_2*X2*fb_2 + 0.3*P_2) - p'_{24}*\mu max_4*X4*(1 - TF_{24}) - D_2$
$dX3/dt = \mu max_3*\tanh(\alpha*I_m/\mu max_3)*X3*(1 - fb_3) - p'_{34}*\mu max_4*X4*(1 - TF_{34}) - te_3*X3 - D_3$
$dX4/dt = p'_{24}*\mu max_4*X4*(1 - TF_{24}) + p'_{34}*\mu max_4*X4*(1 - TF_{34}) - R_4 - G_4 - D_4$

δs = stratification/destratification cycle driven by tide; h = mixed layer depth; $h' = dh/dt$
D_i = biomass change due to advective and diffusive mixing ($i = 2,4$); m = diffusive mixing
X_i and Xb_i = biomass of surface mixed and bottom water ($i = 2,4$), respectively
fb_{ij}, fb_j, and TF_{ij} = resource-controlled, recipient-controlled, and combined feedback functions, respectively
G_{ij} = resource density below which the resource is not available as a food source (i.e. refuge level)
A_{ij} = resource density below which uptake by the recipient is limited
A_j = recipient density above which uptake of a resource is less than maximum (i.e. crowding)
G_j = maximim recipient density that a population can maintain when other resources are not limiting
C_j = metabolic correction factor; tr_2 = specific rate of respiration of bacteria
I_o and I_m = incident light and average light in the surface mixed layer, respectively
α = initial slope of production vs irradiation curve; k = attenuation coefficient
p_{i4} and p'_{i4} = assigned and weighted feeding preference term ($i = 2,3$), respectively
μmax = maximum growth rate; te_3 = specific excretion rate of dissolived organic carbon be cyanobacteria
Ex_4 = excretion rate of dissolved organic carbon by heterotrophic nanoplankton
R_4 and G_4 = rate of respiration and predation loss of heterotrophic nanoplankton, respectively

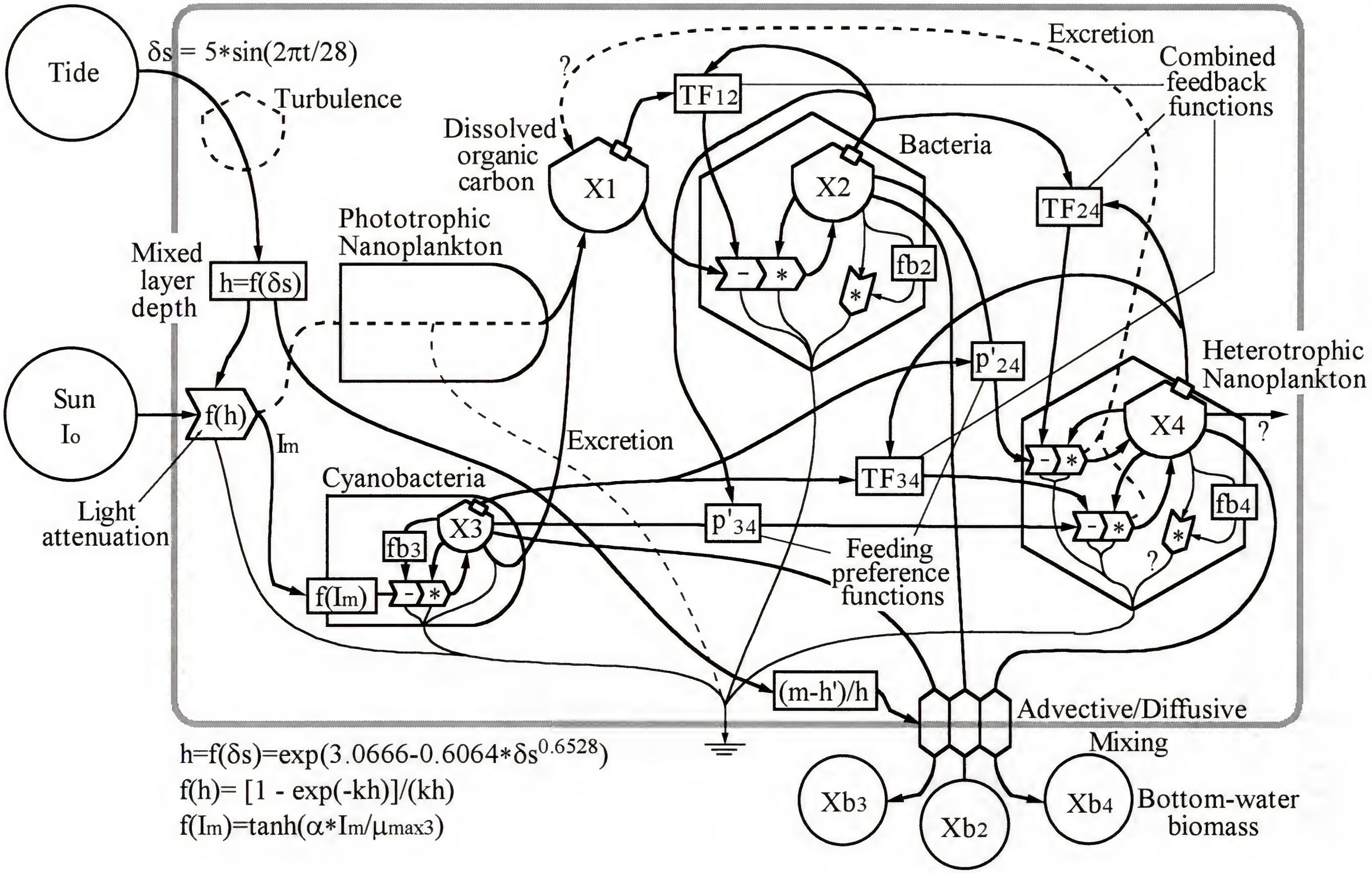

$h=f(\delta s)=\exp(3.0666-0.6064*\delta s^{0.6528})$

$f(h)= [1 - \exp(-kh)]/(kh)$

$f(I_m)=\tanh(\alpha*I_m/\mu_{max3})$

Increased mixed layer depth (h) during destratification reduces average light (Im) in the surface mixed layer, and during stratification period average light increases, stimulating primary production. Heterotrophic bacteria were closely related to the stratification and destratification cycle through fast consumption of dissolved organic carbon (DOC) released by primary producers.

The combined functions of two feedbacks by resources (fb_{ij}) and their recipients (fb_j) in the original equations cause the growth rates of each biological component to dampen in response to increased food. These density dependent feedback functions dampened oscillations of heterotrophic nanoplankton, stabilizing storage. Even though there was no clear periodicity which could be seen in other biological components, the observed variations of heterotrophic nanoplankton were not reproduced in the simulation. Production function in the energy systems diagram shows that the equations include feedbacks in the resource-recipient (prey-predator) pair. Thus, the special feedback functions may be redundant.

Deep-sea bottom ecosystem

Using the STELLA II program, Rowe (1996) simulated and compared responses of three different benthic ecosystems to pulses of organic material (detritus) added to food-limited environments (Figure 1-16). He developed and calibrated his models using published data on benthic ecosystems of the continental shelf of the western Gulf of Mexico, deep-sea bottom below the central gyre of the central North Pacific, and northeast Greenland polynya. Organic material pulses were modeled with a positive sine function in all three models. Simulation showed pulsing oscillations in all three ecosystems. Fluxes and standing stock varied in ranges approximately equal to the standard deviations of the observed data.

Rowe's simulation showed that components in the North Pacific model did not respond to organic material pulses from the surface layer on a seasonal basis, but

Figure 1-16. Energy systems language translation of the models by Rowe (1996) on systems in food limited environments. Original equations are the same as the equations from the systems diagram in which long names for the coefficients and storages are replaced by more abbreviated ones.

a) Deep sea bottom of the North Pacific central gyre

$P = 10*\sin(\pi*t)/182.5 + 1$

$dD = P - k1*H$

$dH = k1*H - k2*H - k3*H*M$

$dM = k3*H*M - k4*M - k5*M$

b) Greenland Polynya

$P = 100*\sin(\pi*t)/182.5 + 10$

$dD = P + k5*D*Me + k5*D*B + k8*Me*Ma + k9*D*Ma$
$+ k12*Ma*Mg - k1*D*Me - k2*D*Ma - k3*D*B$

$dB = k3*D*B - k1*B*Me - k4*B$

$dMe = k1*D*Me + k1*B*Me - k6*Me - k7*Me*Ma$

$dMa = k2*D*Ma + k7*Me*Ma -k10*Ma - k11*Ma*Mg$

$dMg = k11*Ma*Mg - k13*Mg$

c) Benthic system of the Gulf of Mexico

$P = 250*\sin(\pi*t)/182.5 + 50$

$dD = P - k1*D - k2*D - k3*D$

$dB = k3*D - k4*B - k6*B - k7*B$

$dM = k1*D + k4*B - k5*M - f(M)$

$dS = k2*D + k6*B + f(M) - k8*S - k9*S$

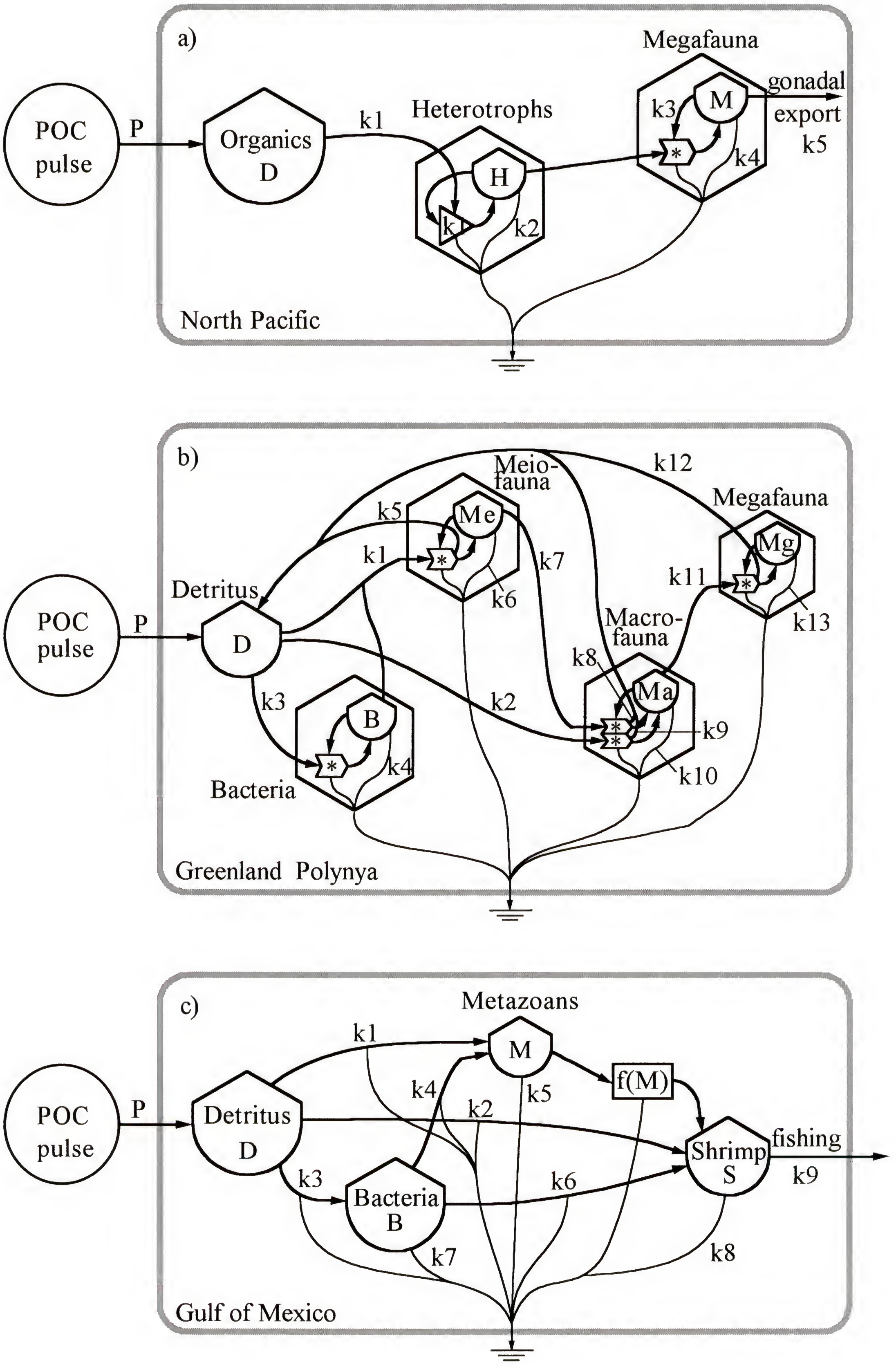
a)
POC pulse
P
Organics D
k1
Heterotrophs
H
k
k2
Megafauna
M
k3
*
k4
gonadal export k5
North Pacific
b)
POC pulse
P
Detritus
D
k1
k2
k3
k4
k5
Meio-fauna
Me
*
k6
k7
k8
k9
k10
k11
k12
Megafauna
Mg
k13
Macro-fauna
Ma
B
Bacteria
Greenland Polynya
c)
POC pulse
P
Detritus D
Metazoans
M
k1
k2
k3
k4
k5
f(M)
Shrimp S
fishing
k9
k6
Bacteria B
k7
k8
Gulf of Mexico

responded in two peaks over a 10-year simulation period. As the energy systems diagram in Figure 1-16a shows, organic material pulses did not have an effect on the dynamics of heterotrophs (H) and megafauna (M) because growth of heterotrophs (k1*H) was only a linear function of heterotrophs. There was no direct or indirect control on heterotrophs and megafauna by organic material pulses and detritus storage (organics) in the system. In this condition, the model turned into a typical prey-predator type model with unlimited energy source. This is why heterotrophs (bacteria) could not follow the seasonal cycle of organic material pulses.

Frequency of oscillations of heterotrophs and megafauna in the North Pacific model (Figure 1-16a) depends on the turnover rate of both storages, as explained above. Without megafauna, storage of heterotrophs can not show any dynamic oscillations because the input and output of the storage (H) are linear. Experimental runs which showed more frequent pulses with changes in the initial organic storage (D) and produced pulsing pattern without megafauna contain some simulation errors.

Pulsing dynamics of the other two models, Greenland polynya and Gulf of Mexico, were controlled by the pulsed input of organic material. Simulation results of both models showed seasonal pulsing of all components. The model for the Gulf of Mexico system showed very simple sine wave variation in the temporal dynamics of each component because all flows between compartments were modeled as first-order, donor-controlled relationships. This seems to be an unrealistic representation of the real system, totally dependent on the variation in the outside pulsing source. Models of the Greenland polynya system showed more complex dynamics because of the recycle pathways of fecal material into detritus storage and autocatalytic functions used for consumers.

Pelagic ecosystems

Moloney and Field (1991) simulated the dynamics of carbon and nitrogen flows in plankton communities using a generic model in which organism size was used to determine the model parameters (Figure 1-17). They divided autotrophs into three different size classes and heterotrophs into four. Heterotrophs in a size class feed on autotrophs and/or heterotrophs in the size class just below their size class. The model represented a hypothetical plankton community in the surface waters of the ocean with spatial extent of one cubic meter. Nitrogen was the only limiting factor to primary production and other physical factors were kept constant.

Model simulation was started with a single pulse of nitrogen upwelling. Heterotrophs in each size class followed the fluctuations of their autotroph prey, forming a pulsing pair. Picophytoplankton, the smallest autotrophs, and heterotrophic nanoplankton pulsed seven times over the 20-day simulation. After the start, recycled nitrogen from heterotrophic nanoflagellates was the main source for picophytoplankton production. Pulse amplitudes decreased during the simulation period because of continuous loss of nitrogen in sinking detritus. Pairs of larger autotrophs and heterotrophs pulsed once over the same simulation period.

Moloney et al. (1991) used the same size-based model to simulate the dynamics of two coastal and one oceanic plankton ecosystem in the southern Benguela region off the west coast of South Africa. They divided phytoplankton into four size categories and zooplankton into five. Temperature dependence of ecological processes was also included in the model parameters to reflect different temperature regimes for each system.

Simulation results of Moloney et al. (1991) were compared with field observations of biomass range and size composition. Their simulation also showed that the different size classes of phytoplankton and zooplankton fluctuate on different time scales. The two coastal ecosystems which started with initial pulse input of nitrogen showed four distinct pulsing frequencies of phytoplankton and zooplankton pairs. Smaller size classes produced more frequent pulses with shorter duration. In contrast, the oligotrophic oceanic system which had constant low input of nitrogen showed fast oscillations in the smallest components of the system. Larger components decreased over the simulation

Figure 1-17. Energy systems language translation of the size-based plankton ecosystem model by Moloney and Field (1991). Dashed are inferred elements from the original model. Author's original equations are shown below.
PI = Picophytoplankton, NA = Nanophytoplankton,
NE = Netphytoplankton, B = Bacterioplankton, HF = Heterotrophic nanoflagellates, MI = Microzooplankton, ME = Mesozooplankton,
DOC = Dissolved Organic Carbon, DON = Dissolved Organic Nitrogen

dACj/dt = carbon fixation - PDOC - respiration - senescence - grazing - sinking
dANj/dt = nitrogen uptake - senescence - grazing - sinking
dHCj/dt = ingestion/uptake - egestion - respiration - predation
dHNj/dt = ingestion/uptake - egestion - excretion - predation
dDET/dt = faeces - sinking
dPDOC/dt = PDOC production by autotrophs - uptake by bacterioplankton
dDOC/dt = lysis of senescent phytoplankton cells - uptake by bacterioplankton
dNEWN/dt = (upwelling/mixing/diffusion) - uptake by bacteria and phytoplankton
dREGN/dt = excretion by heterotrophs - uptake by bacterioplankton and phytoplankton
dDON/dt = lysis of senescent phytoplankton cells - uptake by bacterioplankton

AC = autotroph carbon, AN = autotroph nitrogen, HC = heterotroph carbon,
HN = heterotroph nitrogen, DET = detrital carbon and nitrogen,
NEWN = new nitrogen (nitrate), REGN = regenerated nitrogen (ammonia, urea)
PDOC = photosynthetically produced dissolved organic carbon
j = size class subscript

Primary production: $Pj = VmaxjN/(Ksj + N) * Bj$
PDOC production: 15 % of primary production
Senescence:
  POC/PON production = senescence rate * Bj
  DOC/DON production = lysis rate * POC/PON
Heterotroph uptake/ingestion
  Bacterioplankton growth rate
    $P'j = Vj * Bj$
      $VjC = Vmaxj*(PDOC+DOC)/(Ksj + (PDOC+DOC))$
      $VjN = Vmaxj*N/(Ksj + N)$
  Heterotrophs
      Ingestion rate = Imaxj*(B'k - refugek)/(Kk + sum(B'r - refuger))
Egestion = a proportion of ingested material released as faeces
Respiration rate = Rj*Bj
Excretion rate = Rj*Bj
Sinking losses = (Sj/D)*Bj

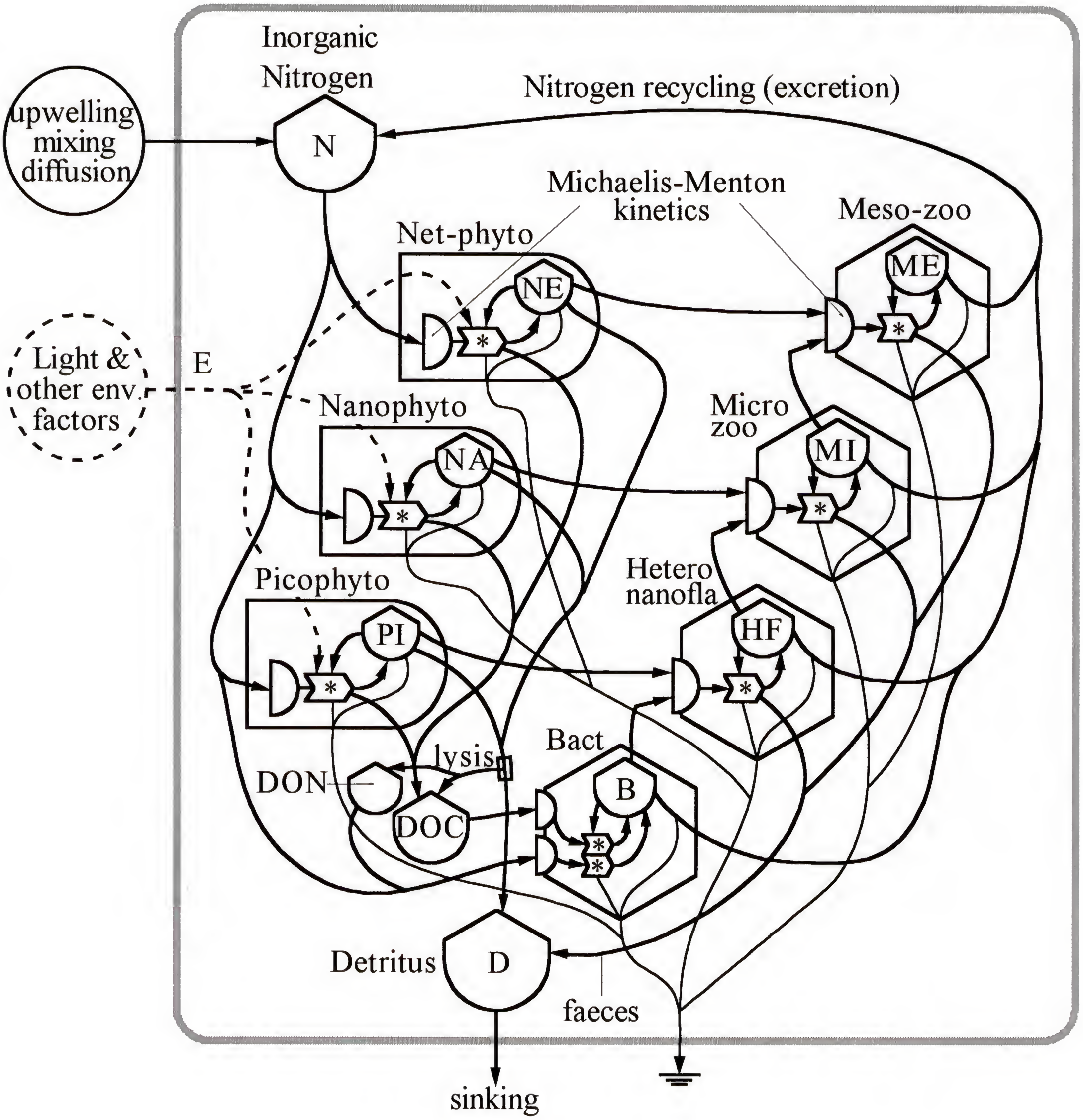
Inorganic
Nitrogen
Nitrogen recycling (excretion)
upwelling
mixing
diffusion
N
Michaelis-Menton
kinetics
Net-phyto
Meso-zoo
NE
ME
Light &
other env.
factors
E
Nanophyto
Micro
zoo
NA
MI
*
Hetero
nanofla
Picophyto
PI
HF
lysis
Bact
DON
B
DOC
Detritus
D
faeces
sinking

period possibly because the nitrogen input was too small to support primary production and higher level grazing.

Moloney (1992) connected the size-based micro/mesoplankton model to a macrozooplankton food web model of euphausiids in Benguela current upwelling, which has different time and space scales. Euphausiids in this model consumed three different size classes of phytoplankton and zooplankton, as an omnivore. The simulation also showed the scale dependence of pulsing frequencies and duration. Euphausiid biomass increased based on the food supply from the micro/mesoplankton model, which might imply a longer pulsing period.

Spatial plankton pulses

Dubois (1975) constructed a non-linear model to explain the horizontal structuation of plankton populations in a turbulent sea (Figure 1-18). He used the Lotka-Volterra type prey-predator equations for the relationship between phytoplankton and zooplankton. In the model, turbulent energy controls the spatial pattern of this prey-predator pair. Starting from an initial small patch of prey-predator populations, model simulation showed pulses of plankton populations and their spatial propagation. A ring structure resulted as plankton concentrations decreased at the center after the prey-predator pulse. The ring propagated, increasing its radius with constant intensity and velocity.

Spruce budworm outbreaks

Ludwig et al. (1978) developed a mathematical model for spruce budworm outbreaks (Figure 1-19). They divided tree biomass into two different categories; foliage (E) and branches (S). Foliage provides energy for structural part of the trees, that is, branches in this model, and budworms through photosynthesis. Budworms with fast turnover time are limited by foliage quantity (E) of spruce trees, which have slower turnover time, and by predators (birds in this model). Both numerical integration of

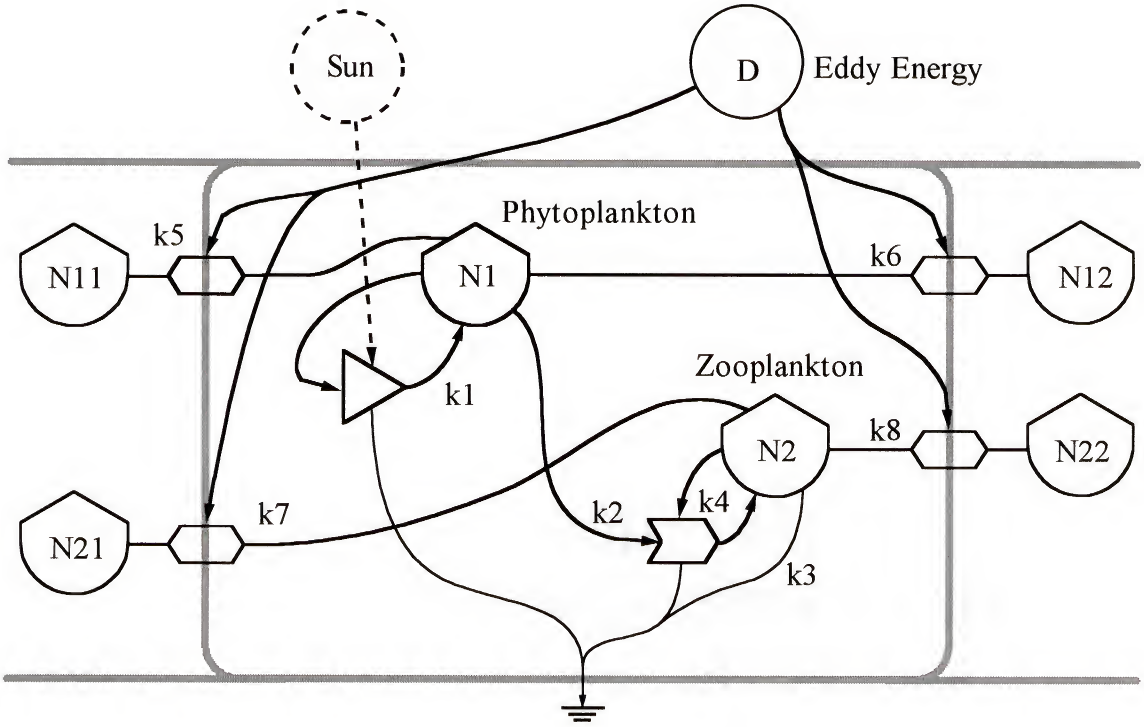

Author's original equations:

$\partial N1/\partial t + V\cdot(U*N1) = k1*N1 - k2*N1*N2 + V\cdot(D\ V\ N1)$
$\partial N2/\partial t + V\cdot(U*N2) = -k3*N2 + k4*N1*N2 + V\cdot(D\ V\ N2)$
where, N1 = phytoplankton population
N2 = zooplankton population
D = eddy diffusivity
k1 = rate of growth of phytoplankton
k2 = rate of interaction between phytoplankton and zooplankton
k3 = grazing rate of zooplankton
k4 = rate of respiration of zooplankton

Figure 1-18. Energy systems language translation of the spatial plankton pulse model of Dubois (1975). Dashed are inferred elements from the original equations. Author's original equations are shown below the diagram.

Figure 1-19. Energy systems lanuage translation of the model of spruce budworm oscillation by Ludwig et al. (1978). Dashed are inferred elements from the original equations. Author's equations are shown below.

$dE/dt = r_E*E(1 - E/K_E) - P*(B/S)$

$dS/dt = r_S*S(1 - (S/K_S)*(K_E/E))$

$dB/dt = r_B*B(1 - B/K_B) - \beta*B^2/(\alpha^2+B^2)$

where, E = Energy reserve of trees stored in foliage

r_E = rate at which trees recover from the stress of defoliation

K_E = maximum energy reserve

P = consumption rate of energy reserve by budworm

B = budworm density

S = total surface area of the branches in a stand

r_S = specific growth rate of trees

K_S = upper limit of surface area (S)

r_B = specific growth rate of budworm

K_B = carrying capacity of budworm

β = upper limit of predation by birds

α = budworm density at which saturation in predation of birds begins to take place

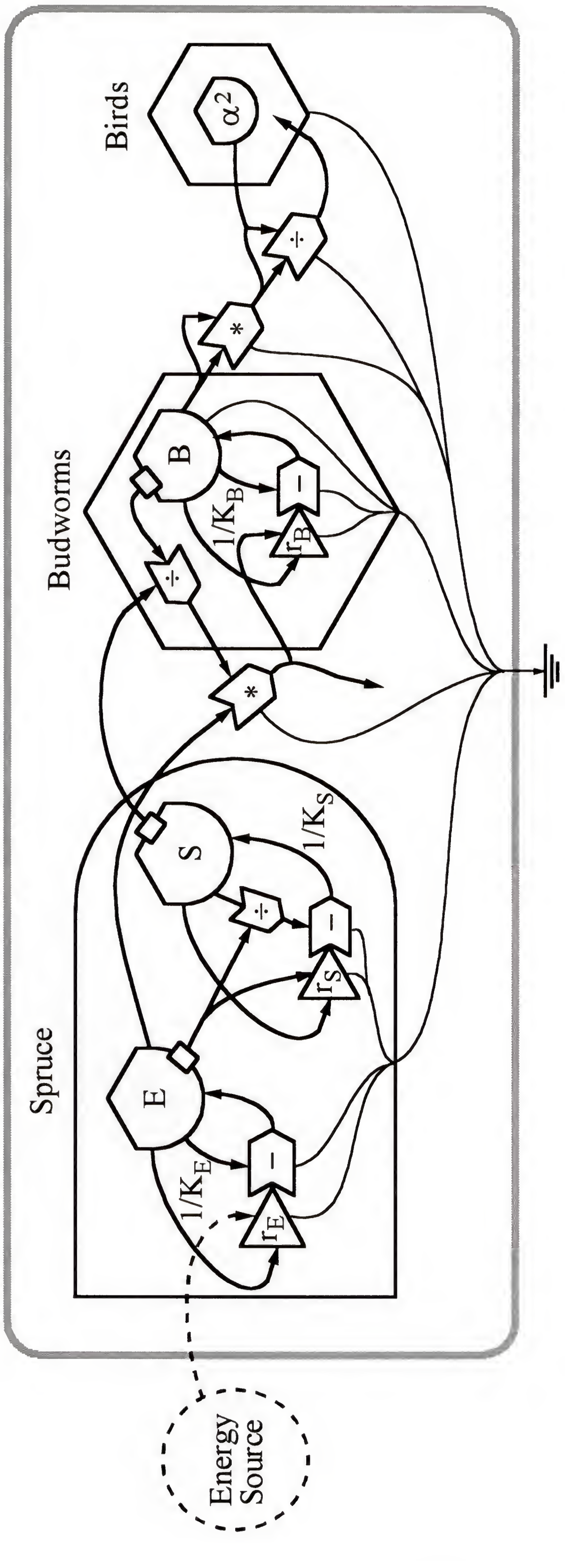
Birds
α²
÷
*
Budworms
B
1/K_B
r_B
−
÷
*
Spruce
S
1/K_S
r_S
÷
−
E
1/K_E
r_E
−
Energy
Source

differential equations and the simulation model showed the typical pattern of pulsing in which gradual buildup of spruce biomass was followed by frenzied consumption by budworms.

Clark et al. (1978) simulated spatial population dynamics of spruce budworms by including a spatial dispersal term into the model by Lugwig et al. (1978). Simulation without human management showed spatial waves and 30-odd year periodicity observed in real systems.

Production and pulse frequency

Stone and Berman (1993) found the resonance effect in their model simulations. They constructed a simple linear compartmental model with two compartments of phytoplankton and microbial loop consisting of bacteria and protozoans. Time delays were incorporated in nutrient cycling by the microbial loop and phytoplankton loss through grazing and sinking. The model simulated the dynamics of phytoplankton production in terms of nitrogen throughflow, without the actual population dynamics investigated. Their model showed explosive growth in nitrogen production through the phytoplankton compartment followed by crashes at a certain frequency range of nutrient input pulses. They argued that the presence of frequency dependent behavior would enhance overall ecosystem productivity.

Diversity and pulsing

Doyle (1981) investigated the effects of hurricanes on a montane rain forest in Puerto Rico, using a tropical forest succession model, FORICO. The model simulated dynamics of a forest gap of 1/30-ha area for 500 years. Simulations with hurricane pulses reflected the compositional variation and species diversity characteristic of the forest. By opening frequent or sizable canopy gaps, hurricane pulses allowed early successional species to coexist with late successional species, increasing species diversity. Without hurricane pulses, a forest community had fewer species and was dominated by late-successional species. The species diversity pattern with and without hurricanes, which was measured as a dominance index determined from the Shannon formula for evenness, diverged after year 60 over a 500-year simulation, and the simulation with hurricanes showed a higher dominance index. Their simulation also showed maximum diversity at intermediate hurricane frequency and intensity.

Ebenhoh (1988), using a mathematical model, showed that variability in environments enables more phytoplankton species to coexist. More algal species coexisted with pulsed input of a single type of nutrient in the model. With increasing intervals between the nutrient pulses, diversity of the model system increased, but the average biomass decreased. Parameter combinations for coexistence of the model phytoplankton species were determined by the frequency of the nutrient pulses. Ebenhoh (1988) argued that the sequential occurrence of favorable conditions for the different species enabled coexistence of species competing for the same resource.

Allen et al. (1993), based on a population model of a species, argued that chaos could reduce species extinction by increasing the degree of asynchrony among local populations. Their simulation results showed that although local extinction rates increased as one moved from stable to chaotic dynamics, species extinction rates of multiple populations weakly coupled by migration declined in the chaotic region in the presence of local perturbations. Protection against extinction was enhanced with increasing amounts of local noise. They suggested a mechanism in which chaotic oscillations decorrelated local populations in such a way that when one goes extinct, recolonization by migrants prevents extinction of the whole.

Global marine diversity, measured as the number of animal families, increases throughout Phanerozoic history, punctuated by mass extinction events (Sepkoski, 1984). Fossils of marine animals showed evolutionary-successional changes which have been grouped as three evolutionary faunas: Cambrian fauna, Paleozoic fauna, and Modern fauna.

Sepkoski (1984) used a three-phase kinetic model (Figure 1-20) to describe the large-scale patterns of the Phanerozoic diversification in the marine record. Simulation results of the model reproduced the diversification pattern of the evolutionary faunas. The equations imply unlimited energy source. The model shows how the diversity of each fauna affects other fauna's diversities.

Diversification of each evolutionary fauna was modeled with a simple logistic equation. Evolutionary faunas interact with each other in such a way that if total diversity of the system increases over the equilibrium diversity of each fauna, diversification of phases becomes negative, decreasing diversity of each phase. Sepkoski viewed mass extinctions as perturbations of the faunal system by external forces, independent of the long-term growth and decay of the evolutionary faunas. In this model major extinction events during the Phanerozoic were modeled with external time-specific perturbations by which extinction rates of each fauna were increased.

Study Plan

A literature review was made of the data and theory offered to explain pulsing in many kinds of systems. Models were developed to consider the general hypothesis that pulsing selected in self-organization increases performance (pulsing paradigm).

Measurements from time series of observed data from published literature were used to analyze pulsing patterns, with emphasis on aquatic ecosystems of lakes and oceans. Measured characteristics were plotted on graphs.

First, single models with two storages each were constructed to investigate characteristics of multiplicative production functions in drawing in power. Simulation results of models with pulsing mechanisms were compared with similar models without pulsing mechanisms.

Figure 1-20. Energy systems laguage translation of Sepkoski's (1984) three phase kinetic model for the diversification of marine fauna during the Phanerozoic. Dashed are inferred elements from the model. Author's original equations are shown below.

Diversification rate of evolutionary fauna

$$dDi/dt = r_{oi}Di(1 - \Sigma Dj/Dki)$$

where, Di = diversity of the i-th phase (i = 1, 3)

r_{oi} = initial per-taxon diversification rate of each phase

Dki = equilibrium diversity

ΣDj = summed diversity of all three phases in the system

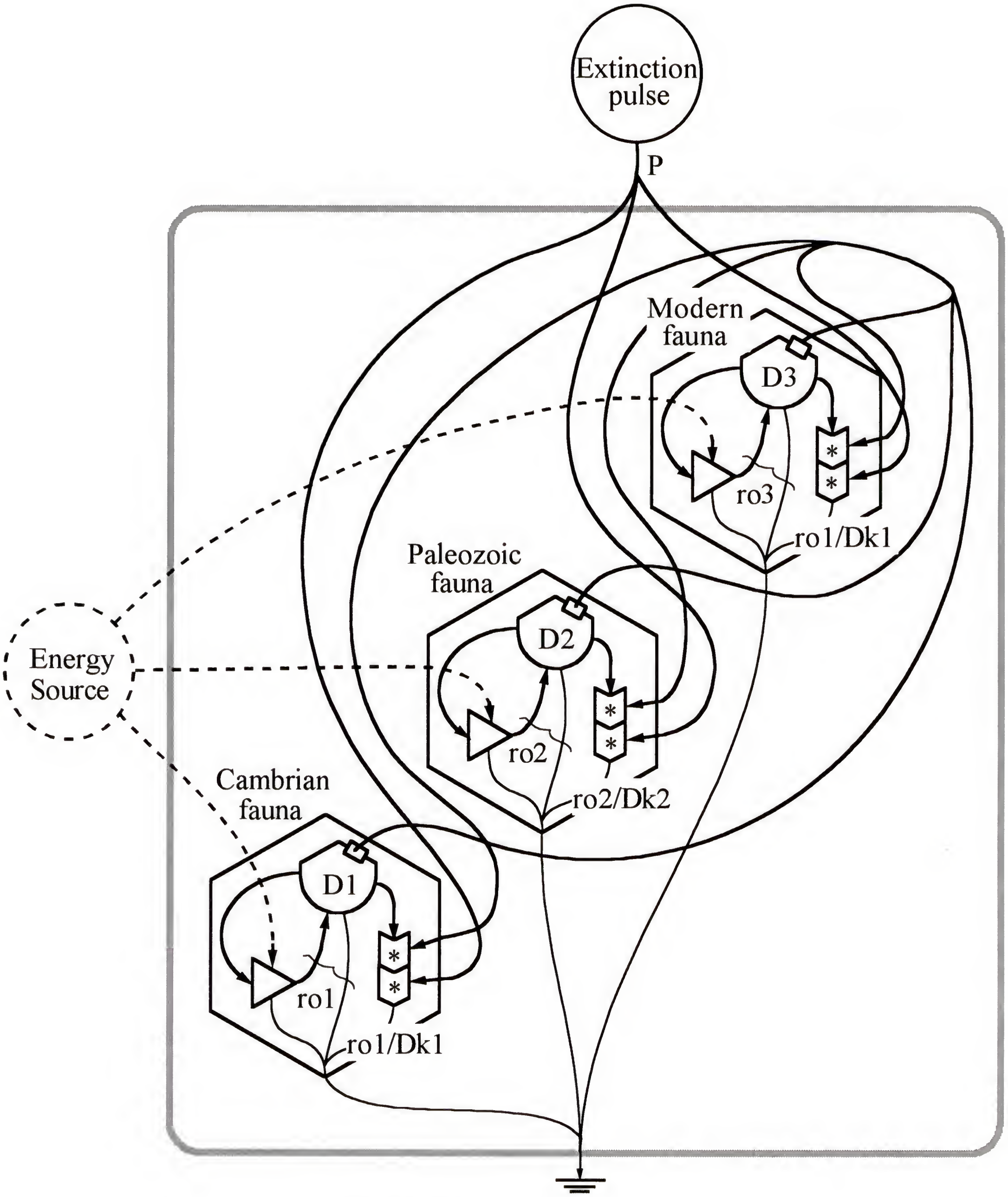

P = time specific perturbations

dD1 = ro1*D1 - P*(ro1/Dk1)*D1*(D1+D2+D3)

dD2 = ro2*D2 - P*(ro2/Dk2)*D2*(D1+D2+D3)

dD3 = ro3*D3 - P*(ro3/Dk3)*D2*(D1+D2+D3)

A basic model of production-consumption with three different consumption pathways was investigated. Input energy levels were varied to study its energetics. Coefficients of production and consumption were also varied to investigate how the efficiencies of production and consumption affect the model dynamics. Starting with the simple pulsing model, various configurations were tested and compared with observed data. These models were calibrated by considering characteristic turnover time in aquatic ecosystems.

Simulation results of the theoretical models were compared to the pulsing pattern analyzed using observed data. Ways of using the pulsing paradigm were considered for policy and management.

CHAPTER 2
METHODS

The pulsing model in Figure 1-7 was used to illustrate the methodology of energy systems modeling and simulation used in this dissertation. This is the basic model for other pulsing models which will be developed in this study. As a minimodel that can be applied to any system in all scales, it is already highly aggregated and can be directly used for simulation. A marine ecosystem was used to show the general procedure of energy systems simulation; how to produce a diagram, such as in Figure 1-7, that can be manageable for simulation and how to set up a computer program from the diagram.

The whole procedure is summarized in Figure 2-1 as a flow chart. Odum and Odum (1996b) give detailed explanations about modeling in the energy systems language.

Energy Systems Diagramming

Energy systems simulation starts with diagramming the system of interest. As a top down modeling, energy systems diagramming helps researchers to understand network organization of the system of their interest and to identify the important flows and interactions most relevant to the problem they are trying to solve.

Detailed Diagram

The first step in the energy systems simulation is to construct an energy systems diagram from verbal descriptions of the system. The initial diagram includes all details identified as relevant to the system of interest. A detailed systems diagram gives an

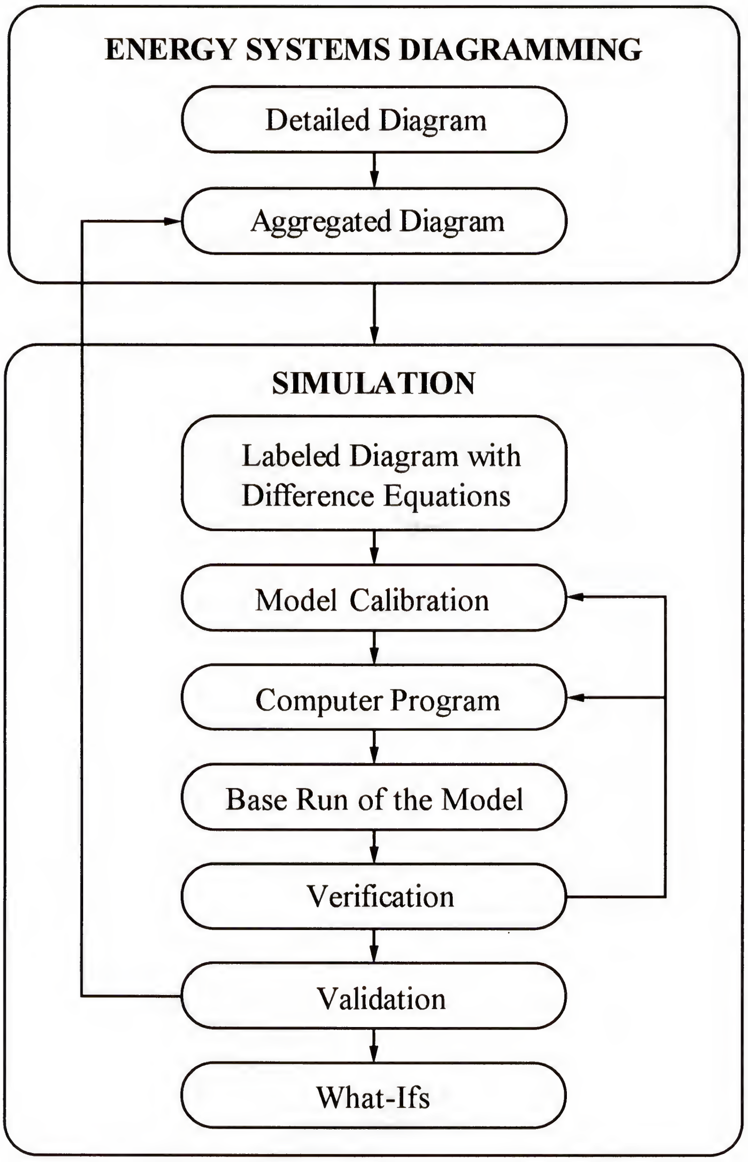

Figure 2-1. A flow chart summarizing the overall procedure in the energy systems simulation methodology.

overview of how the system is organized into a network and clarifies the problems and discussions of the system.

The following steps are used in the initial diagramming of systems under consideration (Doherty et al., 1992).

1. Define boundary of the system; that is, define the problem to be investigated.
2. Make a list of important outside sources (causes, energies, and materials).
3. Make a list of principal components believed important, considering the scale of the defined system.
4. Make a list of processes (flows, interactions, production and consumption processes, etc.).
5. Develop an energy systems diagram based on the above lists, while following the rules of energy systems language diagramming.

Symbols: Each symbol in energy systems language has rigorous energetic and mathematical meaning (Figure 1-3).

System Frame: A rectangular box is drawn to represent the boundary that is selected

Arrangement of Sources: Any input that crosses the boundary is identified as a source, including pure energy flows, materials, information, services, as well as inputs that are destructive. All sources are represented as a circular symbol. Sources are arranged around the border from left to right in order of their transformities starting with sunlight on the left and information and human services on the right.

Pathway Line: Any flow is represented by a line, including pure energy, materials, and information. Money is shown with dashed lines. Lines without barbs flow in proportion to the difference between two forces connected, and may flow in either direction.

Outflows: Any outflow which still has available potential, materials more concentrated than the environment, or usable information is shown as a pathway from either of the three upper system borders, but not out the bottom.

Adding Pathways: Pathways add their flows when they join or when they go into the same tank. Every flow in or out of a tank must be the same type of flow and measured in the same units.

Degraded Energy: Energy that had lost its ability to do work according to the second law of thermodynamics is represented as pathways converging to a heat sink at the bottom center of the diagram. Included are heat energy as byproducts of processes and the dispersed energy from depreciation of storages.

Interactions: Two or more flows that are different, but are both required for a process are drawn to an interaction symbol. The flows to an interaction are connected from left to right in order of their transformity, the lowest quality one connecting to the notched left margin.

Counterclockwise Feedbacks: High-quality outputs from consumers such as information, controls, and scarce materials are fed back from right to left in the diagram. Feedbacks from right to left represent a loss of concentration because of divergence, the service usually being spread out to a larger area.

Material Balances: Since all inflowing materials either accumulate in system storages or flow out, each inflowing material needs to have outflows drawn.

Position of Symbols within Diagram: Symbols are arranged according to their energy hierarchy, that is, in order of their transformity. Components low in the hierarchy are drawn on the left and those high in the hierarchy on the right.

Figure 2-2 is a detailed energy systems diagram of the upper part of an ocean ecosystem. It illustrates a pelagic food web with the system boundary of upper open oceans. The diagram shows energy sources, a producer, and consumers. It also has flows in and out of the system, and nutrient recycling inside the system. Phytoplankton converts inorganic nutrients into organic material using sunlight energy. Physical processes in the ocean also influence the rate of primary production and other processes in the system. Organic material produced by phytoplankton is consumed directly by herbivorous zooplankton and fishes and by heterotrophic microorganisms as detritus before it becomes available to higher energy levels. Part of the organic material produced is lost to the ocean bottom due to sedimentation of particulate organic material. Nektonic species

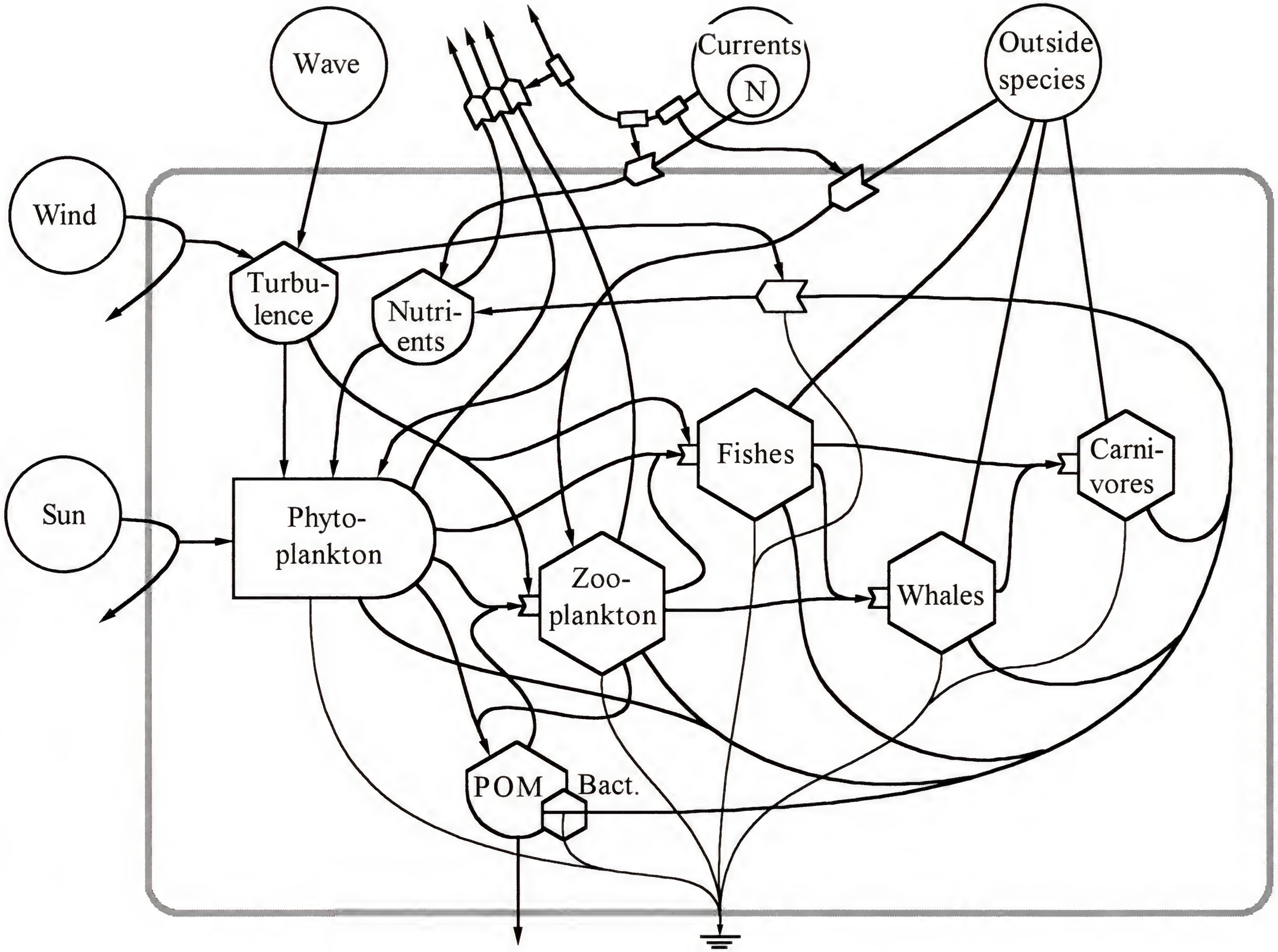

Figure 2-2. Detailed overview diagram of the upper part of an open ocean ecosystem. POM = Particulate Organic Material

moves in and out of the system, and planktonic organisms are carried into and out of the system by currents.

Aggregated Diagram

To be understandable and manageable for systems evaluation and simulation, the detailed diagram has to be reduced in its complexity. From the detailed diagram produced above, a simplified diagram is obtained by aggregating components and pathways into important categories. Aggregated diagrams have to show sources, components, and pathways most relevant to the study, and have to keep energy and material balances. It is required to have an appropriate level of aggregation needed for the purpose of the study.

Figure 2-3 is an aggregated form of the detailed systems diagram in Figure 2-2. The diagram is reduced to a three energy level model of phytoplankton, zooplankton, and carnivores by aggregating higher energy levels into one category of the carnivore component. Sun, wind, and wave energies are grouped into one category. There are still important inflows into the system and outflows to the surrounding environment. Details of production function in producer and consumer units are not represented in group symbols used in this diagram nor in the detailed diagram in Figure 2-2.

Simulation

The aggregated diagrams produced above are calibrated with data and a computer program is written using the mathematical relationships of energy systems symbols to study systems dynamics over time.

Labeled Diagram with Difference Equations

For computer simulation, an aggregated systems diagram in the previous section is used, or it can be aggregated further in a more manageable form for simulation purposes. The aggregated diagram in Figure 2-3 can be further aggregated into the production-

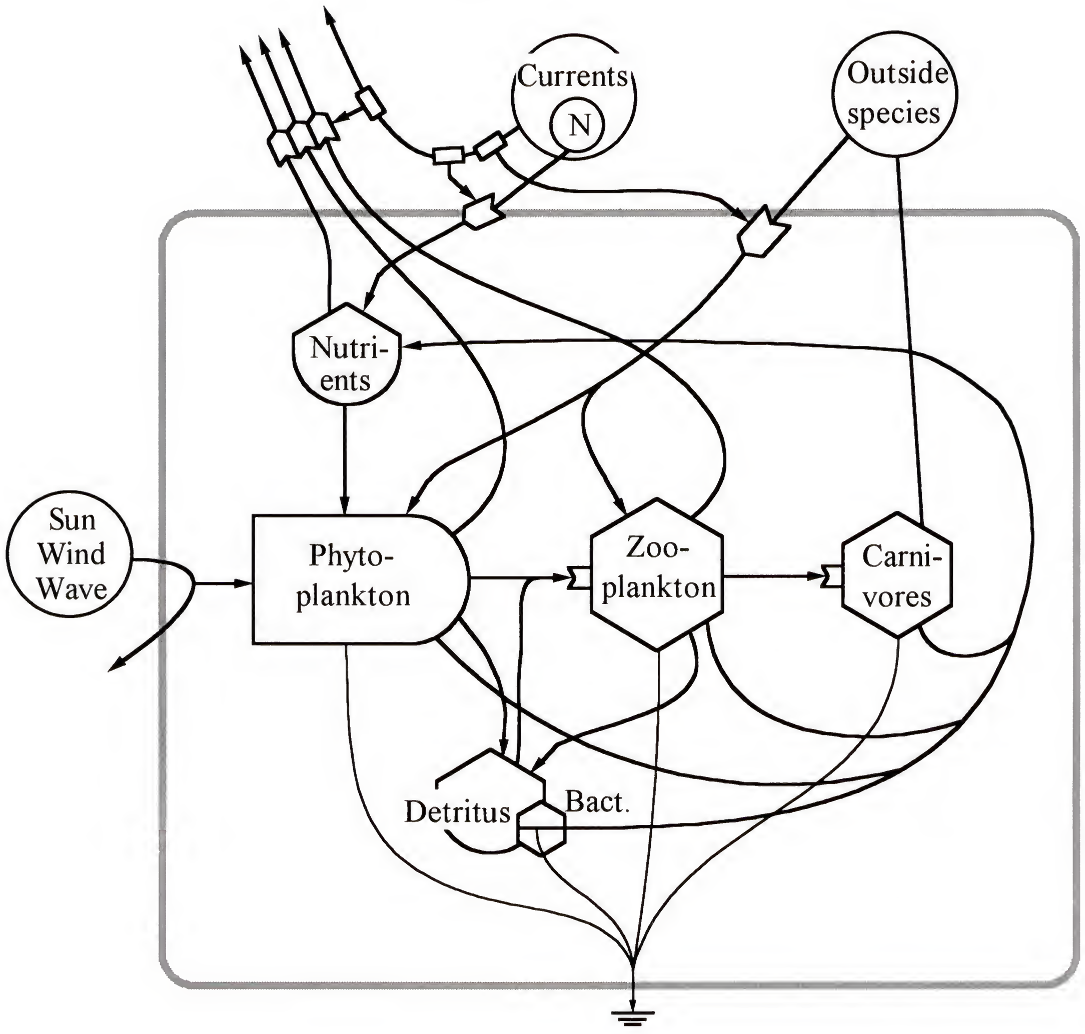

Figure 2-3. Aggregated diagram of the upper open ocean ecosystem in Figure 2-2.

consumption model (Figure 2-4). For theoretical studies of how systems develop different pathways to maximize performance, the system is assumed to be a closed system in terms of material flows, resulting in the model in Figure 1-7. Material is conserved in the system. The diagram has three storage components of producer, consumer, and material. The consumer uses primary production by the producer through three different pathways: slow linear, autocatalytic, and fast quadratic autocatalytic pathways.

In Figure 2-4, letters are assigned for pathway coefficients and for sources and storages. Difference equations for storages are obtained directly from the systems diagram because the network of energy systems symbols has mathematical relationships defined as well as energetic meanings. These equations are used in the computer program.

Model Calibration

To calculate coefficient values for each pathway in the systems diagram which are used in the simulation, numbers for sources, storages and flows are put into the diagram (Figure 2-5). By putting numbers on pathways and storages, the diagram becomes a quantitative model. These numbers can be values from real measurements or arbitrary values reflecting important systems characteristics, such as turnover times. These may be data at a specific moment in time, or average values of the storages and flows for a certain time period. All data have to be in the same space and time units.

In Figure 2-5, the basic pulse model in Figure 2-4 was calibrated for a hypothetical case with phytoplankton, zooplankton, and nutrients. Storages and flows were assigned so that all storages have turnover times in days. Also, the model was calibrated in a dynamic condition, as opposed to steady state. Producer storage is declining because total inflow (250) is less than total outflow (660). On the other hand, consumer storage is growing with total inflow (220.5) greater than total outflow (100). Using these numbers, coefficients are calculated in a spreadsheet (Table 2-1), and then are used in the computer

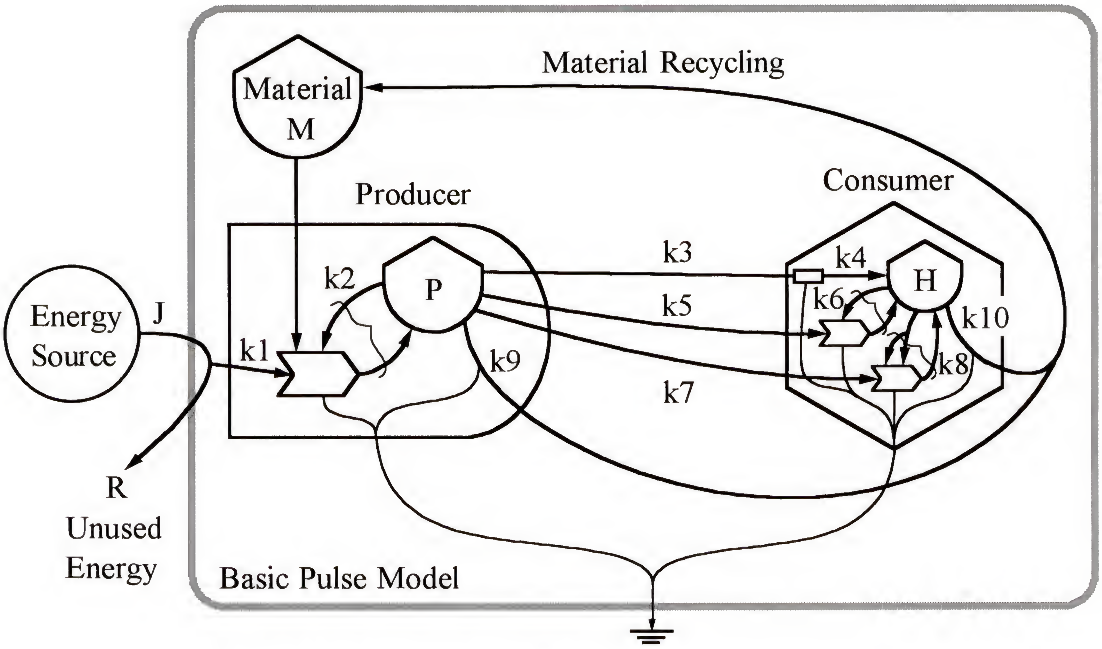

$$M = MT - f1*P - f2*H$$
$$R = J / (1 + k1*M*P)$$
$$dP = k2*R*M*P - k3*P - k5*P*H - k7*P*H*H - k9*P$$
$$dH = k4*P + k6*P*H + k8*P*H*H - k10*H$$

Figure 2-4. Systems diagram of the basic pulse model as in Figure 1-6, with labels for sources, storages and pathways, and difference equations derived from the model. MT = Total material in the system; f1 and f2 = Material fraction of producer (P) and consumer (H) storages, respectively.

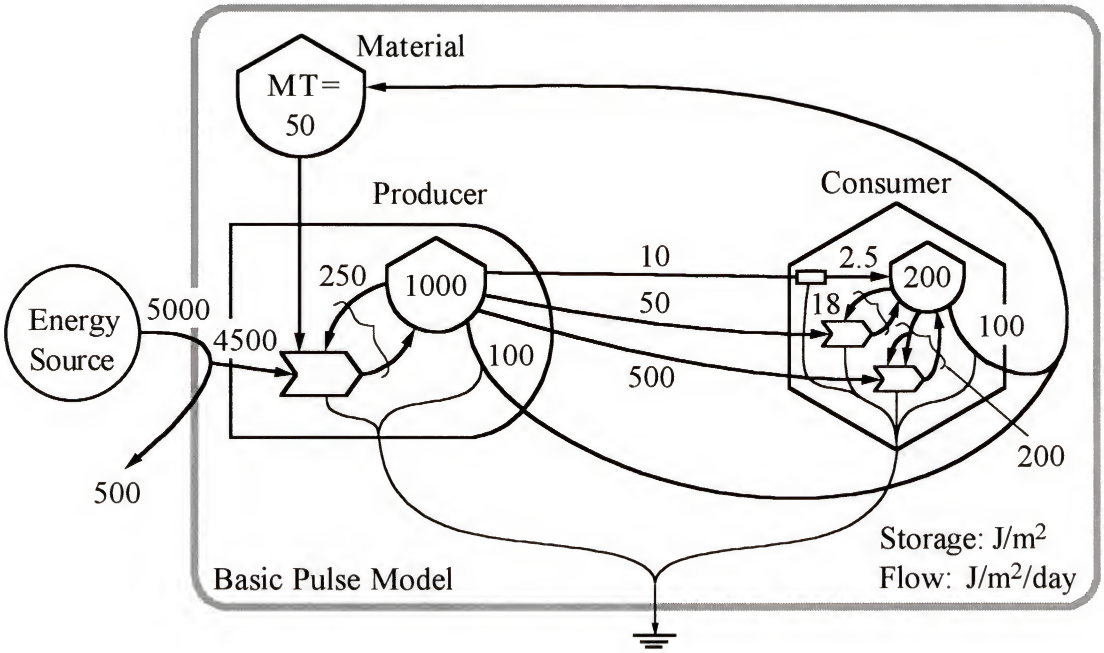

Figure 2-5. Systems diagram of the basic pulse model in Figure 2-4 with flow and storage values for calibration.

Table 2-1. Calibration of the pathway coefficients for the computer simulation of the basic pulse model with a flow limited energy source in Figure 2-4.

Items	Symbols	Values	Units	Coefficients	
Sources					
Sunlight	J	5000	$J/m^2/day$		
Unused energy	R	500	$J/m^2/day$		
Storages					
Producer	P	1000	J/m^2		
Consumer	H	200	J/m^2		
Material available	M	20	g/m^2	M = MT-f1*P-f2*H	
Total Material	MT	50	g/m^2		
Material fraction					
Producer	f1	0.02	g/J		
Consumer	f2	0.05	g/J		
Flows					
Energy used	J1 = k1*R*M*P	4500	$J/m^2/day$	k1 =	0.00045
Primary production	J2 = k2*R*M*P	250	$J/m^2/day$	k2 =	0.000025
Linear consumption	J3 = k3*P	10	$J/m^2/day$	k3 =	0.01
	J4 = k4*P	2.5	$J/m^2/day$	k4 =	0.0025
Autocatalytic consumption	J5 = k5*P*H	50	$J/m^2/day$	k5 =	0.00025
	J6 = k6*P*H	18	$J/m^2/day$	k6 =	0.00009
Quadratic autocatalytic	J7 = k7*P*H*H	500	$J/m^2/day$	k7 =	0.0000125
consumption	J8 = k8*P*H*H	200	$J/m^2/day$	k8 =	0.000005
Producer respiration	J9 = k9*P	100	$J/m^2/day$	k9 =	0.1
Consumer respiration	J10 = k10*H	100	$J/m^2/day$	k10 =	0.5

program in the next section. Notes can be added in the table to explain about data used in the calibration; literature sources of data, calculations needed to get those data, assumptions, and so on.

Computer Program

Using the difference equations (Figure 2-4) and coefficient values (Table 2-1) obtained in previous sections, a computer program is written for simulation using BASIC computer language (Table 2-2). In this dissertation, PowerBASIC 3.2® by PowerBASIC, Inc. is used to write and run simulation programs. The program contains lines for plotting simulation results on the computer screen, initial values of storages and sources, scaling factors for plotting, coefficient values for each pathway, and difference equations to calculate storage changes over time. Initial values of the storages and sources are put into the computer program as starting points of the simulation. Detailed information on the programming in BASIC can be found in any BASIC programming references (e.g., Inman, 1992).

Emergy and transformity simulation

By including equations for emergy and transformity, the BASIC program in Table 2-2 can produce graphs of changes in emergy and transformity of storages, and of patterns in emergy flows on the pathways. These results can also be used to calculate various emergy indices.

Figure 2-6 shows the way by which emergy and transformity of storages and on pathways are calculated. These are implemented in program lines from 300 to 501 in Table 2-2. The statements in the computer program stop adding new emergy when growth of storage is within 5% of steady state. In real systems, variations of storages within this range do not add new storage because fluctuations of this magnitude are present from the smaller scale as a noise to the larger scale.

Table 2-2. BASIC program listing of the basic pulse model in Figure 2-4.

```
' Basic Pulse Model
' File Name: Pulse.bas

' Plotting Frames
10 SCREEN 12
11 LINE (20, 10)-(270, 175), 15, B
12 LINE (20, 65)-(270, 65), 15
13 LINE (20, 120)-(270, 120), 15
15 LINE (20, 190)-(270, 310), 15, B
16 LINE (20, 250)-(270, 250), 15

17 LINE (300, 10)-(550, 170), 15, B
18 LINE (300, 50)-(550, 50), 15
19 LINE (300, 90)-(550, 90), 15, B
20 LINE (300, 130)-(550, 130), 15
21 LINE (300, 190)-(550, 310), 15, B
22 LINE (300, 250)-(550, 250), 15

' Sources and Initial Values
30 MT = 50
31 J = 5000: TrJ = 1
32 P = 10: EP = 10: TrP = EP/P
33 H = .1: EH = 10: TrH = EH/H

' Iteration Time Step during Simulation
40 dt = .01

' Scaling Factors for Plotting
50 P0 = 70: EP0 = 3000: TrP0 = 1.5
51 H0 = 20: EH0 = 3000: TrH0 = 25
52 M0 = 1
53 t0 = 1.46

' Material Fraction of Storages
70 f1 = .02
71 f2 = .05

' Pathway Coefficients
101 k1 = .00045
102 k2 = .000025
103 k3 = .01
104 k4 = .0025
```

Table 2-2 -- continued

```
105 k5 = .00025
106 k6 = .00009
107 k7 = .0000125
108 k8 = .000005
109 k9 = .1
110 k10= .5

' Simulation Loop
200 M = MT - f1 * P - f2 * H
201 IF M < 0 THEN M = 0
202 R = J / (1 + k1*M*P)
211 J1 = k1 * R * M * P
212 J2 = k2 * R * M * P
213 J3 = k3 * P
214 J4 = k4 * P
215 J5 = k5 * P * H
216 J6 = k6 * P * H
217 J7 = k7 * P * H * H
218 J8 = k8 * P * H * H
219 J9 = k9 * P
220 J10= k10* H

300 dP = J2 - J3 - J5 - J7 - J9
301 IF (dP/P)>.05 THEN dEP = TrJ*J1-TrP*J3-TrP*J5-TrP*J7
302 IF (dP/P)<=.05 and (dP/P)>=0 THEN dEP = 0
303 IF (dP/P)<0 THEN dEP = TrP*dP

310 dH = J4 + J6 + J8 - J10
311 IF (dH/H)>.05 THEN dEH = TrP*J3+TrP*J5+TrP*J7
312 IF (dH/H)<=.05 and (dH/H)>=0 THEN dEH = 0
313 IF (dH/H)<0 THEN dEH = TrH*dH

400 P = P + dP * dt
401 IF P < .01 THEN P = .01
402 EP = EP + dEP * dt

410 H = H + dH * dt
411 IF H < .001 THEN H = .001
412 EH = EH + dEH * dt

500 TrP = EP/P
501 TrH = EH/H
```

Table 2-2 -- continued

```
550 Total_P = Total_P + P
551 Total_H = Total_H + H
560 Total_Power = Total_Power + J1
561 Total_EP = Total_EP + EP
562 Total_EH = Total_EH + EH
563 Trans_P = Trans_P + TrP
564 Trans_H = Trans_H + TrH
570 I = I + 1

' Plotting Simulation Result
600 PSET (T / t0 + 20, 65 - P / P0), 15
601 PSET (T / t0 + 20, 120 - H / H0), 15
602 PSET (T / t0 + 20, 175 - M / M0), 15
603 PSET (T / t0 + 20, 250 - J2 / 6), 15
604 PSET (T / t0 + 20, 310 - J1*60/J), 15
605 PSET (T / t0 + 300, 250 - P/J2/.2), 15
606 PSET (T / t0 + 300, 310 - H/(J4+J6+J8)/.2), 15

610 PSET (T / t0 + 300, 50 - EP/EP0), 15
611 PSET (T / t0 + 300, 90 - EH/EH0), 15
612 PSET (T / t0 + 300, 130 - TrP/TrP0), 15
613 PSET (T / t0 + 300, 170 - TrH/TrH0), 15

700 T = T + dt

' Repeat the Simulation Loop
800 IF T / t0 < 250 GOTO 200

LOCATE 23
PRINT "Total Power Input              = ", Total_Power*dt, "J/m2"
PRINT "Average storage of P           = ", Total_P/I, "J/m2"
PRINT "Average storage of H           = ", Total_H/I, "J/m2"
PRINT "Average EMERGY storage of P = ", Total_EP/I, "sej/m2"
PRINT "Average EMERGY storage of H = ", Total_EH/I, "sej/m2"
PRINT "Average transformity of P   = ", Trans_P/I, "sej/J"
PRINT "Average transformity of H   = ", Trans_H/I, "sej/J"
```

Change in energy storage (Q)

$$dQ/dt = J - k1*Q - k2*Q$$

Change in emergy storage (EQ)

IF $dQ > 0$ THEN $dEQ/dt = TrJ*J - TrQ*(k2*Q)$

IF $dQ = 0$ THEN $dEQ/dt = 0$

IF $dQ < 0$ THEN $dEQ/dt = TrQ*(dQ/dt)$

where, TrJ = Transformity of J

TrQ = Transformity of Q = EQ/Q

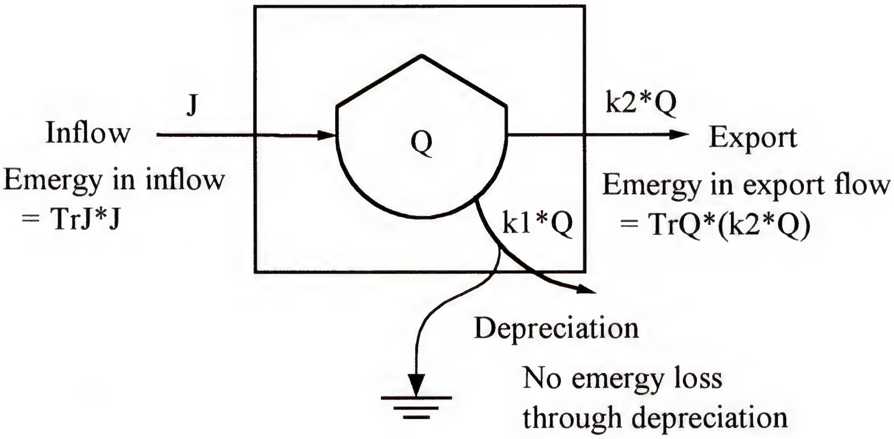

Figure 2-6. Equations for simulating emergy and transformity of storages and flows.

Base Run of the Model

Figure 2-7 shows the result of the base run of the model in Figure 2-4. It shows the basic pattern of pulsing dynamics, cycles of slow buildup of producer storage and frenzied consumption by consumer. Storage of phytoplankton builds up slowly using sunlight energy and material. Material storage decreases while producer storage continues to grow. The consumer pulses after the producer storage reaches a certain level. Material storage builds up again after this fast consumption.

Results of the base run are used to verify whether the internal logic of the program does what was expected (verification). If the simulation results do not show any expected trends in storage changes and flow patterns, program lines have to be examined for errors first (debugging). If the program lines do not include any mistakes, the calibration step must be checked for unreasonable values.

Validation

Validation is the process with which researchers can check their simulation results against real data. If the calibration is done using real measurements, the results can be validated using different sets of real data that were not used in the calibration step. If the results match real data, the model reflects important aspects of the system and can be used for prediction of systems dynamics over time. If the results do not show any trends in real data sets, it means that the model may lack essential elements of the system. Modelers have to return to the diagramming part to change model configuration. After that, the whole process described above is repeated to get the simulation results. If coefficient values are calculated using arbitrary numbers, modelers can return to the calibration step to check any unreasonable flow and storage values. Simulation is an iterative process.

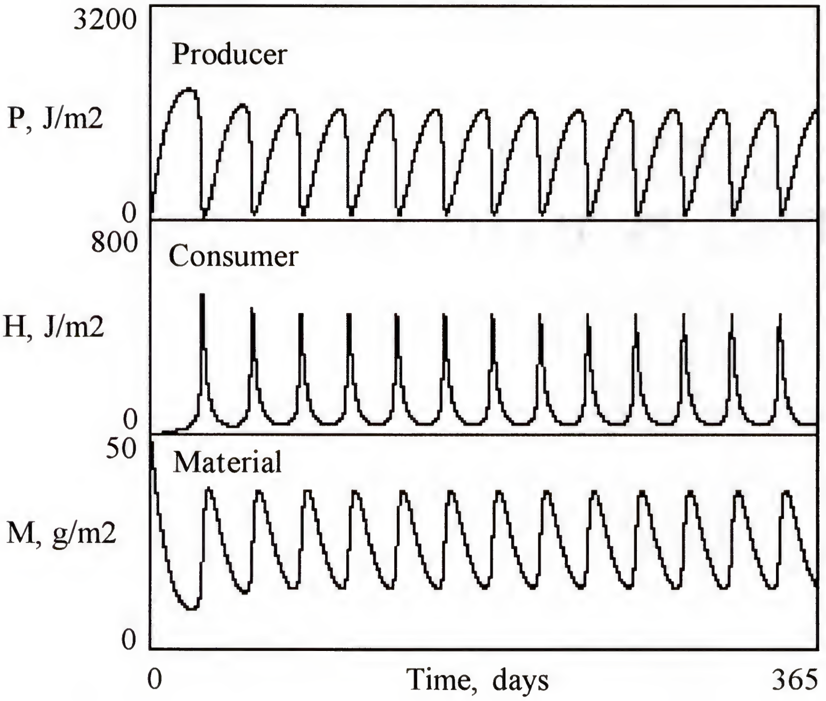

Figure 2-7. Simulation results of the basic pulse model in Figures 2-4 and 2-5, calibrated in Table 2-1, with the program listing in Table 2-2.

Even though the basic pulse model in Figure 2-4 is a very simple model with the assumption of closed material cycles, the simulation results showed patterns of frequent fluctuations observed in real planktonic ecosystems.

What-Ifs

A validated model can be used to test model behavior when there is a change in model parameters. This is a controlled experiment to study how system properties which can not be tested directly in real world experiments are affected by changes in energy sources, flows, and storages; that is, how sensitive the system is to changes.

Figure 2-8 shows an experimental run of the model in Figure 2-4. Energy input to the system (J) was halved to see how input energy affects the system dynamics. With decrease in energy level, there was no pulsing. The system reached a steady state with very low consumer storage. The producer did not grow to the level above which the consumer can start to grow.

Analysis of Published Pulsing Data

To find general characteristics of pulsing in real systems, time series graphs in the literature were selected and analyzed using the method illustrated in Figure 2-9. Height (D in Figure 2-9) of each peak represents amplitude of pulse. Peaks that were less than 10% of the maximum peak in the graphs were not included in this measurement, because the sampling frequency at one scale can not give enough resolution to show smaller scale oscillations. Base width of each pulse measured duration (C in Figure 2-9) from trough to trough. Pulse interval was measured as the average time between earlier and later peaks of equal or greater amplitude (B in Figure 2-9). Pulse amplitude, duration, and interval were measured on the graphs using a ruler. Pulse frequency was calculated as the inverse of pulse interval. Duration of pulse in percent was calculated as 100*(pulse duration) /

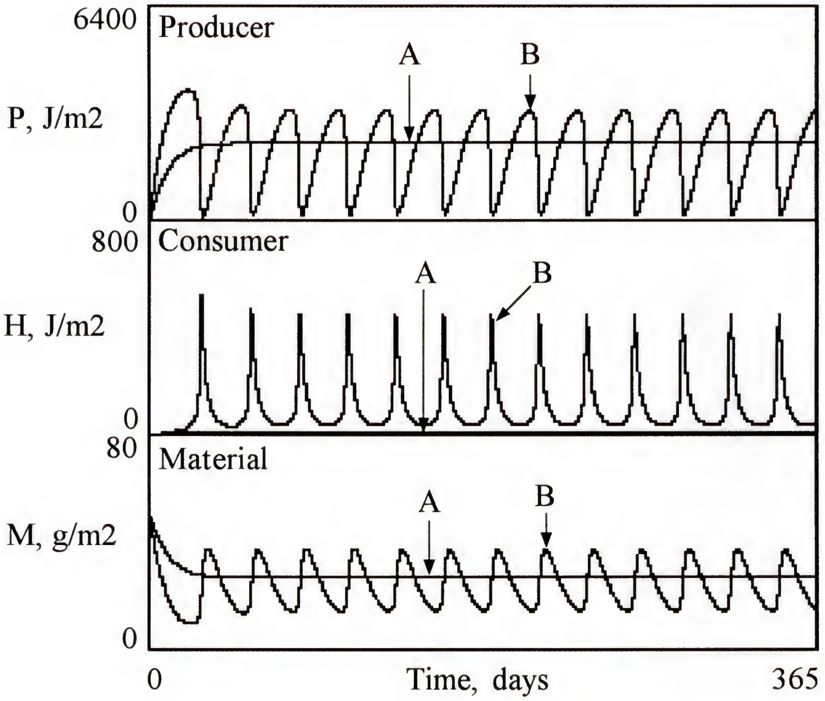

Figure 2-8. A what-if run of the basic pulse model in Figure 2-4. A. 50% decrease in energy input (J). B. The base run in Figure 2-7.

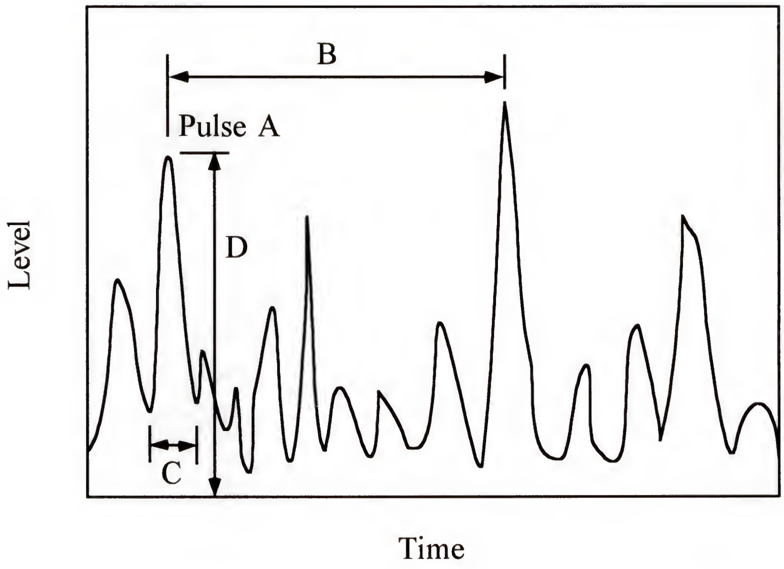

Pulse A

1) Amplitude, D
2) Interval, B = time to previous pulse of equal or greater amplitude
3) Duration, C
4) Percent of time in pulse = (C / B)*100

Figure 2-9. Illustration of the method used to analyze pulsing patterns in time series graphs found in literature.

(pulse interval). Measurements in Figure 2-9 were plotted in three ways: amplitude as a function of interval, pulse duration in percent as a function of interval, and pulse frequency as a function of pulse amplitude.

An alternate way of evaluating graphs in Appendix A is Fourier decomposition of time. Time series data are converted into frequency domain graphs through Fourier transform. The resulting frequency domain graphs enable researchers to analyze repeating patterns in those data (see Platt and Denman, 1975). To apply Fourier transform, consistent data collection is required at equally spaced intervals, with enough data points. If a time series has unequal spacings, a new data set at equal intervals may be obtained from the original data set by interpolation (Platt and Denman, 1975). Precise application requires a Gaussian distribution. Time series data used in this study (Appendix A) did not provide consistent data collection with enough data points for Fourier analysis. In most cases, there were changes in sampling frequency over the study period. For many data sets, the method used in this dissertation may be a practical alternative to Fourier analysis. This method analyzes time series from the perspective of sharp dynamic pulses which tend to be homogenized in statistical methods. In contrast, Fourier analysis investigates time series from the perspective of random distribution.

CHAPTER 3
RESULTS

Data from the published literature were used to seek general patterns in pulsing dynamics, focusing on aquatic ecosystems including lakes and oceans. Theoretical models were constructed to find appropriate designs that could represent observed pulsing patterns. Energetics and kinetics of pulsing systems were investigated by calibrating theoretical models with data from aquatic ecosystems.

Pulsing Patterns in Observed Data

In the literature reviewed, several sources with fairly good time series were selected and their time series graphs were analyzed graphically, as discussed in the methods chapter, to extract general pulsing patterns in real systems. These included plankton records from Lake Okeechobee, Florida (Philips et al., 1993), Lake Mendota, Wisconsin (Lathrop and Carpenter, 1992a and 1992b), Lago Maggiore, Italy (de Bernardi et al., 1988), a microcosm (Kersting, 1985), Lake Kinneret, Israel (Berman et al., 1995), Chubut River, Argentina (Sastre et al., 1994), Gulf of Maine (Balch, 1981), St. Lawrence Estuary (Demers and Legendre, 1981), production estimate in Biosphere 2 (Kang and Engel, 1996), proxy time series of pelagic fish abundance in the California Current (Baumgartner et al., 1992), and vole population (Getz et al., 1997). The original graphs used in this analysis are included in Appendix A.

Figure 3-1 shows pulse amplitude as a function of interval between successive pulses for chlorophyll-a, phytoplankton, zooplankton, Biosphere 2 production, fishes, and a vole population. Pulse amplitude increased with interval between pulses. The pulsing

Figure 3-1. Relationship between pulse interval and amplitude in the observed data.

a),b),c)	Chlorophyll-a in Lake Okeechobee
d)	Chlorophyll-a in Lake Mendota
e)	Chlorophyll-a in Lago Maggiore
f)	Phytoplankton in a microcosm

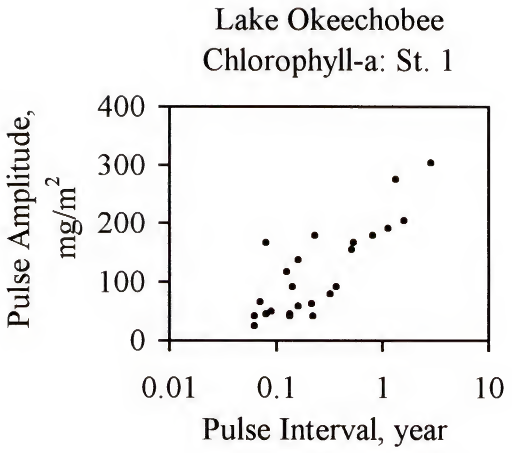
Lake Okeechobee
Chlorophyll-a: St. 1
Pulse Amplitude, mg/m^2
400
300
200
100
0
0.01
0.1
1
10
Pulse Interval, year

a)

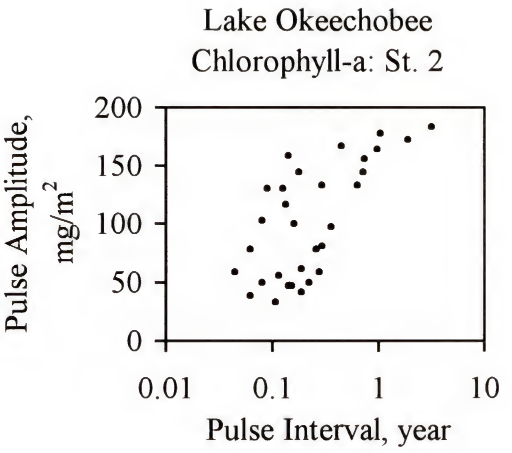
Lake Okeechobee
Chlorophyll-a: St. 2
Pulse Amplitude, mg/m^2
200
150
100
50
0
0.01
0.1
1
10
Pulse Interval, year

b)

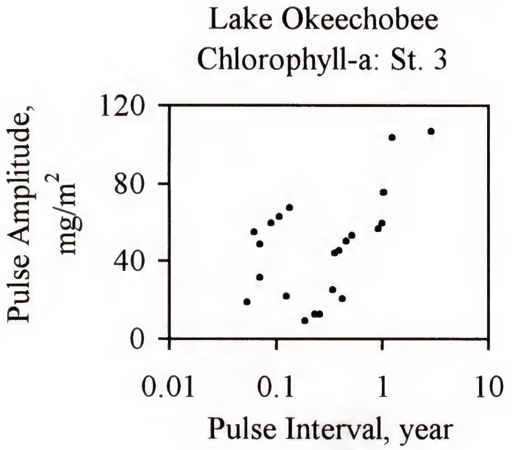
Lake Okeechobee
Chlorophyll-a: St. 3
Pulse Amplitude, mg/m^2
120
80
40
0
0.01
0.1
1
10
Pulse Interval, year

c)

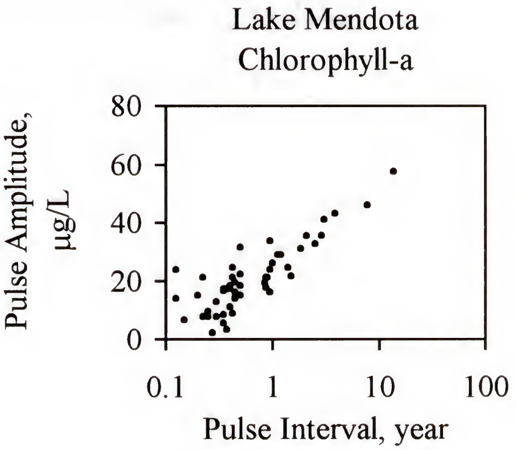
Lake Mendota
Chlorophyll-a
Pulse Amplitude, µg/L
80
60
40
20
0
0.1
1
10
100
Pulse Interval, year

d)

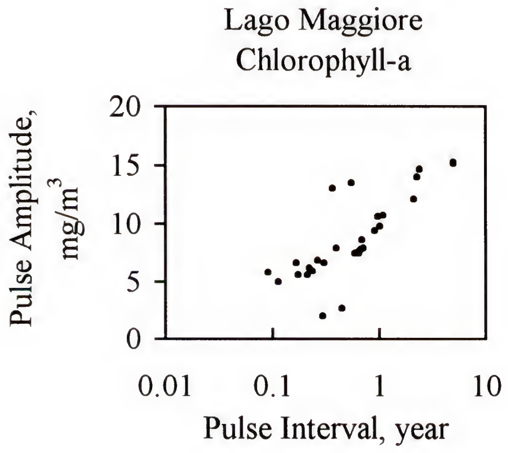
Lago Maggiore
Chlorophyll-a
Pulse Amplitude, mg/m^3
20
15
10
5
0
0.01
0.1
1
10
Pulse Interval, year

e)

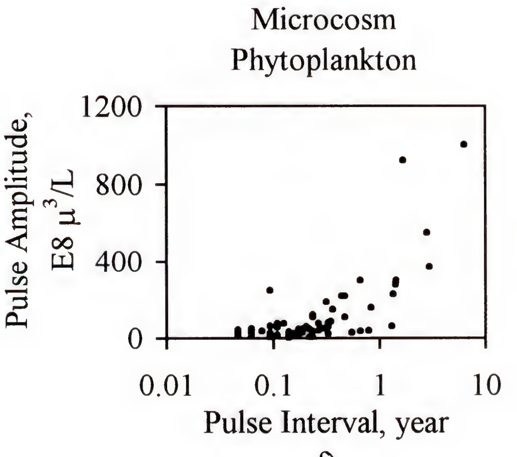
Microcosm
Phytoplankton
Pulse Amplitude, E8 µ^3/L
1200
800
400
0
0.01
0.1
1
10
Pulse Interval, year

f)

Figure 3-1. Continued

g)	Phytoplankton in Lake Mendota
h)	Phytoplankton in Lago Maggiore
i)	Phytoplankton in Lake Kinneret
j), k)	Phytoplankton in Chubut River
l)	Phytoplankton in Gulf of Maine

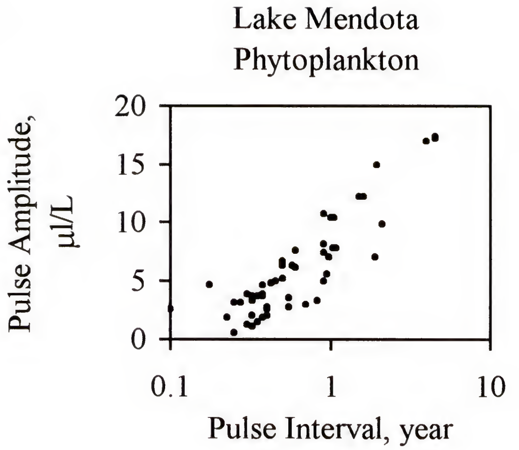
Lake Mendota
Phytoplankton
Pulse Amplitude,
µl/L
20
15
10
5
0
0.1
1
10
Pulse Interval, year

g)

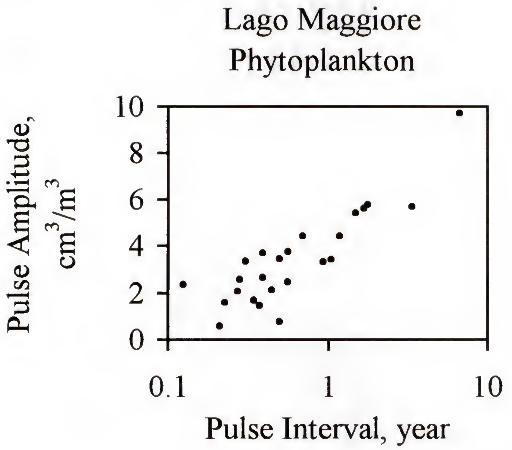
Lago Maggiore
Phytoplankton
Pulse Amplitude,
cm^3/m^3
10
8
6
4
2
0
0.1
1
10
Pulse Interval, year

h)

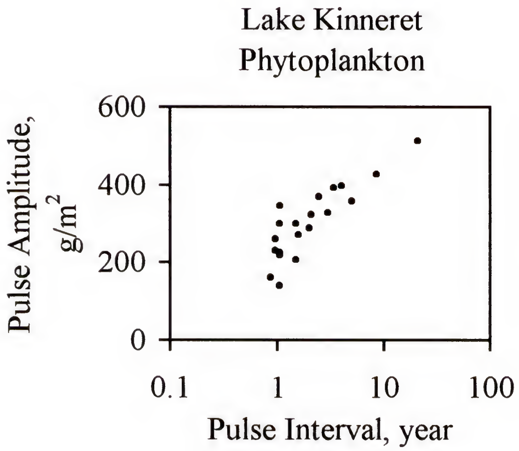
Lake Kinneret
Phytoplankton
Pulse Amplitude,
g/m^2
600
400
200
0
0.1
1
10
100
Pulse Interval, year

i)

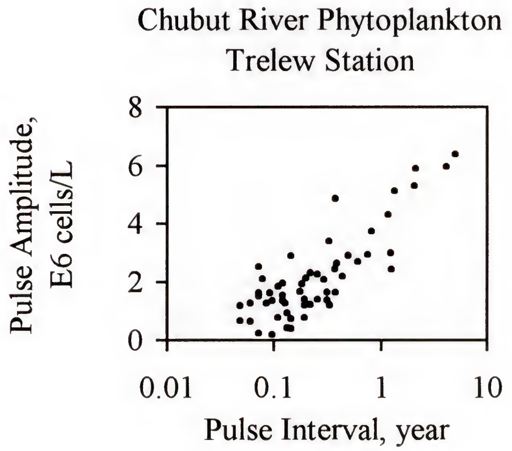
Chubut River Phytoplankton
Trelew Station
Pulse Amplitude,
E6 cells/L
8
6
4
2
0
0.01
0.1
1
10
Pulse Interval, year

j)

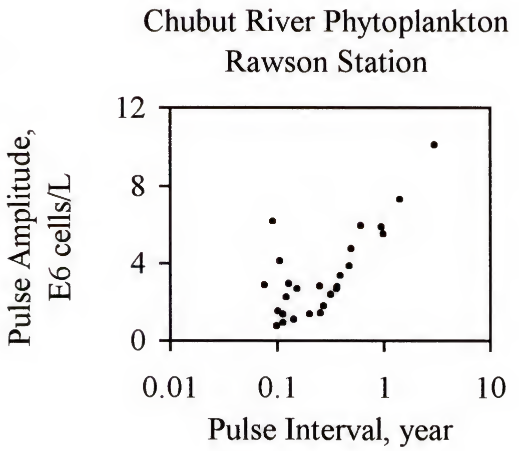
Chubut River Phytoplankton
Rawson Station
Pulse Amplitude,
E6 cells/L
12
8
4
0
0.01
0.1
1
10
Pulse Interval, year

k)

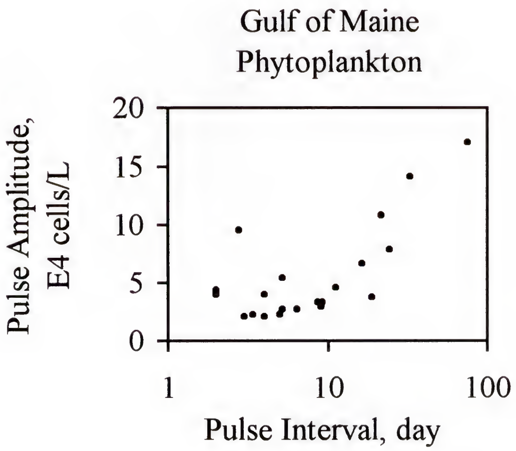
Gulf of Maine
Phytoplankton
Pulse Amplitude,
E4 cells/L
20
15
10
5
0
1
10
100
Pulse Interval, day

l)

Figure 3-1. Continued

m) Phytoplankton in St. Lawrence Estuary
n) Gross production in Biosphere2
o) Zooplankton in Lake Mendota
p) Northern anchovy
q) Pacific sardine
r) Vole population

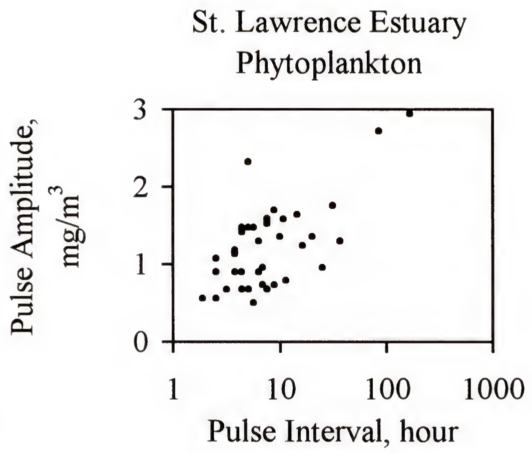
St. Lawrence Estuary
Phytoplankton
Pulse Amplitude,
mg/m^3
0
1
2
3
1
10
100
1000
Pulse Interval, hour

m)

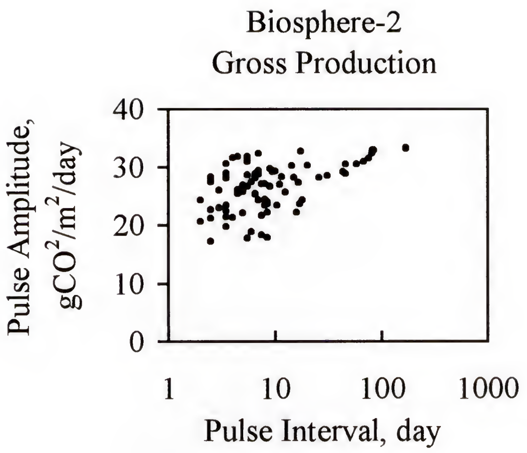
Biosphere-2
Gross Production
Pulse Amplitude,
gCO^2/m^2/day
0
10
20
30
40
1
10
100
1000
Pulse Interval, day

n)

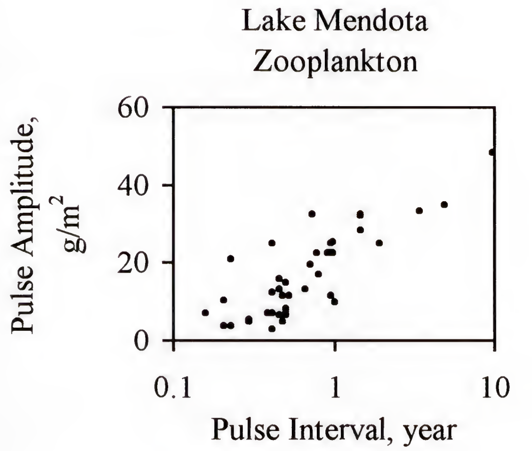
Lake Mendota
Zooplankton
Pulse Amplitude,
g/m^2
0
20
40
60
0.1
1
10
Pulse Interval, year

o)

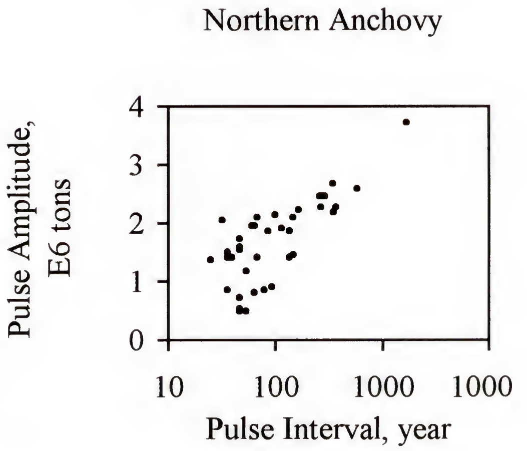
Northern Anchovy
Pulse Amplitude,
E6 tons
0
1
2
3
4
10
100
1000
1000
Pulse Interval, year

p)

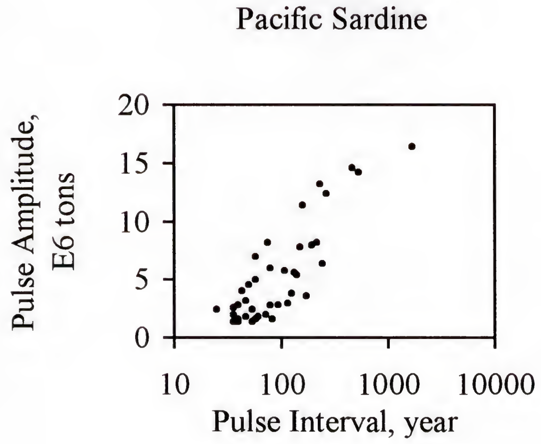
Pacific Sardine
Pulse Amplitude,
E6 tons
0
5
10
15
20
10
100
1000
10000
Pulse Interval, year

q)

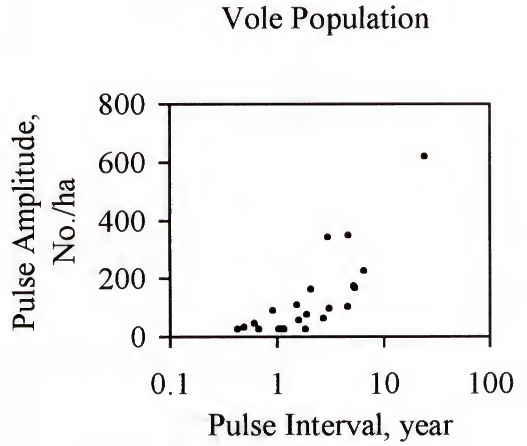
Vole Population
Pulse Amplitude,
No./ha
0
200
400
600
800
0.1
1
10
100
Pulse Interval, year

r)

hierarchy theory discussed in the introduction chapter seems to explain these results since larger pulses require more time between pulses. More time was required to accumulate stored energy to deliver larger pulses.

Each component in Figure 3-1, which spans several energy hierarchies, shows a range of pulse interval and amplitude. This appears to show that variations in time in each hierarchy could be results of concurrent pulsing on many scales in the energy hierarchy. Interconnected through energy transformations, components in each hierarchy receive required energy from the lower hierarchy and contribute to the higher hierarchy.

Also, according to the pulsing paradigm, bigger pulses deliver sharper effects than smaller ones do. This was measured as the ratio of time in pulse to pulse interval in Figure 3-2. Percent of time in pulse decreased as pulse amplitude increased, agreeing with the pulsing hierarchy theory.

In Figure 3-3, the graphs in Figure 3-1 were converted into frequency-size graphs, which can be seen in the literature in many fields. Pulse frequency was obtained by taking the inverse of the pulse interval. It shows a typical size-frequency relationship, even though more frequent, smaller pulses had a more scattered pattern. This could be partly due to errors involved in measuring pulse amplitude and interval on the figures in the literature. Also, lack of sufficient resolution in observations on smaller time scales could result in the scattered pattern in Figure 3-3.

Production Function and Power Inflow

To understand the characteristics of the multiplicative production function in drawing power into systems, two simple models with only two storages were constructed in Figure 3-4 and Figure 3-5, following Alexander (1978) and McGrane (1998). These may be the simplest ways of representing real systems of production and recycle, such as the whole earth system and a microcosm without any material inflow and outflow.

Figure 3-2. Relationship between pulse interval and percent of time in pulse in the observed data.

a),b),c)	Chlorophyll-a in Lake Okeechobee
d)	Chlorophyll-a in Lake Mendota
e)	Chlorophyll-a in Lago Maggiore
f)	Phytoplankton in a microcosm

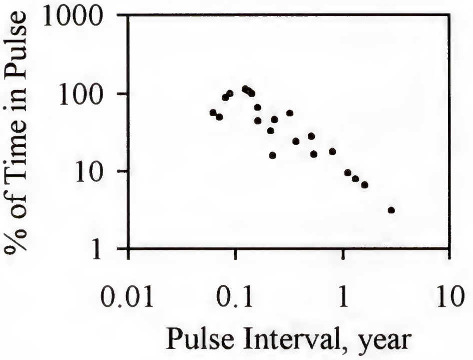
Lake Okeechobee
Chlorophyll-a: St. 1

a)

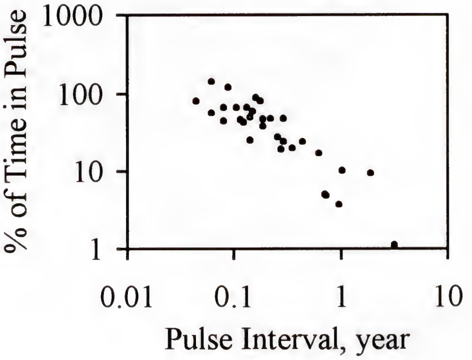
Lake Okeechobee
Chlorophyll-a: St. 2

b)

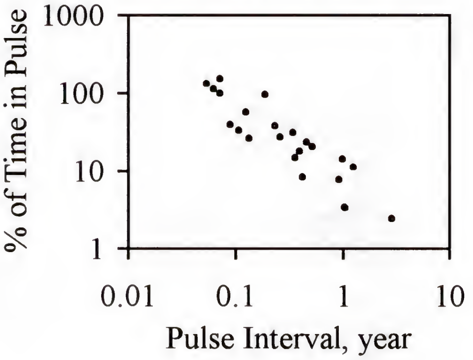
Lake Okeechobee
Chlorophyll-a: St. 3

c)

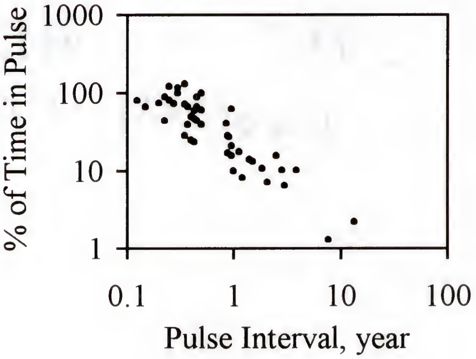
Lake Mendota
Chlorophyll-a

d)

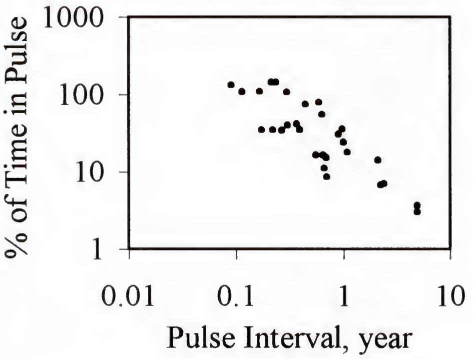
Lago Maggiore
Chlorophyll-a

e)

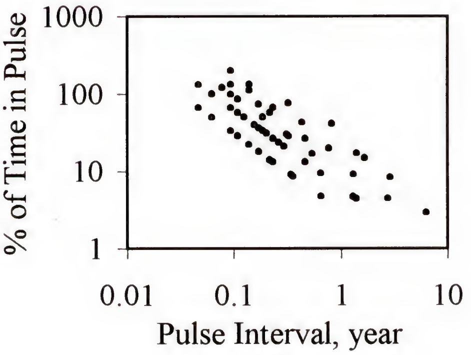
Microcosm
Phytoplankton

f)

Figure 3-2. Continued

g)	Phytoplankton in Lake Mendota
h)	Phytoplankton in Lago Maggiore
i)	Phytoplankton in Lake Kinneret
j), k)	Phytoplankton in Chubut River
l)	Phytoplankton in Gulf of Maine

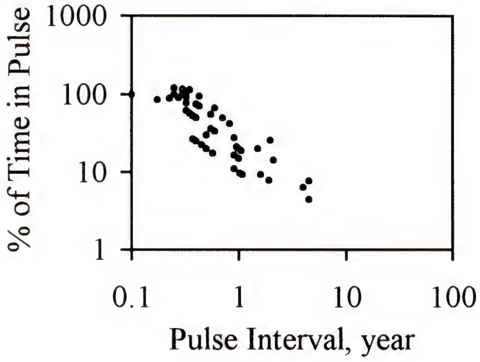

Lake Mendota Phytoplankton

g)

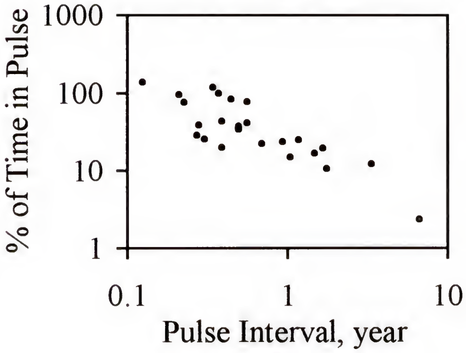

Lago Maggiore Phytoplankton

h)

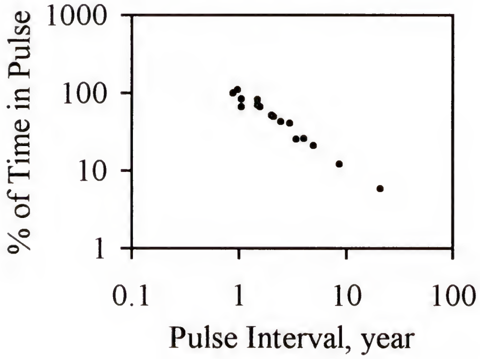

Lake Kinneret Phytoplankton

i)

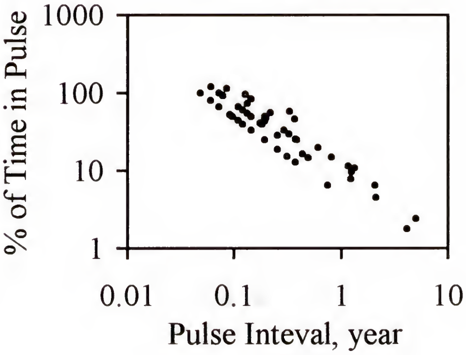

Chuhut River Phytoplankton Trelew Station

j)

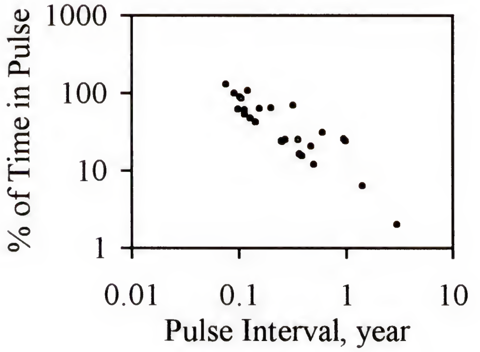

Chuhut River Phytoplankton Rawson Station

k)

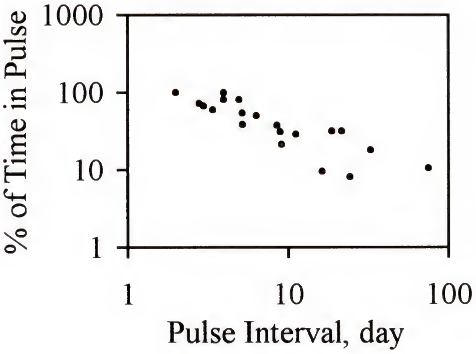

Gulf of Maine Phytoplankton

l)

Figure 3-2. Continued

m) Phytoplankton in St. Lawrence Estuary
n) Gross production in Biosphere2
o) Zooplankton in Lake Mendota
p) Northern anchovy
q) Pacific sardine
r) Vole population

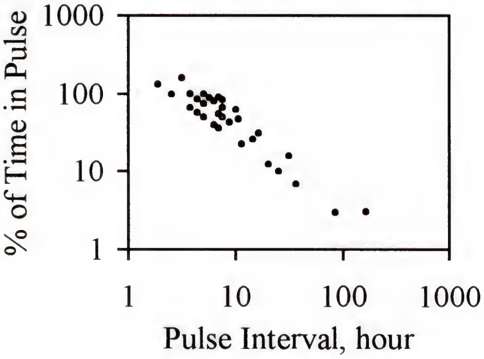
St. Lawrence Estuary Phytoplankton

n)

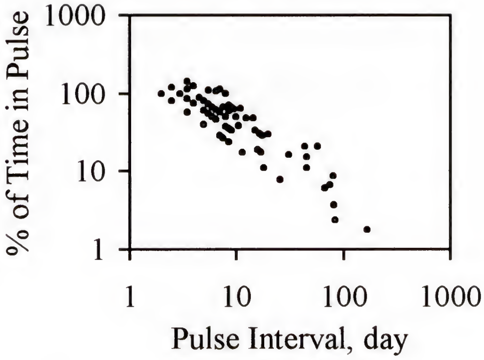
Biosphere-2 Gross Production

n)

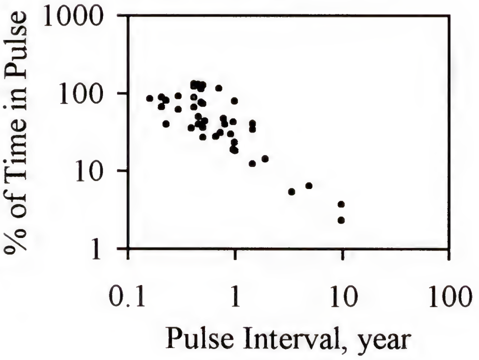
Lake Mendota Zooplankton

o)

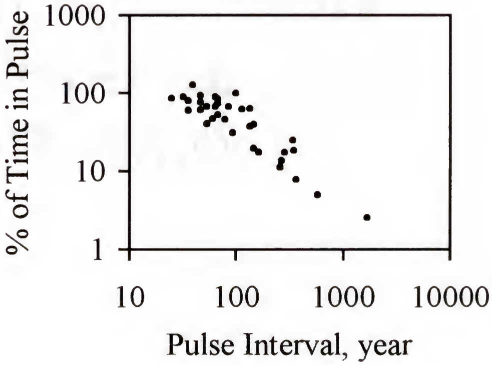
Northern Anchovy

p)

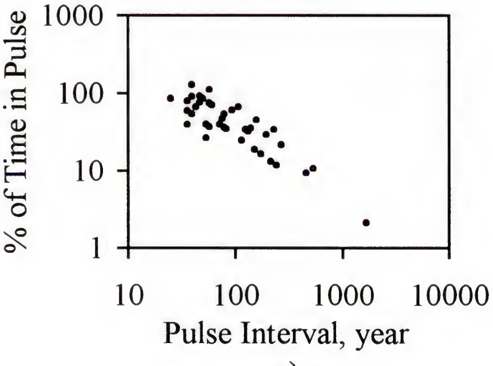
Pacific Sardine

q)

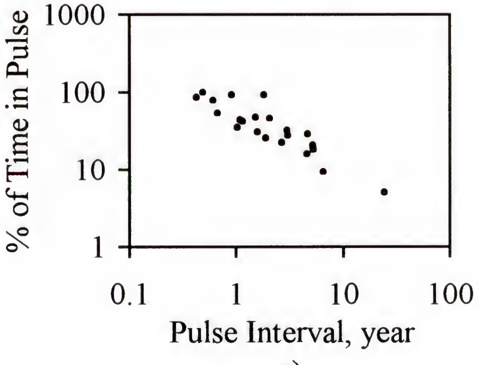
Vole Population

r)

Figure 3-3. Relationship between pulse amplitude and frequency in the observed data.

a),b),c)	Chlorophyll-a in Lake Okeechobee
d)	Chlorophyll-a in Lake Mendota
e)	Chlorophyll-a in Lago Maggiore
f)	Phytoplankton in a microcosm

Lake Okeechobee
Chlorophyll-a: St. 1

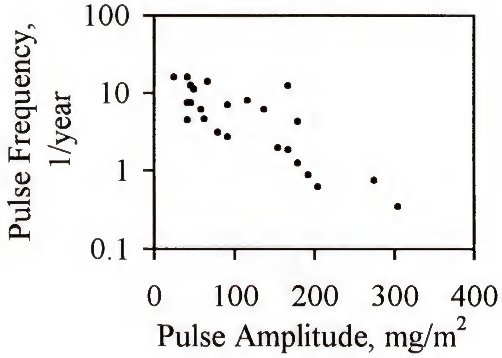

a)

Lake Okeechobee
Chlorophyll-a: St. 2

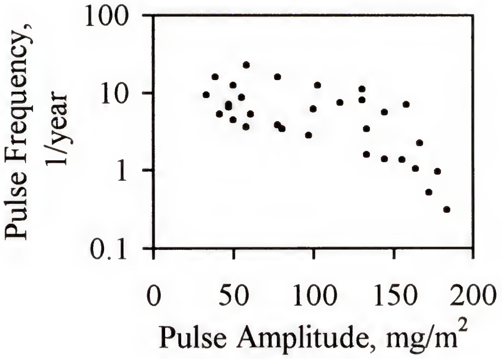

b)

Lake Okeechobee
Chlorophyll-a: St. 3

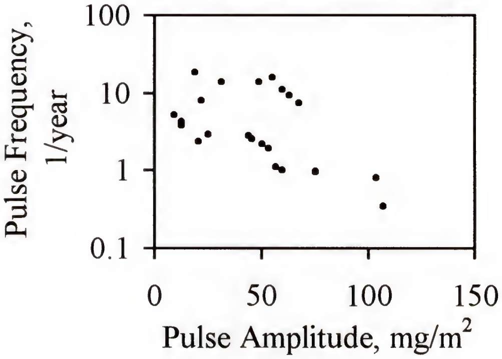

d)

Lake Mendota
Chlorophyll-a

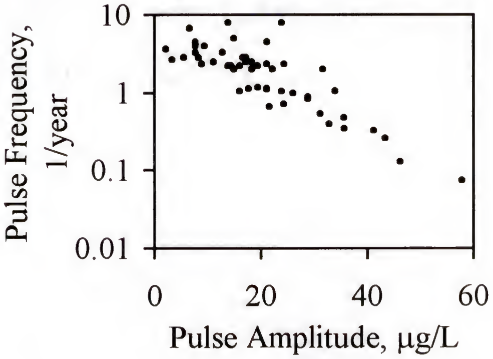

d)

Lago Maggiore
Chlorophyll-a

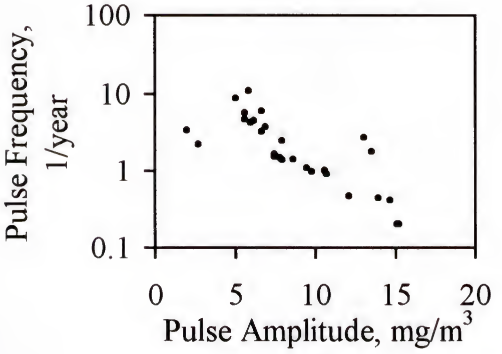

e)

Microcosm
Phytoplankton

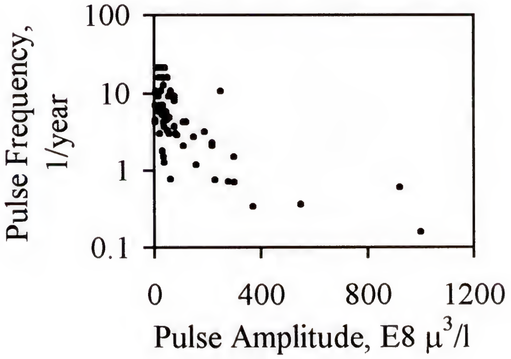

f)

Figure 3-3. Continued

g)	Phytoplankton in Lake Mendota
h)	Phytoplankton in Lago Maggiore
i)	Phytoplankton in Lake Kinneret
j), k)	Phytoplankton in Chubut River
l)	Phytoplankton in Gulf of Maine

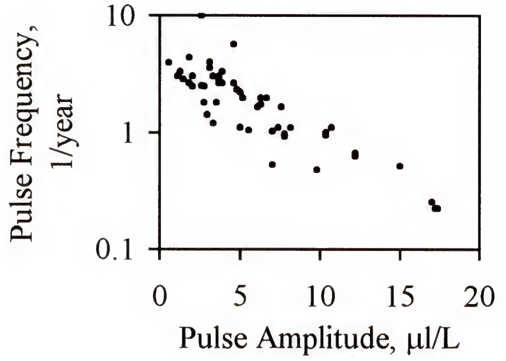

Lake Mendota
Phytoplankton

g)

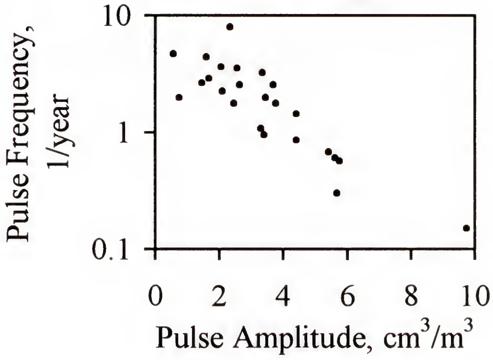

Lago Maggiore
Phytoplankton

h)

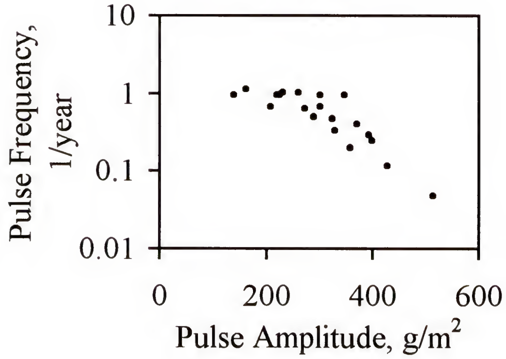

Lake Kinneret
Phytoplankton

i)

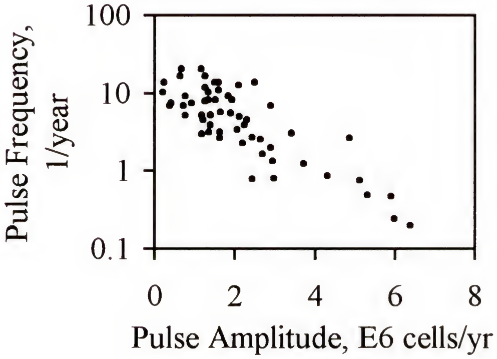

Chubut River Phytoplankton
Trelew Station

j)

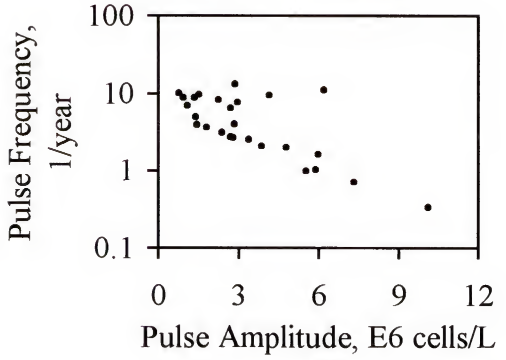

Chubut River Phytoplankton
Rawson Station

k)

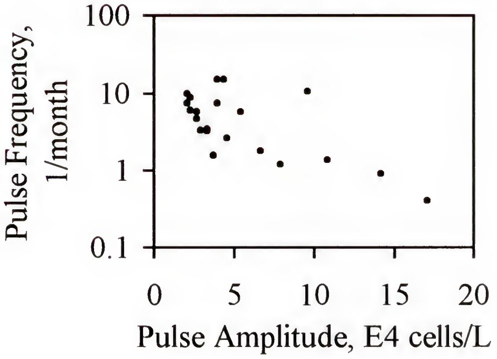

Gulf of Maine
Phytoplankton

l)

Figure 3-3. Continued

m)	Phytoplankton in St. Lawrence Estuary
n)	Gross production in Biosphere2
o)	Zooplankton in Lake Mendota
p)	Northern anchovy
q)	Pacific sardine
r)	Vole population

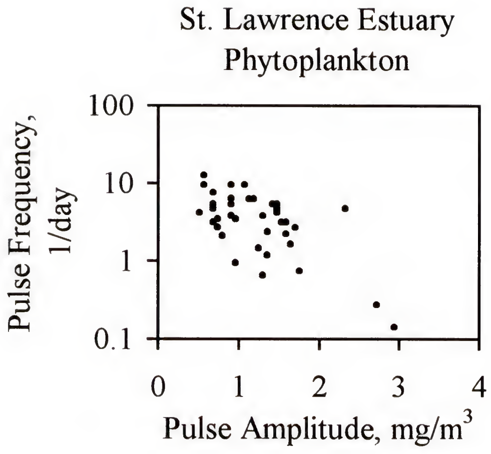
St. Lawrence Estuary
Phytoplankton
Pulse Frequency, 1/day
100
10
1
0.1
0
1
2
3
4
Pulse Amplitude, mg/m3

m)

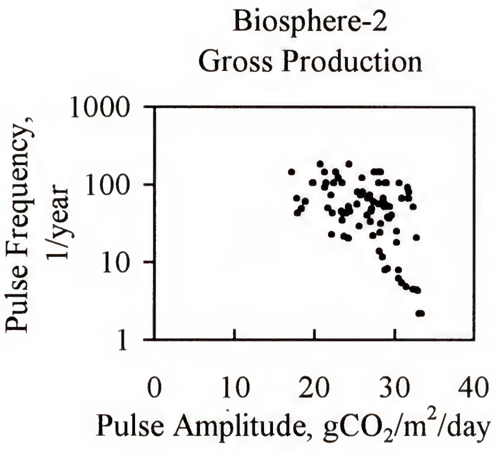
Biosphere-2
Gross Production
Pulse Frequency, 1/year
1000
100
10
1
0
10
20
30
40
Pulse Amplitude, gCO2/m2/day

n)

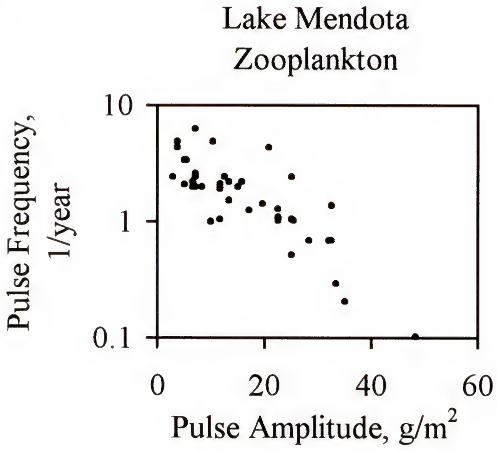
Lake Mendota
Zooplankton
Pulse Frequency, 1/year
10
1
0.1
0
20
40
60
Pulse Amplitude, g/m2

o)

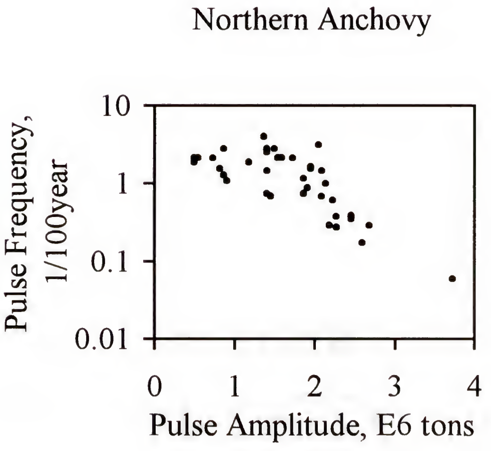
Northern Anchovy
Pulse Frequency, 1/100year
10
1
0.1
0.01
0
1
2
3
4
Pulse Amplitude, E6 tons

p)

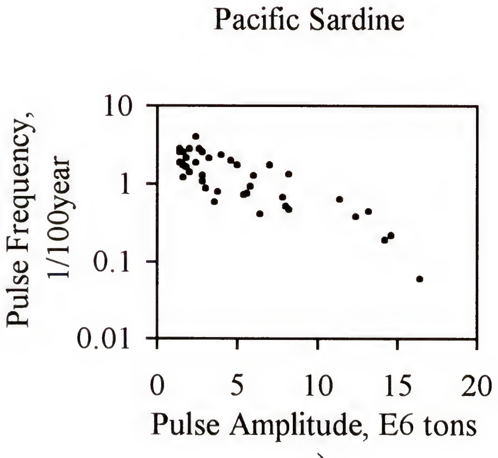
Pacific Sardine
Pulse Frequency, 1/100year
10
1
0.1
0.01
0
5
10
15
20
Pulse Amplitude, E6 tons

q)

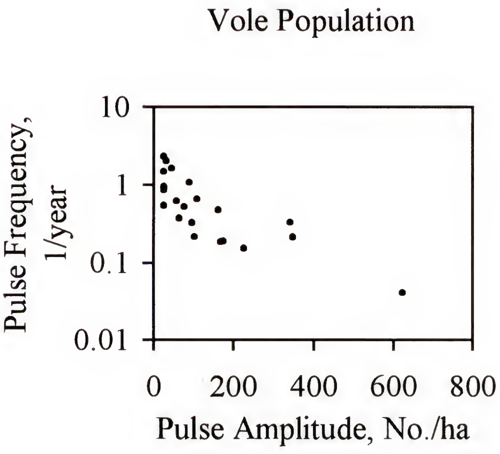
Vole Population
Pulse Frequency, 1/year
10
1
0.1
0.01
0
200
400
600
800
Pulse Amplitude, No./ha

r)

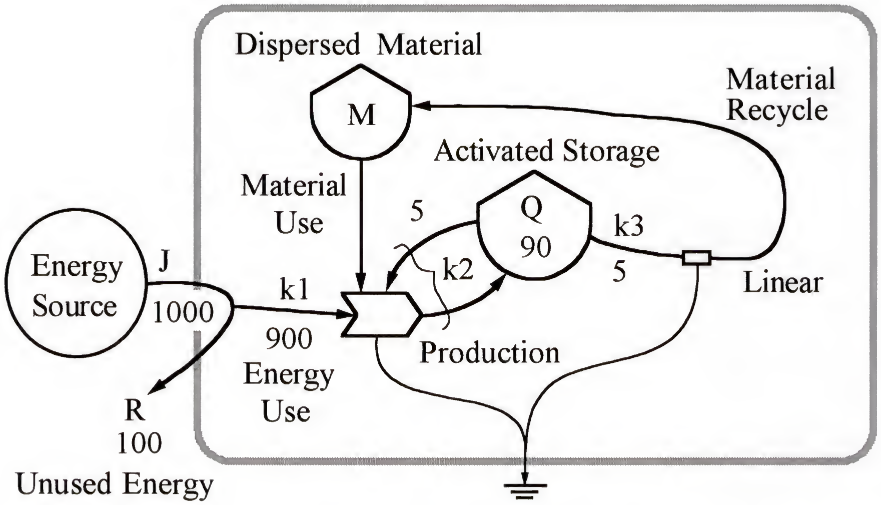

$M = MT - f*Q; MT = 15; f = 0.15$

Power Inflow, $J1 = k1*R*M*Q$

$R = J / (1 + k1*M*Q)$

$dQ = k2*R*M*Q - k3*Q$

Figure 3-4. Systems diagram of the simple two storage model with a flow limited energy source and the linear recycle pathway (k3), to investigate characteristics of the production function in relation to power inflow. Calibration values are given in steady state. MT = Total material inside the system; f = Material fraction of the activated storage (Q).

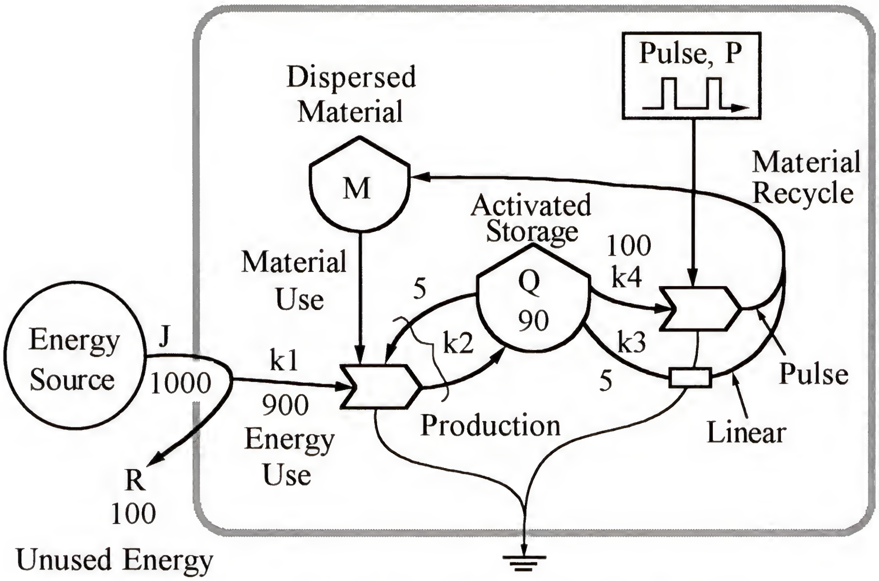

M = MT - f*Q; MT = 15; f = 0.15

Power Inflow, J1 = k1*R*M*Q

R = J / (1 + k1*M*Q)

dQ = k2*R*M*Q - k3*Q - k4*Q*P

Figure 3-5. Systems diagram of the simple two storage model as in Figure 3-4, but with an additional recycle pathway (k4) by an internal pulsing mechanism. Pulsing is given as a step function which turns on the additional material recycle at a given time interval. MT = Total material inside the system; f = Material fraction of the activated storage (Q).

Models by Alexander and McGrane were extended for more general cases and for investigating effects of pulsing amplitude and frequency. Both Alexander and McGrane represented the activated storage consisting only of material upgraded through the production process, which is true for some cases. To be more realistic, only a fraction of the activated storage (Q) was considered as material in the models in Figures 3-4 and 3-5. Thus, instead of plotting power inflow against the activated storage (Q) as in McGrane (1998), power draw is investigated as a function of the dispersed material (M) in the following.

In both models in Figures 3-4 and 3-5, the dispersed material (M) is transformed through an autocatalytic production process into the activated storage (Q), using a flow limited energy source (J). Material bound up in the activated storage recycles back through the linear pathway (k3) in the model in Figure 3-4, while energy is used up in the process. The model in Figure 3-5 has two different recycle pathways; linear pathway (k3) as in Figure 3-4 and pulse recycle pathway (k4). In this model, pulsing is considered as an already established internal mechanism to compare two different systems on the same energy and emergy input basis. The internal pulsing mechanism activates the recycle pathway (k4) for a short time period at a given time interval, and the rate is determined by a specified intensity of the pulsing mechanism. For simplicity, the model in Figure 3-5 does not include any energy support for the pulsing mechanism that might be required to maintain it. Material is conserved inside the systems, that is, $M+f*Q = MT =$ constant. Because both models have only one energy source, empower is proportional to power. In the following, power is measured to compare performance of different model cases.

For simulation, the models in Figures 3-4 and 3-5 were calibrated using flow and storage values on each diagram. Calibration values for the steady model in Figure 3-4 are given in Appendix Table B-1. The pulse model in Figure 3-5 used the same calibration values in Appendix Table B-1. For the pulsing recycle pathway (k4), the same coefficient for the linear pathway (k3) was used, but the pulsing mechanism recycles material through this pathway at much higher rate than through the linear pathway. Both models are calibrated at steady state. Computer programs written in BASIC are listed in Appendix Table C-1 for the steady model in Figure 3-4 and in Appendix Table C-2 for the pulse model in Figure 3-5.

There are two different calibration cases in Appendix Table B-1 to look at the effects of the amount of the dispersed material at steady state, that is, at calibration, in drawing power: material fraction of Q, f = 0.15 and 0.05. These numbers were selected based on McGrane (1998). In the first case (f=0.15), the dispersed material storage has 10% of total material (MT) at steady state. This represented a case in which the pre-pulse value of the material storage was less than 50% of total material. The dispersed material storage contains 70% of total material in the second case of f=0.05, at steady state. In this case, the pre-pulse value of the material storage was greater than 50% of total material.

Simulation results of both steady and pulsing recycle models are given in Figure 3-6 when the material fraction of the activated storage was set at 0.15. Both models showed maximum power inflow at the moment when 50% of the total material was in the dispersed storage and the remaining 50% in the activated storage (see also Figure 3-8). Even though average Q over the simulation period was lower, the system with pulsing recycle drew in more total power (ΣJ1) than the steady state configuration. In this case, pulsing maintained the level of the dispersed storage closer to the 50% level, resulting in more total power draw; average 20.3% in the pulsing model and 11.7% in the steady model.

Figure 3-7 shows simulation results when both steady and pulsing models were calibrated for f=0.05, that is, 70% of total material in the dispersed material storage. Maximum instantaneous power inflow was achieved when the dispersed material storage had 70% of total material (see also Figure 3-8). This is the lowest level of the dispersed material that can be obtained under the given calibration conditions in Figures 3-4 and 3-5. The pulsing model drew less total power than the model without it. More material (74.7%

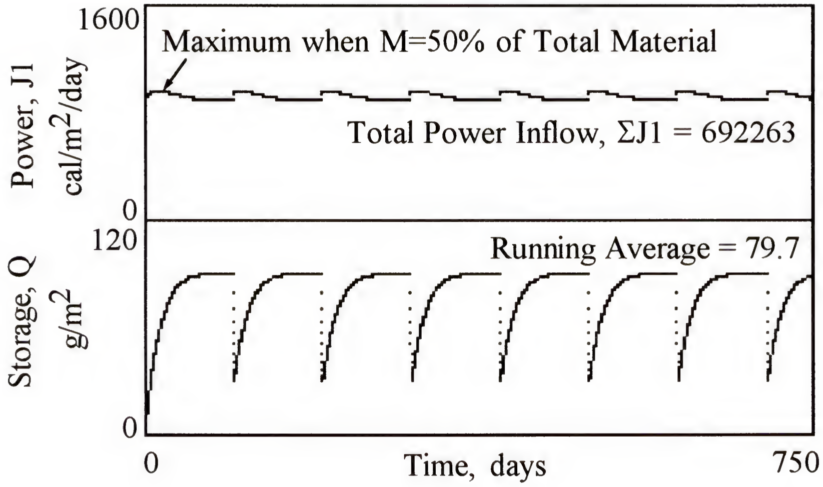

a)

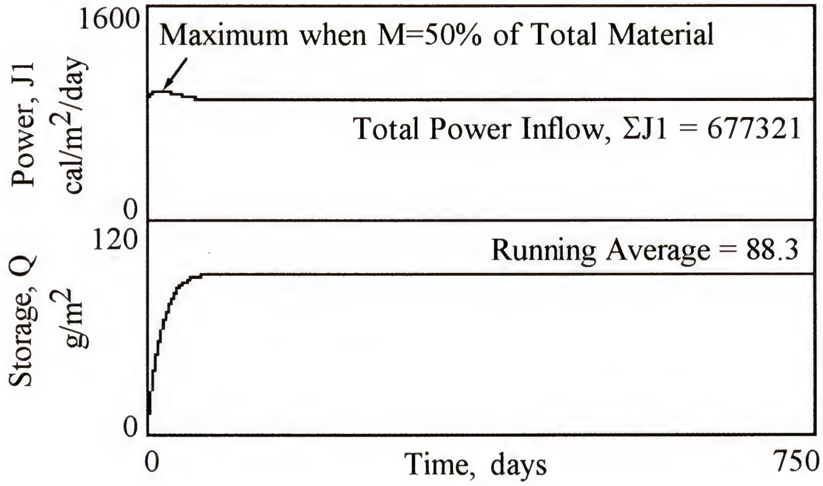

b)

Figure 3-6. Simulation results of the pulse model in Figure 3-5 (a) and the steady model in Figure 3-4 (b), when material fraction (f) of the activated storage (Q) is 0.15.

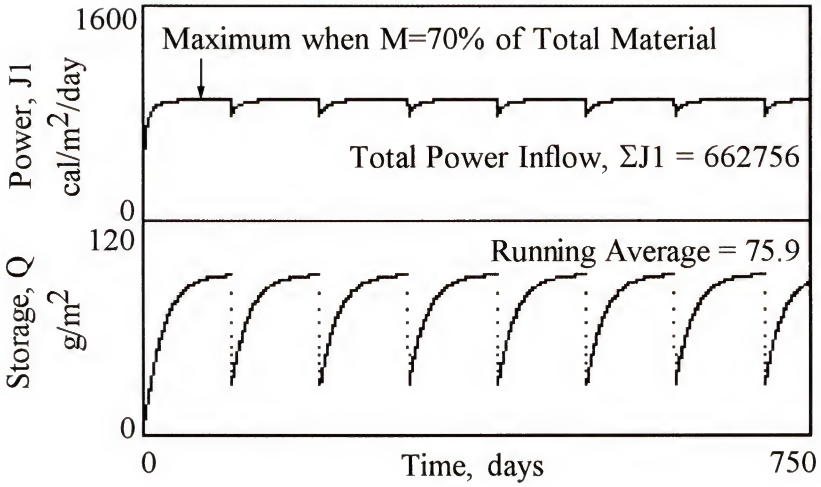

a)

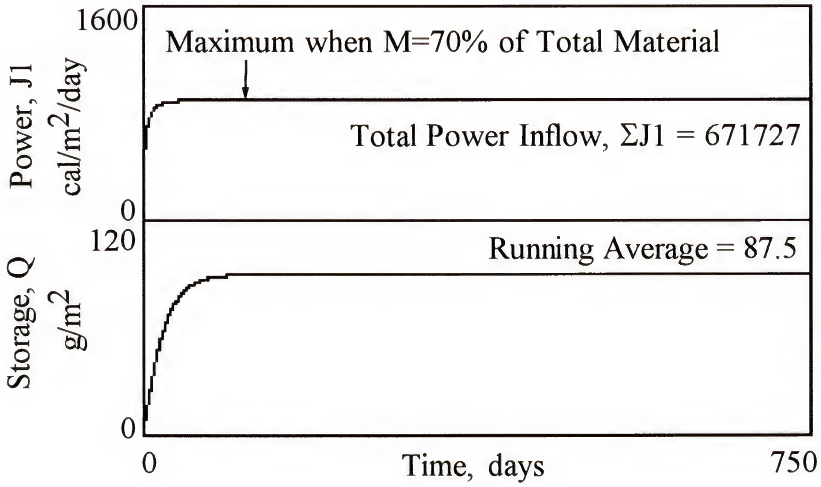

b)

Figure 3-7. Simulation results of the pulse model in Figure 3-5 (a) and the steady model in Figure 3-4 (b), when material fraction (f) of the activated storage (Q) is 0.05.

of total material) on the average stayed in the dispersed material storage in the pulsing model than in the steady model (70.8%).

In Figure 3-8a, power inflow (J1) was plotted as a function of the dispersed material over the simulation period, for both calibration cases of f=0.15 and 0.05. It shows clearly the relationship between the amount of total material in the dispersed material storage and the power inflow to the system. The amount of material in the dispersed storage at steady state determined the level of maximum power inflow. Equation for the power inflow (J1) is given in Figure 3-8b as a function of the dispersed material by expressing other variables (R and Q) in terms of the dispersed material (M). Solving the differentiated equation with respect to M for local minimum or maximum yielded M=MT/2, agreeing with the simulation results in Figures 3-7 and 3-8. Power inflow, J1, was maximum when the dispersed material, M, was a half of total material, MT.

The pulse model in Figure 3-5 was simulated with varying pulse amplitudes (Figure 3-9a) and intervals (Figure 3-9b), and total power inflow was compared with that of the steady model. In the system calibrated for f=0.05 (70% of total material in M), total power inflow decreased with increase in pulse amplitude (Figure 3-9a) and with decrease in pulse interval (Figure 3-9b). In other words, lower pulse amplitude and longer pulse interval enabled the system to maintain its average material storage level close to 50%, drawing in more power. For the system calibrated for f=0.15 (10% of total material in M), there was an optimum level of pulse amplitude (Figure 3-9a) and interval (Figure 3-9b), even though it was less distinct in the case of pulse amplitude variation. There was an optimum pulse level which maintained the dispersed material storage close to 50% of total material. Both results show that pulsing would maximize total power inflow for the system calibrated so that long term average of material content in the dispersed storage is less than 50%, depending on the pulse amplitudes and intervals, but not for the systems calibrated over 50%.

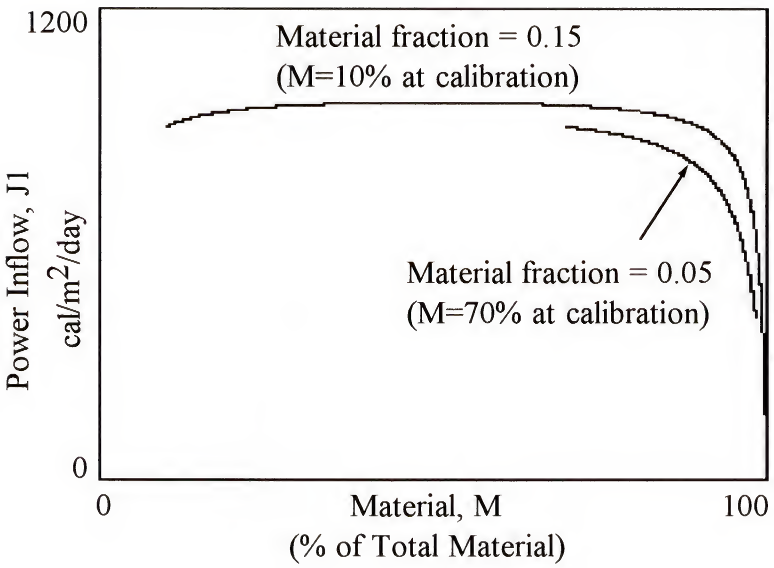

a)

Power Inflow

$$J1 = k1*R*M*Q \tag{1}$$

Remaining Energy

$$R = J / (1 + k1*M*Q) \tag{2}$$

Activated Storage as a function of material, M

$$MT = M + f*Q$$

$$\text{Thus, } Q = (MT - M) / f \tag{3}$$

Substituting for (2) and (3) into (1)

$$J1 = \frac{K*J*MT*M \; - \; K*J*M^2}{1 \; + \; K*MT*M \; - \; K*M^2} \quad \text{, where } K = k1/f \tag{4}$$

Differentiating equation (4) with respect to M,

$$dJ1/dM = \frac{K*J*MT \; - \; 2*K*J*M}{(K*J*MT*M \; - \; K*J*M^2 \;)(1 \; + \; K*MT*M \; - \; K*M^2)} \tag{5}$$

b)

Figure 3-8. Power inflow as a function of the dispersed material (M). a) Simulation results of the models in Figures 3-4 and 3-5. Dispersed material is given as the percentage of the total material; b) Equations of the power inflow (J1) as a function of the dispersed material.

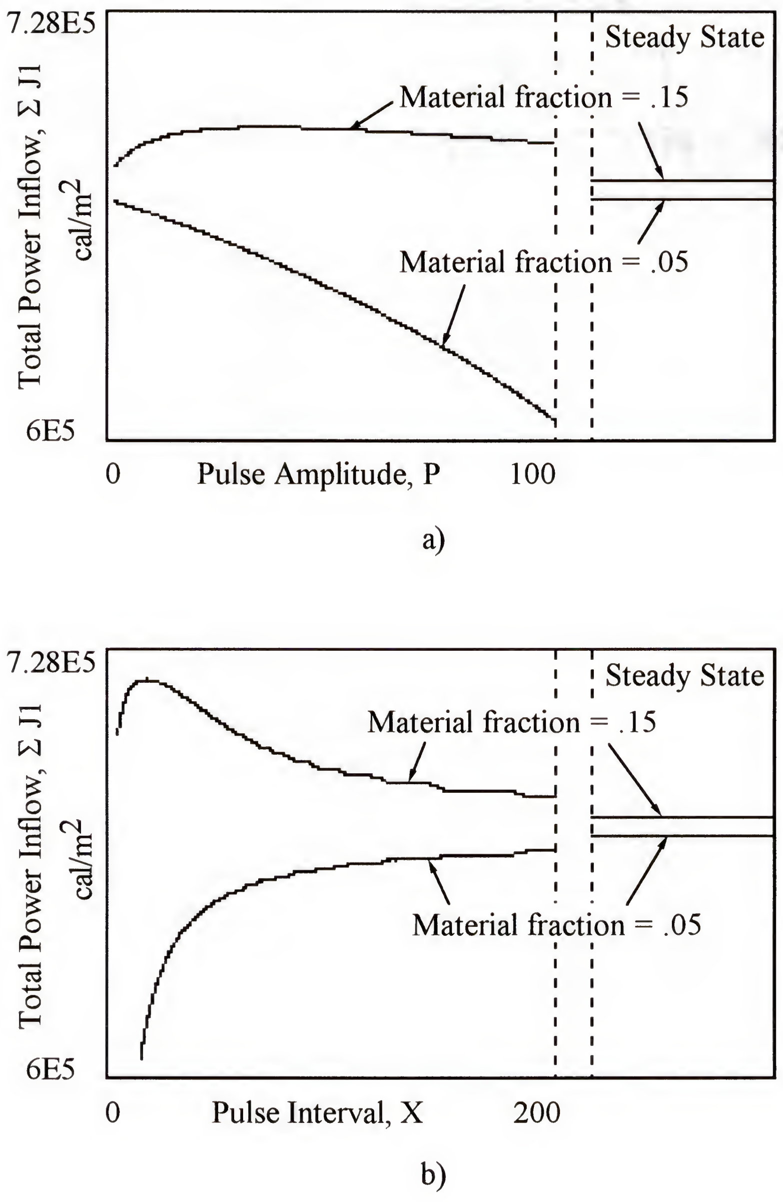

Figure 3-9. Effects of variations in pulse amplitude (a) and pulse interval (b) on the total power inflow in the pulse model in Figure 3-5. In each case, two different material fractions of the activated storage (Q) were compared with those in the steady model in Figure 3-4.

Figure 3-10 clearly shows the effect of the calibration conditions, that is, the material fraction of the activated storage and, thus, material content in the dispersed storage. It shows that there is a material fraction above which pulsing draws in more power than in the steady state model. It will depend on the level of pulse amplitudes and intervals.

Basic Pulse Model

The basic pulse model (Figures 1-7, 2-4, and 2-5) is the simplest model that was used to develop more complex pulsing models in this dissertation. This model was used in the methods chapter to illustrate the methodology used in this dissertation. Figures 2-4 and 2-5 are the energy systems diagrams of the model. The model was calibrated in Table 2-1 and the computer program is listed in Table 2-2.

Base Run

The base run of the basic pulse model in Figure 2-7 generated a typical pattern of pulsing dynamics. The producer storage (P) increased using input energy (J) and material (M). The consumer (H) grew slowly through the linear pathway (k4) until the producer reached a certain level, after which first the autocatalytic pathway (k6) and then the quadratic autocatalytic pathway (k8) took over to pulse. Material (M) was recycled after pulsed consumption by the consumer unit, providing necessary material for the primary production to start over again.

Figure 3-11 shows the base run of emergy and transformity simulation of the basic pulse model in Figure 2-4. Emergy storage (Figure 3-11a) of both producer (EP) and consumer (EH) units followed the same pattern of energy storage in Figure 2-7. Plateaus in the emergy storage of the producer reflect the 5% limitation imposed in the computer program for noises from the smaller scales, as explained in the methods chapter.

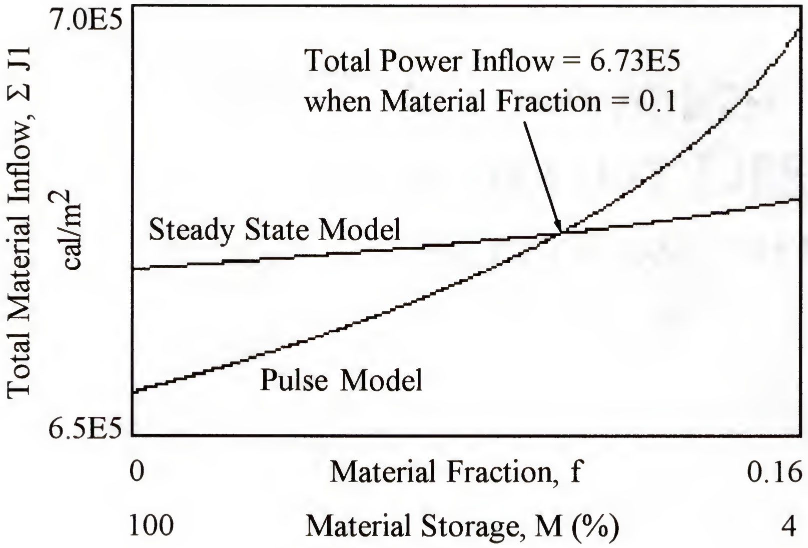

Figure 3-10. Effects of change in the material fraction (f) of the activated storage (Q) which was used to calibrate the model in Figures 3-4 and 3-5, on the total power inflow. Pulse interval and amplitude for the base case in Figure 3-5 were used in this simulation: Pulse interval (X) = 100 and amplitude (P) = 20.

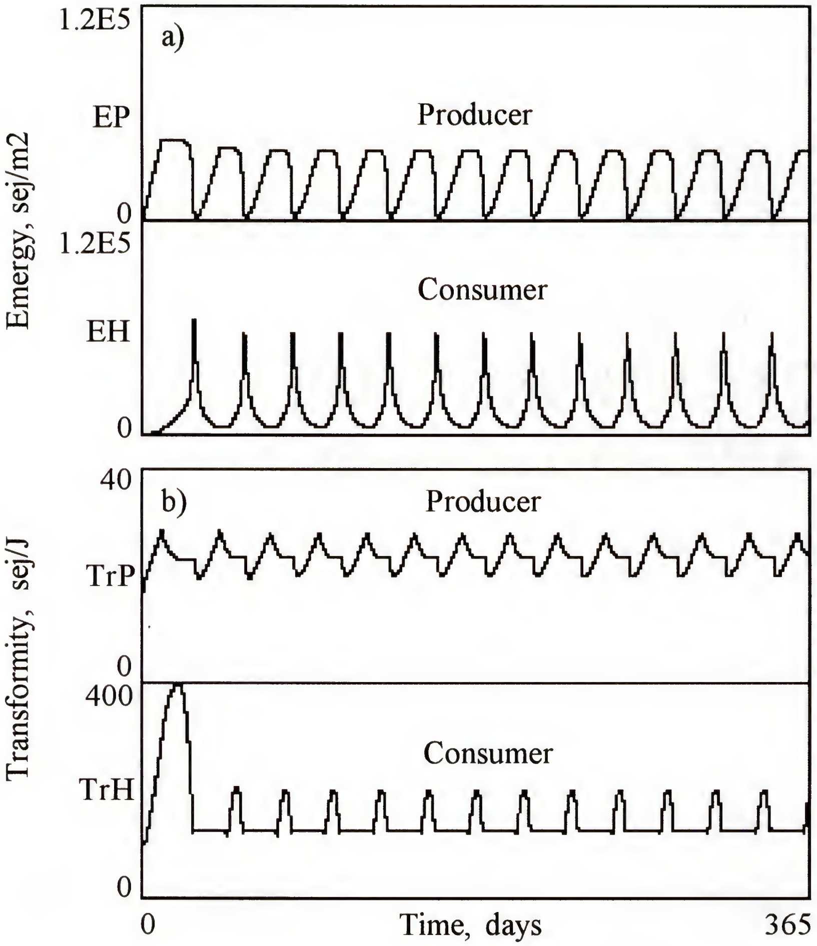

Figure 3-11. Emergy (a) and transformity (b) simulation of the basic pulse model in Figure 2-4.

Even though the transformities (Figure 3-11b) of producer and consumer storages reflected the pulsing pattern in energy (Figure 2-7) and emergy (Figure 3-11a), they did not reach maximum values at the same time as energy and emergy storages. The transformity of the producer storage increased while the emergy storage of the producer increased, reaching maximum at the point where the emergy storage leveled off. The transformity of the producer decreased right after reaching its maximum because the energy storage was increasing while the emergy storage was not changing. Transformity of a storage is obtained by dividing emergy content of the storage by its energy content. When the producer storage reached a peak value, transformity did not change because there were no changes in both energy and emergy storages. Also, during the decay phase of the producer storage, the transformity of the producer did not change because in this period change in emergy is proportional to change in energy content (see Figure 2-6).

The transformity of the consumer storage (Figure 3-11b) pulses during the growth phase of the storage through the autocatalytic and quadratic autocatalytic pathways. It reached maximum in the middle part of the growth phase because growth rate of emergy is faster than that of energy storage. Notice that the base of the emergy simulation in Figure 3-11a is more symmetrical than that of energy in Figure 2-7. The transformity of the consumer did not change during the growth period through the linear pathway because both storages did not change much over this period, and during the decay period because the rate of change in both storages was the same (see Figure 2-6).

Figure 3-12a shows the pattern of primary production (J2) and percent power use (PPU) in the base run of the basic pulse model in Figure 2-4. Percent power use is the percentage of input energy source (J) used in the system (J1); that is, PPU = (J1/J)*100. Both followed the pattern of producer storage variation. Highest primary production and power use occurred before the producer storage reached its peak point, when the material storage (M) was about 46% of total material (MT=50). Average percent power use was 87.5% over the simulation period of one year.

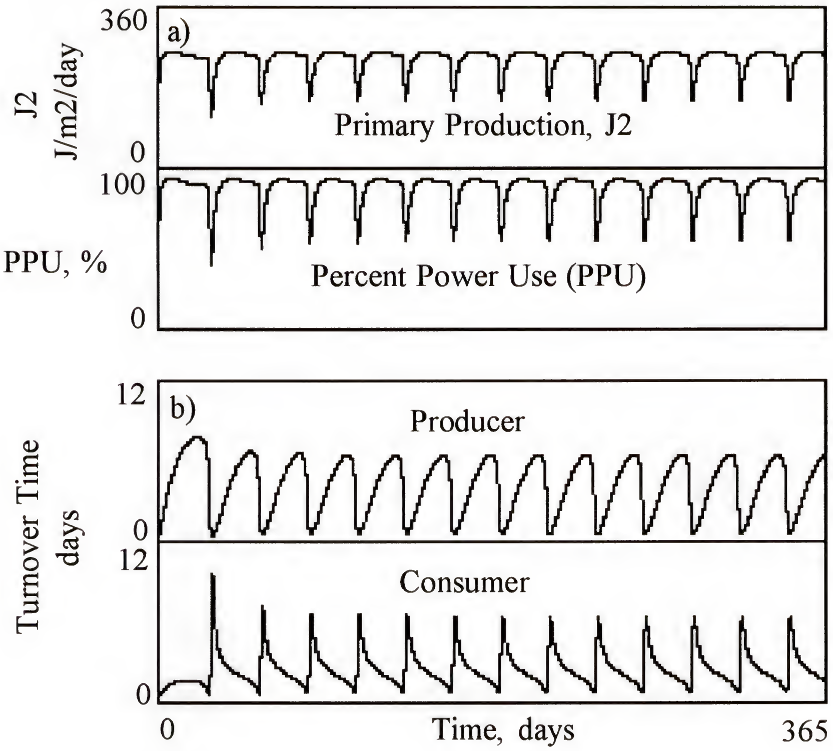

Figure 3-12. Changes in primary production (J2) and percent power use (a) and the turnover time of producer (P) and consumer (H) in the base run of the basic pulse model in Figure 2-4. Percent power use is the percentage of power inflow (J1) used in primary production (J2). Turnover time of each storage is the amount of stored quantity divided by the sum of the inflows to each storage.

Figure 3-12b shows dynamic changes in turnover time of the producer and consumer storages. Among various ways of calculating turnover times in Figure 2-4, turnover times in this base simulation were calculated as the amount of stored quantity divided by total inflows; that is, turnover time of producer = P / J2 and turnover time of consumer = H / (J4+J6+J8). The turnover time of the producer storage followed the pattern of energy storage of the producer (Figure 2-7), turning over more slowly as the storage increased. In contrast, consumer turned over less frequently while it was growing through the linear pathway. The turnover time of the consumer storage decreased as the storage built up, turning over more frequently than the producer during fast growth.

Variation in Energy Input

In Figures 3-13 and 3-14, the basic pulse model in Figure 2-4 was simulated with varying energy input (J) to the system. Average storage of the producer decreased as the energy level increased (Figure 3-13). In contrast, the average consumer storage increased with the energy level. Percent power use decreased with increase in the energy level. The model pulsed for energy inputs from 3900 to 5200. Within this range, pulsing frequency increased as the energy level went up. At low energy level (J=3500), slow growth of the producer did not allow the consumer to build enough storage against depreciation flow (k10), and the autocatalytic and quadratic autocatalytic pathways could not develop for pulsing to occur. The consumer storage leveled off at a very low value. Much of the material was tied up in the producer storage.

At a high energy level (J=5500), the model system showed damped oscillation. The producer started to grow before the consumer storage reached the lowest point after the first pulse, because of a faster growth rate at the higher energy levels. As the simulation continued, the producer storage did not grow to the previous level because available material for production was smaller with material tied up in the consumer

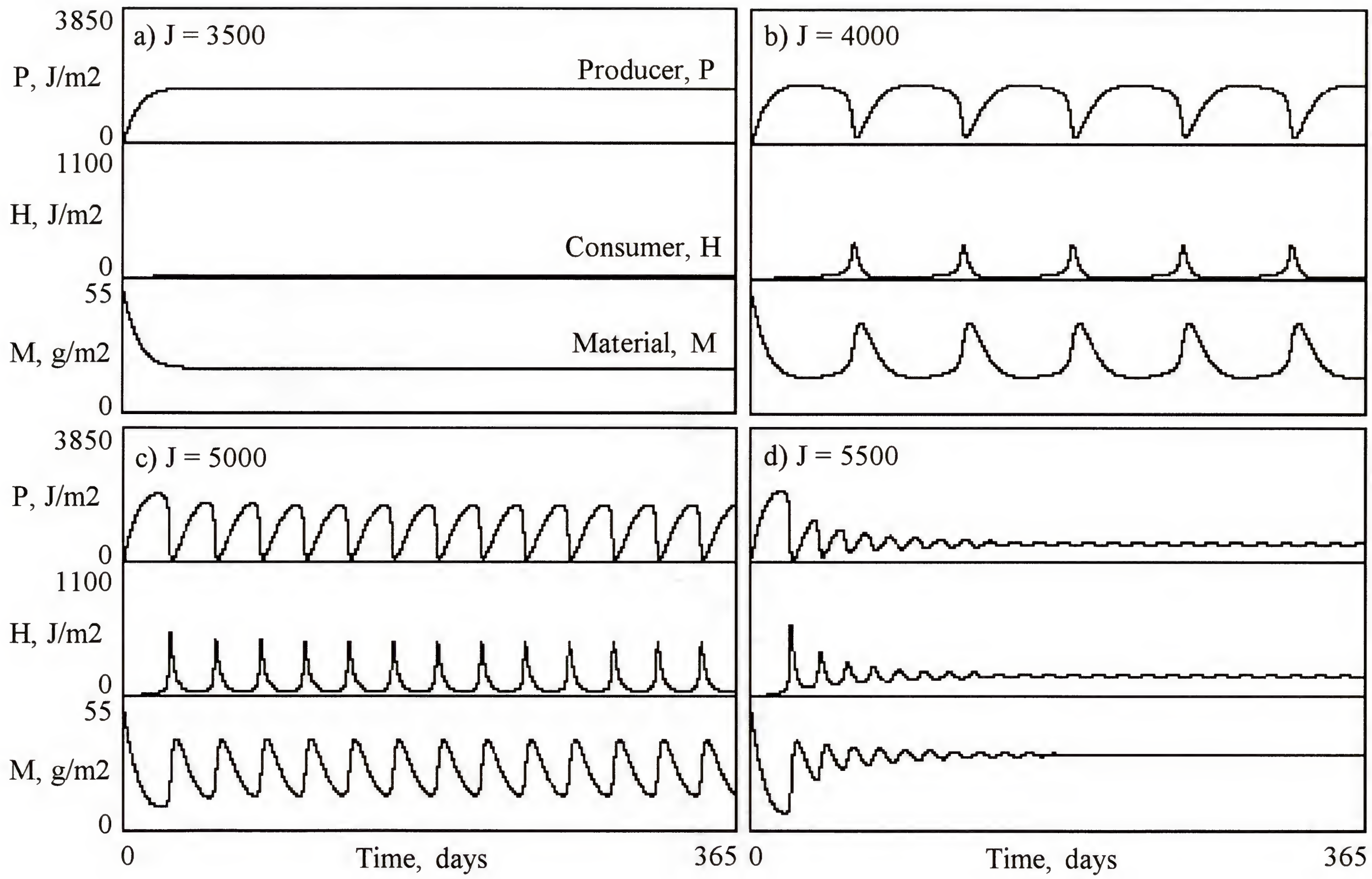

Figure 3-13. Simulation results of the basic pulse model for varied energy input from the source (J). c) is the base case shown in Figure 2-7.

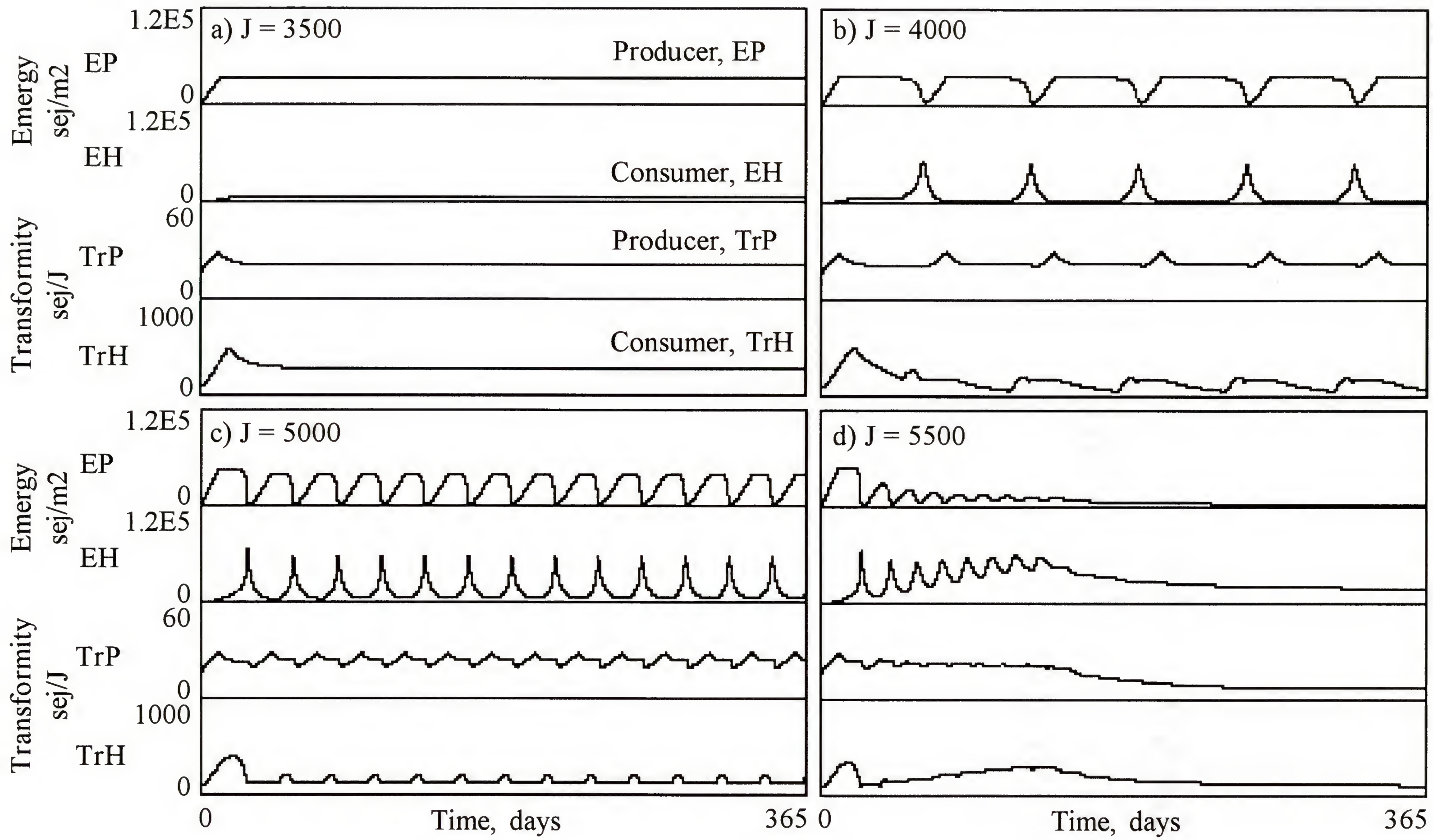

Figure 3-14. Emergy and transformity simulation of the basic pulse model in Figure 2-4, for varied energy input from the source (J). c) is the base case shown in Figure 3-11.

storage. Pulses of the consumer storage continued to get smaller than previous ones in response to this cycle. With increasing input energy level, more energy passed unused through the system; 7.5% at J=3500, 8.9% at J=4000, 12.6% at J=5000, and 12.4% at J=5500.

Emergy storages of both producer and consumer showed the same trend as in energy storage with an increase in the energy level (Figure 3-14): a decrease in producer emergy and an increase in consumer emergy as the energy level goes up. Average transformity of the producer was slightly higher in the pulsing range, and that of the consumer decreased as the energy input increased. Even though the average transformity of the consumer at J=5500 was greater than that of at J=5000 over one year simulation, simulation over a longer period produced lower transformity for the former case. Notice that emergy and transformity of both producer and consumer at J=5500 are still decreasing at the end of the simulation (Figure 3-14d).

Efficiency of Primary Production

In Figures 3-15 and 3-16, the efficiency of primary production was changed to evaluate how production efficiency affects the pulsing pattern. Efficiency of primary production was measured as a ratio of coefficient k2 to coefficient k1. Coefficient k2 was changed to vary the production efficiency of the producer. As in the case of changes in the energy input in Figure 3-13, average producer storage decreased, and that of consumer increased with increase in the efficiency of primary production (Figure 3-15). The model showed the pulsing dynamics in a very narrow range of efficiency, from 4.4% to 5.8%. Within this range, pulsing frequency increased with the production efficiency. Percent power use decreased as the production efficiency increased.

Variations in the emergy and transformity of the producer and consumer showed the same pattern as in the case of energy input change (Figure 3-16). Average emergy and

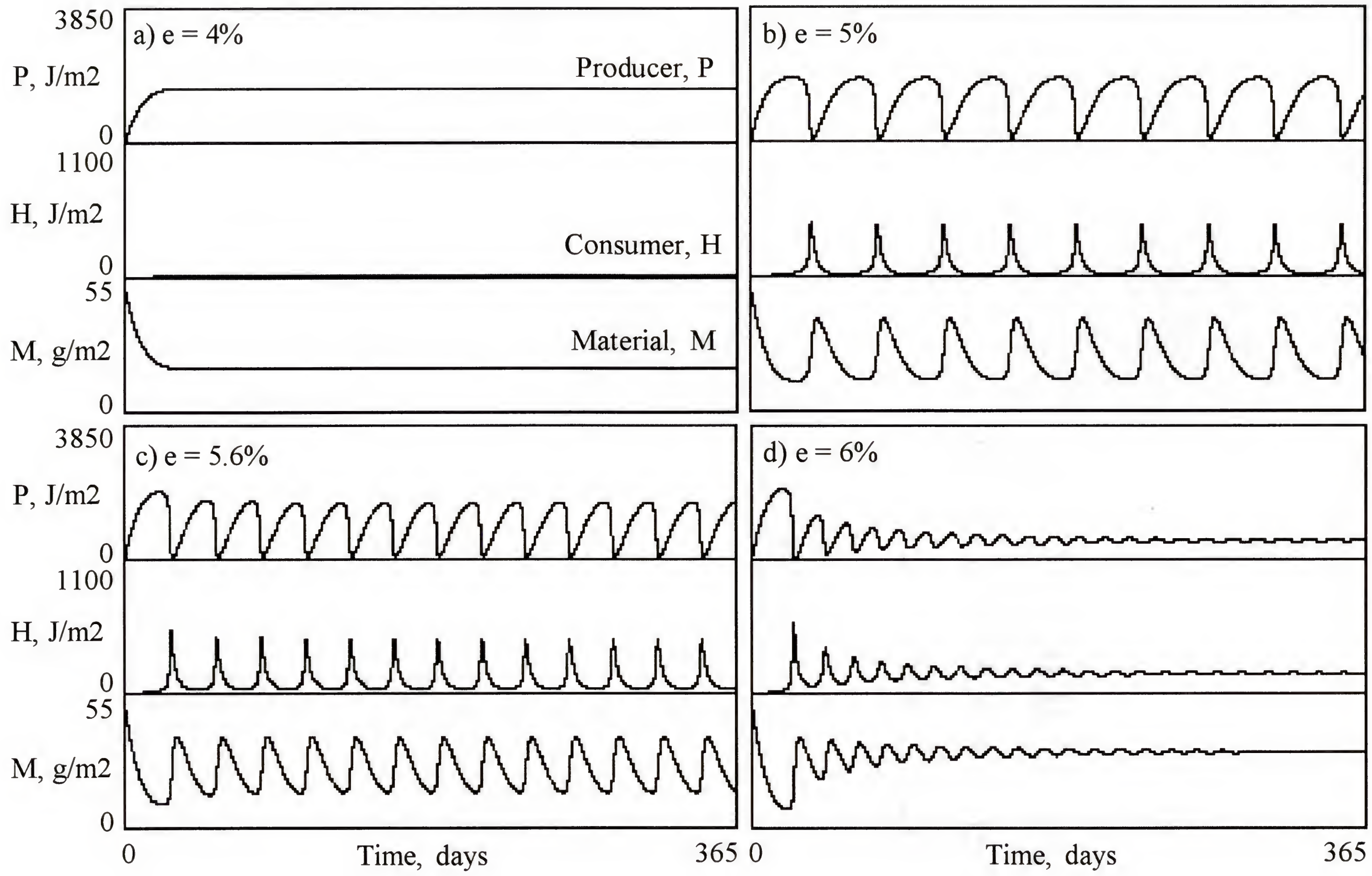

Figure 3-15. Simulation results of the basic pulse model in Figure 2-4, for varied production efficiency of producer (P). Production efficiency = (k2/k1)*100. Production efficiency was varied by changing the coefficient k2. c) is the base case shown in Figure 2-7.

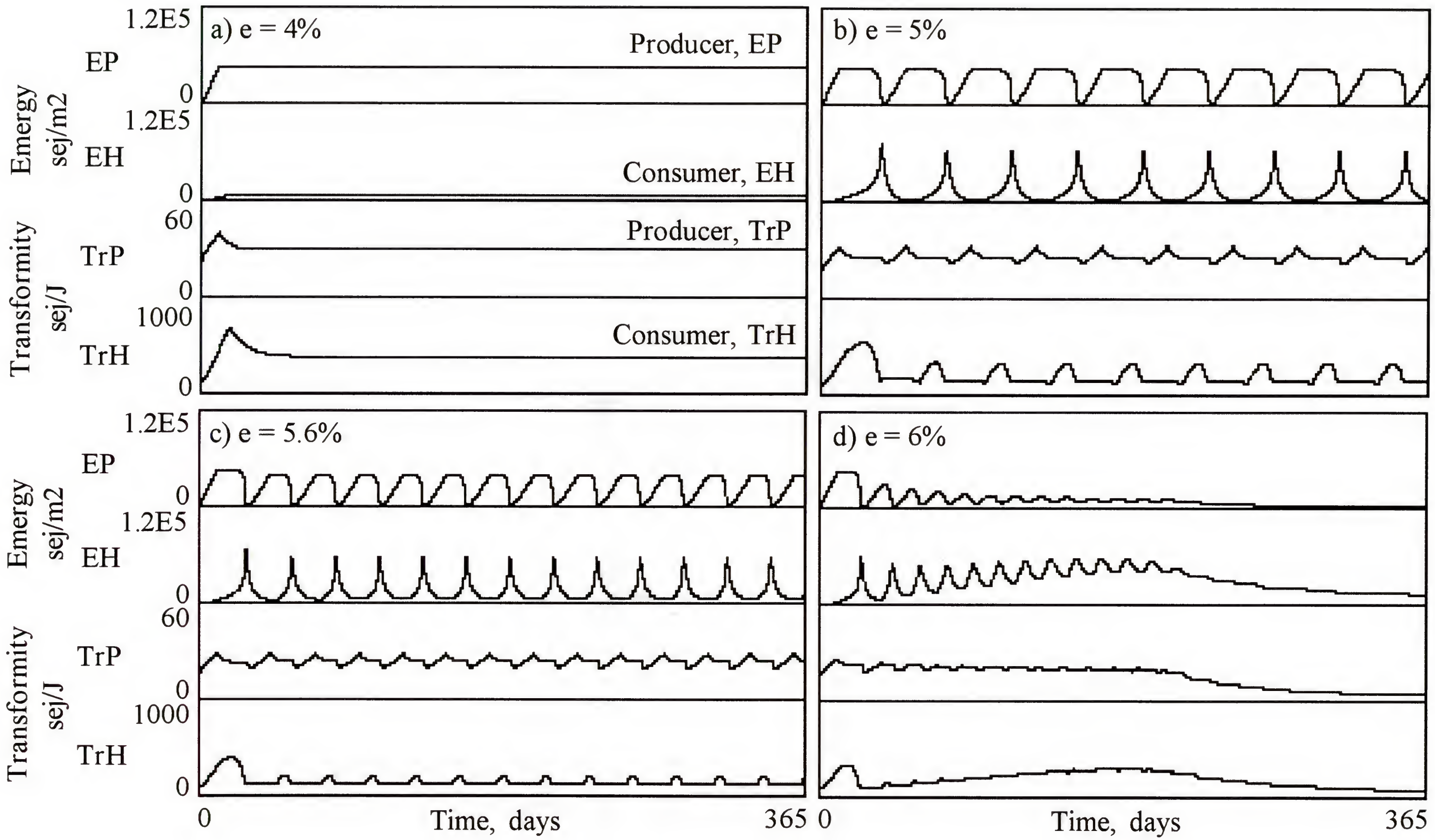

Figure 3-16. Emergy and transformity simulation of the basic pulse model in Figure 2-4, for varied production efficiecy of producer (P). Production efficiency = (k2/k1)*100. Efficiency was varied by changing the coefficient k2. c) is the base case shown in Figure 3-11.

transformity of the producer, and average transformity of the consumer over the simulation period decreased with increase in the efficiency, while average emergy of consumer was increasing.

Changes in Consumption Efficiency

Effects of consumption efficiency on simulation results of the basic pulse model were investigated in Figures 3-17, 3-18, 3-19, 3-20, 3-21, and 3-22. Efficiencies of three different consumption pathways were calculated as follows: efficiency of the linear pathway = (k4/k3)*100, efficiency of the autocatalytic pathway = (k6/k5)*100, and efficiency of the quadratic autocatalytic pathway = (k8/k7)*100. Efficiencies were changed by varying k4 for the linear pathway, k6 for the autocatalytic pathway, and k8 for the quadratic autocatalytic pathway.

In all cases, average storage of the producer decreased and that of the consumer increased as the efficiencies of consumption pathways increased (Figures 3-17, 3-19, and 3-21). Also, the model pulsed in certain ranges of efficiency values; 12%-58% for the linear pathway (k2), 11%-49% for the autocatalytic pathway (k6), and 26%-43% for the quadratic autocatalytic pathway (k8). Within those ranges, pulsing frequency increased with the efficiencies. Percent power use increased with increase in the efficiency of the linear pathway (k4), but decreased with increase in the efficiencies of other consumption pathways (k6 and k8).

Emergy storage of the producer and consumer showed the same pattern as energy storage (Figures 3-18, 3-20, and 3-22). Average emergy storage decreased for the producer and increased for the consumer as the consumption efficiency increased. The transformity of the producer was slightly higher in the pulsing range in all cases. The transformity of the consumer storage decreased with increase in the efficiency in all cases. Simulation over a longer time period resulted in lower transformities for the last cases

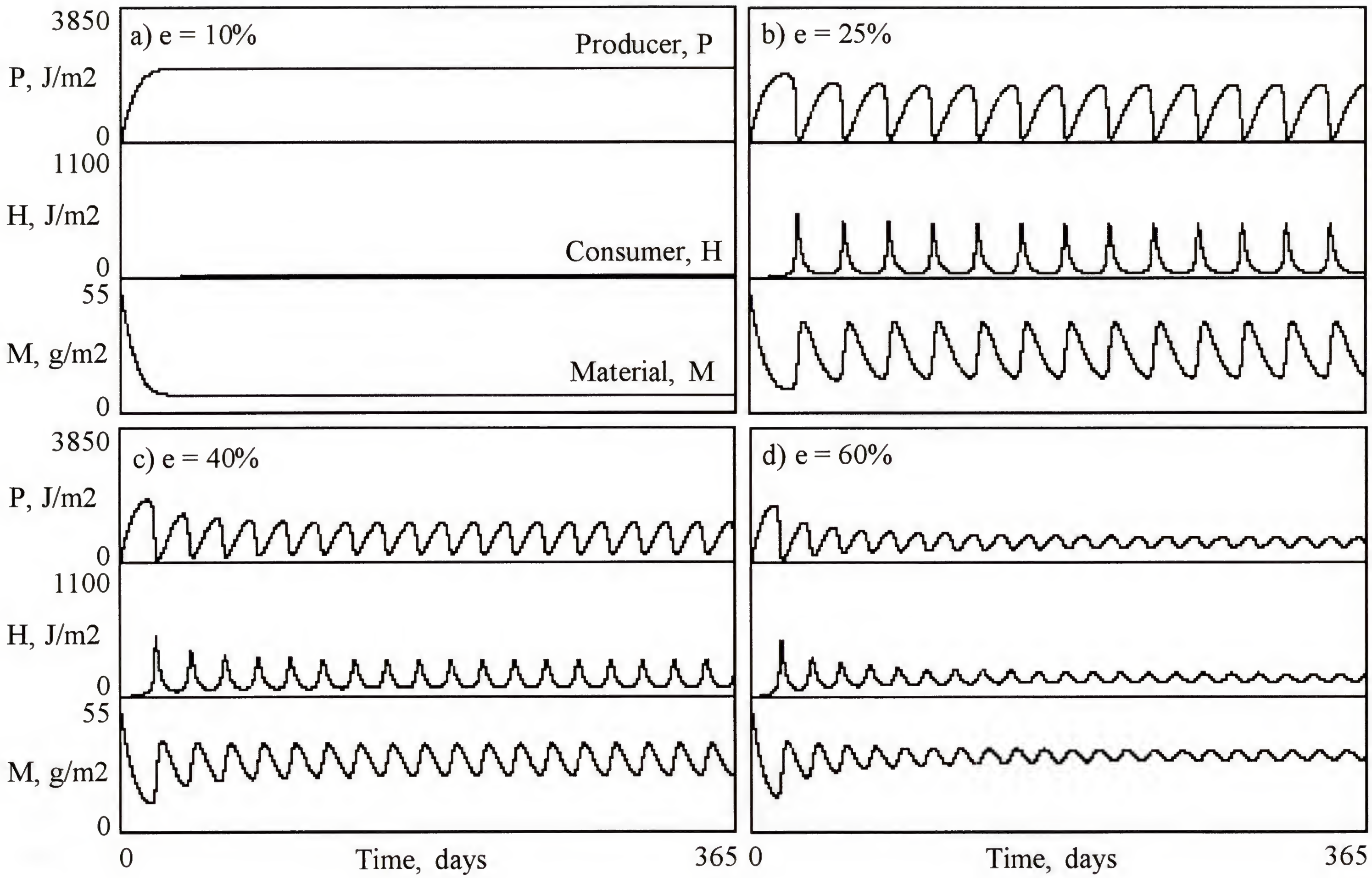

Figure 3-17. Simulation results of the basic pulse model in Figure 2-4, for varied efficiency of energy transfer from producer (P) to consumer (H) through the linear pathway. Efficiency, e = (k4/k3)*100. Efficiency was varied by changing the coefficient k4. b) is the base case shown in Figure 2-7.

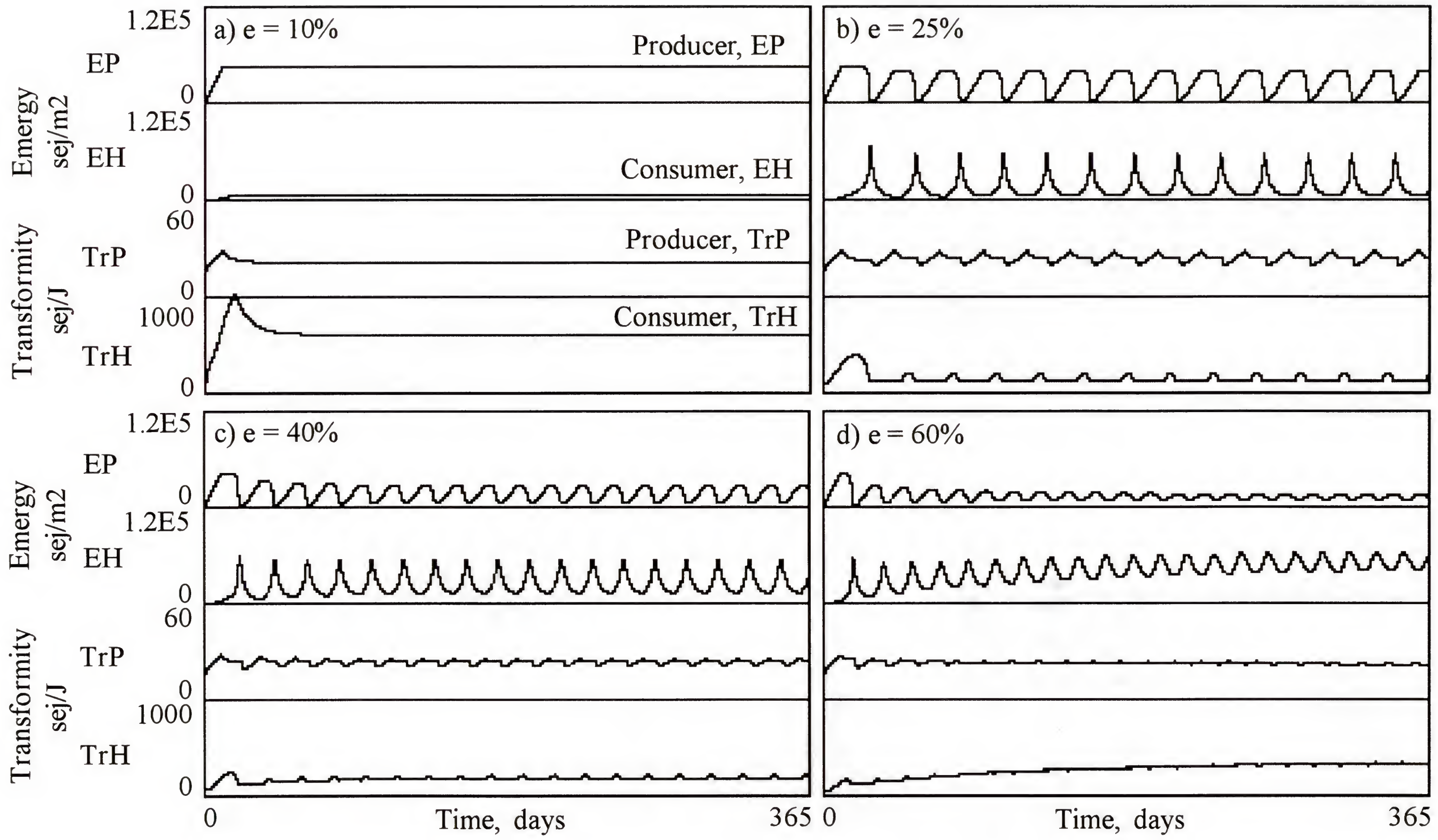

Figure 3-18. Emergy and transformity simulation of the basic pulse model in Figure 2-4, for varied efficiency of energy transfer from producer (P) to consumer (H) through the linear pathway (from k3 to k4). b) is the base case shown in Figure 3-11.

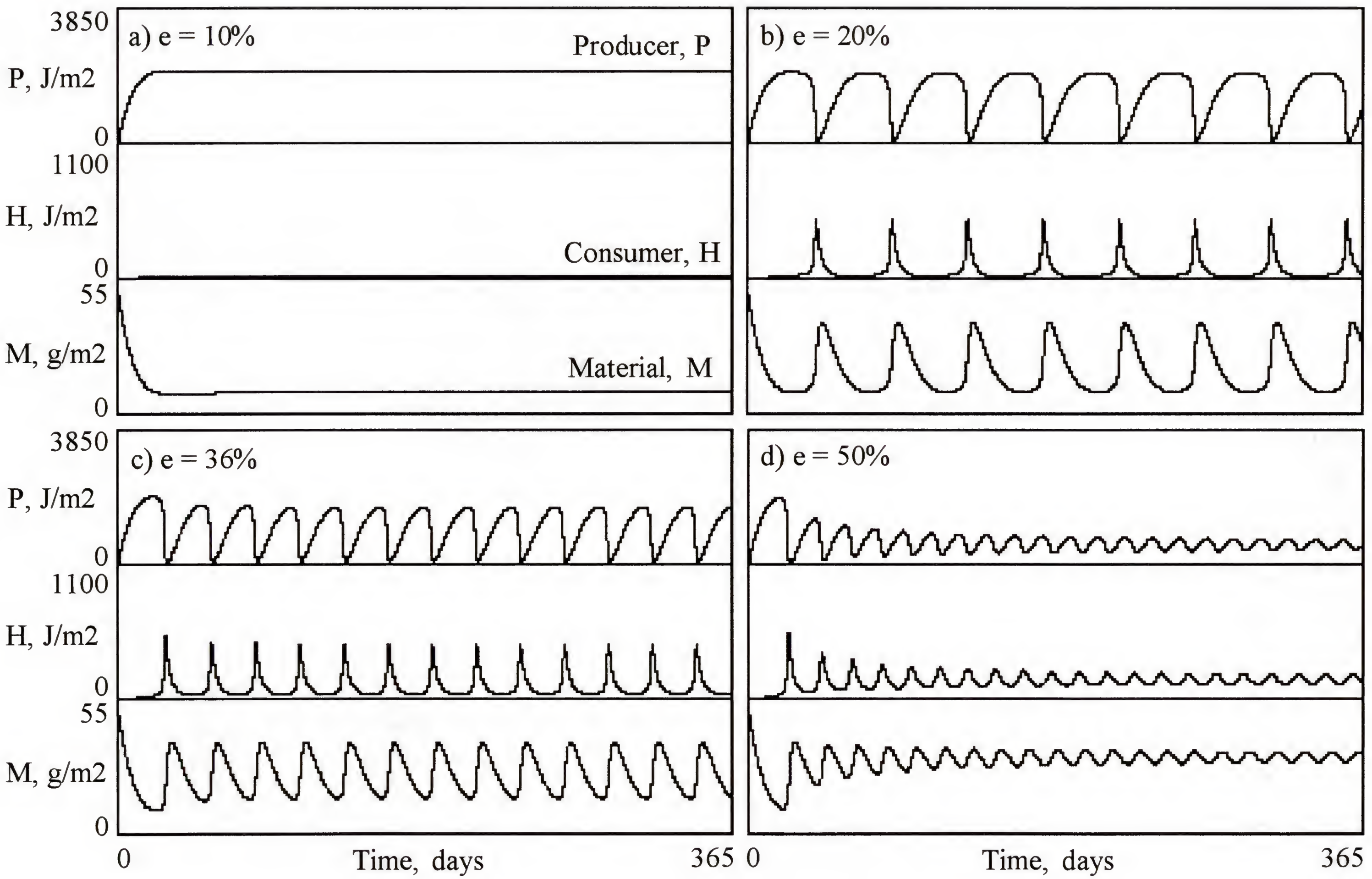

Figure 3-19. Simulation results of the basic pulse model in Figure 2-4, for varied efficiency of energy transfer from producer(P) to consumer (H) through the autocatalytic pathway (from k5 to k6). c) is the base case shown in Figure 2-7.

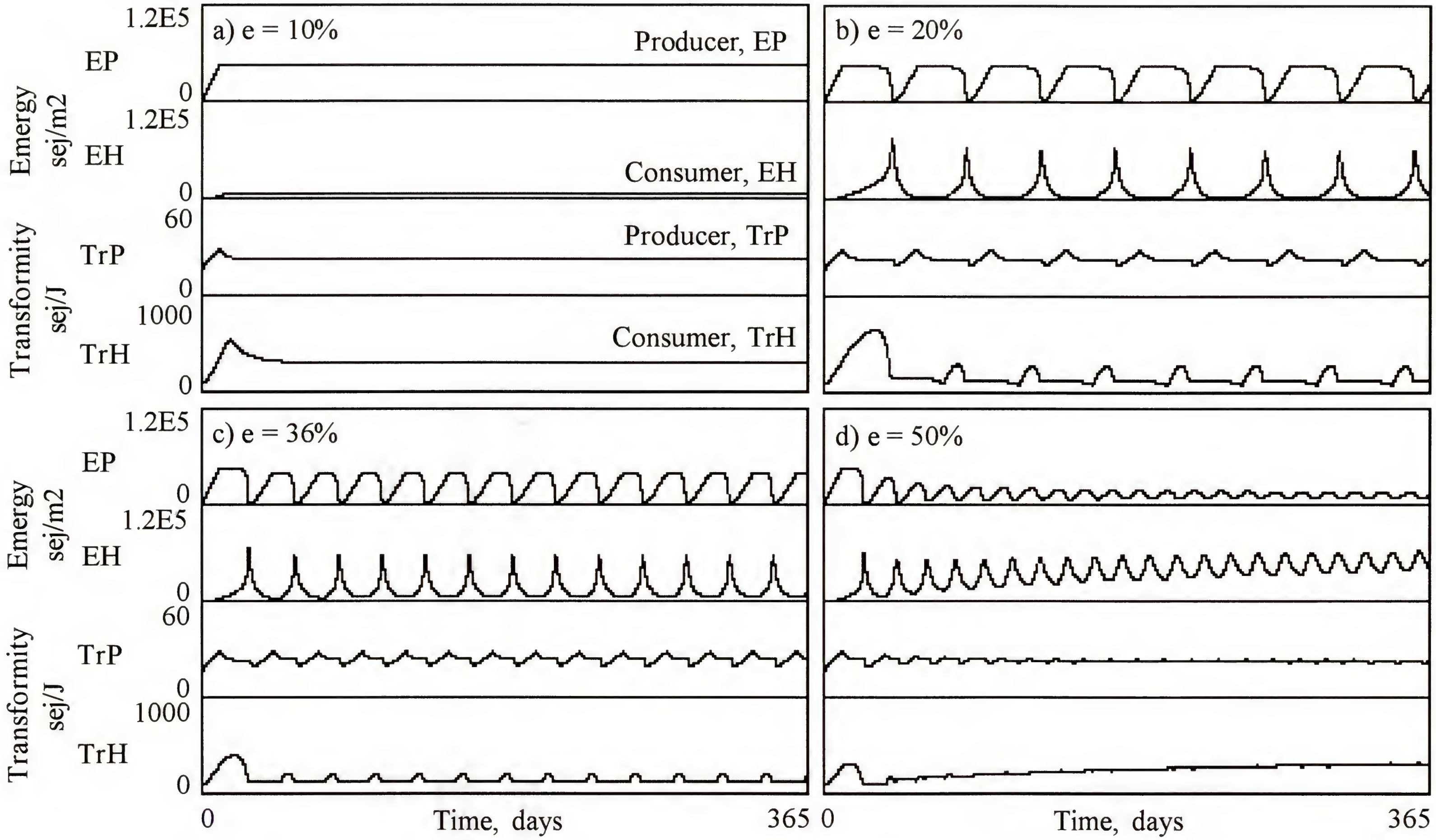

Figure 3-20. Emergy and transformity simulation of the basic pulse model in Figure 2-4, for varied efficiency of energy transfer from producer (P) to consumer (H) through the autocatalytic pathway (from k5 to k6). c) is the base case shown in Figure 3-11.

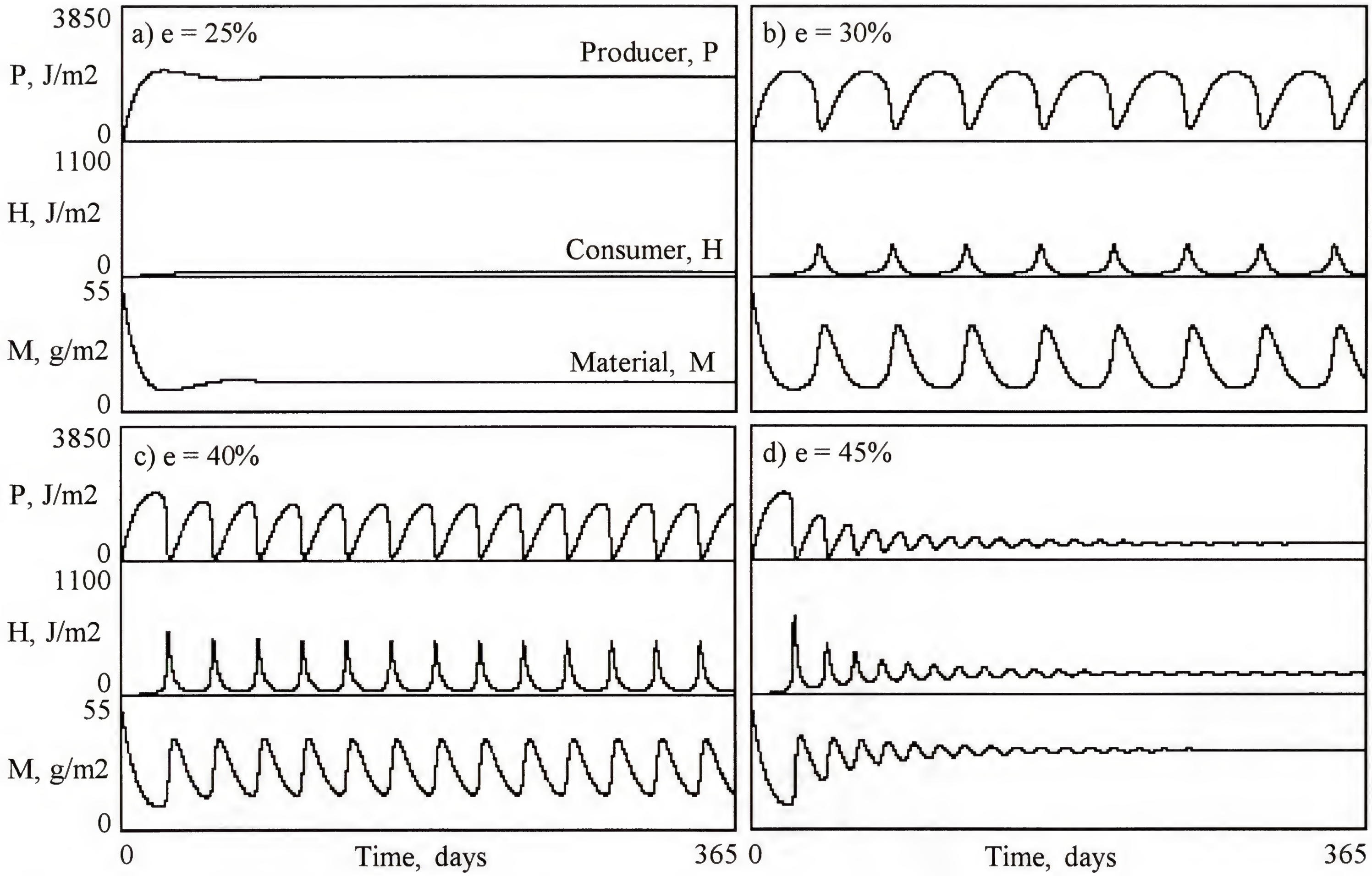

Figure 3-21. Simulation results of the basic pulse model in Figure 2-4, for varied efficiency of energy transfer from producer (P) to consumer (H) through the quadratic autocatalytic pathway (from k7 to k8). c) is the base case shown in Figure 2-7.

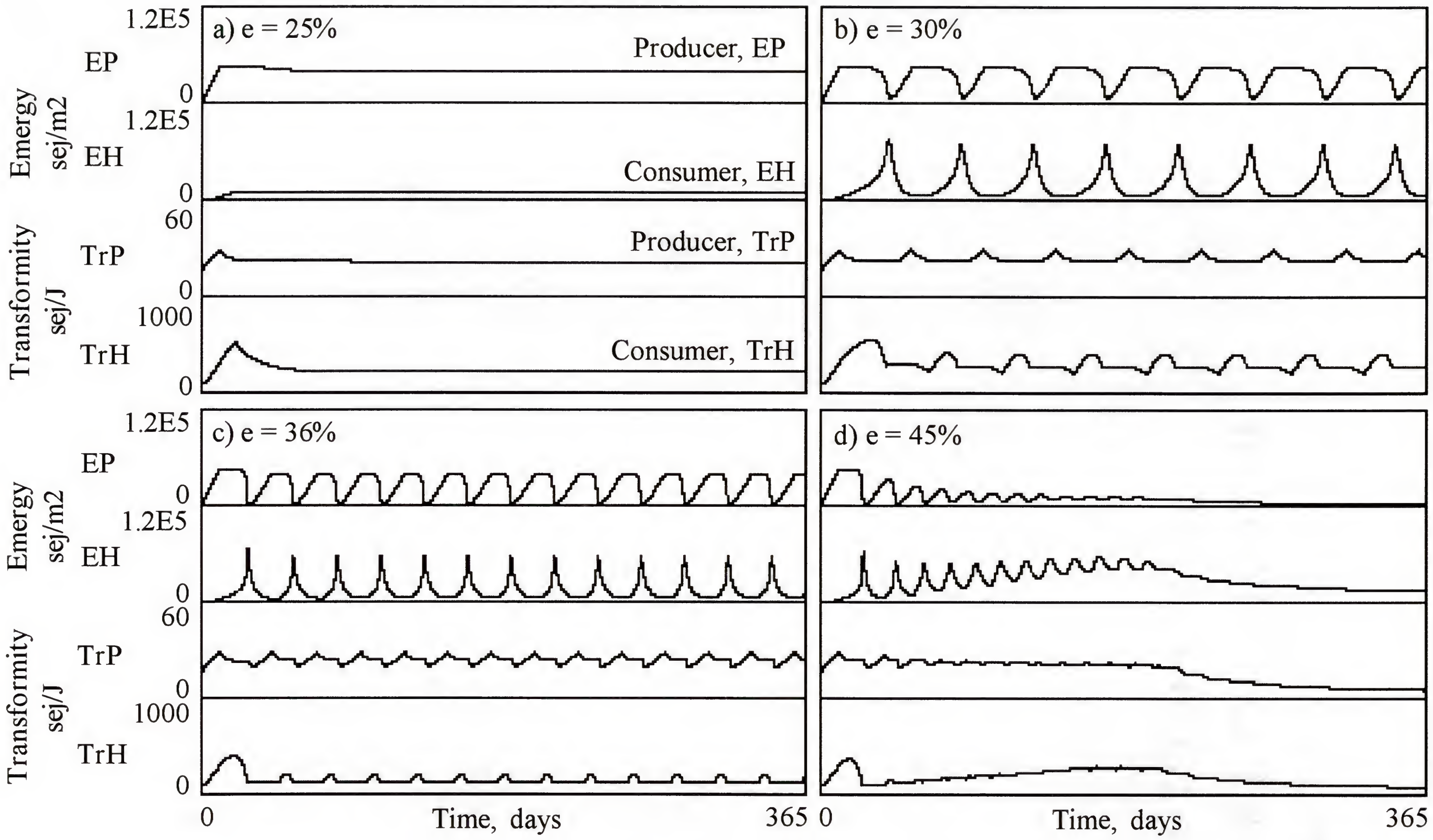

Figure 3-22. Emergy and transformity simulation of the basic pulse model in Figure 2-4, for varied efficiency of energy transfer from producer (P) to consumer (H) through the quadratic autocatalytic pathway (from k7 to k8). c) is the base case shown in Figure 3-11.

(Figures 3-18d, 3-20d, and 3-22d) in all three simulations, even though they had higher transformities than the base run of the model over a one year time period.

Level of Depreciation of Consumer Storage

The depreciation coefficient (k10) of the consumer storage was changed in Figures 3-23 and 3-24, and the model behavior was examined. Increase in depreciation resulted in more average producer storage and less consumer storage, just the reverse of the previous two cases. The model pulsed within a certain range of depreciation, that is, 49%-62%, with less frequent pulses as depreciation increased. At low depreciation flow (d=48%), material recycle was limited by the slowly changing consumer storage, resulting in damped oscillation. The consumer storage did not grow enough for pulsing through the autocatalytic and quadratic autocatalytic pathways at high depreciation flow (d=63%).

As in energy storage (Figure 3-23), emergy storage increased for the producer and decreased for the consumer with increase in depreciation flow of the consumer storage (Figure 3-24). Producer transformity was slightly higher in the pulsing range, while that of the consumer was lower.

Steady Model

Performance of the basic pulse model in Figure 2-4 was compared with a model without pulsing dynamics. The quadratic autocatalytic pathway is responsible for the pulsing dynamics in the model configuration with a flow limited energy source in Figure 2-4. By removing this pathway, a steady state model was constructed in Figure 3-25. This model has only two consumption pathways: linear (k3 and k4) and autocatalytic (k5 and k6). Other model configurations are identical with the basic pulse model. The steady model was calibrated in Figure 3-26 and Appendix Table B-2. Summed flow values on the autocatalytic and quadratic autocatalytic pathways in Figure 2-5, were assigned to the

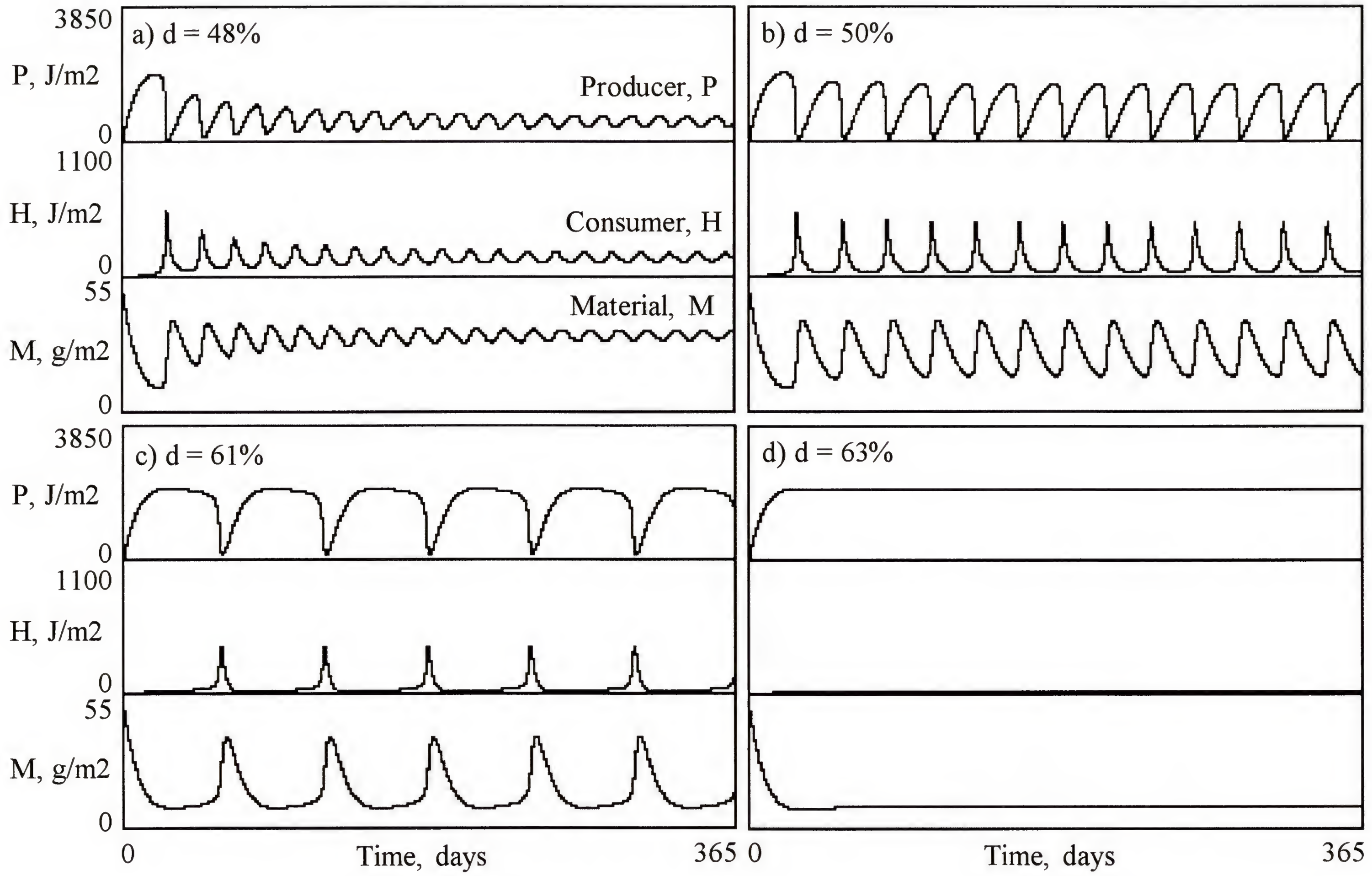

Figure 3-23. Simulation results of the basic pulse model in Figure 2-4, for varied depreciation coefficient (k10) of the consumer unit (H). b) is the base case shown in Figure 2-7.

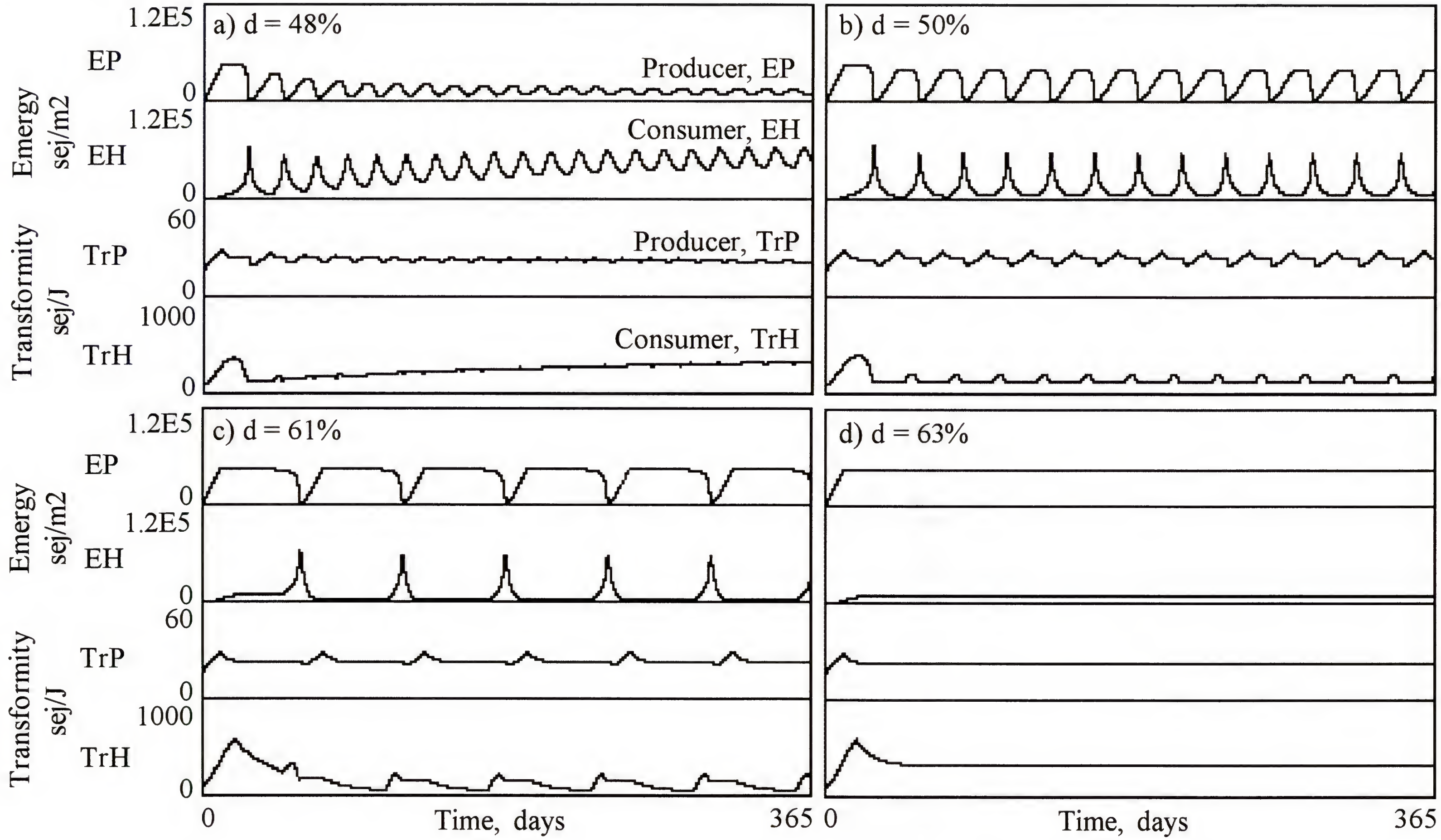

Figure 3-24. Emergy and transformity simulationn of the basic pulse model in Figure 2-4, for varied depreciation coefficient (k10) of the consmer unit (H). b) is the base case shown in Figure 3-11.

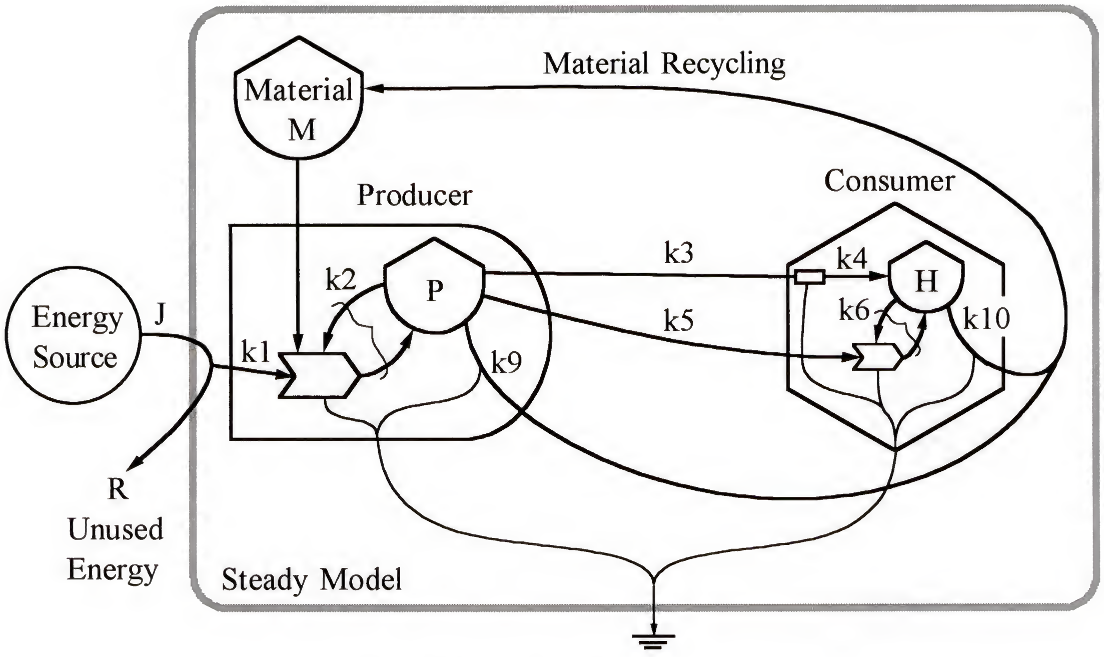

M = MT - f1*P - f2*H

R = J / (1 + k1*M*P)

dP = k2*R*M*P - k3*P - k5*P*H - k9*P

dH = k4*P + k6*P*H - k10*H

Figure 3-25. Systems diagram of the steady model without the quadratic autocatalytic pathway. Other configurations are the same as the basic pulse model in Figure 2-4.

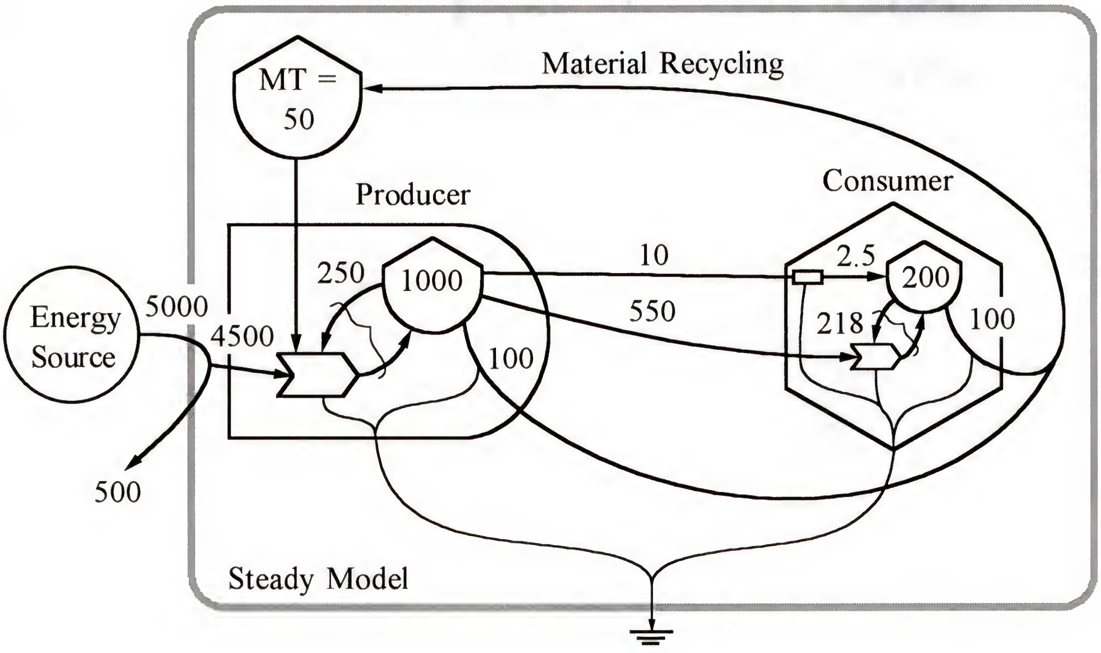

Figure 3-26. Calibration diagram of the steady model in Figure 3-25. Flow values on the autocatalytic pathway were obtained by adding those of the autocatalytic pathway and quadratic autocatalytic pathway in Figure 2-5.

autocatalytic pathway of the steady model in Figure 3-26, to compare both models on the same total consumption flow condition. Appendix Table C-3 lists the simulation program.

Without the quadratic autocatalytic pathway, the model reached a steady state after the initial pulse (Figure 3-27). Average producer storage over the simulation period was lower than in the basic pulse model, but the consumer storage was higher. The material storage was kept higher because of decreased primary production. There was not much difference in percent power use compared to the basic pulse model -- less than 1% difference. Average percent power use over the simulation period was 87.1% in the steady model. Emergy storage of the producer was lower in the steady model and that of the consumer was higher than that of the basic pulse model, reflecting the trend in energy storage (Figure 3-27b). The transformity of both storages was lower in the steady model. The basic pulse model showed 20% higher transformity for the producer and 18% for the consumer.

Pulse Model with Consumer Feedback

Even though the basic pulse model in Figure 2-4 includes feedback to primary production through material recycle by the consumer unit, many real systems show direct feedback on primary production from consumer units. In Figure 3-28, the basic pulse model was extended to include a direct feedback flow from the consumer storage. Primary production was separated into two different pathways; one without consumer feedback and the other with direct feedback. These two processes compete for available energy and material. Production with direct consumer feedback was calibrated so that it had slightly higher efficiency (Figure 3-29 and Appendix Table B-3). The simulation program is listed in Appendix Table C-4.

Figure 3-30 shows the base run of the pulse model with consumer feedback in Figure 3-28. Pulsing frequency decreased compared to the basic pulse model in Figure

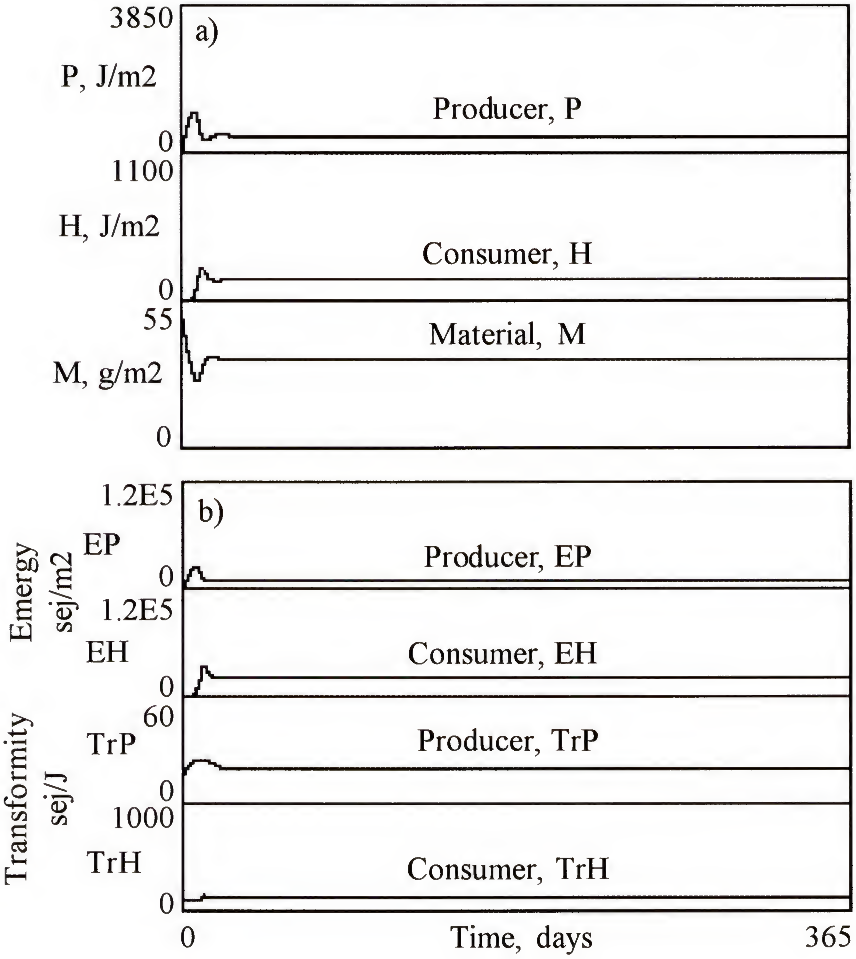

Figure 3-27. Simulation results of the steady model in Figure 3-25, with coefficients calibrated as in Appendix Table B-2. a) Energy simulation and b) emergy and transformity simulation

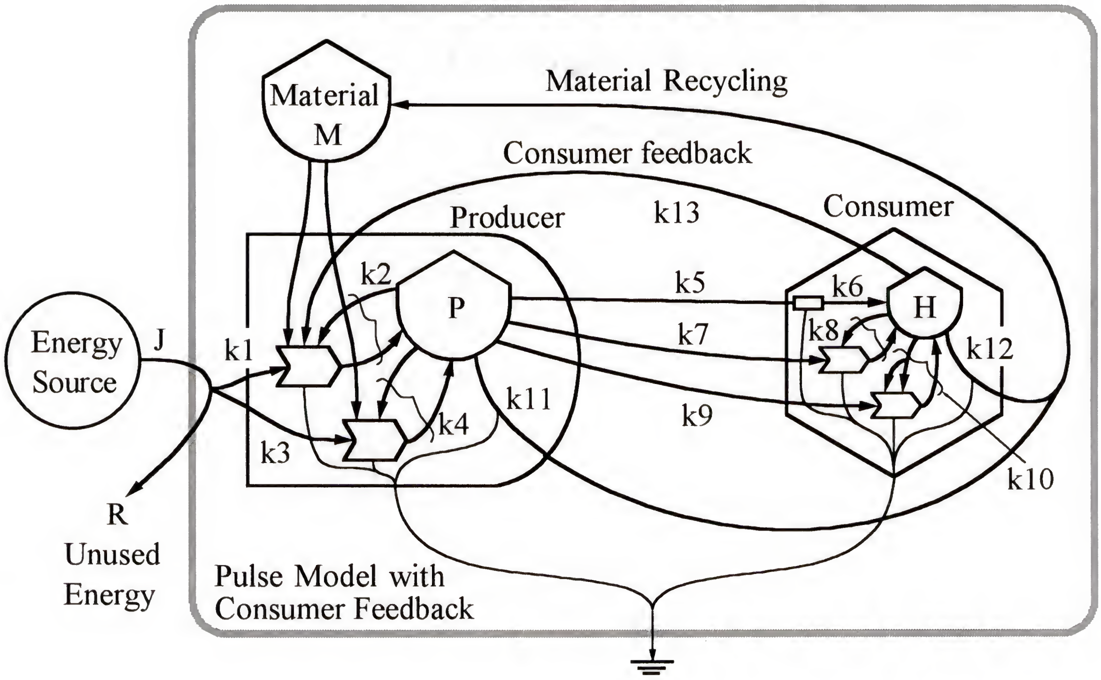

$$M = MT - f1*P - f2*H$$

$$R = J / (1 + k1*M*P*H + k3*M*P)$$

$$\begin{aligned} dP = {} & k2*R*M*P*H + k4*R*M*P - k5*P - k7*P*H \\ & - k9*P*H*H - k11*P \end{aligned}$$

$$\begin{aligned} dH = {} & k6*P + k8*P*H + k10*P*H*H - k12*H \\ & - k13*R*M*P*H \end{aligned}$$

Figure 3-28. Pulse model with direct consumer feedback on primary production. The producer has two different production processes: a process based on its own feedback and available material (k4), and the other with feedback from the consumer unit (H) (k4). MT=total material inside the system; f1 and f2 = Material fraction of the producer and consumer storages, respectively.

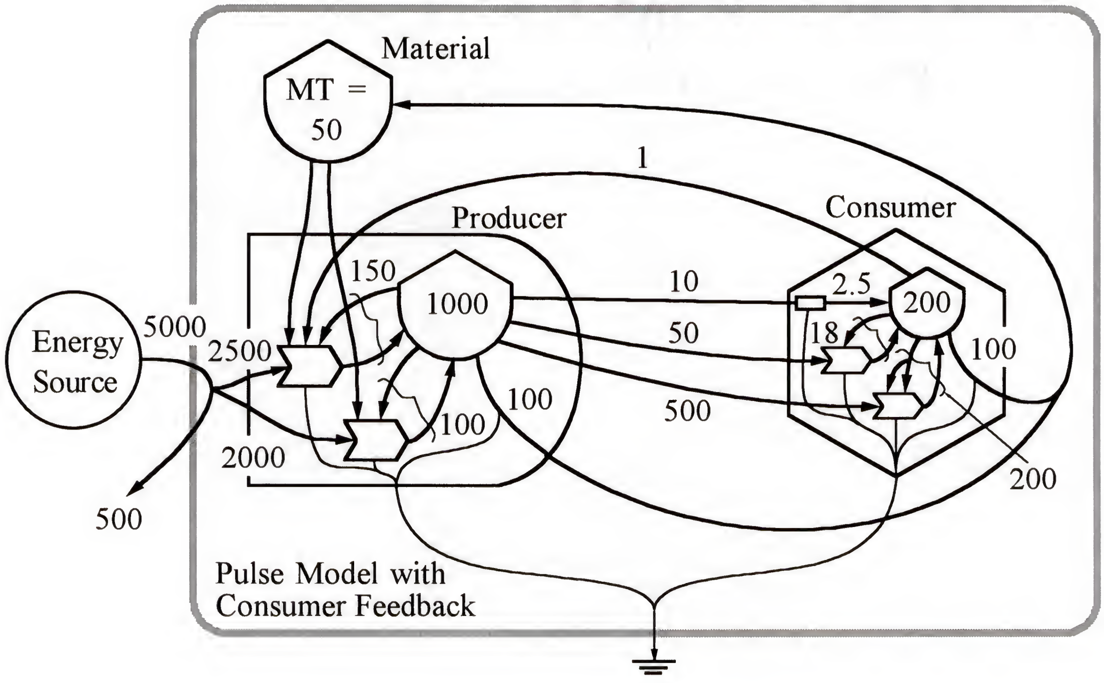

Figure 3-29. Calibration diagram of the pulse model with consumer feedback on primary production in Figure 3-28.

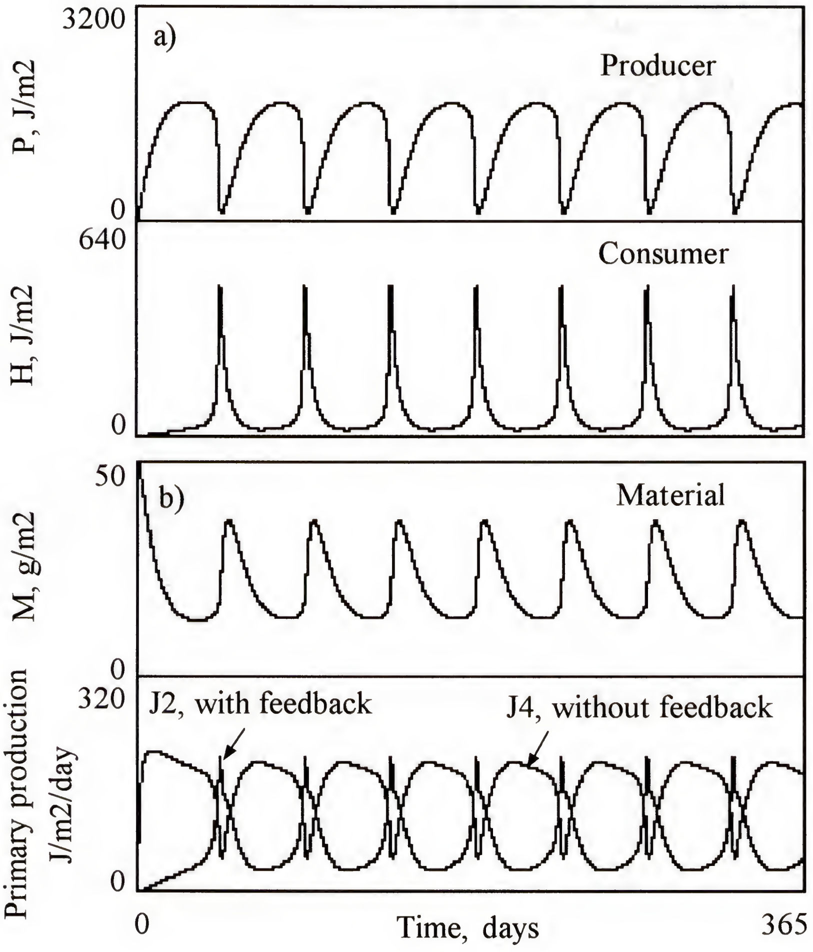

Figure 3-30. Simulation results of the pulse model with consumer feedback on primary production in Figure 3-28, with coefficients as calibrated in Appendix Table B-3.

a) Storage of producer and consumer;

b) Material storage and primary production;

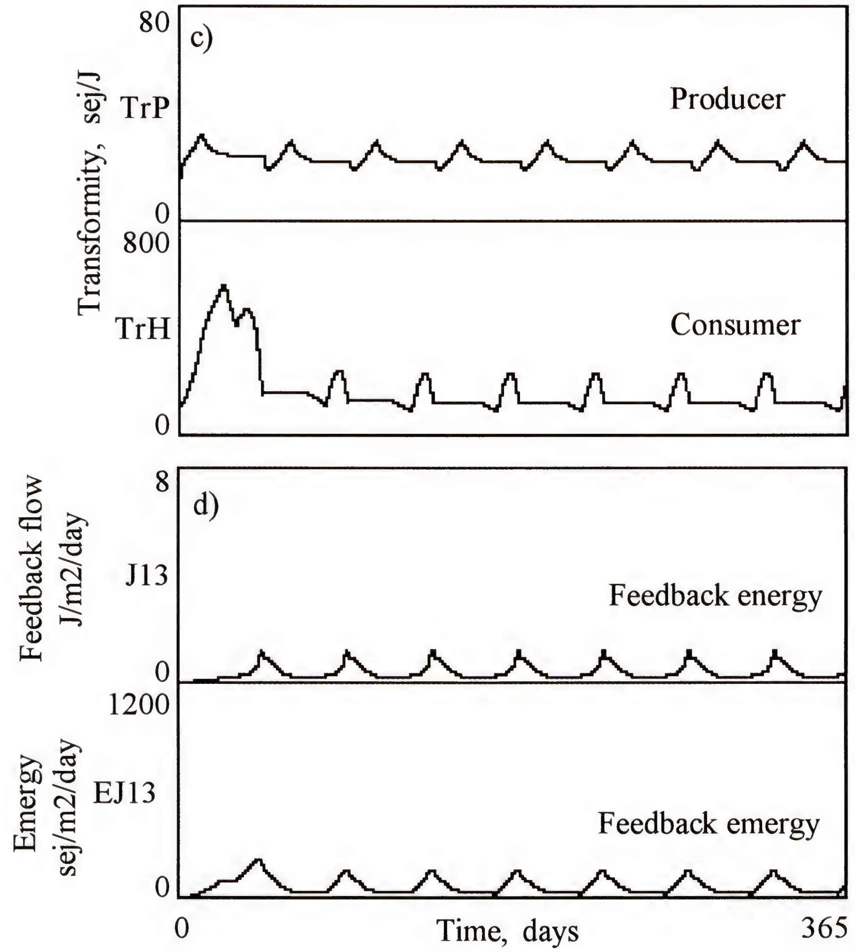

Figure 3-30. Continued.
c) Transformity of producer and consumer;
d) Energy and emergy of feedback flow (k13).

2-4, even though the calibration condition for total energy used (J1+J3) and total production (J2+J4) were the same as in the basic pulse model. The simulation result clearly shows alternation between different production pathways (Figure 3-30b). First, the production process without feedback (k4) accumulated the producer storage when both producer and consumer were low in concentration. Then, the production with consumer feedback (k2) took over based on increased producer and consumer storage. It reached a maximum rate at the peak of the consumer storage.

Transformity was simulated in Figure 3-30c. The transformities of both producer and consumer reached a maximum during the growth phase, as in the basic pulse model in Figure 3-11. Energy and emergy of the feedback flow (k13) followed the pattern of the consumer, reaching maximum value at the peak of the consumer storage (Figure 3-30d).

Effects of the amount of feedback flow on the pulsing pattern were examined in Figure 3-31. The model pulsed without feedback flow (k13 = 0), indicating that the quadratic autocatalytic pathway (k9 and k10) was mostly responsible for the pulsing dynamics in the model. Increase in the feedback flow produced less frequent pulses. Further increase in the flow resulted in a steady state with very low consumer storage. It took longer for the consumer storage to reach the level for the pulsing pathway to start, due to increased outflow from the storage. Percent power use decreased with increase in the feedback flow, but the difference between them was very small, less than 2%. The average transformity of the producer over the simulation period did not change much with increase in the feedback flow (Figure 3-32). The transformity of the consumer storage, however, decreased in the pulsing range.

In Figure 3-33, variations in energy and emergy flow of the feedback (k13) were plotted as the coefficient k13 was changed. The average flow of feedback energy over the simulation period was maximum with k13 = 2.5E-9. Average emergy flow (empower) increased with increasing coefficient k13. Maximum instantaneous empower, however, was greatest at k13 = 2.5E-9, implying maximum feedback effect at this coefficient value.

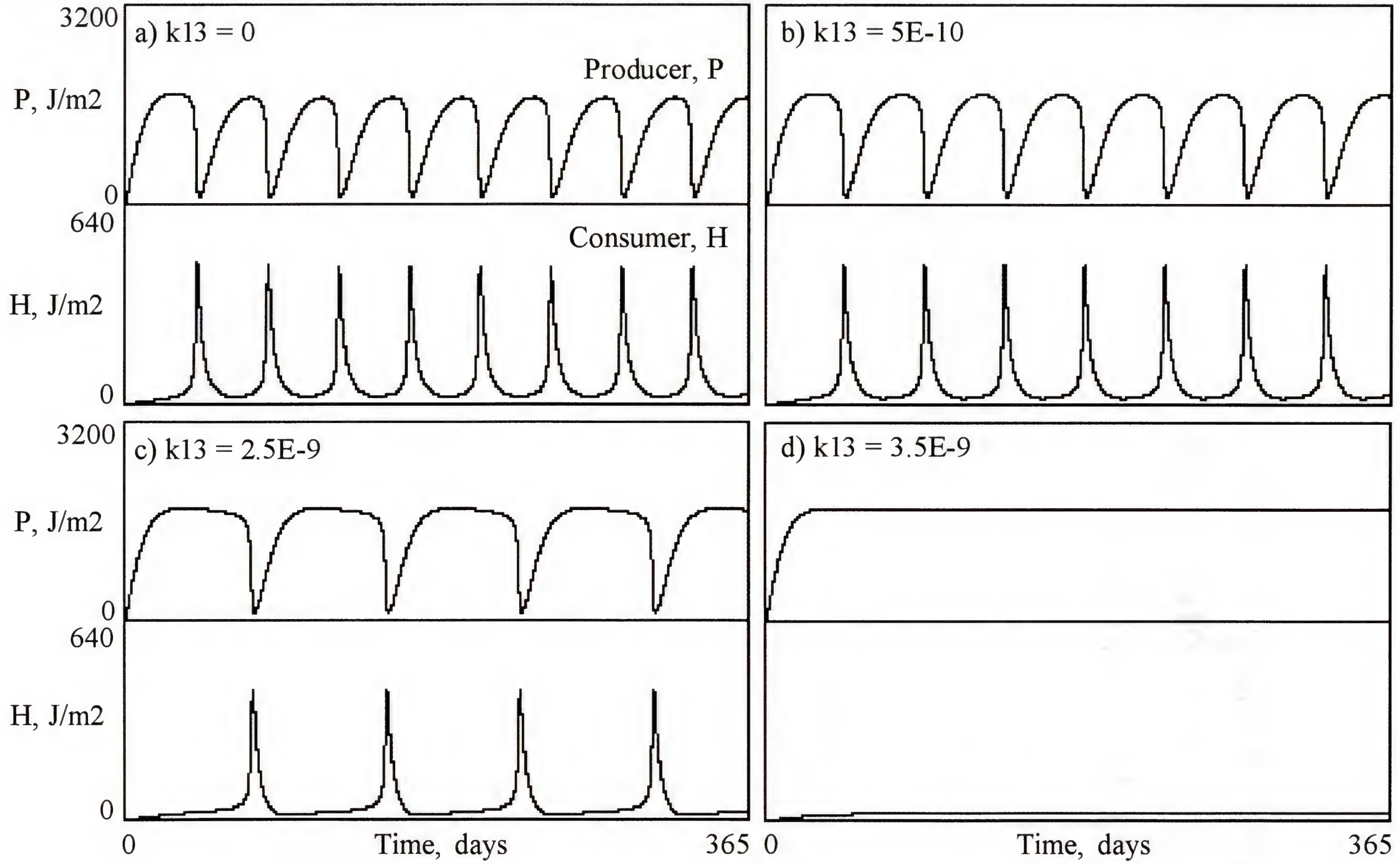

Figure 3-31. Simulation results of the pulse model with consumer feedback on primary production in Figure 3-28, for varied feedback flow (k13). b) is the base case shown in Figure 3-30.

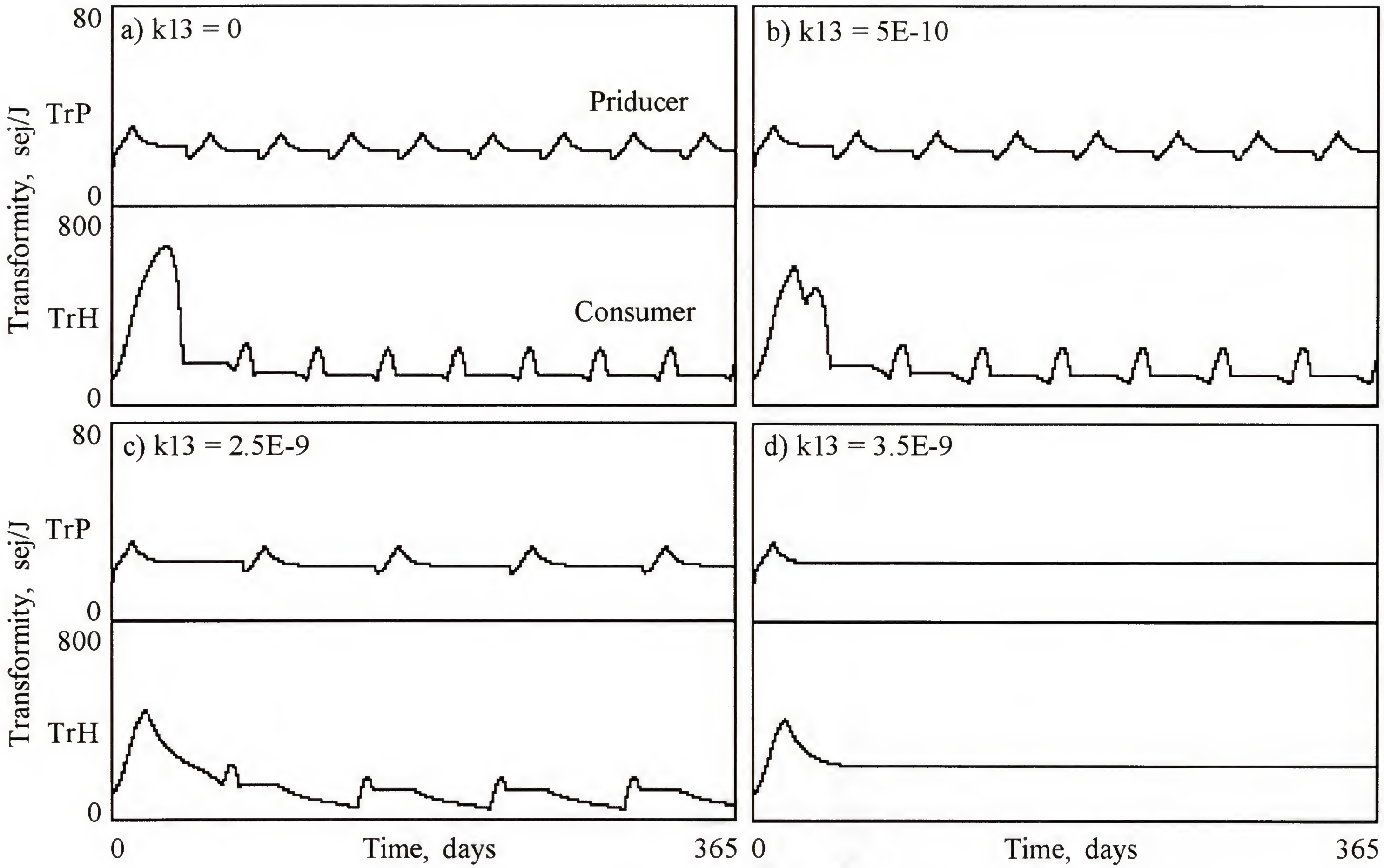

Figure 3-32. Transformity simulation of the pulse model with consumer feedback on primary production in Figure 3-28, for varied feedback flow (k13). b) is the base case shown in Figure 3-30.

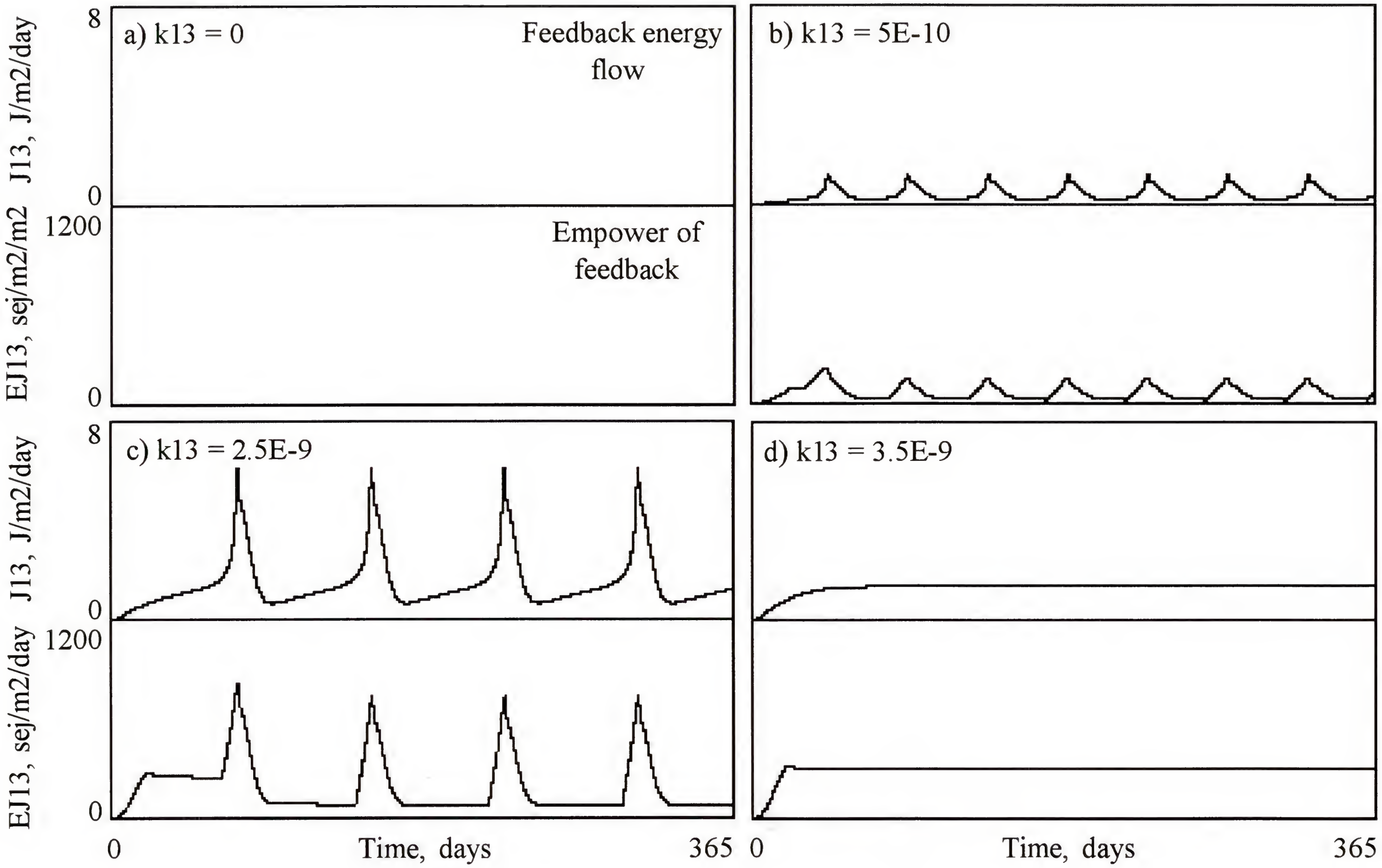

Figure 3-33. Energy and emergy of feedback flow (k13) in the pulse model with consumer feedback on primary production in Figure 3-28, for varied coefficient k13. b) is the base case shown in Figure 3-30.

In Figures 3-34 and 3-35, efficiencies of both primary production processes were changed to see how the model system responded to them. Efficiency of the production process with consumer feedback was defined as (k2/k1)*100 and defined as (k4/k3)*100 for the production process without consumer feedback. Efficiencies were varied by changing the coefficients k2 and k4.

Both cases showed pulsing patterns in very narrow ranges of efficiency; 3.1% - 7.1% with consumer feedback, and 4.5% - 5.8% without consumer feedback. Within those ranges, pulsing frequency increased with increasing efficiencies. At low production efficiencies, growth of the producer storage was not fast enough for the consumer storage to overcome depreciation loss (k12). Fast growth of the producer at high efficiency did not provide enough time for decrease in the consumer storage. Material recycle was a limiting factor for primary production. Even though the percent power use was less in the pulsing range, the difference was less than 2%.

Detritus Model

Figure 3-36 shows a pulse model that includes a detritus storage (D). Detritus is an important and significant component in aquatic ecosystems. The detritus storage receives particulate organic material through three different pathways; directly from the producer (k9) and consumer (k10), and through messy feeding of the producer by the consumer (k16). Many herbivores feed on both producers and detritus. Bacterial decomposition recycles material incorporated in detritus. For model simplicity and because it may act as a passive accumulator of small scale inputs, an autocatalytic pathway was not included in the consumption pathways of producer and detritus. The model was calibrated in Figure 3-37 and Appendix Table B-4, and the simulation program is listed in Appendix Table C-5.

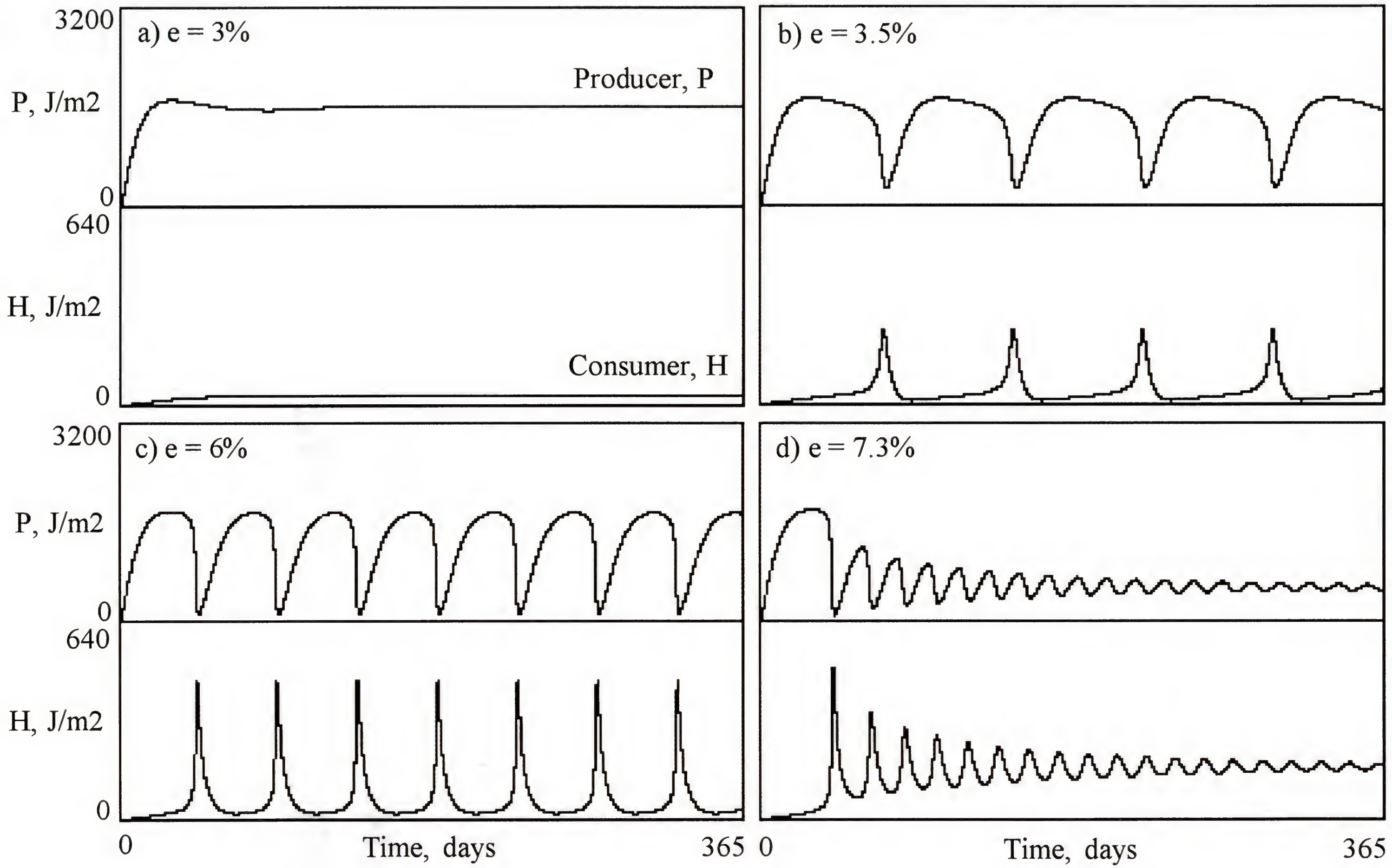

Figure 3-34. Simulation results of the pulse model with consumer feedback on primary production in Figure 3-28, for varied efficiency of primary production with consumer feedback (k2). c) is the base run in Figure 3-30.

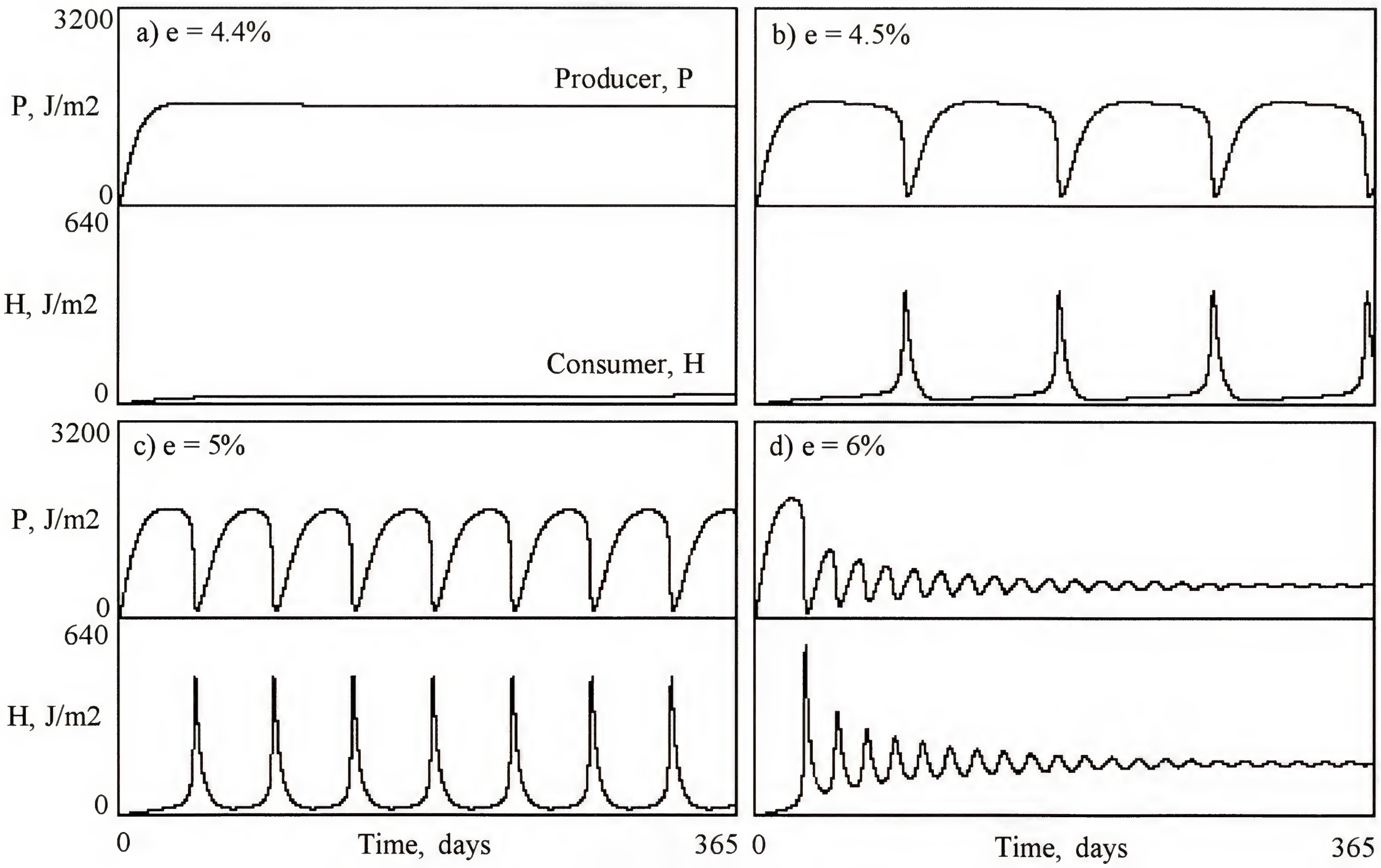

Figure 3-35. Simulation results of the pulse model with consumer feedback on primary production in Figure 3-28, for varied efficiency of primary production without consumer feedback (k4). c) is the base run in Figure 3-30.

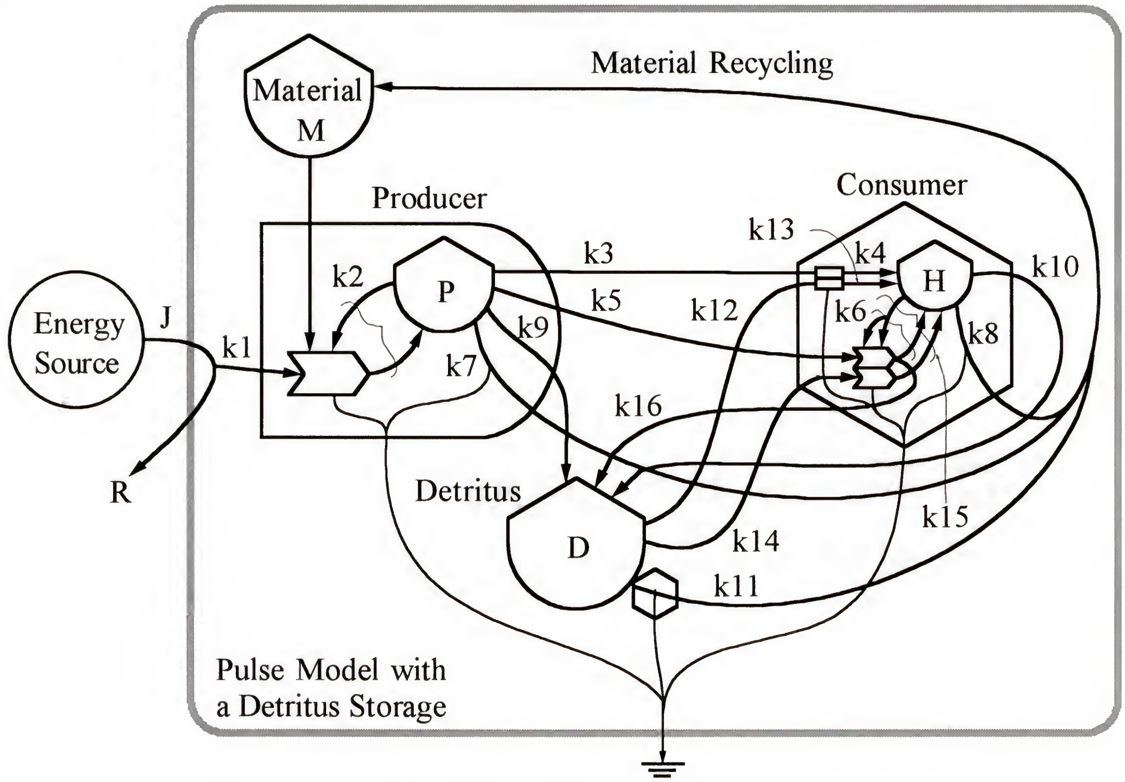

M = MT - f1*P -f2*H - f3*D

R = J / (1 + k1*M*P)

dP = k2*R*M*P - k3*P - k5*P*H*H - k7*P - k9*P

dH = k4*P + k6*P*H*H + k13*D + k15*D*H*H - k8*H - k10*H

dD = k9*P + k10*H + k16*P*H*H - k11*D - k12*D - k14*D*H*H

Figure 3-36. Pulse model with a detritus storage. Detritus is supplied through three different pathways: directly from the producer (k9) and consumer (k10), and through messy feeding of the consumer (k16). The consumer unit feeds on both producer and detritus. MT = Total material in the system; f1, f2, and f3 = Material fraction of the producer (P), consumer (H), and detritus (D), respectively.

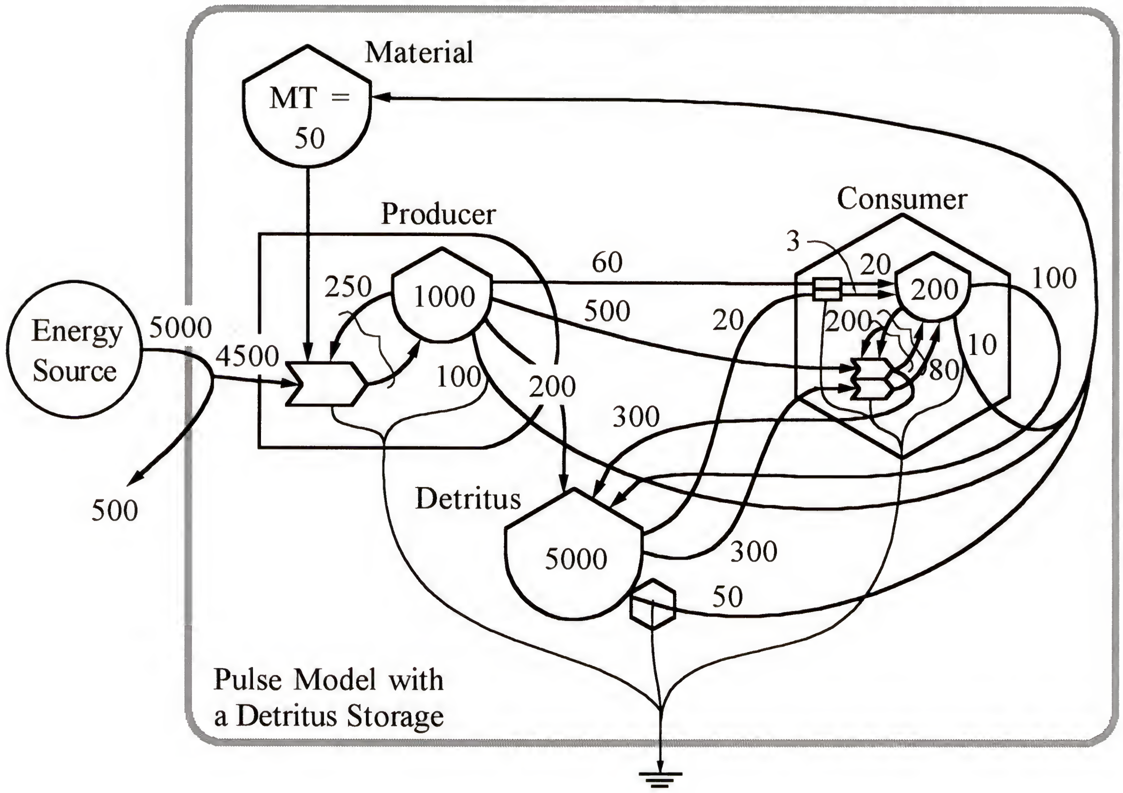

Figure 3-37. Calibration diagram of the pulse model with a detritus storage in Figure 3-36.

The base run of the detritus model in Figure 3-36 is shown in Figure 3-38. Herbivore pulses were related to the detritus storage. Consumption pathways feeding on producers kept the consumer storage higher than in the previous pulsing models. Average transformity of the consumer over the simulation period was greater than that of the producer. The detritus, however, had lower transformity than the producer. Slower growth rate of the detritus might cause the 5% limitation in emergy growth, explained in the methods chapter, to be active early, resulting in lower transformity. It represents the low quality early successional net production.

Figure 3-39 shows the effects of changes in production efficiency of the producer (P). The efficiency was calculated as follows: $e = (k2/k1)*100$. It was varied by changing the coefficient k2. The model pulsed in a very narrow range of efficiency, from 4.3% to 6.7%. Pulsing frequency increased with increasing efficiency within the pulsing range. Average storage of the producer and detritus decreased with increase in the efficiency, while that of the consumer increased. Percent power use decreased with increase in the efficiency. At low production efficiency, growth of the producer storage was slow for the consumer to build storage to pulse. Fast growth of the producer before the consumer reached the lowest level caused limitation in material recycle, leading to damped oscillation.

Figure 3-40 shows results of transformity simulation for varied efficiency of primary production. The average transformity of the producer decreased with increase in the efficiency, while those of the consumer and detritus increased. At 6.8% of efficiency, the transformity of the detritus became greater than that of the producer.

Layered Pulse Model

In aquatic ecosystems, there are several different size classes of producers and consumers. They alternate their production and consumption contributing to the systems

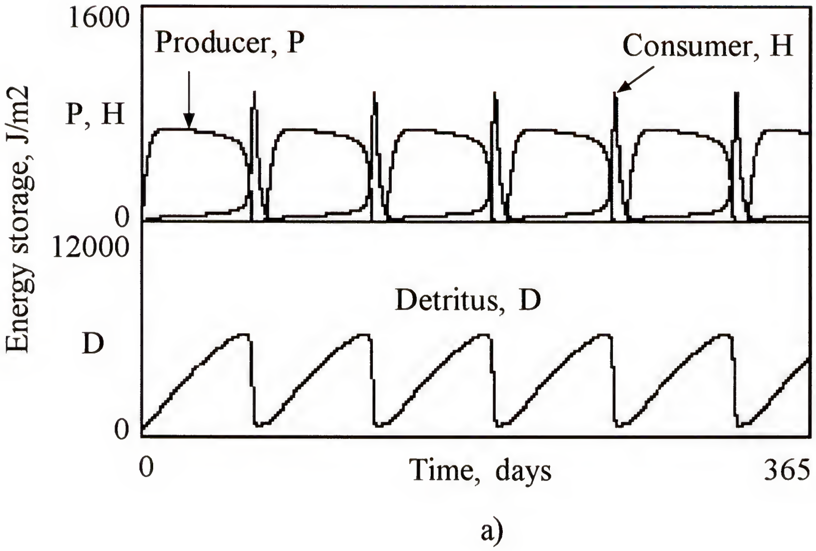

a)

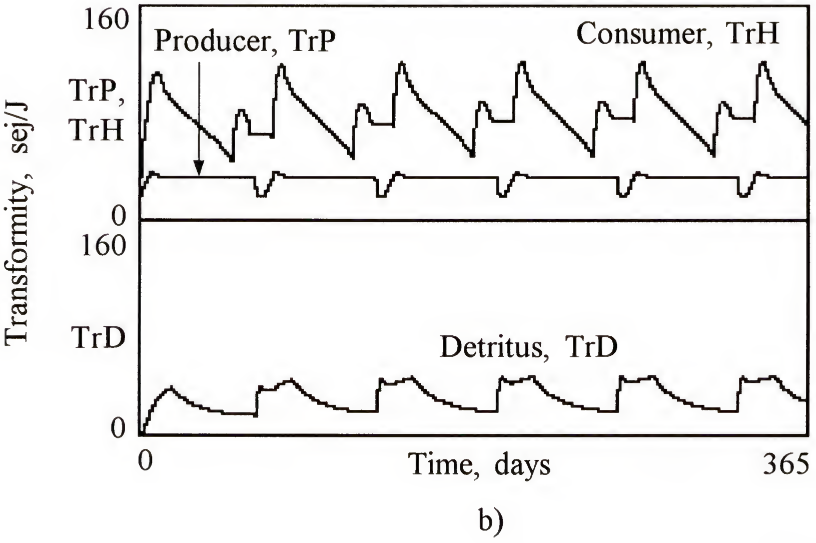

b)

Figure 3-38. Simulation results of the pulse model with a detritus storage in Figure 3-36, with coefficients as calibrated in Appendix Table B-4. a) Simulation of energy storages and b) transformity simulation.

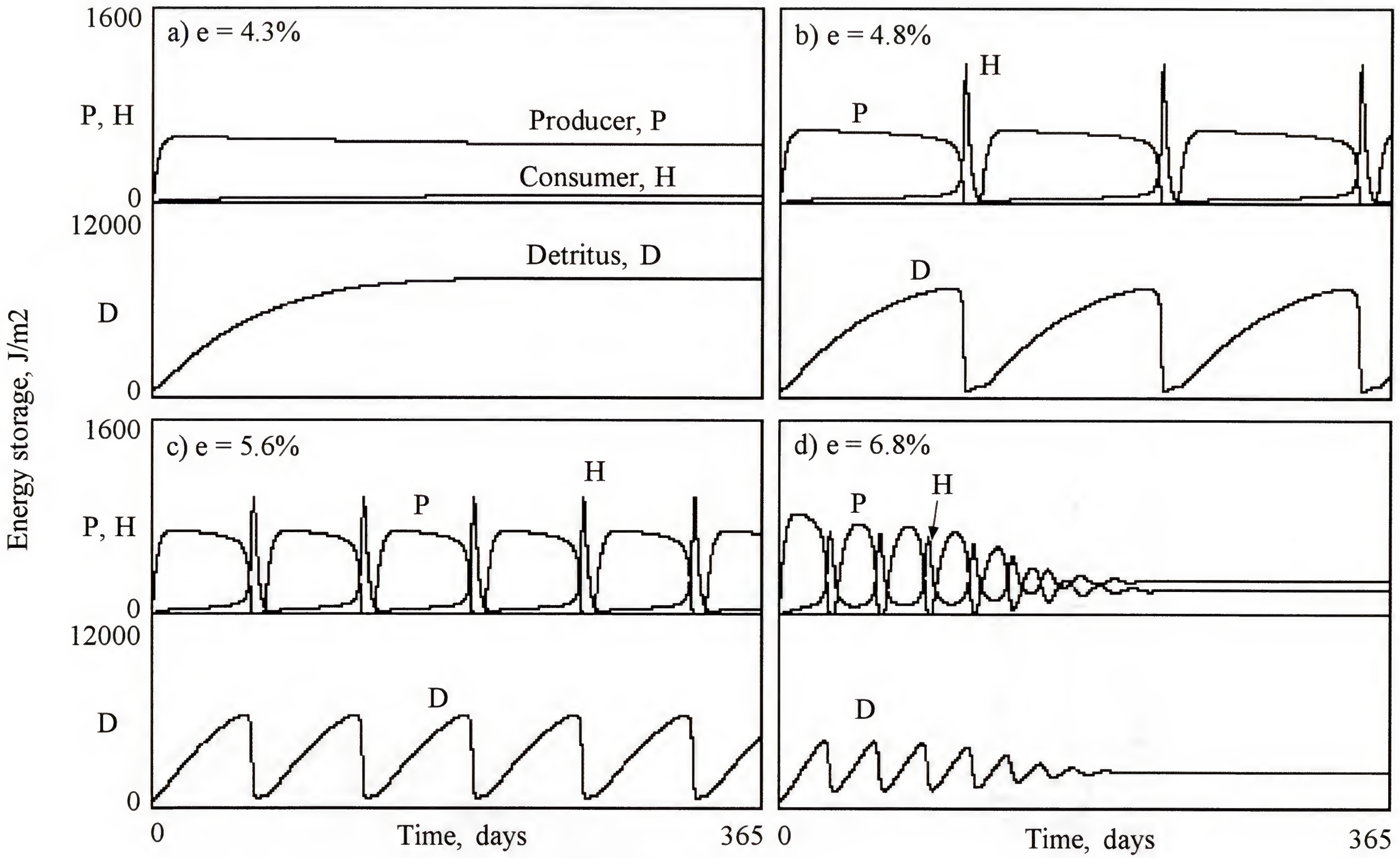

Figure 3-39. Simulation results of the pulse model with a detritus storage in Figure 3-36, for varied production efficieny of the producer (P). c) is the base case shown in Figure 3-38.

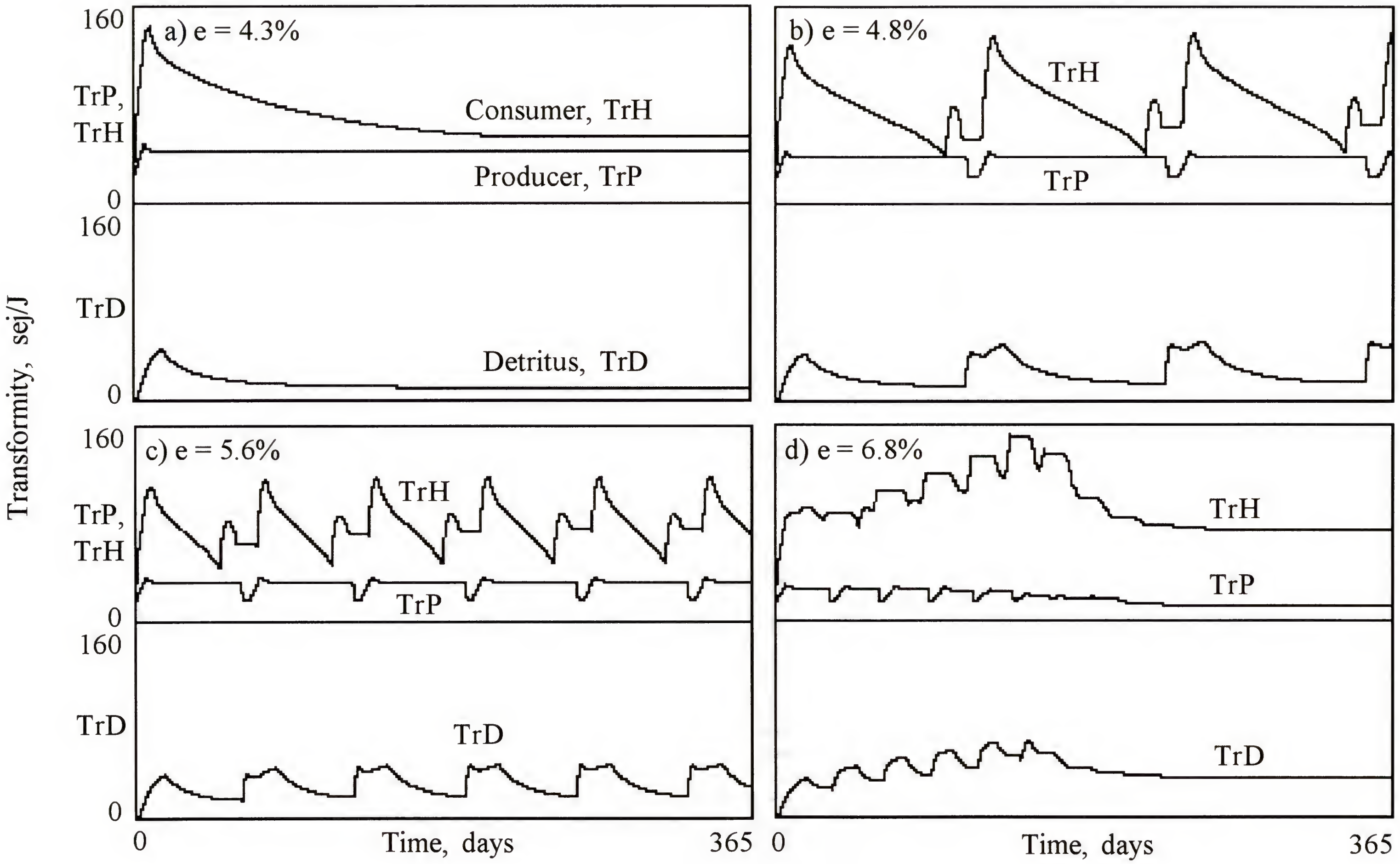

Figure 3-40. Transformity simulation of the pulse model with a detritus storage in Figure 3-36, for varied production efficiency of the producer (P). c) is the base case shown in Figure 3-38.

production in different times. To reflect this ecosystem structure in a simple way, the pulsing pair in Figure 2-4 was put in parallel units (Figure 3-41). Producers in both pairs competed for available energy (J) and for material (M). The upper pulsing pair was connected to the lower pulsing pair through an autocatalytic consumption pathway (k21) from the consumer 1 (H1) to the consumer 2 (H2). The model was calibrated so that the lower pulsing pair turned over slower than the upper pulsing pair. The model was calibrated in Appendix Table B-5 using values in Figure 3-42. The simulation program is listed in Appendix Table C-6.

The base run of the layered pulse model in Figure 3-41 is shown in Figure 3-43 for energy storages and in Figure 3-44 for emergy and transformity simulation. Pulses of both pairs alternated each other with the same frequency (Figure 3-43). The upper pulsing pair turned over faster and was first to pulse. The lower pulsing pair with slower turnover times took over after the upper pair pulsed, using material recycled by the upper pulsing consumer. Total storage of the producers and consumers generated a more realistic pattern that can be observed in real systems.

Emergy storages followed the same trend in the energy storage (Figure 3-44). Plateaus in the emergy storages of the producers represent the 5% limitation for noises from smaller scales in adding emergy to storages. Average transformity of both producers and consumers was slightly higher in the lower pulsing pair (P2 and H2). However, the transformity of the producer 2 (P2) had as much variation as the transformity of the producer 1 (P1).

Figure 3-45 shows effects of changes in energy input to the system (J). Increase in the energy level produced more frequent pulses. Both pulsing units pulsed at the same frequency regardless of the energy level. At low energy level, storages of the upper pulsing pair (P1 and H1) reached only a half of the base case. The model system showed pulsing dynamics over a wide range of energy level. The percent power used overall decreased with increase in the energy level, that is, more input energy passed unused

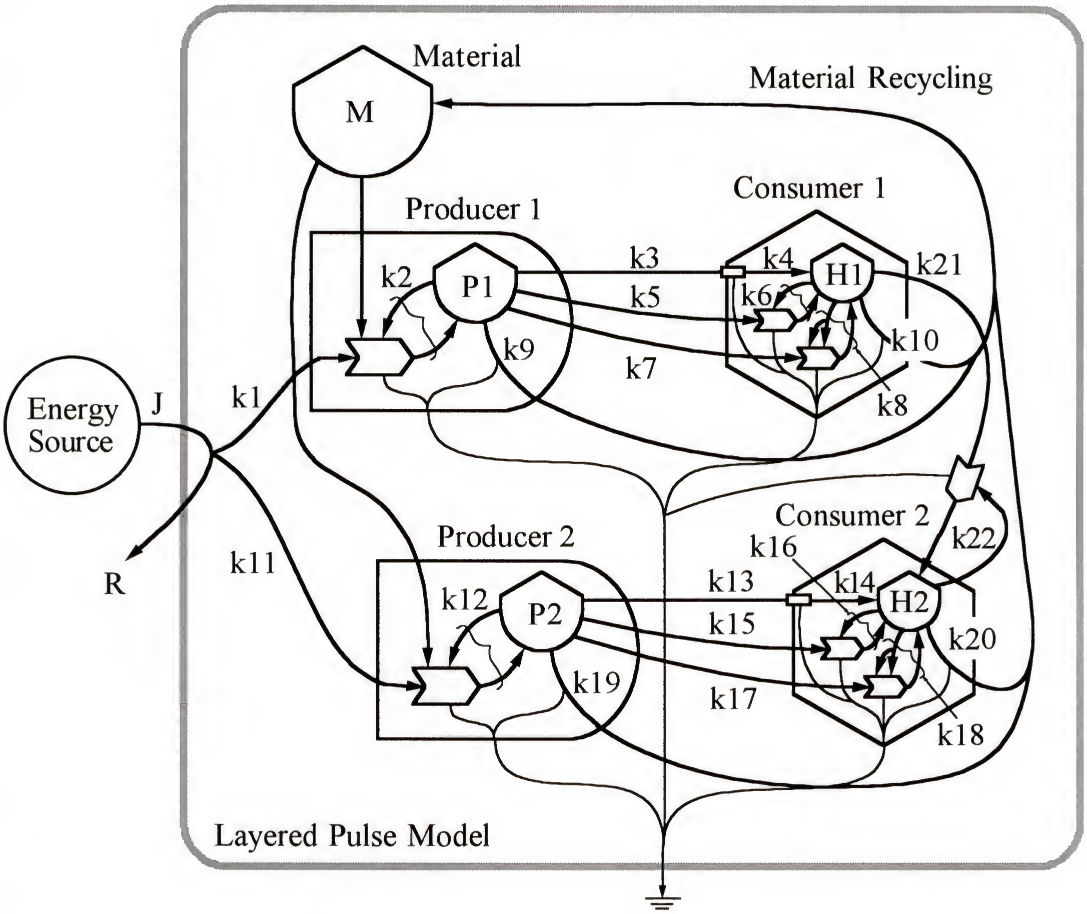

M = MT - f1*P1 - f2*H1 - f3*P2 - f4*H2
R = J / (1 + k1*M*P1 + k11*M*P2)
dP1 = k2*R*M*P1-k3*P1-k5*P1*H1-k7*P1*H1*H1-k9*P1
dP2 = k12*R*M*P2-k13*P2-k15*P2*H2-k17*P2*H2*H2-k19*P2
dH1 = k4*P1+k6*P1*H1+k8*P1*H1*H1-k10*H1-k21*H1*H2
dH2 = k14*P2+k16*P2*H2+k18*P2*H2*H2+k22*H1*H2-k20*H2

Figure 3-41. Layered pulse model with the pulsing pair in the basic pulse model in Figure 2-4 arranged in parallel. The pulsing pairs compete for the available energy and material, and connected through the autocatalytic pathway from the upper pair to the lower pair. MT=Total material inside the system; f1, f2, f3, and f4 = Material fraction of producer 1, consumer 1, producer 2, and consumer 2 storage, respectively.

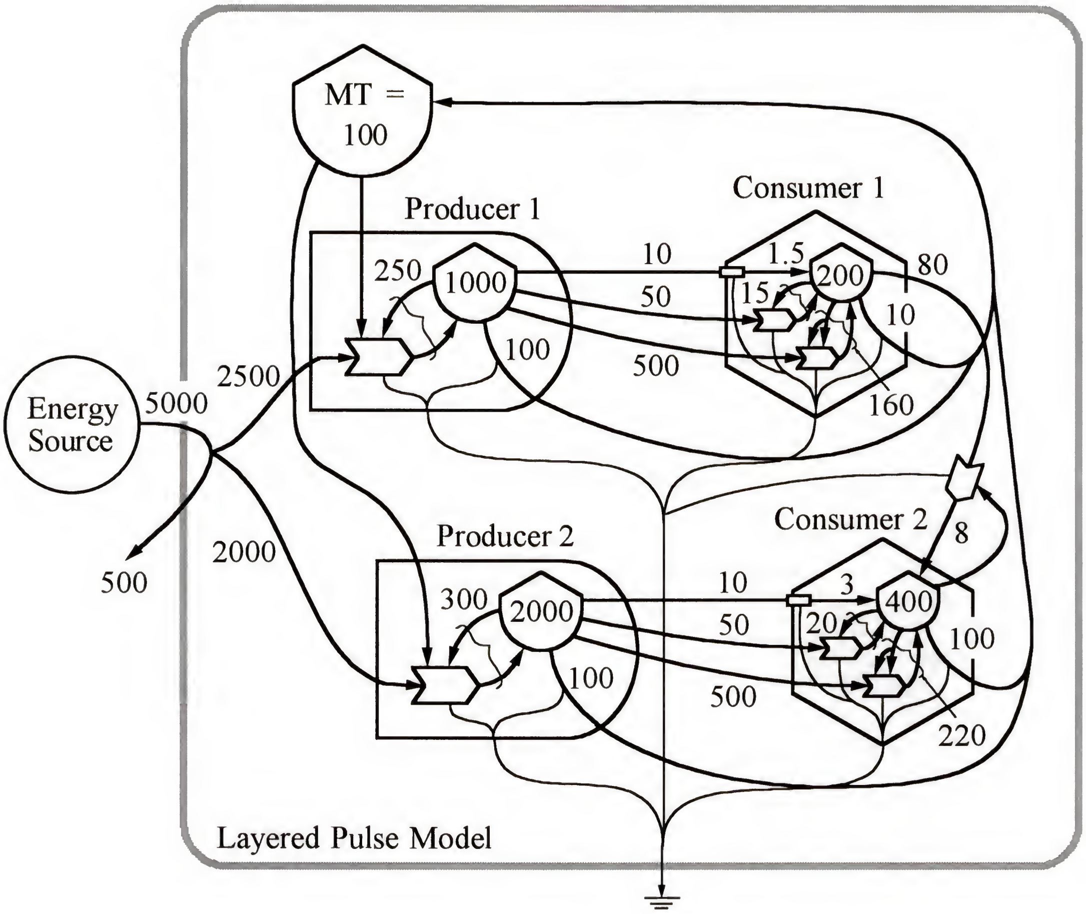

Figure 3-42. Calibration diagram of the layered pulse model in Figure 3-41.

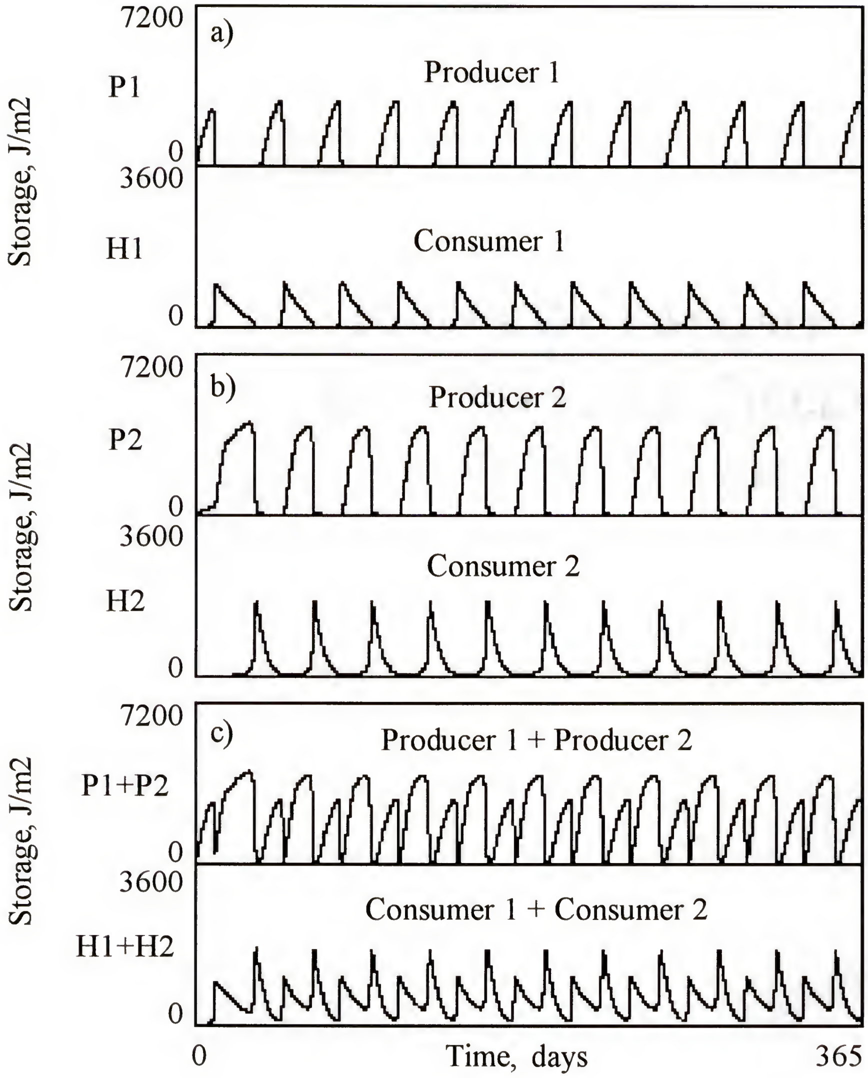

Figure 3-43. Simulation results of the layered model in Figure 3-41, with coefficients as calibrated in Appendix Table B-5.
a) Upper pulsing pair of producer 1 (P1) and consumer 1 (H1);
b) Lower pulsing pair of producer 2 (P2) and consumer 2 (H2);
c) Total producer and consumer in the system.

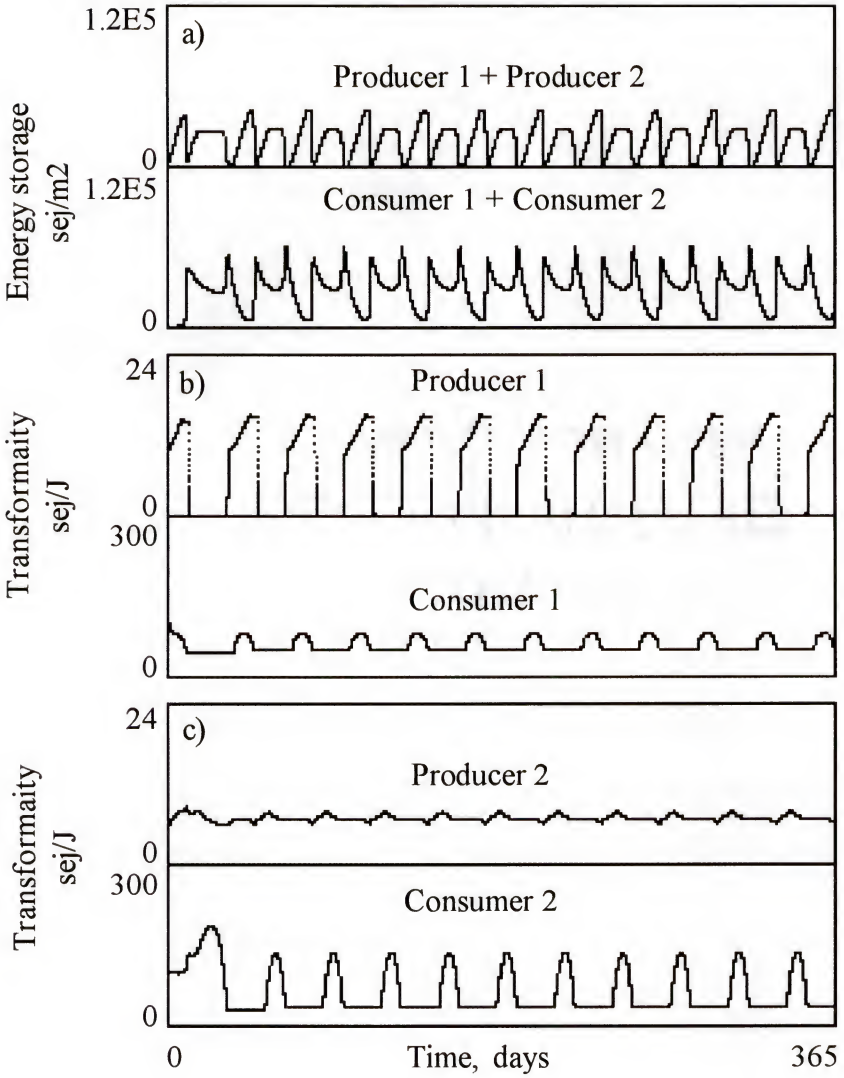

Figure 3-44. Emergy (a) and transformity (b and c) simulation of the layered model in Figure 3-41, with coefficients as calibrated in Appendix Table B-5.

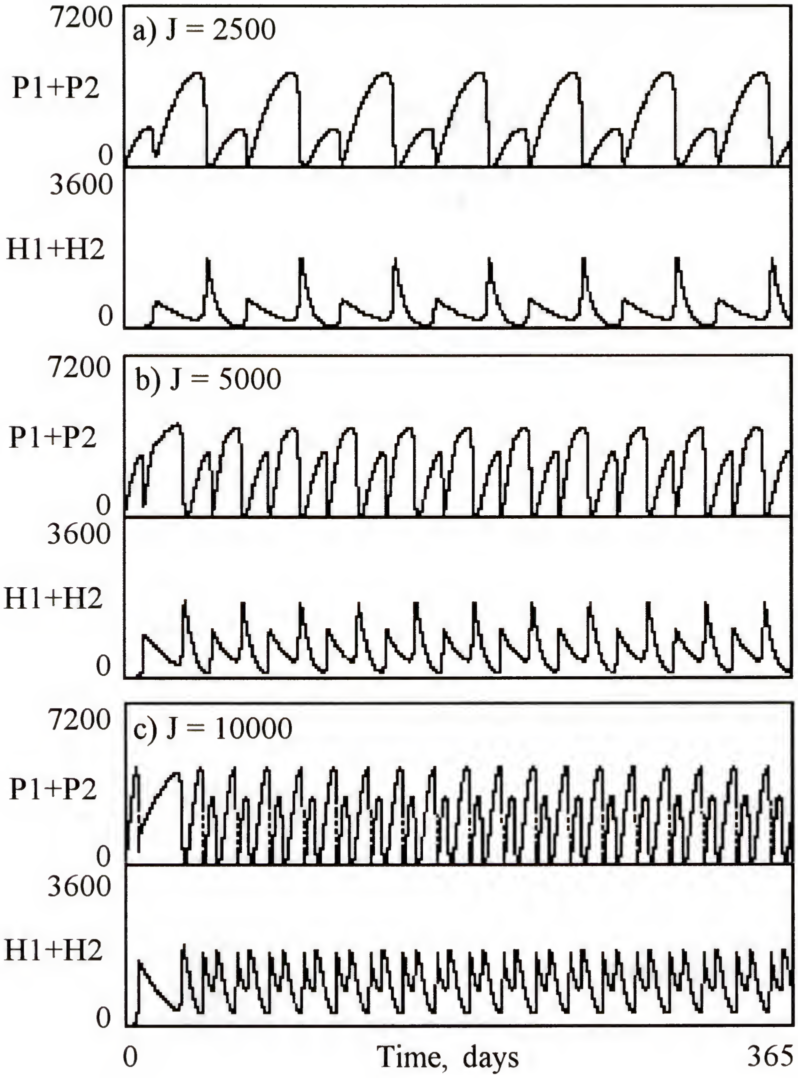

Figure 3-45. Simulation results of the layered model in Figure 3-41, for varied energy input from the source (J). b) is the base case shown in Figure 3-43.

through the system. The fraction of total power inflow through the lower pulsing pair decreased with increase in the energy level.

Figure 3-46 shows how the production efficiency of the producer 1 (P1) affected the model dynamics. Pulsing frequency of the model increased with increase in the efficiency. At very low efficiency (e=1%), the model reached a steady state after an initial pulse by the lower pulsing pair of the producer 2 (P2) and consumer 2 (H2). Storages of the producer 1 and consumer 1 were very low over the simulation period. The model pulsed over a wide range of efficiency. The overall percent power use decreased with increase in the efficiency.

Production efficiency of the producer 2 (P2) was varied in Figure 3-47 to see how the model dynamics responds to it. The system pulsed over a wide range of efficiency, with more frequent pulses with increase in the efficiency. At 1% efficiency (Figure 3-47a), the system reached a steady state after an initial pulse of the upper pulsing pair (P1 and H1). The producer 2 (P2) and consumer 2 (H2) were kept in very low concentration. At 100% efficiency, the combined result in Figure 3-47d did not show separate pulses by each pulsing unit. With this much high efficiency, there was little time delay in pulses by the lower pulsing unit after pulses by the upper pulsing pair, resulting in the pattern in Figure 3-47d. Power inflow through the upper pulsing pair increased and power inflow through the lower pulsing pair decreased with increase in the efficiency, resulting in decrease in overall power inflow.

In Figure 3-48 and 3-49, consumption efficiency of the consumer 1 (H1) by the consumer 2 (H2) was varied to see how the pulsing pattern of the model system changes. The system showed a pulsing pattern regardless of the efficiency, while the pulsing frequency increased with more efficient consumption (Figure 3-48). Pulse amplitude decreased as the consumption efficiency increased. Power inflow through the upper pulsing pair (J1) increased with increase in the efficiency, but power inflow through the

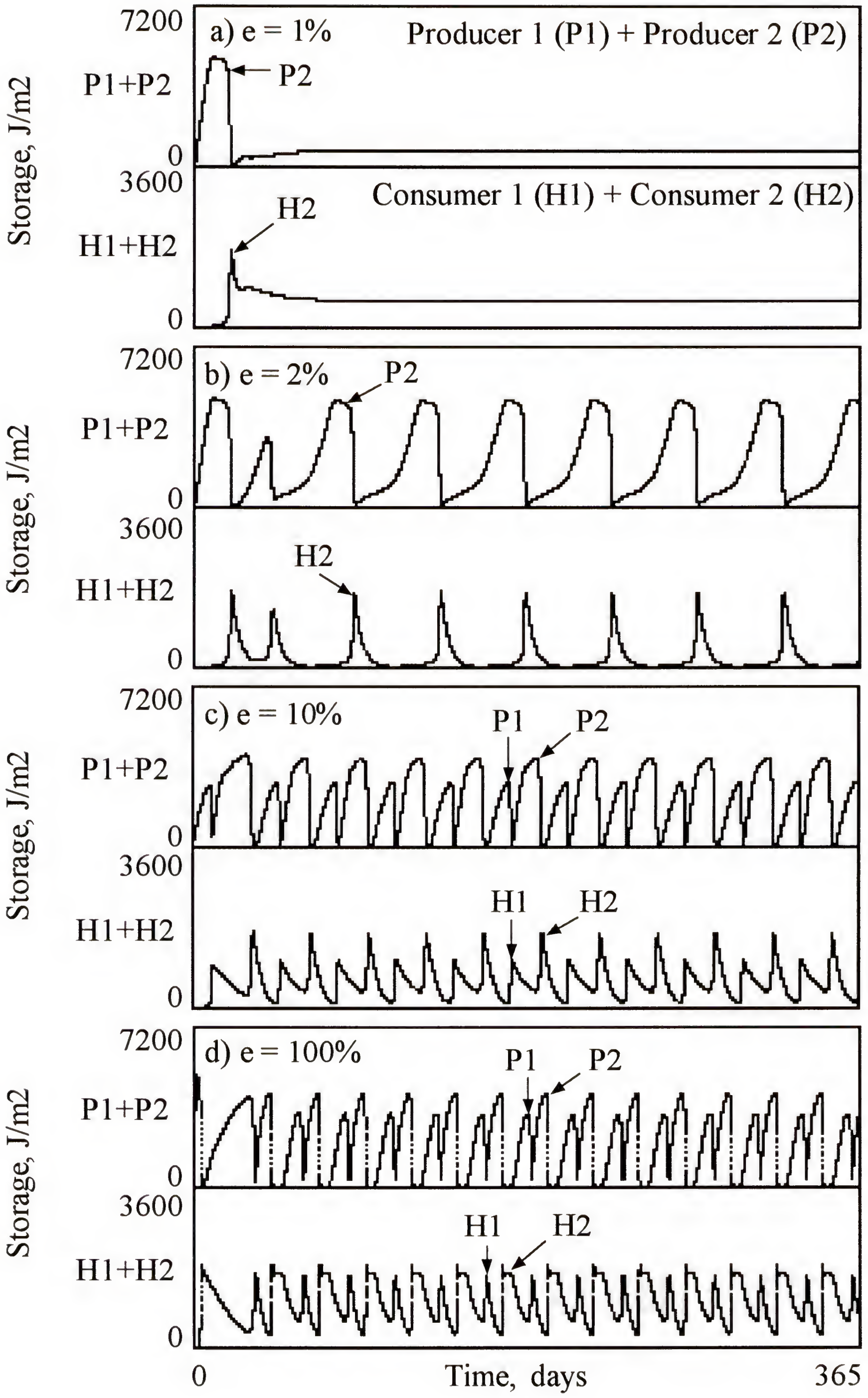

Figure 3-46. Simulation results of the layered model in Figure 3-41 when the production efficiency, e, of producer 1 (P1) was varied. c) is the base case shown in Figure 3-43.

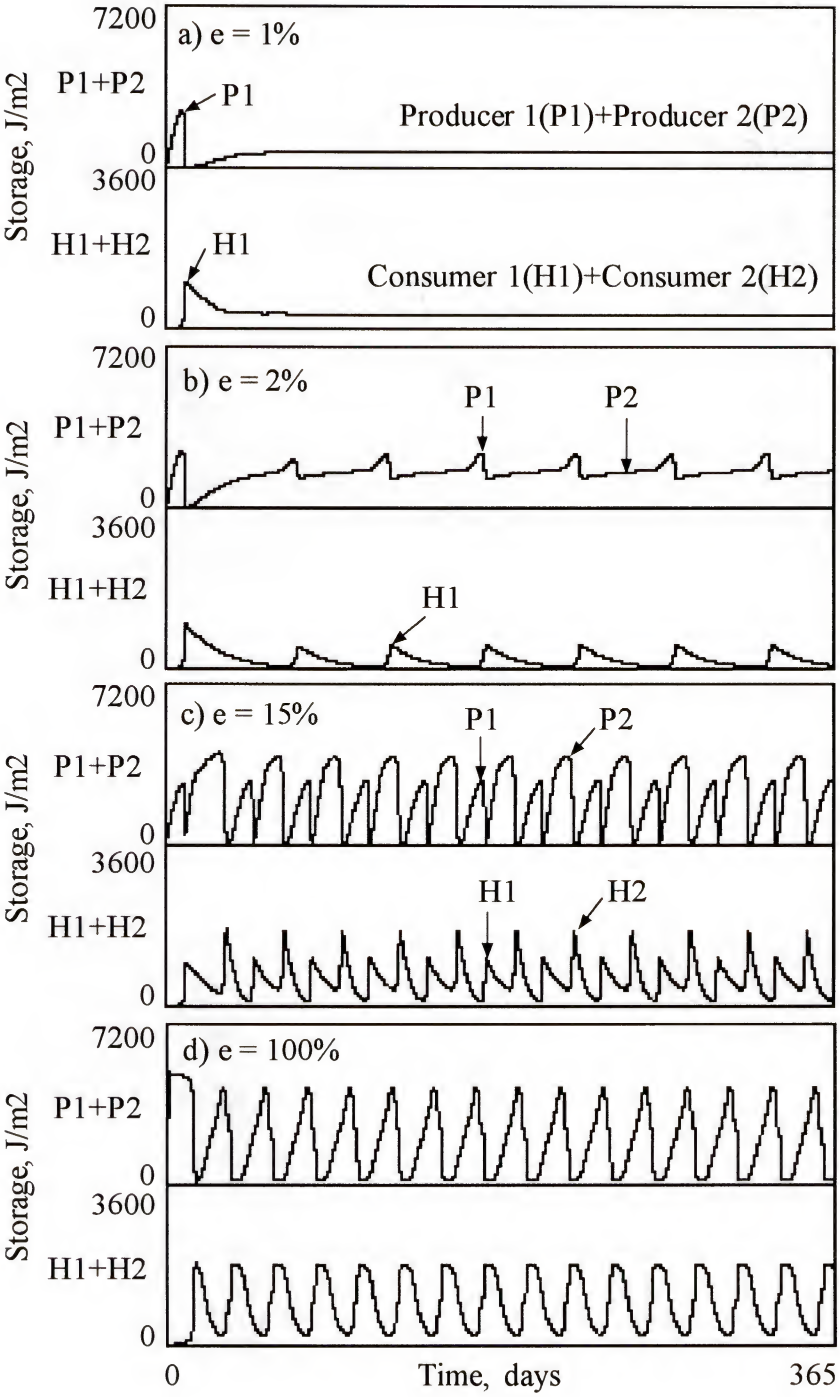

Figure 3-47. Simulation results of the layered model in Figure 3-41 when the production efficieny, e, of producer 2 (P2) was varied. c) is the base case shown in Figure 3-43.

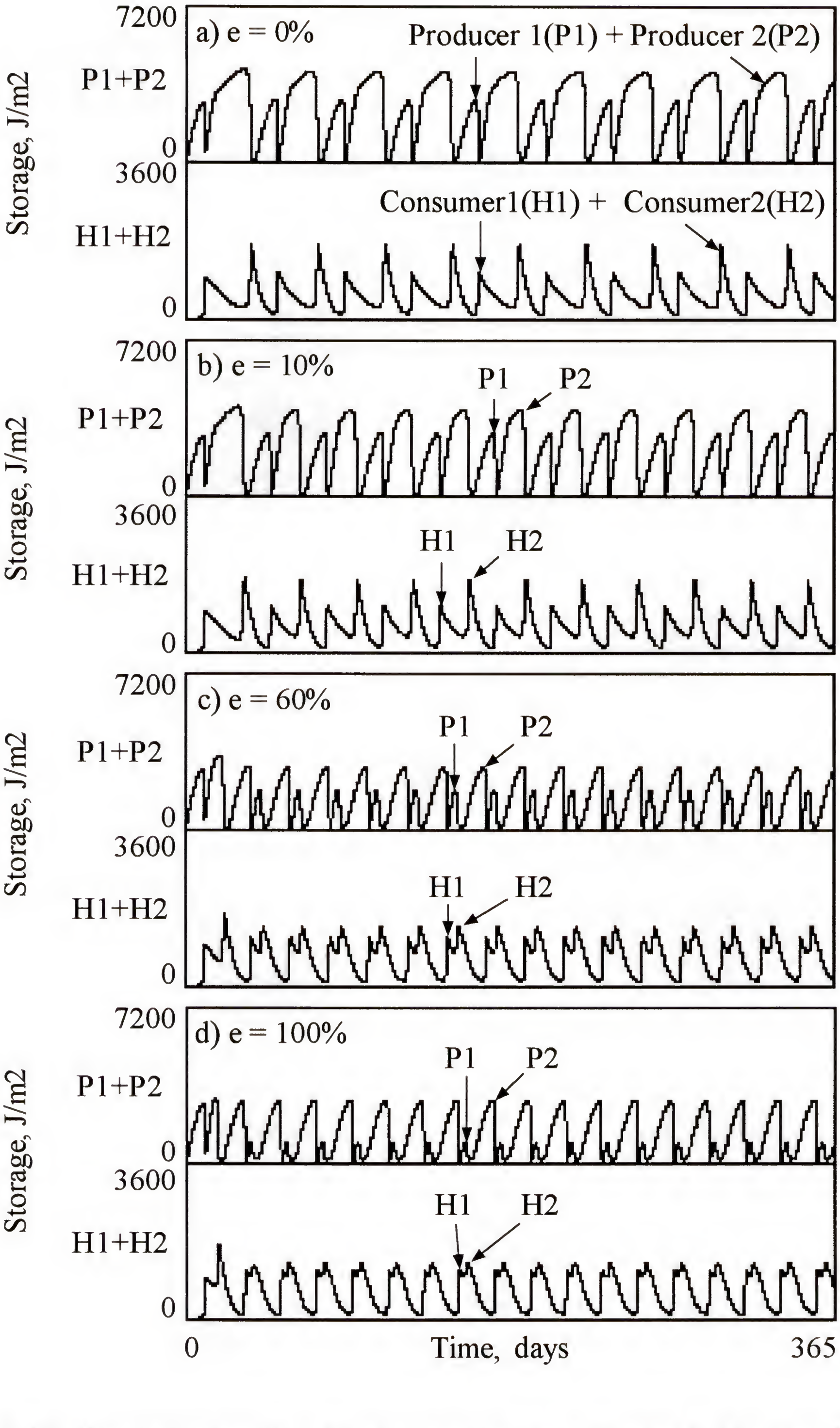

Figure 3-48. Simulation results of the layered model in Figure 3-41 when the efficiency, e, of energy transfer from the consumer 1 (H1) to the consumer 2 (H2) was varied. Pulse frequency of both producers and consumers increased, and pulse amplitude decreased as the efficiency increased. b) is the base case shown in Figure 3-43.

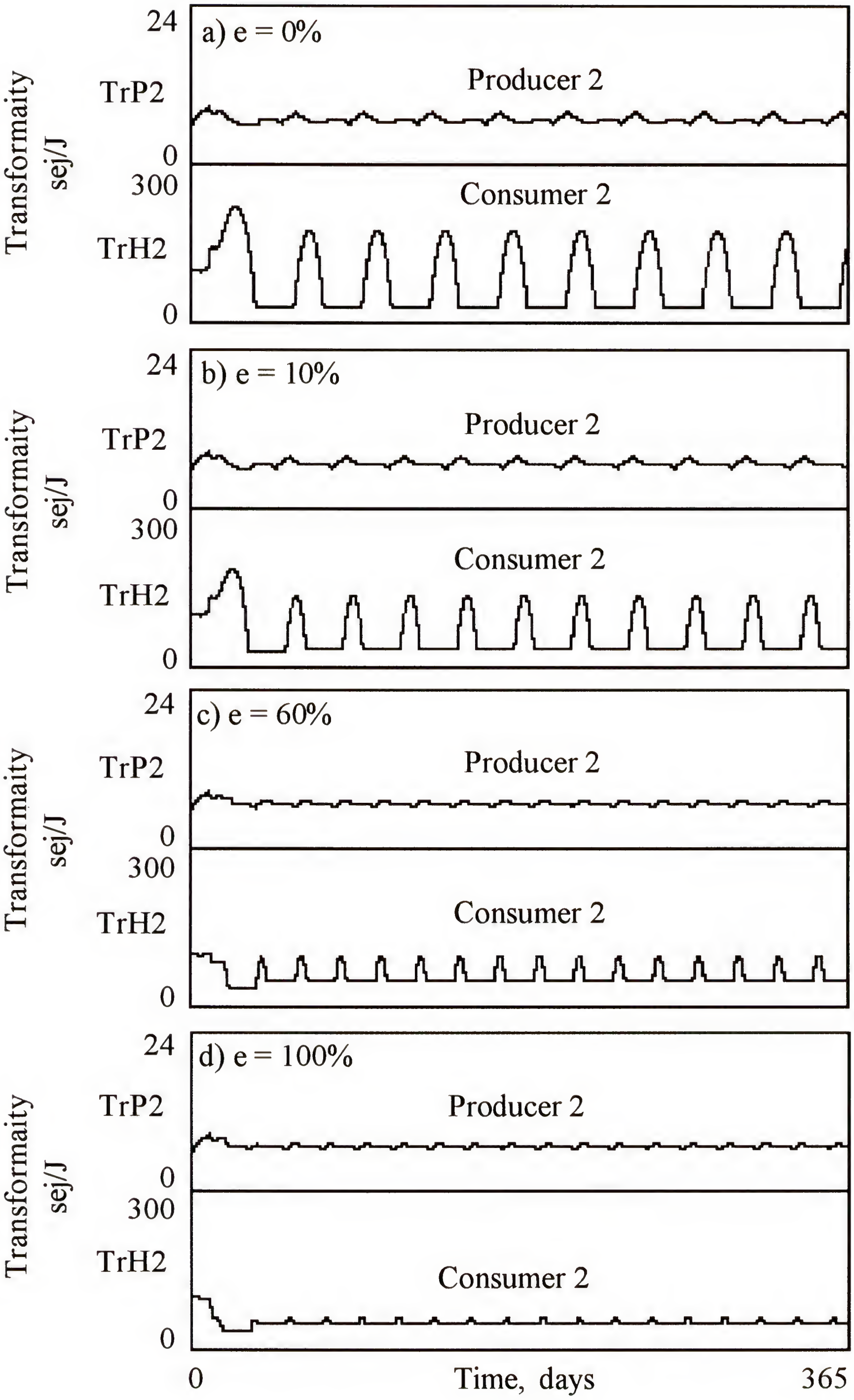

Figure 3-49. Transformity simulation results of the layered model in Figure 3-41 when the efficiency, e, of energy transfer from the consumer 1 (H1) to the consumer 2 (H2) was varied. Variability of the transformity of both producer 2 and consumer 2 decreased as the efficiency increased, and the average transformities of storages also decreased. b) is the base case shown in Figure 3-44.

producer 2 decreased. Overall, the percent power use increased with the consumption efficiency.

Variation in the efficiency made little change in average transformity of the producer 2 (Figure 3-49). The transformity of the consumer 2 decreased with increase in the consumption efficiency.

Two Module Pulse Model

Real ecosystems have more than two energy levels (trophic levels). In Figure 3-50, two pulsing pairs from Figure 2-4 were connected to represent multiple energy levels in nature. Two pulsing pairs were connected with two different pathways to provide alternative consumption modes; the linear pathways (k10 and k11) and the autocatalytic pathways (k12 and k13). Material was conserved in the system and all components participated in material recycle. The model was calibrated so that the second pulsing pair had slower turnover time (Figure 3-51). Model coefficients were calculated in Appendix Table B-6 and the simulation program is listed in Appendix Table C-7.

The base run of the model in Figure 3-52 produced two different pulsing frequencies for each pulsing pair. The producer-herbivore pair pulsed three times for every pulse by the second pulsing pair. Pulsing by the first and second carnivores required energy from the herbivore to build up storage enough to pulse. Varying properties of the first carnivore caused pulses in the lower hierarchy. Feeding back, the pulsing of the first and second carnivores controlled the pattern of the producer-herbivore pair. Pulse amplitude of the producer and herbivore was highest right after the second carnivore pulses. Average percent power use was about 89.7%, 2.2% higher than in the basic pulsing model in Figure 3-12a.

In the model in Figure 3-50, average transformity over the simulation period increased up the chain from the producer to the second carnivore. All storages had the

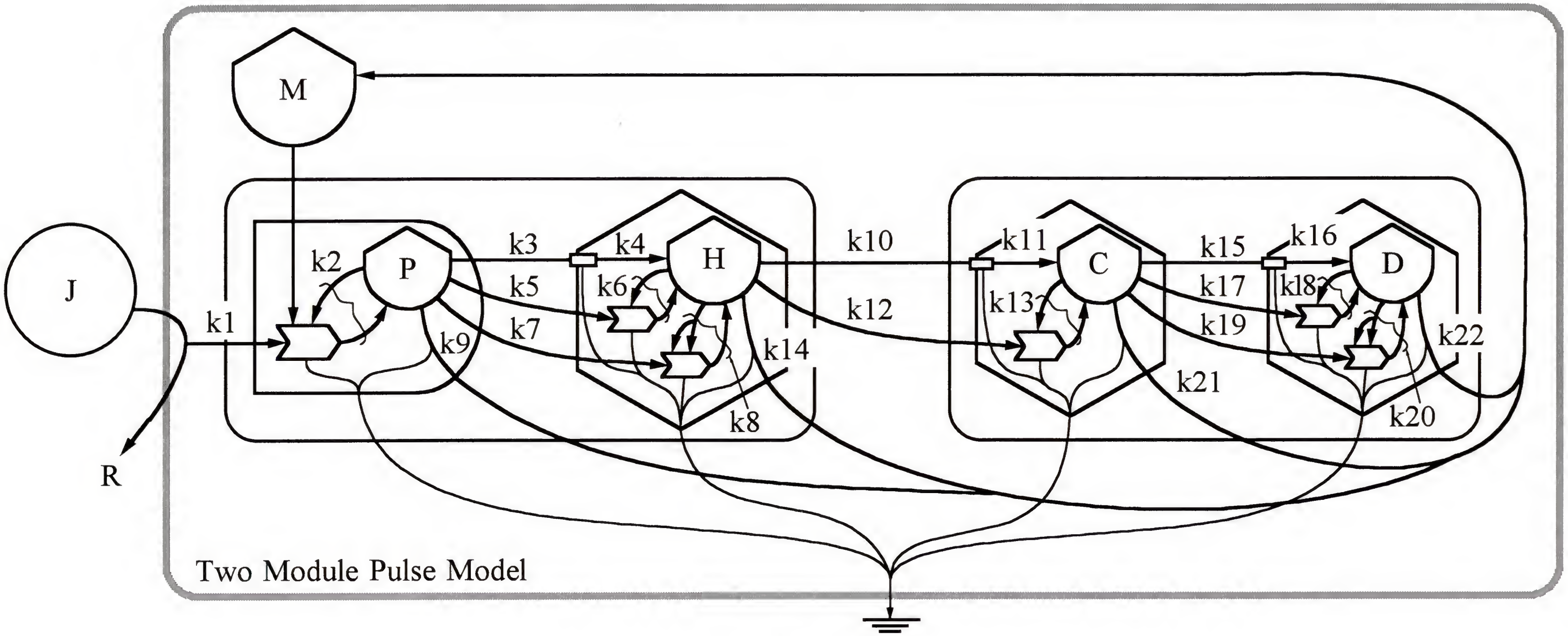

$M = MT - f1*P - f2*H - f3*C - f4*D$
$R = J / (1 + k1*M*P)$
$dP = k2*R*M*P - k3*P - k5*P*H - k7*P*H*H - k9*P$
$dH = k4*P + k6*P*H + k8*P*H*H - k10*H - k12*H*C - k14*H$
$dC = k11*H + k13*H*C - k15*C - k17*C*D - k19*C*D*D - k21*C$
$dD = k16*C + k18*C*D + k20*C*D*D - k22*D$

Figure 3-50. Two module pulse model with two pulsing pairs connected in series. Two pulsing pairs are connected through two different pathways: linear and autocatalytic. MT = Total material conserved in the system; f1, f2, f3, and f4 = Material fraction of the producer (P), herbivore (H), 1st carnivore (C), and 2nd carnivore (D), respectively.

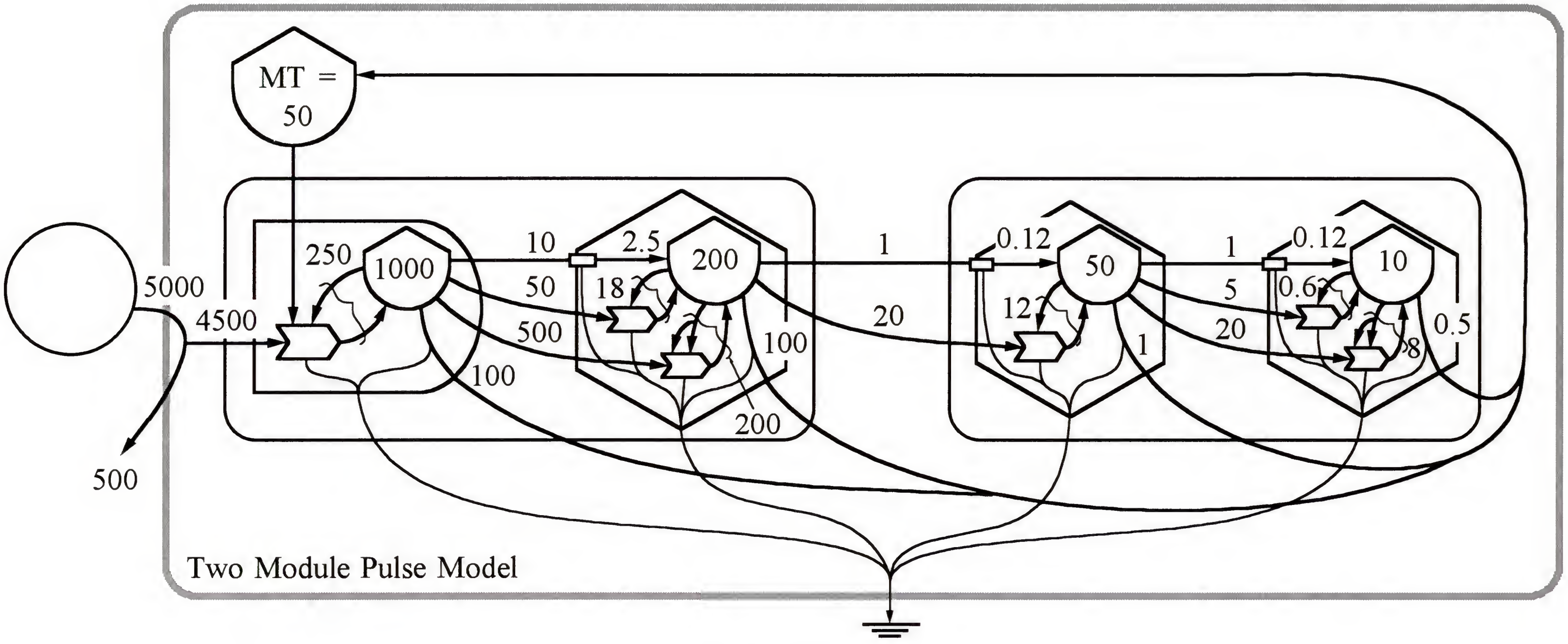

Figure 3-51. Calibration diagram of the two module pulse model in FIgure 3-50. MT = Total material conserved in the system.

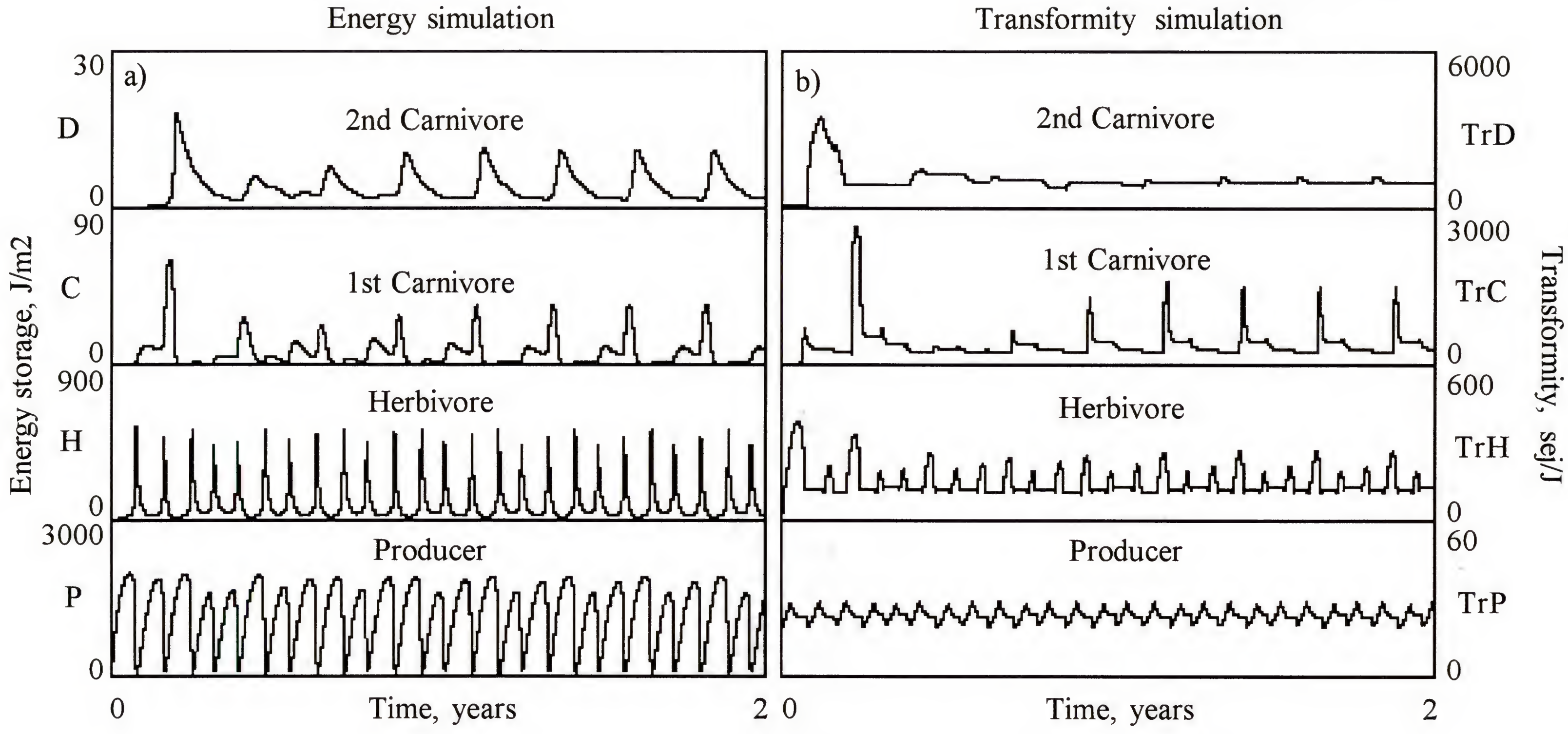

Figure 3-52. Simulation results of the two module pulse model in Figure 3-50, with coefficients as calibrated in Appendix Table B-6. a) Simulation of energy storages and b) transformity simulation.

highest transformity during the fast growth period before their storages reached maximum. Thus, transformity simulation (Figure 3-52b) clearly showed the energy hierarchy.

Figure 3-53 shows how input energy level (J) affected the dynamics of the model system. Pulse frequency increased as the energy input increased. However, there was only a short range of energy level for pulsing to occur. With lower energy input, the producer could not produce fast enough and pulsing pathways of the consumers were not activated. Percent power use decreased with increase in the energy input, leaving more energy unused.

Changes in the transformity of storages are plotted in Figure 3-54, where the energy input was varied. The transformities of the producer (P), herbivore (H), and first carnivore (C) were maximum in the pulsing range, but the transformity of the second carnivore (D) decreased with increase in the energy level (J). Even though the average transformity of the second carnivore at J=5500 over the simulation period was greater than that at J=5000, it decreased to a very low level at the end of the simulation.

Figure 3-55 shows effects of changes in the production efficiency (k1 to k2) of the producer unit (P). The model had a very short range of production efficiency to pulse, from 4.4% to 5.9%. Within this range, increase in the production efficiency produced more frequent pulses. Percent power use decreased with increase in the production efficiency from 4.3% to 5.6%, and at 6% efficiency percent power use increased again. The second pulsing pair did not have a chance to develop structures at low production efficiency.

Figure 3-56 shows changes in transformity for varied efficiency of primary production. In any case, transformity increased with increase in the energy level. The transformities of the producer (P), first carnivore (C), and second carnivore (D) decreased with increase in the production efficiency. But, the herbivore (H) showed maximum transformity in the pulsing range.

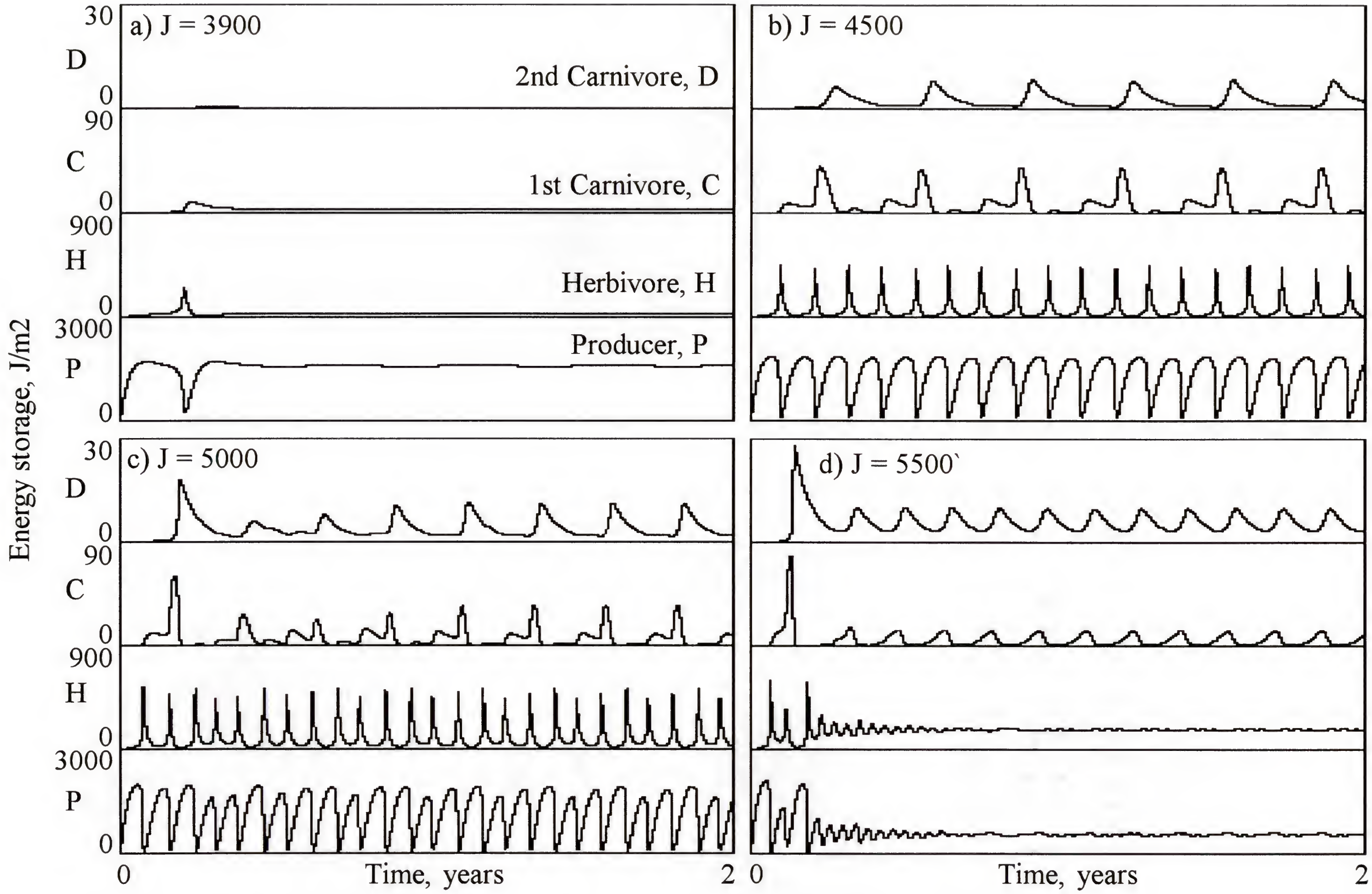

Figure 3-53. Simulation results of the two module pulse model in Figure 3-50, for varied level of energy input (J) to the system. c) is the base case shown in Figure 3-52.

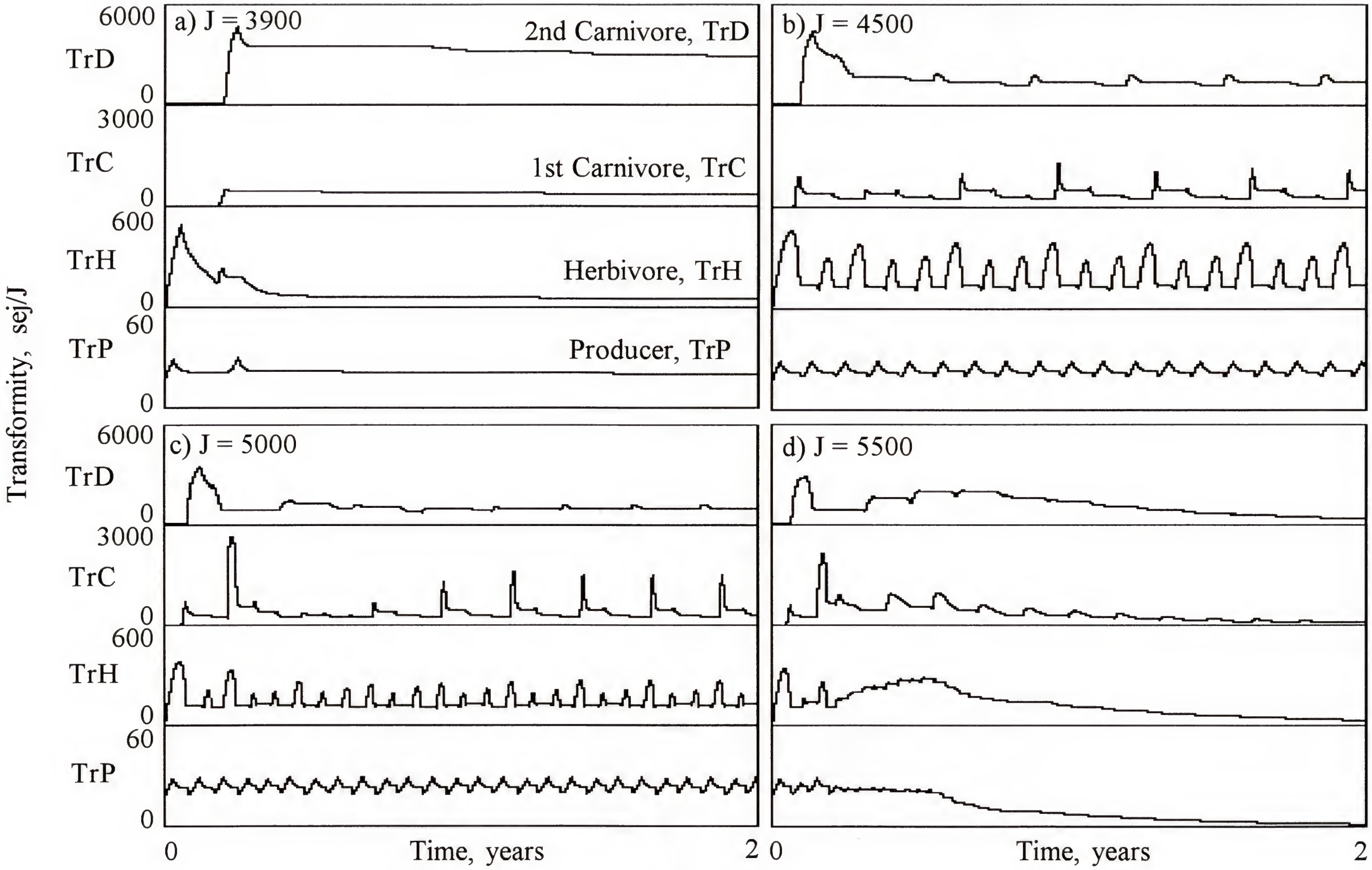

Figure 3-54. Transformity simulation of the two module pulse model in Figure 3-50, for varied level of energy input (J) to the system. c) is the base case shown in Figure 3-52.

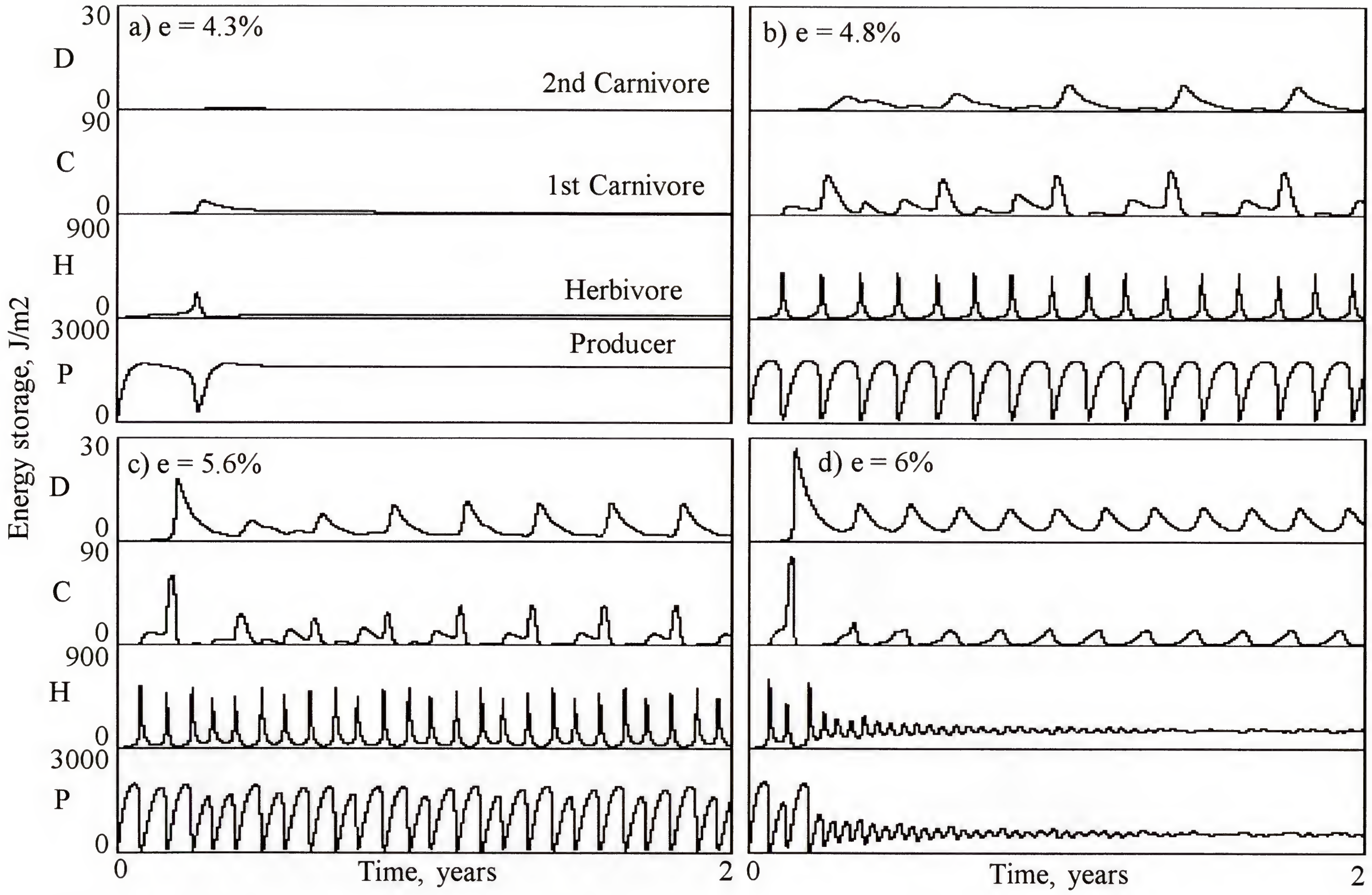

Figure 3-55. Simulation results of the two module pulse model in Figure 3-50, for varied efficiency of primary production of the producer (P). c) is the base case shown in Figure 3-52.

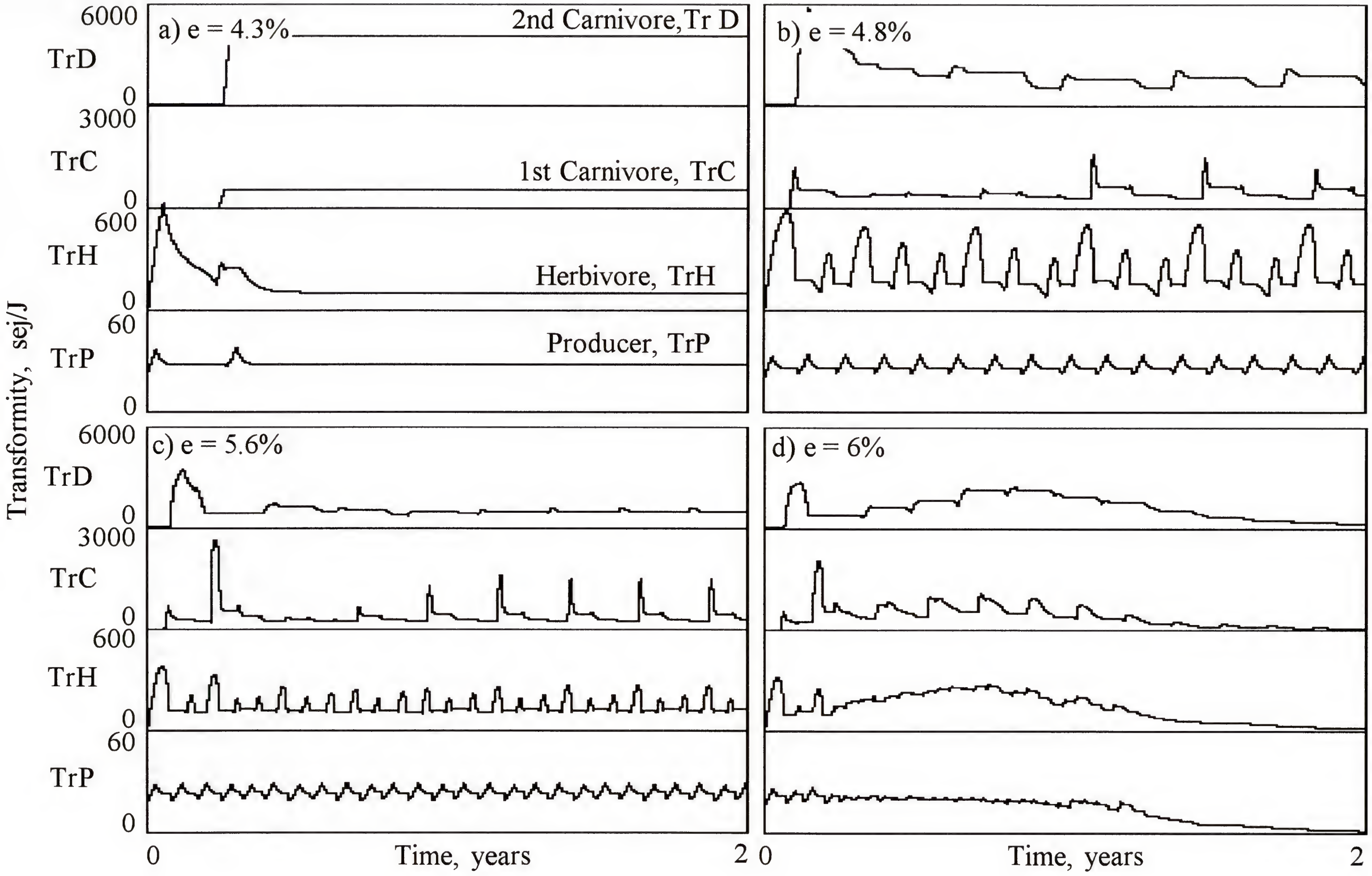

Figure 3-56. Transformity simulation of the two module pulse model in Figure 3-50, for varied efficiency of primary production of the producer (P). c) is the base case shown in Figure 3-52.

Three Module Pulse Model

The two module pulse model in Figure 3-50 was extended into a six energy level model by adding one more pulsing pair (Figure 3-57). A third pulsing pair is connected to the second pulsing pair through the linear (k22 and k23) and autocatalytic (k24 and k25) pathways. Figure 3-58 is a calibration diagram that was used to calculate the pathway coefficients in Appendix Table B-7. The simulation program is listed in Appendix Table C-8.

Simulation results in Figure 3-59 shows three different pulsing frequencies for each pulsing pair, with decreasing pulsing frequency as they go up the food chain. Variations in the first carnivore (C) and the third carnivore (E) reflected more frequent pulses from one scale below. Controls from pulses in the higher energy levels were reflected in variations of pulse amplitudes in the lower energy levels. Results of the transformity simulation revealed the hierarchy in energy levels. The producer had lowest average transformity and the top predator the highest transformity. Average percent power use was 89.8%.

Characteristics of Simulation Pulses

Figure 3-60 shows pulse characteristics in regard to interval and intensity, using various runs of the basic pulse model from Figures 3-13 to 3-23. Pulse intensity was measured in emergy units (emergy storage during a pulse divided by the emergy storage in a complete pulse cycle). As defined, pulse intensity is the portion of cumulative emergy in a complete pulse cycle that is added during a pulse. In these runs there was an optimum pulse interval (45-50 days) for maximum pulsed feedback effect (Figure 3-60a). Figure 3-60b shows an optimum pulse interval for maximum transformity. In this graph, transformity is the maximum transformity that occurred in a complete pulse cycle. Transformity increased as pulse intensity increased (Figure 3-60c).

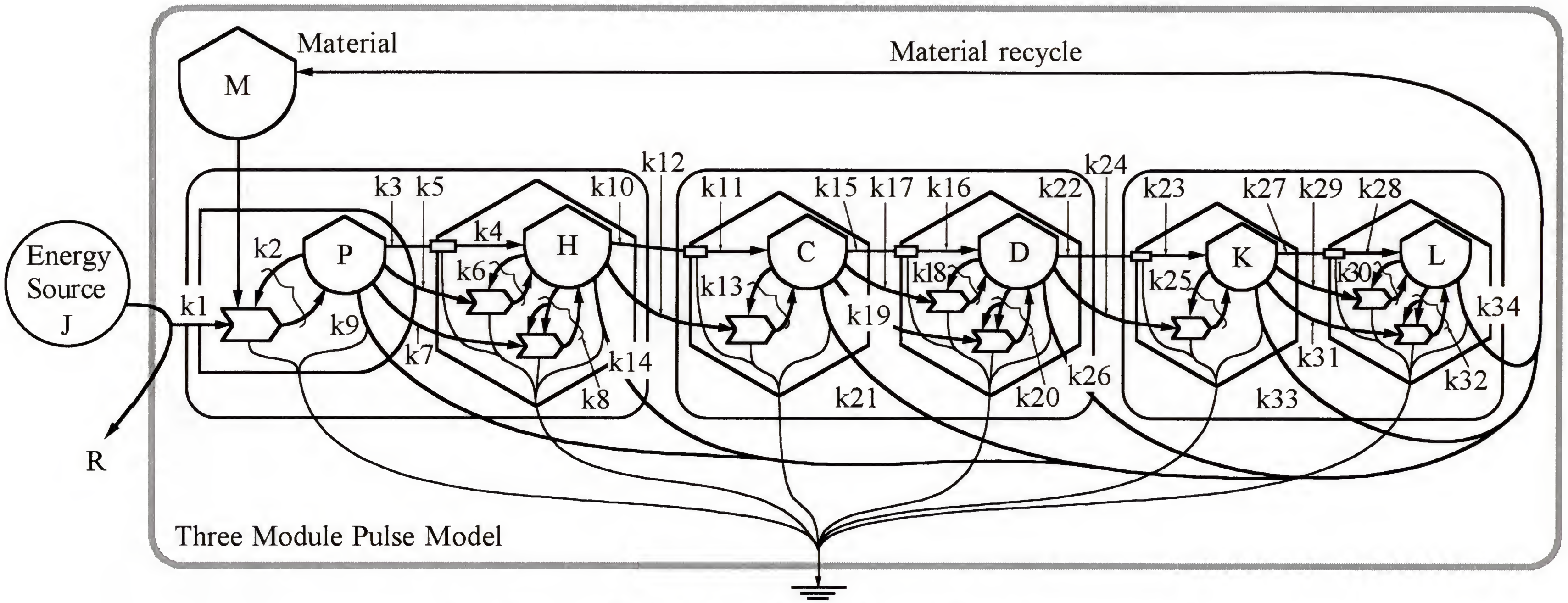

$$M = MT - f1*P - f2*H - f3*C - f4*D - f5*K - f4*L$$
$$R = J / (1 + k1*M*P)$$
$$dP = k2*R*M*P - k3*P - k5*P*H - k7*P*H*H - k9*P$$
$$dH = k4*P + k6*P*H + k8*P*H*H - k10*H - k12*H*C - k14*H$$
$$dC = k11*H + k13*H*C - k15*C - k17*C*D - k19*C*D*D - k21*C$$
$$dD = k16*C + k18*C*D + k20*C*D*D - k22*D - k24*D*K - k26*D$$
$$dK = k23*D + k25*D*K - k27*K - k29*K*L - k31*K*L*L - k33*K$$
$$dL = k28*K + k30*K*L + k32*K*L*L - k34*L$$

Figure 3-57. Three module pulse model in which three pulsing pairs are connected in series. Each pulsing pair is connected through two different pathways: linear and autocatalytic. MT = Total material conserved in the system; f1, f2, f3, f4, f5, and f6 = Material fraction of the producer (P), herbivore (H), 1st carnivore (C), 2nd carnivore (D), 3rd carnovore (K), and top predator (L), respectively.

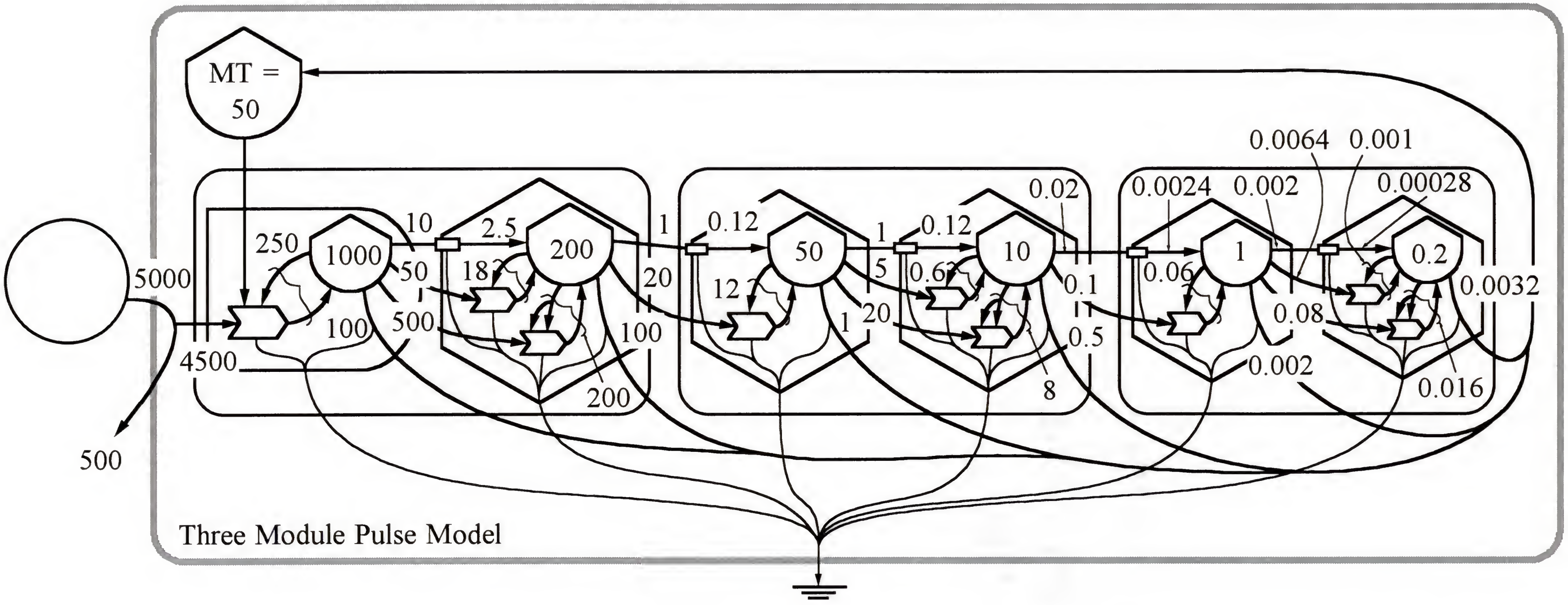

Figure 3-58. Calibration diagram of the three module pulse model in Figure 3-57. MT = Total material conserved in the system.

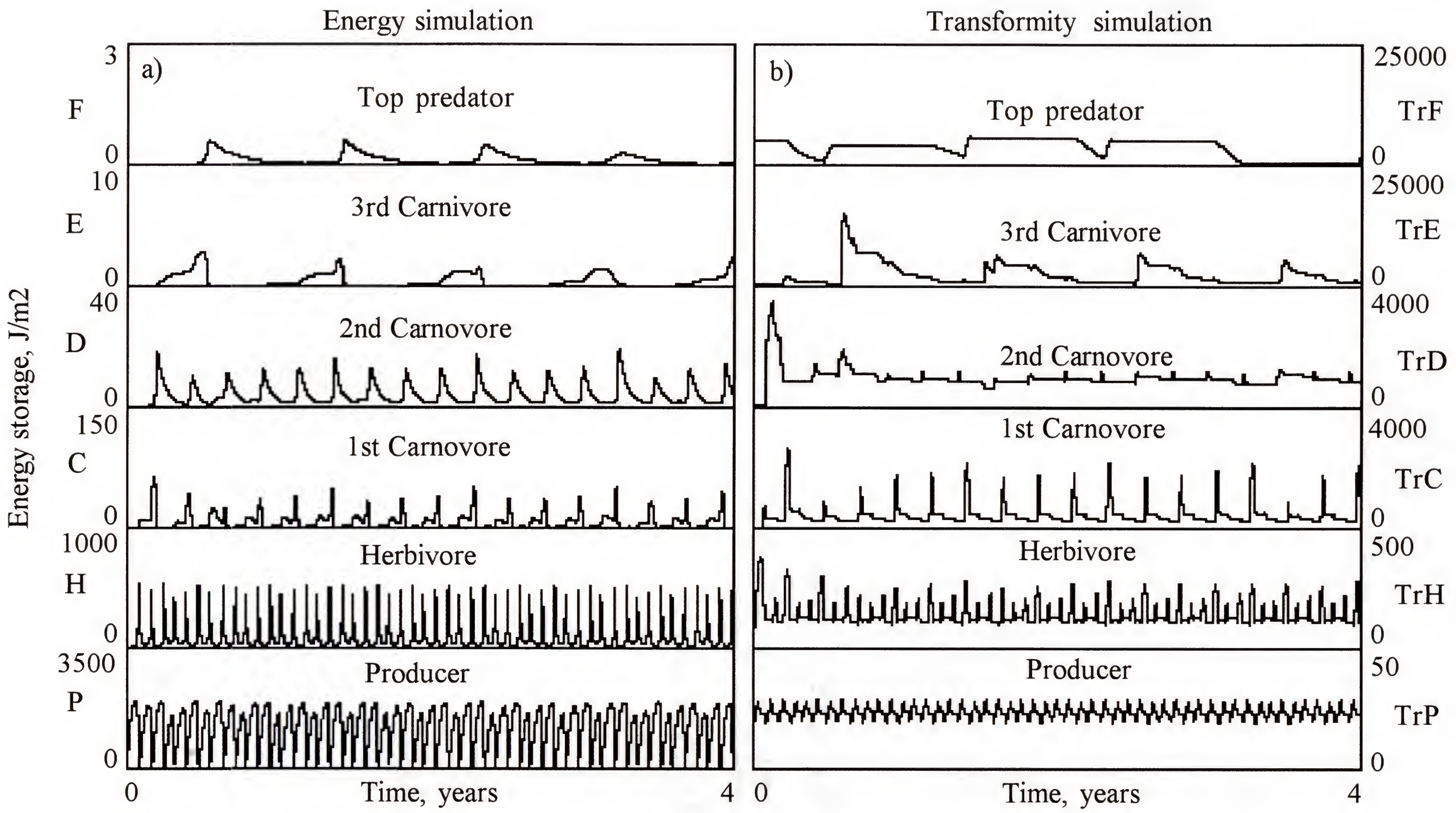

Figure 3-59. Simulation results of the three module pulse model in Figure 3-57, with coefficients calibrated as in Appendix Table B-7. a) Simulation of energy storages and b) transformity simulation.

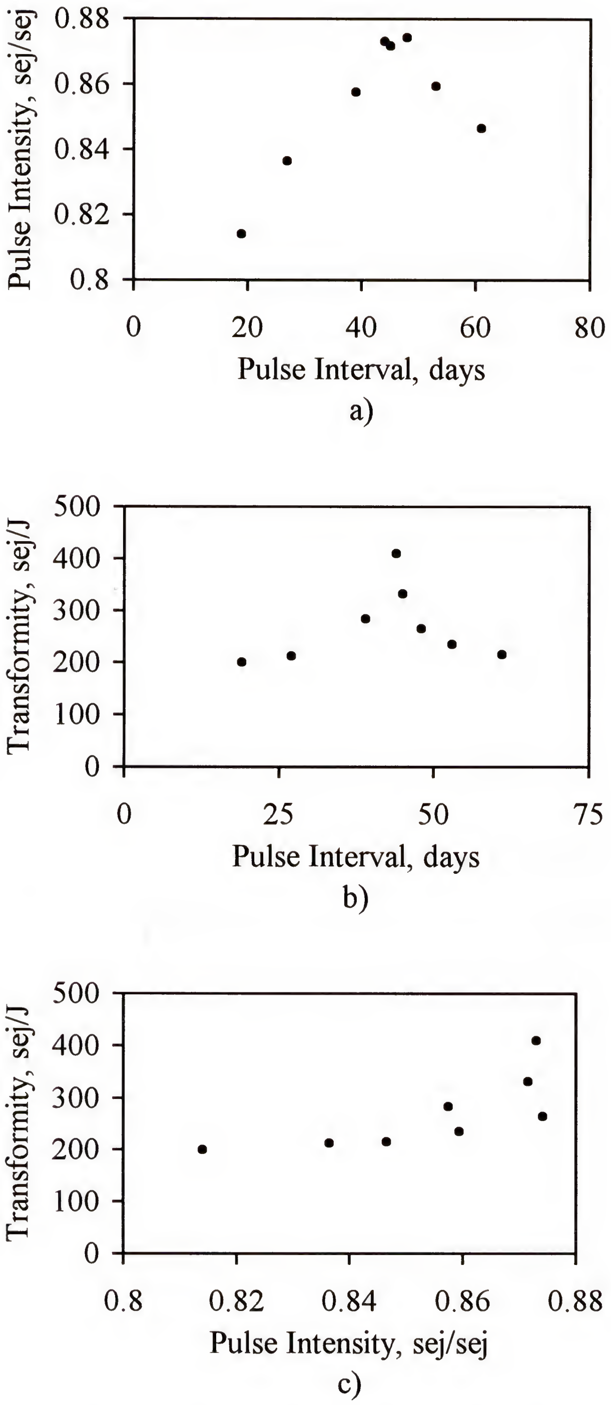

Figure 3-60. Characteristics of pulses in the simulation results of the basic pulse model in Figure 2-4. a) Relationship between pulse interval and intensity; b) Maximum transformity over the simulation period as a function of pulse interval; c) Relationship between pulse intensity and transformity.

In Figure 3-61, average quantities of the storages of the two module and three module pulse models over simulation time periods were plotted as a function of transformity, on a log-log plot. As the energy was transformed from producer to carnivores, the amount of energy stored in a hierarchy decreased and the transformity of each hierarchy increased.

Simulation results of the three module pulse model were used to plot on similar coordinates for comparison with the field data in Figures 3-1 to 3-3 (Figure 3-62). Pulses of the producer storage were used to plot those graphs. Graphs in Figure 3-62 show the same pattern in observed data in Figures 3-1 to 3-3.

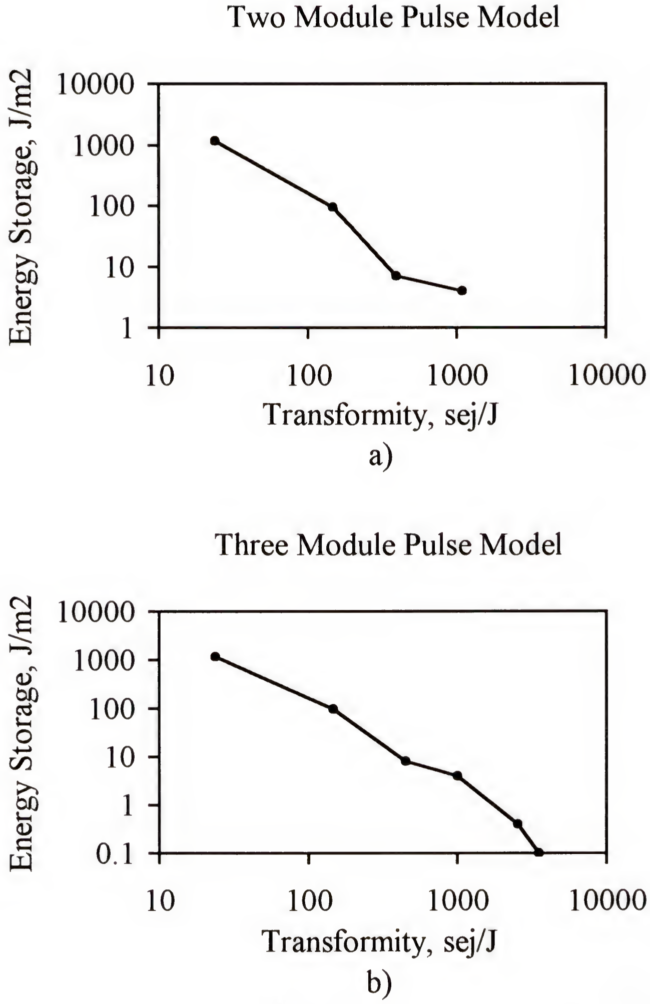

Figure 3-61. Quantity-quality diagram on a log-log plot, using the simulation results of the two module pulse model in Figure 3-50 (a) and the three module pulse model in Figure 3-57 (b).

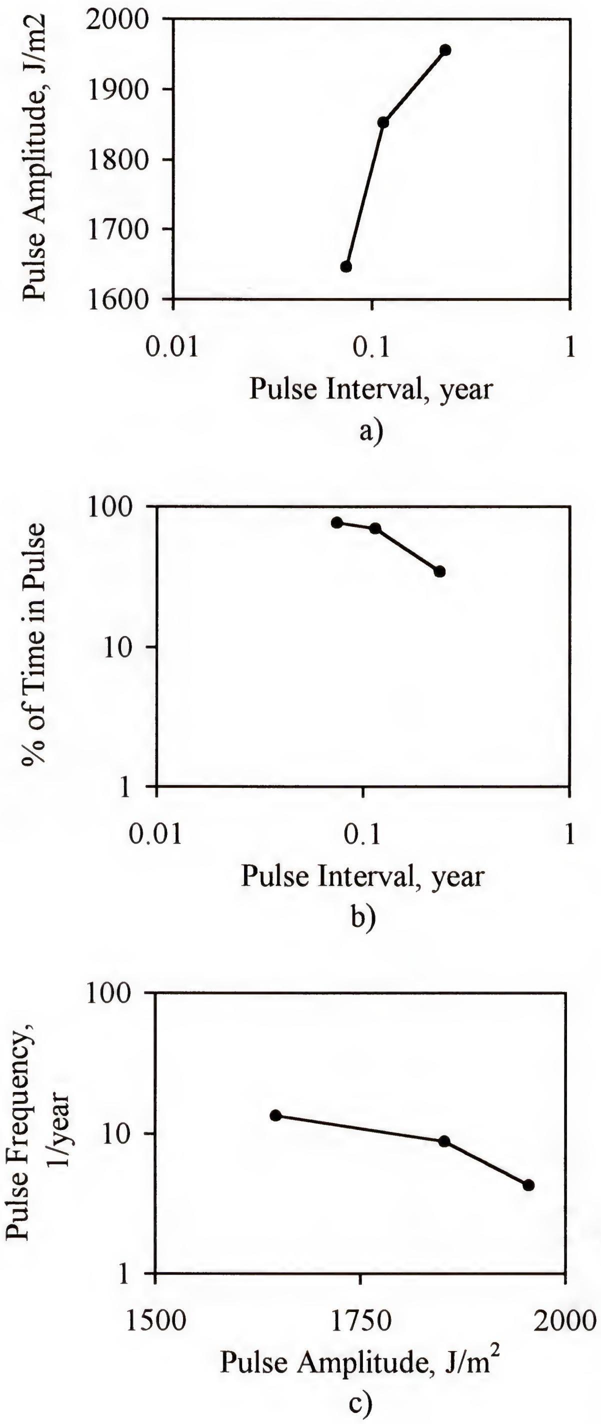

Figure 3-62. Pulsing patterns in the simulation results of the three module pulse model in Figure 3-57. a) Relationship between pulse interval and amplitude; b) Relationship between pulse interval and percent of time in pulse; c) Relationship between pulse amplitude and frequency.

CHAPTER 4
DISCUSSION

Suggested as a new paradigm by Odum et al. (1995), pulsing concepts (Odum, 1983) may give a new insight on systems development, compared to the steady state concept. This paradigm views systems development as composed of slow accumulation of production followed by frenzied consumption in a short time period. Different pathways between the production-consumption pair provide alternatives for energy flow in a system, under different input energy levels and material inputs. Pulsing may maximize empower by utilizing more energy and providing better loading than steady state. Self-organizing processes form complex webs that contain producer-consumer pairs, which produces a hierarchy of pulses. Appropriate matching of internal pulsing mechanisms and external pulse inputs may be required for a system to maximize performance.

Attributes of the Pulse Mechanism

The basic pulse model in Figure 2-4 was investigated with variations in input energy level and efficiencies of production and consumption. The linear pathway operates at low energy level, providing the system subsistence level of energy. As the energy builds up in the system, nonlinear, higher order pathways develop for the system to pulse. The highest order pathway, that is, the quadratic autocatalytic pathway, is mostly responsible for recycling materials tied up in the storages, so that the slow build-up process can start over again. Interspecific cooperation between species that perform similar function in an ecosystem can provide an example of quadratic autocatalytic pathway. Energy cost associated with developing this higher order pathway may be overcome by the material recycle that may keep optimum loading for the production process.

Systems in nature receive variable energy inputs from many energy sources at the same time. In this dissertation, steady energy input from one source was used as a controlled experiment to simply study energy use by pulsing designs. Providing a constant source was equivalent to filtering incoming pulses from smaller scales. The models may produce richer pulsing dynamics if supplied variable energy inputs from several sources. The results suggested that those systems with internal pulsing pathways can better utilize variable inputs.

As shown by Richardson (1988) with a similar unit model applied spatially this pulsing occurred in the middle ranges of energy level and efficiencies. At low energy level or low efficiency of production and consumption, the system did not have enough energy to develop high order pathways necessary for pulsing. The system could not pulse at high energy level or high efficiency of production and consumption because the material recycle was limiting the production process. In the middle range of input energy or efficiencies, the system showed more frequent pulses with increase in the energy input.

In the pulsing models investigated in this dissertation, the system puts its own self-organized pulse on each pathway that is in competition, constrained by a flow limited energy and material recycle. The thresholds by which higher order pathways predominate are inherent in the mathematics and were not switches artificially placed in the programs. The models self-control their pulsing consumption pathways.

Production Function and Maximum Power

Based on the results in Figures 3-6, 3-7, and 3-8, it can be restated what McGrane (1998) found in his study as follows: where materials are divided between dispersed and bounded stages, maximum power inflow is obtained when the dispersed material storage has 50% of total material and the activated storage has the rest. If pulsing occurs when the dispersed material storage has more than 50% of total material, it will decrease power inflow to the system. By recycling material tied up in the activated storage, pulsing will increase power when it occurs after the dispersed storage decreases below the 50% level, by recycling material tied up in the activated storage. Self-organization can help maximize power by reinforcing components that allocate 50% of the materials to storage of available materials.

Comparison of Pulsing and Steady States

The basic pulse model in Figure 2-4 did not pulse when the quadratic autocatalytic pathway was removed in Figure 3-24, as predicted y the pulsing paradigm. For the range of calibrations tested, the quadratic pathway was the internal source of the pulsing dynamics in the model. This shows that the pulsing dynamics can be initiated internally with appropriate fine tuning of rates. In ecosystems, many organisms have different modes of affecting process rates depending on energy levels and other factors such as nutrients and species composition of the systems. Different species may carry out the same functional role in ecosystems, but are active in different times.

In this simple model the pulsing system utilized slightly more power than the one adjusted to be in steady state. This may be due to better material loading caused by pulsed consumption which recycles material. Transformities of both producer and consumer were higher in the pulsing system. A pulsing unit pair may be more competitive because it delivers impact with high quality of energetic interaction. Where the basic pulse model has only one energy source, empower is proportional to power.

Internal and External Pulses

Most authors relate pulses to oscillating inputs. Consideration on a larger scale often shows these oscillations internally generated from the larger system. For example, an earthquake pulse impacts a pond, as an external input. On a larger scale, however, earthquakes come from accumulation and subsequent quick transformations of energy, which is an internal cycle at that larger scale. If the scale difference between two energy levels is too great, small scale pulses are filtered out and do not affect large scale pulses.

Pulsing and Complex Webs

The real world is an energy hierarchy of many levels with many alternative species in parallel with opportunity to dominate the pulsing at their level. The diversity of species supplies many choices that can become a pulsing pair appropriate for any particular condition. Multiple hierarchy in real ecosystems was represented in the models by connecting the production-consumption pair in the simple basic pulse model in parallel (Figure 3-38) and in series (Figures 3-47 and 3-54).

In the layered pulse model with parallel pulsing pairs in Figure 3-38, two pairs of units alternated their pulses with the same frequency. The model pulsed over a wide range of input energy and efficiencies. The model seems to generate more realistic results compared to the basic pulse model in Figure 2-4 alone.

The two module pulse model in Figure 3-47 represents four levels of energy hierarchy (trophic levels). The three module pulse model in Figure 3-54 has six hierarchical levels. By connecting the basic pulse module in series, several different pulse frequencies were obtained concurrently with one frequency for each pulsing pair. These models suggest the multiple frequencies of pulsing observed in nature (Figures 3-1, 3-2, and 3-3). Larger scale pulses (higher in hierarchy) were modified by variations on a small scale (lower in hierarchy) that provide necessary energy for them. Controls by the pulses of larger units (higher in hierarchy) caused variation of pulse amplitude in units lower in hierarchy.

Pulses in real systems are the combined result of internal designs and external inputs. Pulsing patterns viewed on one time scale contain pulses from several different scales, resulting in multiple amplitude distribution. If the models in this dissertation include multiple energy sources with varying input, they may generate the rich amplitude distribution that is observed in real systems.

Average percent power used over the simulation period was greater in models with the basic pulse pair connected in series in Figures 3-47 and 3-54. This may be one reason systems develop complex webs with many duplicate components and processes. By developing complex webs, systems minimize wasted energy and utilize input energies with better efficiency through cooperation of component units. These models and the basic pulse model decreased percent power use when input energy level was increased, leaving more energy unused for other units. By developing other components and processes, adapted systems can utilize this unused energy, thus maximizing empower of whole systems.

Fluctuations in many systems have been studied with stochastic theories. Irregular pulse intervals and amplitudes are considered as responses of systems to random influences. Statistical equations used in those studies often have an inherent premise of randomness, not causal actions. However, complex models developed in this dissertation through cooperation of deterministic pulsing pairs generate patterns that look like skewed, random distributions.

An aggregated model of a system ought to include essential features of the system. Inappropriate aggregations would not provide correct systems dynamics. The highly aggregated basic two unit pulse model in Figure 2-4 can be used for any kind of system. It generated essential features of pulsing systems, even though there was only one pulse frequency. Connecting the basic pulsing pair into complex webs produced more realistic patterns observed in nature. Degree of aggregation appears to affect detailed pattern of systems dynamics, but not basic pattern. In modeling there is an optimum aggregation which generates realistic patterns, but requires moderate time, effort, and computing power.

Emergy and Transformity Characteristics of Pulses

Emergy content of the storages followed the same pattern of the energy storages in pulsing cycles, reaching peak values at the same time as the storages do. But, transformity of the storages showed different patterns in variations. Even though variations in transformity reflect the pulsing dynamics in some aspect, they did not reach the maximum values at the same time as the storages. Transformity of the storages reached the maximum value during the growth period of the storages because during this period growth rate of emergy storage was greater than that of energy storage. Transformity of a storage is obtained by dividing emergy content of the storage by its energy content.

Pulse Intensity and Transformity

Analysis of various runs of the basic pulse model revealed an optimum pulse interval (45-50 days) for maximum pulsed feedback effect (Figure 3-59a). There was also an optimum pulse interval for maximum transformity. Transformity increased as pulse intensity increased (Figure 3-59c), delivering higher quality feedback actions in shorter duration. Feedbacks that control by sharp action may cause pulsing designs to prevail in many systems in nature.

Transformity and Hierarchy

A general way of representing energy hierarchy is to plot energy quantity versus energy quality measured as transformity. Because of the second energy law, the quantity of energy flow decreases as most of the energy is lost during energy transformation processes. The two module pulse model in Figure 3-47 contains four levels of hierarchy and the three module pulse model in Figure 3-54 six levels. In food chain ecology, level of energy hierarchy has been called trophic level.

In Figure 3-60, average quantities of the storages of the two models over simulation time periods were plotted as a function of transformity, on a log-log plot. The amount of energy stored in a hierarchy decreased as transformity of storages in each hierarchy increased, which is typical of the pattern of energy transformation hierarchy observed in the many different kinds of systems.

Comparison of Observed Pulses with Simulation Pulses

According to pulsing hierarchy theory based on energy accumulations, the larger the pulses the more time is required between successive pulses. Also, bigger pulses deliver sharper effects than the smaller ones. Analysis of the observed data in Figure 3-1 to 3-3 was consistent with the theory.

Sampling frequency affected the observed data graphs in Figures 3-1 to 3-3. With more frequent sampling, more small scale pulses would appear. There is a lower limit to the sampling frequency which produces enough time series data for meaningful analysis at a selected time scale. The patterns in Figures 3-1 to 3-3, however, were obtained where the sampling frequency was greater than the pulse periods studied. Garnier and Benest (1991) measured primary production in Lake Creteil with variable sampling frequencies of a week, two weeks, three weeks, and a month over 8 year period. Overall pattern of time series of primary production was similar for all sampling frequencies, even though the number of peaks decreased with less frequent sampling. The patterns in Figures 3-1 to 3-3 may not be an artifact of the sampling frequency.

The same pattern in the observed data was produced when the simulation results of the three module pulse model were plotted for comparison with the observed data (Figure 3-61). The pulsing models simulated real systems in this regard, implying that model configurations investigated in this dissertation are correct in representing real systems. Observed data were sometimes more complex with some ranges of pulse amplitude and frequency that could be explained as the interaction of external and internal pulsing mechanisms.

Adaptation to the Edge of Chaos

Using examples and simulations of molecular, organismal and population biology, Kauffman (1993) sought general systems principles about the evolution of life. He proposed a hypothesis that "complex systems constructed such that they are poised on the boundary between order and chaos are the ones best able to adapt by mutation and selection. Such poised systems appear to be best able to coordinate complex, flexible behavior and best able to respond to changes in their environment." His models showed the best fitness in intermediate range of carrying capacity which resulted in pulsing patterns.

All pulsing models simulated in this dissertation showed pulsing patterns in the middle range of energy levels and efficiencies. Pulsing patterns appeared within narrow ranges of energy levels and efficiencies. Even though increases in energy level did not cause choatic pattern in the models, the models investigated appear to be adapted to the edge of chaos. Chaos in the dynamic modeling sense is a shifting of the pathways and timing of oscillations. As shown by Beyers and Odum (1993) oscillation on one scale can interact with that on another scale to generate chaotic oscillations.

Information and Pulsing

All systems have information storages to sustain and manage organizations of their own systems. Odum (1996 and 1997) discussed information hierarchy, with increasing territory and transformity as going up the hierarchy. Information from smaller scale with fast turnover times is synthesized and selected for transfer to the upper hierarchy, and this high quality information organizes small scale information to sustain the system.

Information content of systems may pulse as other system components pulse, to provide appropriate feedback control during different phases of fluctuations. Margalef (1958) and Travers (1971) observed pulsed variations of species diversity along the successional stages of coastal phytoplankton. Balch (1981) also observed pulses in phytoplankton diversity that coincided with total phytoplankton abundances in the Gulf of Maine. In the world of global networks, we are experiencing surges of information often through television news. These information pulses have a wide range of turnover times. Cultural information, with longer turnover time and territory, pulses less frequently. On the geologic time scale there are pulses of genetic information encoded in DNA of organisms in speciation and extinction.

Short-term pulses of information provide inputs to higher levels that can filter and select information that is repeated. Information selected repeatedly is reinforced and retained as higher levels of information. The pulse models developed in this dissertation could also be used to explain information hierarchy and pulses. Odum (1997) provided a simulation model of diversity pulsing and selection.

Adaptive Cooperative Oscillator Theory

Multiple pulsing frequencies were obtained when the production-consumption pair in the basic pulse model in Figure 2-4 was connected in series in Figures 3-47 and 3-54. In each pulsing pair, two units were connected through three different pathways, with quadratic autocatalytic pathway responsible for the pulsing dynamics. Pulsing pairs in lower energy hierarchy provided energy to the higher pulsing pairs. Pulsing pairs in higher energy hierarchy pulsed when enough energy is accumulated from fast, smaller scale pulses. The higher pulsing pair provided support energy to even higher pulsing pairs. Accumulation of energy from the pulsing pair at one level below triggers pulsing patterns in the hierarchy above, and that returns feedback to control the lower hierarchy.

Beckerman (1997) discussed cooperative processes in which pulses of small-scale components can generate large-scale pulses, using examples in neural networks. Coupled populations of oscillatory units synchronize their motions if the native frequencies are not too dissimilar, through phase pulling mechanism or fast threshold modulation depending on types of oscillators. This synchronization produces global motions over a broad range of frequencies. Increased energy use by cooperation among pulsing units during self-organization may be another way to explain the pulsing hierarchy generated by the models in this dissertation.

Pulsing Hierarchy and Episodic Events

Pulsing patterns have been treated as "episodic events" in many fields because of seeming irregularities in pulse interval and magnitude. Volcanic eruptions and earthquakes are examples of episodic events in geology. When McGrane (1998), developing overview models of earth processes, used the same producer-consumer configurations studied in this dissertation, episodic pulsing scenarios were found. For plankton ecologists, red tide by toxic algae in coastal areas is an example of episodic events.

When connected in series in Figures 3-47 and 3-54, the basic pulse model in Figure 2-4 produced a hierarchy of pulsing frequencies. Each pair of slow growth and fast consumption units had its own frequency with increasing pulse interval as going up the energy hierarchy. Pulses in smaller scales appeared as a noise in larger scale pulses. Transformity of storages increased with level in the energy hierarchy. Pulses in higher hierarchy could be considered as episodic when viewed by components with a short time scale. Control effects by pulses from higher in the energy hierarchy are reflected in variations of pulse amplitudes in pulses of lower hierarchy. Simulation results of the three module pulse model in Figure 3-56 shows some variations in pulse amplitudes for the pulsing pair higher in the hierarchy. The models with complex combinations of pulsing pairs seem to generate episodic events which are observed in many real systems, further supporting the plausibility of the pulsing pair concept used in this dissertation.

Pulsing Cycles in Economy

Fluctuations in economic activities seem to be represented using the pulsing models in this dissertation. In business cycles, economic growth is periodically interrupted by various pulses in production, demand, and supply, which is similar to the concept of slow growth and frenzied consumption in the pulsing paradigm. Inventory cycle represents pulsed consumption of stocks accumulated over time.

There is a hierarchy of pulsing economic activities. Every day activities accumulate to support monthly or seasonal pulses, and seasonal pulses supports longer term pulses of the business cycles. Long-wave pulses in economy and world power with about 50-year cycle can be thought of as pulses higher in hierarchy than the short-term business cycles. Controls are fed back to the lower hierarchies. The pulse models in Figures 3-47 and 3-54 have hierarchy of pulses in which higher energy levels pulse less frequently. To pulse, larger pulses in economic activities will need enough time to accumulate economic assets. Also, both models show irregularities in pulse amplitudes which may explain the episodic nature of business cycles.

Recognizing the effect of an accumulation followed by a period of replacement, Mosekilde et al. (1992) simulated an economic long wave model and obtained a pulsing cycle with a period of about 47 years. The long wave cycles (Kondratief cycles) were produced endogenously by the investment behavior of the capital producing sector. They also investigated the interaction of the long wave with the building cycles (Kuznets cycles) and business cycles by imposing a sinusoidal variation in the demand for capital derived from the consumer goods sector. Watt (1989) traced long waves in the economy to fluctuations in global energy prices.

Sampling Frequency and Systems Dynamics

If pulsing dynamics is general for all systems, sampling strategies to investigate dynamics of a system of interest should take into account pulsing patterns. Without appropriate sampling frequencies, real patterns of systems are not revealed, and measurements based on inappropriate sampling schemes can not show how a system behaves and interacts with various disturbances. Single or short period measurements of productivity in open oceans incorrectly evaluated primary productivity in open ocean ecosystems, underestimating primary productivity in open oceans. Zimmerman and Kremer (1984) showed how the sampling frequency could affect the resources available to a kelp forest. Reduced sampling frequencies underestimated nutrient availability because they missed many of the short pulses of nitrate input. High frequency sampling revealed a 2-per-day frequency of pulsed input of nitrate into the kelp forest throughout the year. This frequent pulsing was linked to internal waves and semidiurnal tides.

Wheeler et al. (1989) observed diel periodicity of ammonium uptake and regeneration, bacterial production, and abundance of autotrophic and heterotrophic plankton in nutrient-rich oceanic water. Apparently short-term pulses of production and consumption occur within the microbial food web. This also emphasizes the importance of frequent sampling.

Implications of Pulsing Concepts for Ecosystem Management

Many policies on economy and environment have been organized around the steady state concept in which systems reach a steady state after growth phase and stay there for long time. If pulsing is an inherent characteristic of any system, those policies need to be restructured to be successful. Wu and Loucks (1995) argued that the classical equilibrium view in ecology has failed not only because equilibrium conditions are rare in nature, but also because of our past inability to incorporate heterogeneity and scale multiplicity into our quantitative expressions for stability. The theories and models built around these equilibrium and stability principles led to poor policies for resource management, nature conservation, and environmental protection. Below are three examples where the pulsing paradigm in this dissertation might be relevant.

An appropriate policy is to adapt human uses to fit the pulsing that is appropriate for each scale. The examples below suggest that the best way to preserve diversity is to preserve entire ecosystems and their landscape-level pulsing.

Management of Deltaic Systems

Sediment input by pulsing events, such as river floods and storms, is very important in maintaining deltaic systems (Day et al., 1995). Deltas have been cut off from input of nutrients, freshwater, and sediments by management practices, such as dams, dikes, impoundment, and canals. These authors discussed roles of pulsing events in functioning of deltaic systems in relation to sea level change. They suggested management approaches for sustainable deltas that take advantage of pulsing events for sediment input to the deltaic systems.

Structures, such as dikes, dams, seawalls, and so on, that have been built to protect properties along the river and coast have exacerbated damages by natural pulsing events of big floods and strong storms. Those structures prevented smaller pulses which can be dissipated in natural ecosystems with little damages to the systems. When too much pulse energy is concentrated on those structures and those structures fail, the whole ecosystem and associated human structures may be severely damaged. Optimum size of the structures could be estimated by considering pulsing hierarchy in a given region as well as economic factors.

Diversity Management

Maintaining diversity of ecosystems has been an important task of many conservation efforts. Without correct understanding of how systems respond to various external and internal agents, those efforts accelerated loss in diversity. Pulsing dynamics investigated in this dissertation may help management of stocks and diversity.

Lewin (1986) discussed the preservation of diversity considering the inevitability of large-scale pulses. He suggested that changes within ecosystems should be seen as natural and inevitable on the larger scale perspectives, even if they may lead to local extinctions. Human interventions that resisted those fluctuations resulted in lost diversity, which is the opposite what many park managers and conservationists believed. Thus, pulsing dynamics of ecosystems and their hierarchical level should be considered in both space and time. There might be a proper matching of natural pulses and pulses in human societies to help conservation efforts of biodiversity in the long-run.

Leach and Givnish (1996) found that suppression of periodic pulses of fire decreased diversity in prairies. Wootton et al. (1996) found that pulses of water release may be important in restoring food web integrity of a river ecosystem.

Fisheries Management and Hierarchy of Pulsing

In many parts of the world, the fisheries industry has been experiencing decline in fish stocks because of over-fishing. Over-fishing might reflect mismatching of pulses on two different scales. Simulation in Figure 3-22 shows a pattern in which poor matching of pulsed consumption led to a crash in the storage. To be sustainable, there must be optimum pulses of fishing effort. To survive, fisheries systems might optimize yields by controlling pulse of capital financing of fishing boats to maximize long-term sustainability. This is likely to occur only when fishery production is considered over a large time scale.

Summary

Analysis of observed data and simulation models suggest that self-organization generates pulsing which increases performance in complex systems through cooperative pulsing of many scales. The following is a numbered list that summarizes the major points in this study.

1. Pulsing patterns in real systems were graphically analyzed using time series graphs from various systems, with emphasis on aquatic ecosystems in lakes and oceans.

2. Time series graphs were obtained from published literature. Size, interval, and duration of pulses were measured on the graphs and plotted.

3. In the observed data, larger pulses occurred less frequently and concentrated in a shorter time period relative to pulse interval. Observed patterns appeared to support the theory of pulsing paradigm.

4. Simple two storage models were constructed to investigate the characteristics of multiplicative production function in drawing power. A model with an internal pulsing mechanism given as a step function was compared with a similar model without the pulsing mechanism.

5. Simulation results showed that pulsing might maximize power by providing optimum load to the production function.

6. A basic pulsing model of producer-consumer-recycle was examined to find characteristics of the model system for variations in input energy level and efficiencies of production and consumption.

7. The basic pulsing model pulsed in an intermediate range of input energy level and efficiencies. Increase in energy level and efficiencies produced more frequent pulses.

8. Emergy storages followed the same trend in energy storages. Transformity varied over the simulation period and reached maximum during the fast growth period of a pulse cycle. These results show that pulsing mechanisms involve high quality consumers.

9. The basic pulsing model was compared with a steady model without a quadratic autocatalytic pathway. Both models were compared in similar calibration conditions. The pulsing model drew slightly more power, but the difference was very small, less than 2%. The pulsing model shows more realistic patterns in the variation of storages that are observed in real ecosystems.

10. Direct feedback effect of consumer on production by producer was included in the basic pulse model. Pulsing delivered a sharp feedback effect.

11. A detritus storage was included in the basic pulse model. The model simulated pulses in producer, consumer, and detrital storages. Consumer pulses were dependent on the detritus storage.

12. A simple pulsing unit of producer-consumer-recycle was connected in parallel. The model was constructed in such a way that two pulsing units competed for the same energy source and material.

13. The model (#13) produced stable pulsing patterns over a wide range of input energy level and efficiencies. Both units pulsed with the same frequencies, but alternated their pulses.

14. Connection of the simple pulsing unit in series simulated several energy levels in real ecosystems. In these models, each pulsing unit was connected through the linear and autocatalytic pathways.

15. Simulation results of the model with the simple pulsing pair in series showed multiple pulse frequencies with less frequent pulses in higher energy levels. Simulation generated transformities, characteristic of the energy hierarchy in the models. The average transformity of storages over the simulation period increased with the energy hierarchy.

16. Simulation pulses were analyzed to find how the models represented the real systems. Pulses from the basic pulse model, the two module pulse model, and the three module pulse model, were used in this analysis.

17. Simulated transformity of pulses increased with pulse intensity. There was an optimum pulse interval for maximum pulsed feedback effect. Graphs of energy storages as a function of transformity showed a typical pattern of the energy transformation hierarchy.

18. Simulation pulses of the three module pulse model were plotted on the same coordinates used for the observed data. Graphs were similar.

19. Studies in economics have revealed fluctuations on several different scales. Pulsing models investigate in this dissertation generated similar fluctuations in the storages to those observed in economic systems.

20. Episodic pulsing scenarios like those of earthquakes and volcanoes in geologic systems were found in the models with the simple pulsing pair in series.

21. In managing systems and anticipating the future, what is sustainable may be repeating pulses rather than a steady state. Management of ecosystems may need different policies for each stage in oscillation.

Conclusion

The concepts of pulsing paradigm were investigated using general systems concepts of energy transformation hierarchy. Analyses of observed data and simulation models suggest that pulsing patterns with many frequencies occur simultaneously in many different kinds of systems.

The pulsing paradigm theory interprets fluctuations in systems as a consequence of the selection during self-organization of designs that pulse simultaneously on many scales. In simulation models pulsing of this kind is generated with combinations of paired producer-consumer units in series, each accumulating products that cause a surge of consumer development and recycle. The pulsing results from the interplay of linear, autocatalytic, and quadratic autocatalytic pathways, which prevail by using available energy more than models running in steady state. Simultaneous pulses of different frequencies result when producer-consumer pairs are connected in an energy transformation network where energy levels decrease, but turnover times increase in successive steps. By cooperative action, the complex of pulsing pairs leaves little energy unused.

Analysis of frequencies, amplitudes, and durations of pulses in published data on plankton and other systems was consistent with the pulsing paradigm hypothesis. What is often interpreted as inherent randomness of these systems can be accounted for as the concurrent dynamic pulsing on many scales. In systems management, performance may be increased by adapting uses to the pulsing regimes rather than by trying to develop steady states.

APPENDIX A
ORIGINAL FIGURES USED TO FIND PULSING PATTERNS IN THE OBSERVED DATA

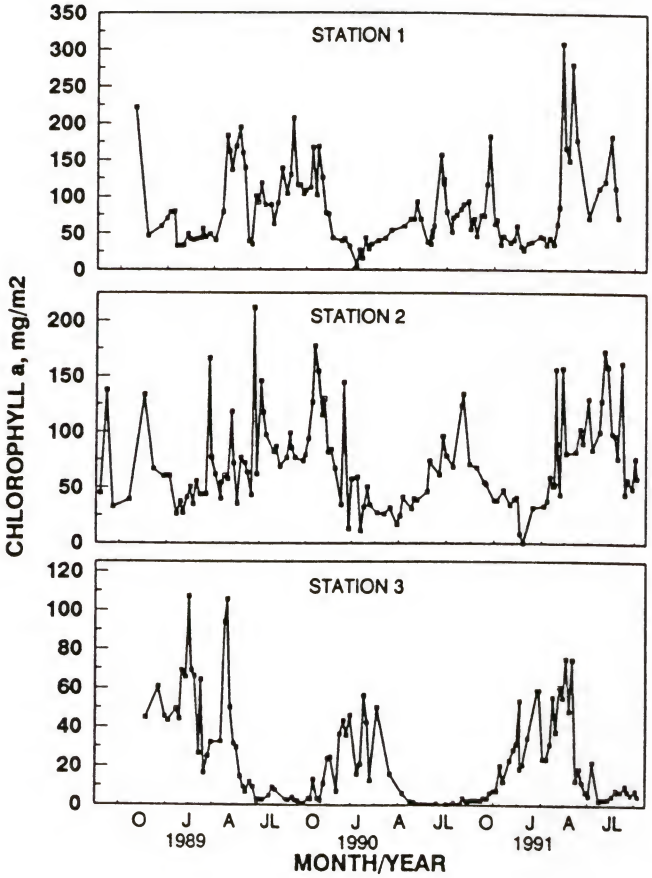

Appendix A-1. Fluctuations in chlorophyll-a levels at three sampling stations of Lake Okeechobee, Florida (Philips et al., 1993).

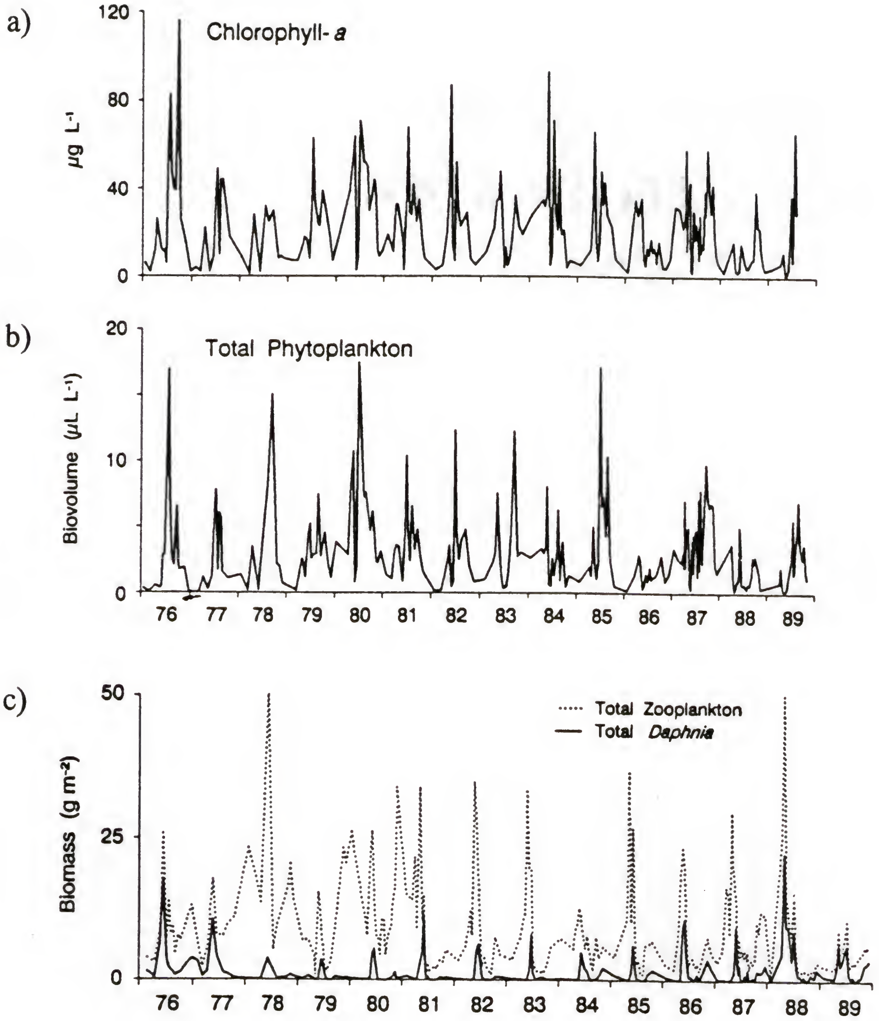

Appendix A-2. Time series of chlorophyll-a (a), total phytoplankton (b), and total zooplankton and total Daphnia (c) in Lake Mendota, Wisconsin during 1976-1989 (Lathrop and Carpenter, 1992a and 1992b).

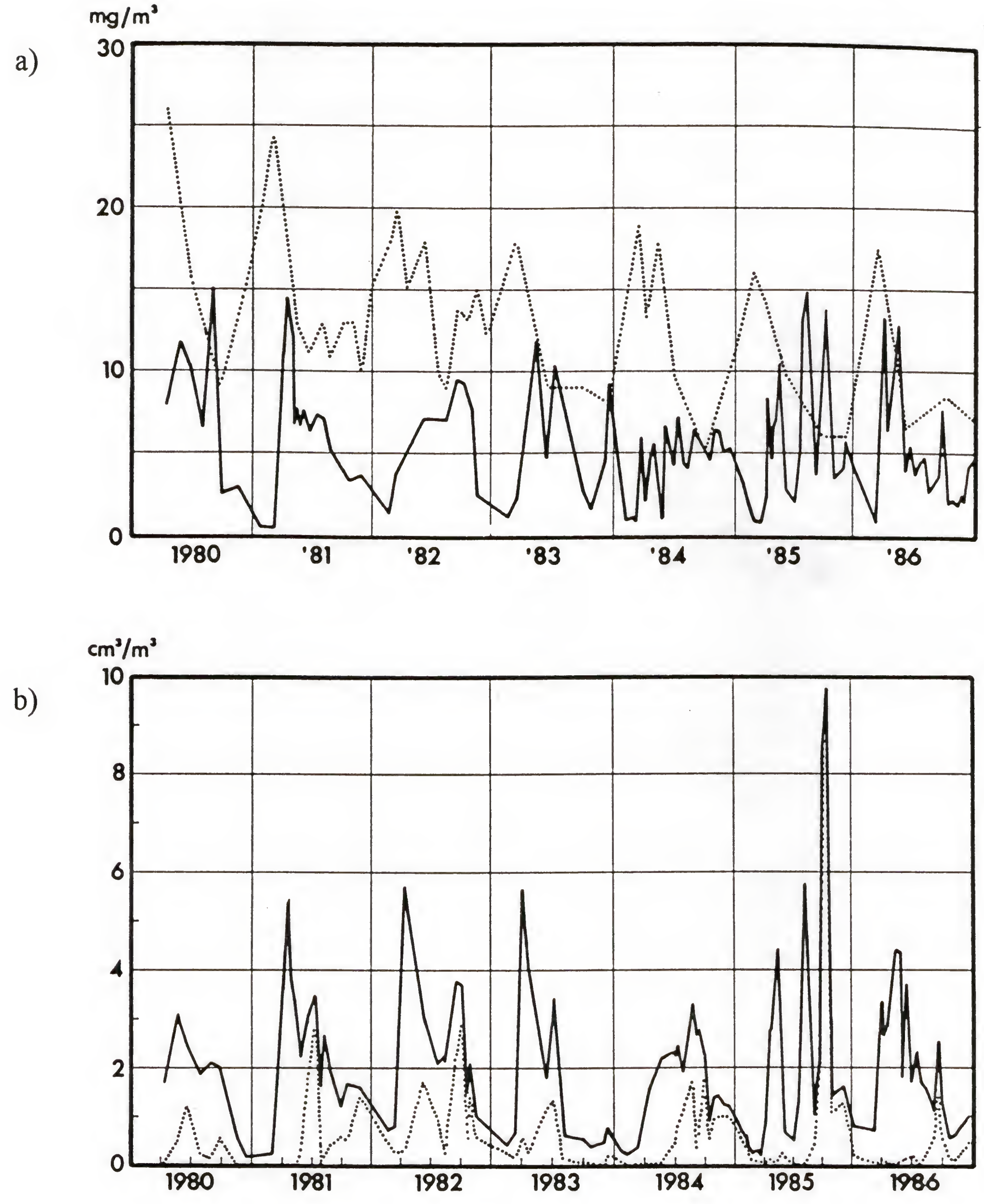

Appendix A-3. Trends of total phosphorus (·····) and chlorophyll-a (—) (a) and biomass (as cell volume) of total phytoplankton (—) and blue-green algae (·····) (b) in the upper 20m of Lago Maggiore, Italy (de Bernardi et al., 1988).

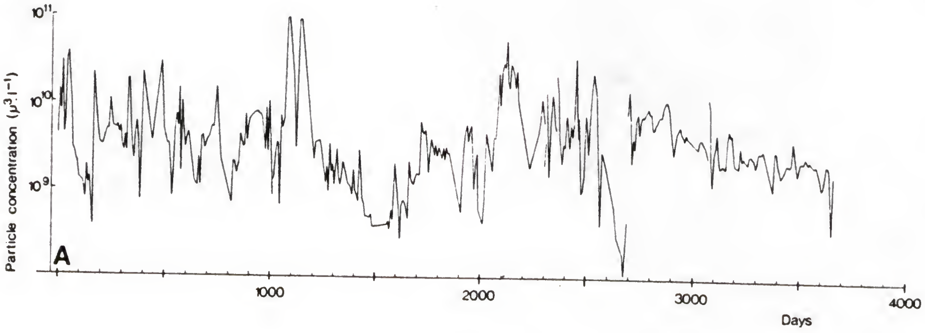

Appendix A-4. Time series of algal concentration in a microcosm over 10 years (Kersting, 1985).

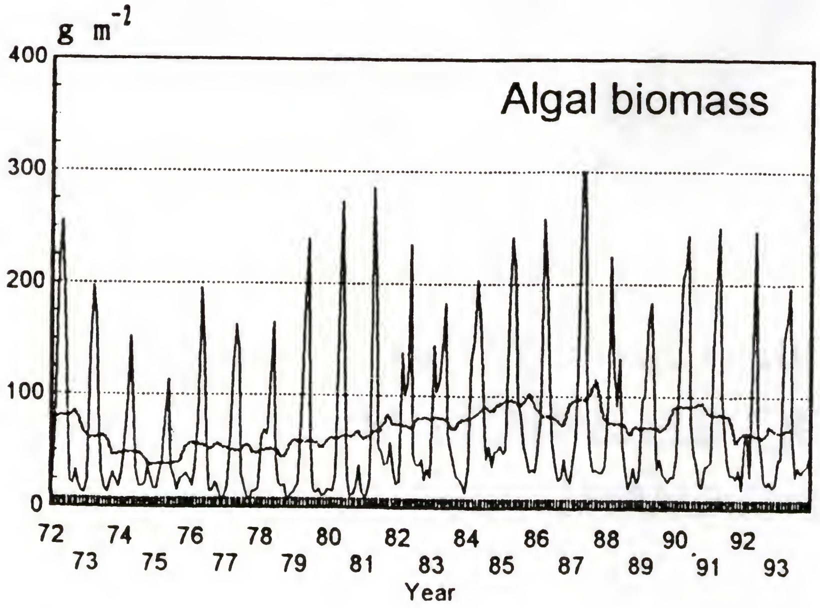

Appendix A-5. Time series of phytoplankton biomass in Lake Kinneret, Israel from 1972 through 1993 (Berman et al., 1995).

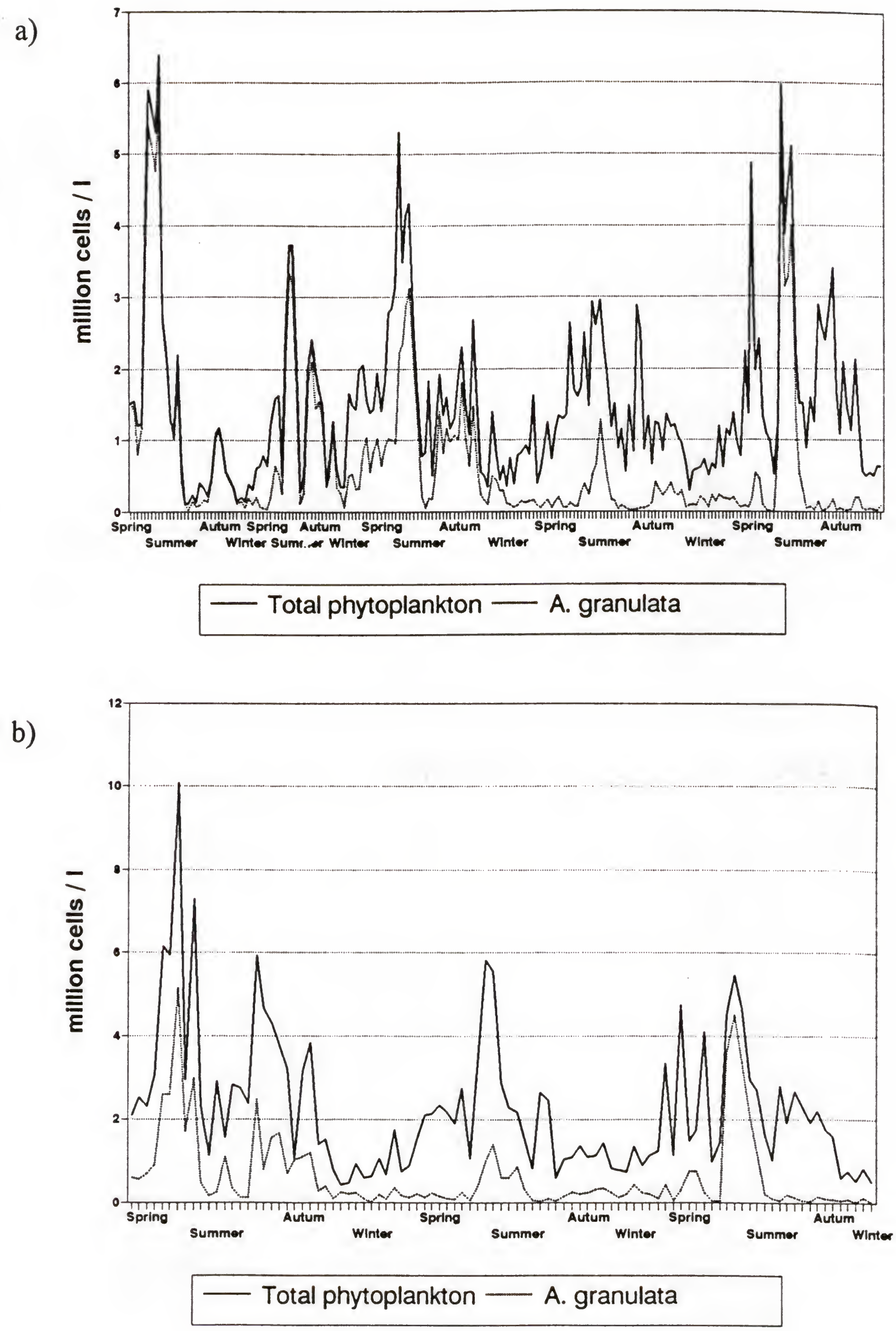

Appendix A-6. Temporal distribution of total phytoplankton and *Aulacoseira granulata* in Trelew station (a) and Rawson station (b) of the Chubut River in Argentina from November 1989 to July 1992 (Sastre et al., 1994).

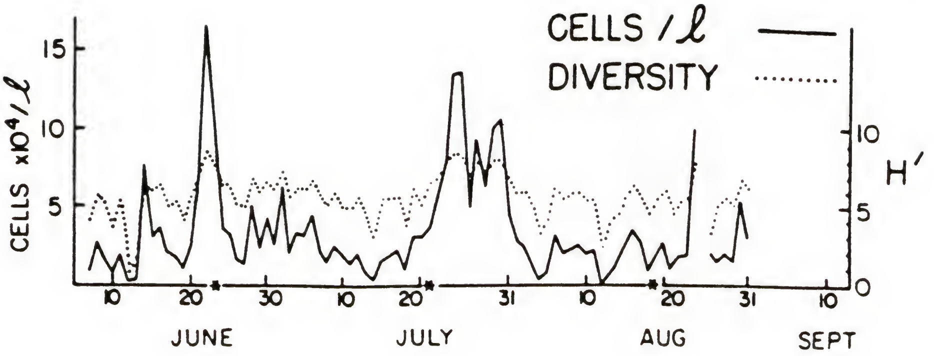

Appendix A-7. Daily variation in total phytoplankton abundance (cells/l) and Shannon-Wiener diversity index during the summer of 1978 in the Gulf of Maine (Balch, 1981).

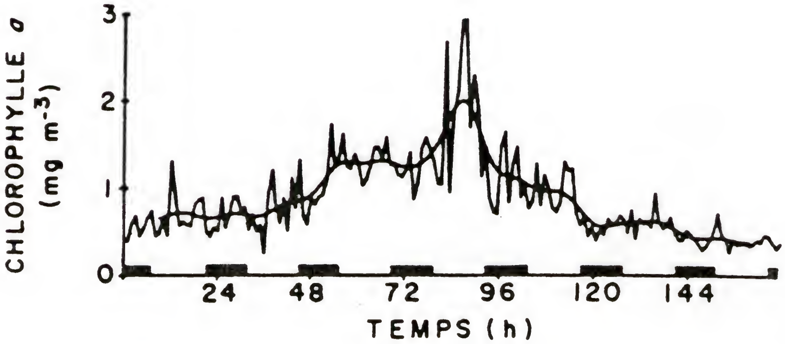

Appendix A-8. Hourly variation of chlorophyll-a at an anchored station in the Middle Estuary of the St. Lawrence River, Canada (Demers and Legendre, 1981).

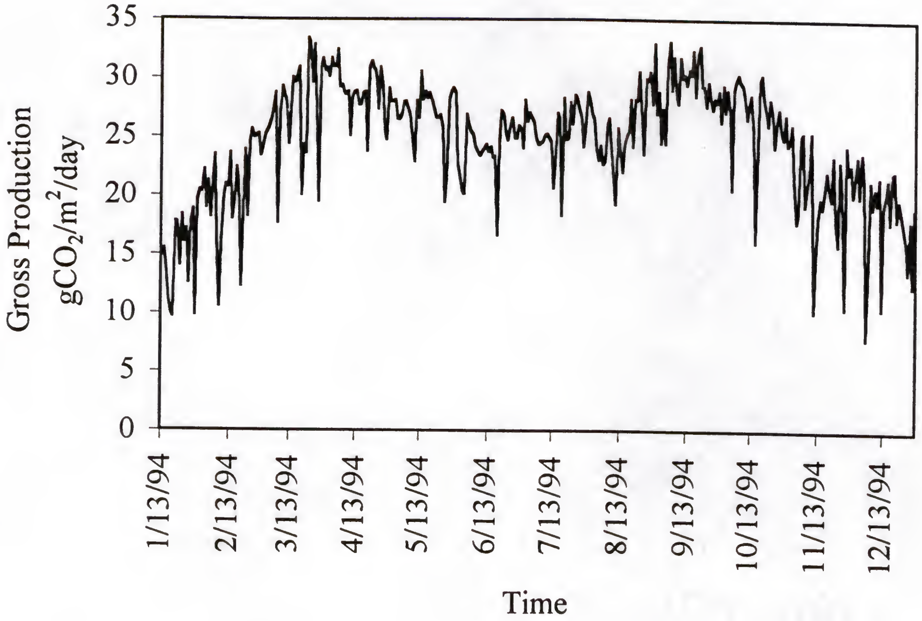

Appendix A-9. Fluctuations in gross production inside Biosphere 2 over a year in 1994 (Kang and Engel, 1996).

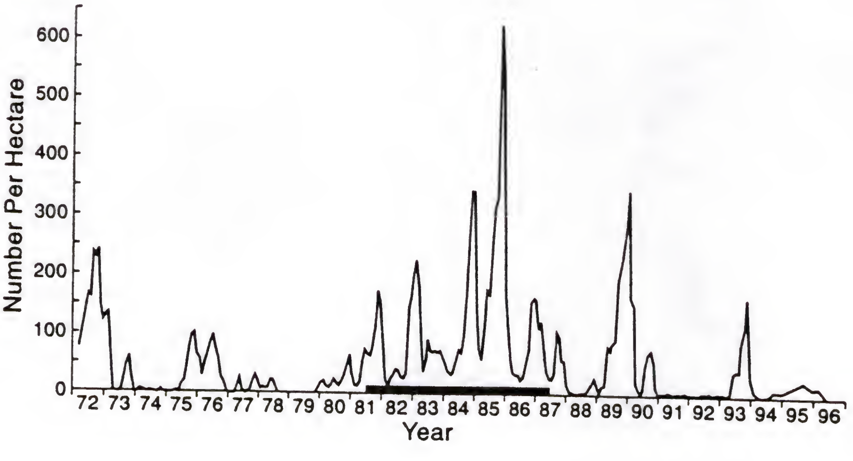

Appendix A-10. Population fluctuations of the prairie vole, *Microtus ochrogaster* (Getz et al., 1997).

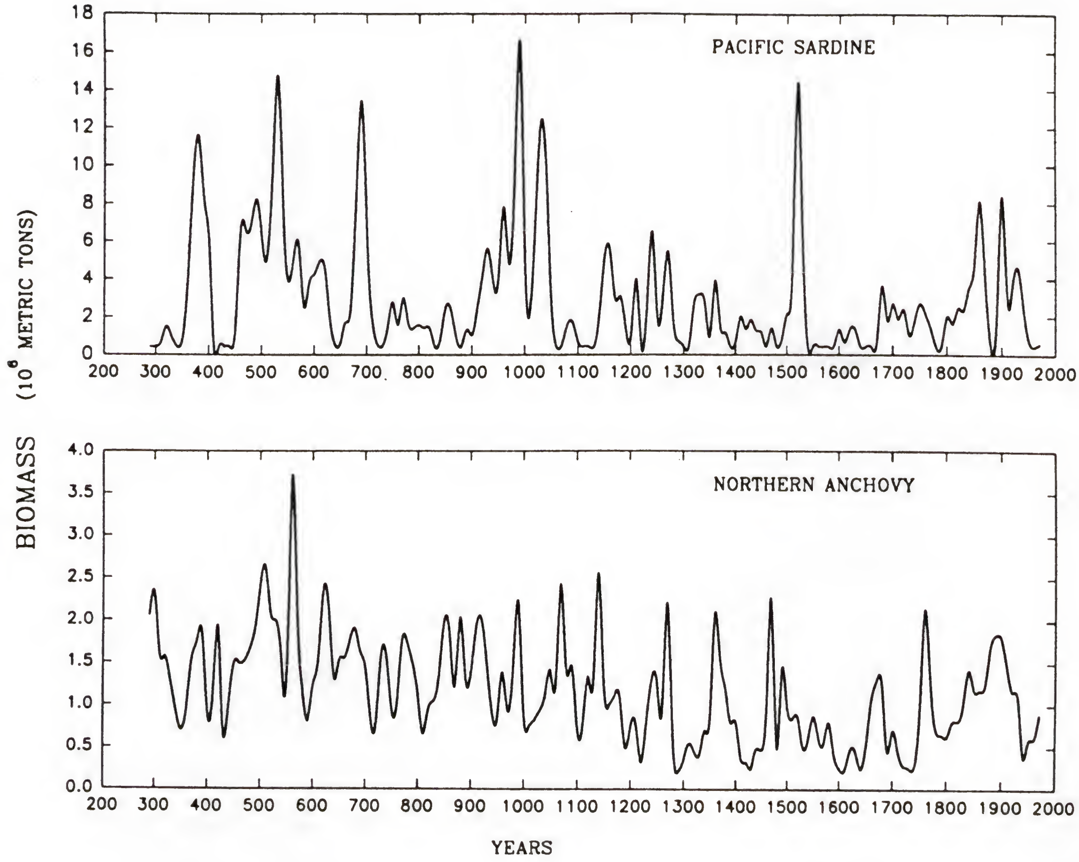

Appendix A-11. 1700-year hindcast series of Pacific sardine and northern anchovy biomasses off California and Baja California obtained by conversion of scale deposition rate data (Baumgartner et al., 1992).

APPENDIX B
CALIBRATION TABLES OF THE MODELS

Appendix Table B-1. Calibration of the pathway coefficients for the computer simulation of the simple two storage model with a flow limited energy source in Figure 3-4.

Items	Symbols	Values	Units	Coefficients
Material Content of Q = 15%				
Sources				
Energy Flow	J	1000	$J/m^2/day$	
Unused Energy	R	100	$J/m^2/day$	
Storages				
Product Storage	Q	90	J/m^2	
Material Fraction of Q,	f	0.15	g/J	
Material Available	M	1.5	g/m^2	(= MT - f*Q)
Total Material	MT	15	g/m^2	
Flows				
Energy Use	J1 = k1*R*M*Q	900	$J/m^2/day$	k1 = 6.667E-02
Production	J2 = k2*R*M*Q	5	$J/m^2/day$	k2 = 3.704E-04
Material Recycle	J3 = k3*Q	5	$J/m^2/day$	k3 = 5.556E-02
Material Content of Q = 5%				
Sources				
Energy Flow	J	1000	$J/m^2/day$	
Unused Energy	R	100	$J/m^2/day$	
Storages				
Product Storage	Q	90	J/m^2	
Material Fraction of Q,	f	0.05	g/J	
Material Available	M	10.5	g/m^2	(= MT - f*Q)
Total Material	MT	15	g/m^2	
Flows				
Energy Use	J1 = k1*R*M*Q	900	$J/m^2/day$	k1 = 9.524E-03
Production	J2 = k2*R*M*Q	5	$J/m^2/day$	k2 = 5.291E-05
Material Recycle	J3 = k3*Q	5	$J/m^2/day$	k3 = 5.556E-02

Appendix Table B-2. Calibration of the pathway coefficients for the computer simulation of the steady model in Figure 3-25.

Items	Symbols	Values	Units	Coefficients
Sources				
Energy source	J	5000	J/m^2/day	
Remaining energy	R	500	J/m^2/day	
Storages				
Producer	P	1000	J/m^2	
Consumer	H	200	J/m^2	
Material available	M	20	g/m^2	M=MT-f1*P-f2*H
Total material	MT	50	g/m^2	
Material fraction				
Producer	f1	0.02	g/J	
Consumer	f2	0.05	g/J	
Flows				
Energy use	J1 = k1*R*M*P	4500	J/m^2/day	k1 = 0.00045
Primary production	J2 = k2*R*M*P	250	J/m^2/day	k2 = 0.000025
Linear consumption	J3 = k3*P	10	J/m^2/day	k3 = 0.01
growth	J4 = k4*P	2.5	J/m^2/day	k4 = 0.0025
Autocatalytic consump.	J5 = k5*P*H	550	J/m^2/day	k5 = 0.00275
growth	J6 = k6*P*H	218	J/m^2/day	k6 = 0.00109
Producer respiration	J9 = k9*P	100	J/m^2/day	k9 = 0.1
Consumer respiration	J10 = k10*H	100	J/m^2/day	k10 = 0.5

Appendix Table B-3. Calibration of the pathway coefficients for the computer simulation of the pulse model with consumer feedback on primary production in Figure 3-28.

Items	Symbols	Values	Units	Coefficients	
Sources					
Sunlight	J	5000	J/m^2/day		
Remaining Sunlight	R	500	J/m^2/day		
Storages					
Producer	P	1000	J/m^2		
Consumer	H	200	J/m^2		
Material available	M	20	g/m^2	M = MT-f1*P-f2*H	
Total material	MT	50	g/m^2		
Material fraction					
Producer	f1	0.02	g/J		
Consumer	f2	0.05	g/J		
Flows					
Sunlight Used	J1 = k1*R*M*P*H	2500	J/m^2/day	k1 =	0.00000125
	J2 = k2*R*M*P*H	150	J/m^2/day	k2 =	8.E-08
Primary production	J3 = k3*R*M*P	2000	J/m^2/day	k3 =	0.0002
	J4 = k4*R*M*P	100	J/m^2/day	k4 =	0.00001
Linear consumption	J5 = k5*P	10	J/m^2/day	k5 =	0.01
growth	J6 = k6*P	2.5	J/m^2/day	k6 =	0.0025
Autocatalytic consump.	J7 = k7*P*H	50	J/m^2/day	k7 =	0.00025
growth	J8 = k8*P*H	18	J/m^2/day	k8 =	0.00009
Quadratic consumption	J9 = k9*P*H*H	500	J/m^2/day	k9 =	0.0000125
growth	J10 = k10*P*H*H	200	J/m^2/day	k10 =	0.000005
Producer respiration	J11 = k11*P	100	J/m^2/day	k11 =	0.1
Consumer respiration	J12 = k12*H	100	J/m^2/day	k12 =	0.5
Feedback flow	J13 = k13*R*M*P*H	1	J/m^2/day	k13 =	5E-10

Appendix Table B-4. Calibration of the pathway coefficients for the computer simulation of the pulse model with a detritus storage in Figure 3-36.

Items	Symbols	Values	Units	Coefficients
Sources				
Sunlight	J	5000	J/m^2/day	
Unused sunlight	R	500	J/m^2/day	
Storages				
Producer	P	1000	J/m^2	
Consumer	H	200	J/m^2	
Detritus	D	5000	J/m^2	
Material available	M	15	g/m^2	MT-f1*P-f2*H-f3*D
Total material	MT	50	g/m^2	
Material fraction				
Producer	f1	0.02	g/J	
Consumer	f2	0.05	g/J	
Detritus	f3	0.001	g/J	
Flows				
Sunlight used	J1 = k1*R*M*P	4500	J/m^2/day	k1 = 0.0006
Primary production	J2 = k2*R*M*P	250	J/m^2/day	k2 = 3.33333E-05
Linear consumption	J3 = k3*P	60	J/m^2/day	k3 = 0.06
growth	J4 = k4*P	20	J/m^2/day	k4 = 0.02
Quadratic consumption	J5 = k5*P*H*H	500	J/m^2/day	k5 = 0.0000125
growth	J6 = k6*P*H*H	200	J/m^2/day	k6 = 0.000005
Producer respiration	J7 = k7*P	100	J/m^2/day	k7 = 0.1
Consumer respiration	J8 = k8*H	10	J/m^2/day	k8 = 0.05
Producer Death	J9 = k9*P	200	J/m^2/day	k9 = 0.2
Consumer Death	J10 = k10*H	100	J/m^2/day	k10 = 0.5
Detritus decomposition	J11 = k11*D	50	J/m^2/day	k11 = 0.01
Linear consumption	J12 = k12*D	20	J/m^2/day	k12 = 0.004
growth	J13 = k13*D	3	J/m^2/day	k13 = 0.0006
Quadratic consumption	J14 = k14*D*H*H	300	J/m^2/day	k14 = 0.0000015
growth	J15 = k15*D*H*H	80	J/m^2/day	k15 = 0.0000004
Fecal pellet production	J16 = k16*P*H*H	300	J/m^2/day	k16 = 0.0000075

Appendix Table B-5. Calibration of the pathway coefficients for the computer simulation of the layered pulse model in Figure 3-41.

Items	Symbols	Values	Units	Coefficients
Sources				
Sunlight	J	5000	J/m^{2}/day	
Remaining sunlight	R	500	J/m^{2}/day	
Storages				
Producer 1	P1	1000	J/m^{2}	
Producer 2	P2	2000	J/m^{2}	
Consumer 1	H1	200	J/m^{2}	
Consumer 2	H2	400	J/m^{2}	
Material available	M	10	g/m^{2}	(MT-f1*P2-f2*H1 -f3*P2-f4*H2)
Total material	MT	100	g/m^{2}	
Material fraction				
Producer 1	f1	0.02	g/J	
Consumer 1	f2	0.05	g/J	
Producer 2	f3	0.02	g/J	
Consumer 2	f4	0.05	g/J	
Flows				
Sunlight used by P1	J1 = k1*R*M*P1	2500	J/m^{2}/day	k1 = 0.0005
Production - producer 1	J2 = k2*R*M*P1	250	J/m^{2}/day	k2 = 5.E-05
Linear consumption	J3 = k3*P1	10	J/m^{2}/day	k3 = 0.01
	J4 = k4*P1	1.5	J/m^{2}/day	k4 = 0.0015
Autocatalytic consump.	J5 = k5*P1*H1	50	J/m^{2}/day	k5 = 0.00025
	J6 = k6*P1*H1	15	J/m^{2}/day	k6 = 0.000075
Quadratic consumption	J7 = k7*P1*H1*H1	500	J/m^{2}/day	k7 = 0.0000125
	J8 = k8*P1*H1*H1	160	J/m^{2}/day	k8 = 0.000004
Producer 1 respiration	J9 = k9*P1	100	J/m^{2}/day	k9 = 0.1
Consumer 1 respiration	J10 = k10*H1	10	J/m^{2}/day	k10 = 0.05
Sunlight used by P2	J11 = k11*R*M*P2	2000	J/m^{2}/day	k11 = 0.0002
Production - producer 2	J12 = k12*R*M*P2	300	J/m^{2}/day	k12 = 0.00003
Linear consumption	J13 = k13*P2	10	J/m^{2}/day	k13 = 0.005
	J14 = k14*P2	3	J/m^{2}/day	k14 = 0.0015
Autocatalytic consump.	J15 = k15*P2*H2	50	J/m^{2}/day	k15 = 0.0000625
	J16 = k16*P2*H2	20	J/m^{2}/day	k16 = 0.000025
Quadratic consumption	J17 = k17*P2*H2*H2	500	J/m^{2}/day	k17 = 1.5625E-06
	J18 = k18*P2*H2*H2	220	J/m^{2}/day	k18 = 6.875E-07

Appendix Table B-5 -- continued

Items	Symbols	Values	Units	Coefficients
Producer 2 respiration	J19 = k19*P2	100	$J/m^2/day$	k19 = 0.05
Consumer 2 respiration	J20 = k20*H2	100	$J/m^2/day$	k20 = 0.25
Predation of consumer 1	J21 = k21*H1*H2	80	$J/m^2/day$	k21 = 0.001
by consumer 2	J22 = k22*H1*H2	8	$J/m^2/day$	k22 = 0.0001

Appendix Table B-6. Calibration of the pathway coefficients for the computer simulation of the two module pulse model in Figure 3-50.

Items	Symbols	Values	Units	Coefficients
Sources				
Sunlight	J	5000	J/m^2/day	
Remaining sunlight	R	500	J/m^2/day	
Storages				
Producer	P	1000	J/m^2	
Herbivore	H	200	J/m^2	
1st Carnivore	C	50	J/m^2	
2nd Carnivore	D	10	J/m^2	
Material available	M	15	g/m^2	M = MT-f1*P-f2*H -f3*C-f4*D
Total material	MT	50	g/m^2	
Material fraction				
Producer	f1	0.02	g/J	
Herbivore	f2	0.05	g/J	
1st Carnivore	f3	0.08	g/J	
2nd Carnivore	f3	0.1	g/J	
Flows				
Sunlight used	J1 = k1*R*M*P	4500	J/m^2/day	k1 = 0.0006
Primary production	J2 = k2*R*M*P	250	J/m^2/day	k2 = 3.33333E-05
Linear consumption	J3 = k3*P	10	J/m^2/day	k3 = 0.01
growth	J4 = k4*P	2.5	J/m^2/day	k4 = 0.0025
Autocatalytic consump.	J5 = k5*P*H	50	J/m^2/day	k5 = 0.00025
growth	J6 = k6*P*H	18	J/m^2/day	k6 = 0.00009
Quadratic consumption	J7 = k7*P*H*H	500	J/m^2/day	k7 = 0.0000125
growth	J8 = k8*P*H*H	200	J/m^2/day	k8 = 0.000005
Producer respiration	J9 = k9*P	100	J/m^2/day	k9 = 0.1
Linear consumption	J10 = k10*H	1	J/m^2/day	k10 = 0.005
growth	J11 = k11*H	0.12	J/m^2/day	k11 = 0.0006
Autocatalytic consump.	J12 = k12*H*C	20	J/m^2/day	k12 = 0.002
growth	J13 = k13*H*C	12	J/m^2/day	k13 = 0.0012
Herbivore respiration	J14 = k14*H	100	J/m^2/day	k14 = 0.5
Linear consumption	J15 = k15*C	1	J/m^2/day	k15 = 0.02
growth	J16 = k16*C	0.12	J/m^2/day	k16 = 0.0024
Autocatalytic consump.	J17 = k17*C*D	5	J/m^2/day	k17 = 0.01
growth	J18 = k18*C*D	0.6	J/m^2/day	k18 = 0.0012

Appendix Table B-6 -- continued

Items	Symbols	Values	Units	Coefficients	
Quadratic consumption	J19 = k19*C*D*D	20	$J/m^2/day$	k19 =	0.004
growth	J20 = k20*C*D*D	8	$J/m^2/day$	k20 =	0.0016
1st Carnivore resp.	J21 = k21*C	1	$J/m^2/day$	k21 =	0.02
2nd Carnivore resp.	J22 = k22*D	0.5	$J/m^2/day$	k22 =	0.05

Appendix Table B-7. Calibration of the pathway coefficients for the computer simulation of the three module pulse model in Figure 3-57.

Items	Symbols	Values	Units	Coefficients
Sources				
Energy source	J	5000	J/m^2/day	
Remaining energy	R	500	J/m^2/day	
Storages				
Producer	P	1000	J/m^2	
Herbivore	H	200	J/m^2	
1st carnivore	C	50	J/m^2	
2nd carnivore	D	10	J/m^2	
3rd carnivore	K	1	J/m^2	
Top predator	L	0.2	J/m^2	
Material available	M	14.5	g/m^2	M=MT-f1*P-f2*H -f3*C-f4*D-f5*K -f6*L
Total material	MT	50	g/m^2	
Material fraction				
Producer	f1	0.02	g/J	
Herbivore	f2	0.05	g/J	
1st carnivore	f3	0.08	g/J	
2nd carnivore	f4	0.1	g/J	
3rd carnivore	f5	0.4	g/J	
Top predator	f6	0.5	g/J	
Flows				
Energy use	J1 = k1*R*M*P	4500	J/m^2/day	k1 = 0.00062069
Primary production	J2 = k2*R*M*P	250	J/m^2/day	k2 = 3.44828E-05
Linear consumption	J3 = k3*P	10	J/m^2/day	k3 = 0.01
growth	J4 = k4*P	2.5	J/m^2/day	k4 = 0.0025
Autocatalytic consump	J5 = k5*P*H	50	J/m^2/day	k5 = 0.00025
growth	J6 = k6*P*H	18	J/m^2/day	k6 = 0.00009
Quadratic consump.	J7 = k7*P*H*H	500	J/m^2/day	k7 = 0.0000125
growth	J8 = k8*P*H*H	200	J/m^2/day	k8 = 0.000005
Producer respiration	J9 = k9*P	100	J/m^2/day	k9 = 0.1
Linear consumption	J10 = k10*H	1	J/m^2/day	k10 = 0.005
growth	J11 = k11*H	0.12	J/m^2/day	k11 = 0.0006
Autocatalytic consump	J12 = k12*H*C	20	J/m^2/day	k12 = 0.002
growth	J13 = k13*H*C	12	J/m^2/day	k13 = 0.0012
Herbivore respiration	J14 = k14*H	100	J/m^2/day	k14 = 0.5

Appendix Table B-7 -- continued

Items	Symbols	Values	Units	Coefficients	
Linear consumption	J15 = k15*C	1	J/m^2/day	k15 =	0.02
growth	J16 = k16*C	0.12	J/m^2/day	k16 =	0.0024
Autocatalytic consump	J17 = k17*C*D	5	J/m^2/day	k17 =	0.01
growth	J18 = k18*C*D	0.6	J/m^2/day	k18 =	0.0012
Quadratic consump.	J19 = k19*C*D*D	20	J/m^2/day	k19 =	0.004
growth	J20 = k20*C*D*D	8	J/m^2/day	k20 =	0.0016
1st carnivore resp.	J21 = k21*C	1	J/m^2/day	k21 =	0.02
Linear consumption	J22 = k22*D	0.02	J/m^2/day	k22 =	0.002
growth	J23 = k23*D	0.0024	J/m^2/day	k23 =	0.00024
Autocatalytic consump	J24 = k24*D*K	0.1	J/m^2/day	k24 =	0.01
growth	J25 = k25*D*K	0.06	J/m^2/day	k25 =	0.006
2nd carnivore resp.	J26 = k26*D	0.5	J/m^2/day	k26 =	0.05
Linear consumption	J27 = k27*K	0.002	J/m^2/day	k27 =	0.002
growth	J28 = k28*K	0.00028	J/m^2/day	k28 =	0.00028
Autocatalytic consump	J29 = k29*K*L	0.0064	J/m^2/day	k29 =	0.032
growth	J30 = k30*K*L	0.001	J/m^2/day	k30 =	0.005
Quadratic consump.	J31 = k31*K*L*L	0.08	J/m^2/day	k31 =	2
growth	J32 = k32*K*L*L	0.016	J/m^2/day	k32 =	0.4
3rd carnivore resp.	J33 = k33*K	0.002	J/m^2/day	k33 =	0.002
Top predator resp.	J34 = k34*L	0.0032	J/m^2/day	k34 =	0.016

APPENDIX C
LISTINGS OF THE SIMULATION PROGRAMS

Appendix Table C-1. Program listing of the simple two storage model in Figure 3-4.

```
' Simple Two Storage Model – Steady Model
' FILE Name: Power-S.BAS

' Plotting Frames
10  SCREEN 12
11 LINE (20, 10)-(270, 170), 15, B
12 LINE (20, 90)-(270, 90), 15
13 LINE (290, 10)-(490, 170), 15, B

' Sources and Initial Values
20 MT = 15   ' Total Material
21 J = 1000
22 Q = .1
23 f = .15   ' Material fraction of Q

' Iteration Time Step during Simulation
40 dt = .01

' Scaling Factors for Plotting
50 Q0 = 1.5
51 M0 = 1
52 J10 = 20
53 t0 = 3

' Pathway Coefficients
60 k1 = 6.667E-2
61 k2 = 3.704E-2
62 k3 = 5.556E-2

' Simulation Loop
200 M = MT - f*Q
201 If M <= 0 THEN M = 0
202 R = J / (1 + k1 * Q * M)
211 J1 = k1 * R * Q * M
212 J2 = k2 * R * Q * M
213 J3 = k3 * Q

300 dQ = J2 - J3

350 IF Max_Power <= J1 THEN Max_Power = J1
351 IF Max_Power <= J1 THEN Max_Q = Q
352 IF Max_Power <= J1 THEN Max_T = T
```

Appendix Table C-1 -- continued

```
400 Q = Q + dQ * dt

550 Sum_Q = Sum_Q + Q
551 Total_Power = Total_Power + J1*dt
552 Total_Production = Total_Production + J2*dt
554 I = I + 1      ' Number of Iteration

' Plotting Simulation Result
600 PSET (T / t0 + 20, 170 - Q / Q0), 15
601 PSET (T / t0 + 20, 90 - J1 / J10), 15
603 PSET ((M*100/MT)/.5 + 290, 170 - J1 / 8), 15

700 T = T + dt

' Repeat the Simulation Loop
800 IF T / t0 < 250 GOTO 200

' Print the Key Values
900 LOCATE 15
901 PRINT "Average Storage        = ", Sum_Q/I, "J/m2"
902 PRINT "Total Power Inflow     = ", Total_Power, "J/m2"
903 PRINT "Total Production       = ", Total_Production, "J/m2"
904 PRINT Max_Power, Max_Q, Max_T
```

Appendix Table C-2. Program listing of the simple two storage model with a pulsing recycle pathway in Figure 3-5.

```
' Simple Two Storage Model with Pulsing Recycle
' FILE Name: Power-P.BAS

' Plotting Frames
10 SCREEN 12
11 LINE (20, 10)-(270, 170), 15, B
12 LINE (20, 90)-(270, 90), 15
13 LINE (290, 10)-(540, 210), 15, B

' Sources and Initial Values
20 MT = 15    ' Total Material
21 J = 1000
22 Q = .1
23 f= .15    ' Material fraction of Q
24 X = 100    ' Pulse Frequency
25 PP = 20    ' Pulse Amplitude

' Iteration Time Step during Simulation
40 dt = .01

' Scaling Factors for Plotting
50 Q0 = 1.5
51 M0 = 1
52 J10 = 20
53 t0 = 3

' Pathway Coefficients
60 k1 = 6.667E-2
61 k2 = 3.704E-4
62 k3 = 5.556E-2
63 k4 = 5.556E-2

' Simulation Loop
200 M = MT - f*Q
201 If M <= 0 THEN M = 0
202 R = J / (1 + k1 * Q * M)
203 IF (T MOD X)<=(X-1) AND (T MOD X)>=(X-2) THEN P=PP ELSE P=0
211 J1 = k1 * R * Q * M
212 J2 = k2 * R * Q * M
213 J3 = k3 * Q
214 J4 = k4 * Q * P
```

Appendix Table C-2 -- continued

```
300 dQ = J2 - J3 - J4

350 IF Max_Power <= J1 THEN Max_Power = J1
351 IF Max_Power <= J1 THEN Max_Q = Q
352 IF Max_Power <= J1 THEN Max_T = T

400 Q = Q + dQ * dt

550 Sum_Q = Sum_Q + Q
551 Total_Power = Total_Power + J1*dt
552 Total_Production = Total_Production + J2*dt
554 I = I + 1  ' Number of Iteration

' Plotting Simulation Result
600 PSET (T / t0 + 20, 170 - Q / Q0), 15
601 PSET (T / t0 + 20, 90 - J1 / J10), 15
603 PSET ((M*100/MT)/.4 + 290, 210 - J1 / 6), 15

700 T = T + dt

' Repeat the Simulation Loop
800 IF T / t0 < 250 GOTO 200

' Print the Key Values
900 LOCATE 15
901 PRINT "Average Storage       = ", Sum_Q/I, "J/m2"
902 PRINT "Total Power Inflow    = ", Total_Power, "J/m2"
903 PRINT "Total Production      = ", Total_Production, "J/m2"
904 PRINT Max_Power, Max_Q, Max_T
```

Appendix Table C-3. Program listing of the steady model in Figure 3-25.

```
' Steady Model
' File Name: Steady.bas

' Plotting Frames
10 SCREEN 12
11 LINE (20, 10)-(270, 175), 15, B
12 LINE (20, 65)-(270, 65), 15
13 LINE (20, 120)-(270, 120), 15
15 LINE (20, 190)-(270, 310), 15, B
16 LINE (20, 250)-(270, 250), 15

17 LINE (300, 10)-(550, 170), 15, B
18 LINE (300, 50)-(550, 50), 15
19 LINE (300, 90)-(550, 90), 15, B
20 LINE (300, 130)-(550, 130), 15
21 LINE (300, 190)-(550, 310), 15, B
22 LINE (300, 250)-(550, 250), 15

' Sources and Initial Values
30 MT = 50
31 J = 5000: TrJ = 1
32 P = 10: EP = 10: TrP = EP/P
33 H = .1: EH = 10: TrH = EH/H

' Iteration Time Step during Simulation
40 dt = .01

' Scaling Factors for Plotting
50 P0 = 70: EP0 = 3000: TrP0 = 1.5
51 H0 = 20: EH0 = 3000: TrH0 = 25
52 M0 = 1
53 t0 = 1.46

' Material Fraction of Storages
70 f1 = .02
71 f2 = .05

' Pathway Coefficients
101 k1 = .00045
102 k2 = .000025
103 k3 = .01
104 k4 = .0025
```

Appendix C-3 -- continued

```
105 k5 = .00275
106 k6 = .00109
109 k9 = .1
110 k10= .5

' Simulation Loop
200 M = MT - f1 * P - f2 * H
201 IF M < 0 THEN M = 0
202 R = J / (1 + k1*M*P)
211 J1 = k1 * R * M * P
212 J2 = k2 * R * M * P
213 J3 = k3 * P
214 J4 = k4 * P
215 J5 = k5 * P * H
216 J6 = k6 * P * H
219 J9 = k9 * P
220 J10= k10* H

300 dP = J2 - J3 - J5 - J9
301 IF (dP/P)>.05 THEN dEP = TrJ*J1-TrP*J3-TrP*J5
302 IF (dP/P)<=.05 and (dP/P)>=0 THEN dEP = 0
303 IF (dP/P)<0 THEN dEP = TrP*dP

310 dH = J4 + J6 - J10
311 IF (dH/H)>.05 THEN dEH = TrP*J3+TrP*J5
312 IF (dH/H)<=.05 and (dH/H)>=0 THEN dEH = 0
313 IF (dH/H)<0 THEN dEH = TrH*dH

400 P = P + dP * dt
401 IF P < .01 THEN P = .01
402 EP = EP + dEP * dt

410 H = H + dH * dt
411 IF H < .001 THEN H = .001
412 EH = EH + dEH * dt

500 TrP = EP/P
501 TrH = EH/H

550 Total_P = Total_P + P
551 Total_H = Total_H + H
560 Total_Power = Total_Power + J1
561 Total_EP = Total_EP + EP
```

Appendix C-3 -- continued

```
562 Total_EH = Total_EH + EH
563 Trans_P = Trans_P + TrP
564 Trans_H = Trans_H + TrH
570 I = I + 1

' Plotting Simulation Result
600 PSET (T / t0 + 20, 65 - P / P0), 15
601 PSET (T / t0 + 20, 120 - H / H0), 15
602 PSET (T / t0 + 20, 175 - M / M0), 15
603 PSET (T / t0 + 20, 250 - J2 / 6), 15
604 PSET (T / t0 + 20, 310 - J1*60/J), 15
605 PSET (T / t0 + 300, 250 - P/J2/.1), 15
606 PSET (T / t0 + 300, 310 - H/(J4+J6)/.1), 15

610 PSET (T / t0 + 300, 50 - EP/EP0), 15
611 PSET (T / t0 + 300, 90 - EH/EH0), 15
612 PSET (T / t0 + 300, 130 - TrP/TrP0), 15
613 PSET (T / t0 + 300, 170 - TrH/TrH0), 15

700 T = T + dt

' Repeat the Simulation Loop
800 IF T / t0 < 250 GOTO 200

LOCATE 23
PRINT "Total Power Input           = ", Total_Power*dt, "J/m2"
PRINT "Average storage of P        = ", Total_P/I, "J/m2"
PRINT "Average storage of H        = ", Total_H/I, "J/m2"
PRINT "Average EMERGY storage of P = ", Total_EP/I, "sej/m2"
PRINT "Average EMERGY storage of H = ", Total_EH/I, "sej/m2"
PRINT "Average transformity of P   = ", Trans_P/I, "sej/J"
PRINT "Average transformity of H   = ", Trans_H/I, "sej/J"
'print jmax, MaxM, MaxT, TJ*dt
```

Appendix Table C-4. Program listing of the pulse model with consumer feedback on primary production in Figure 3-28.

```
' Pulse Model with Feedback from Consumer
' File Name: Feedback.BAS

' Plotting Frames
10 SCREEN 12
11 LINE (20, 10)-(270, 170), 15, B
12 LINE (20, 90)-(270, 90), 15
13 LINE (20, 180)-(270, 340), 15, B
14 LINE (20, 260)-(270, 260), 15

15 LINE (300, 10)-(550, 170), 15, B
16 LINE (300, 90)-(550, 90), 15
17 LINE (300, 180)-(550, 340), 15, B
18 LINE (300, 260)-(550, 260), 15

' Sources and Initial Values
30 MT = 50
31 J = 5000: TrJ = 1
32 P = 10: EP = 10: TrP = EP/P
33 H = .1: EH = 10: TrH = EH/H

' Iteration Time Step in Simulation
40 dt = .01

' Scaling Factors for Plotting
50 P0 = 40: EP0 = 3000: TrP0 = 1
51 H0 = 8: EH0 = 3000: TrH0 = 10
52 M0 = .625
53 J20 = 4
54 J40 = 4
56 t0 = 1.46

' Material Fraction of Storages
70 f1 = .02
71 f2 = .05

' Pathway Coefficients
101 k1 = .00000125
102 k2 = 8E-8
103 k3 = .0002
104 k4 = .00001
```

Appendix Table C-4 -- continued

```
105 k5 = .01
106 k6 = .0025
107 k7 = .00025
108 k8 = .00009
109 k9 = .0000125
110 k10= .000005
111 k11= .1
112 k12= .5
113 k13= 5E-10

' Simulation Loop
200 M = MT - f1 * P - f2 * H
201 IF M < 0 THEN M = 0
202 R = J / (1 + k1 * M * P * H + k3 * M * P)
203 J1 = k1 * R * M * P * H
204 J2 = k2 * R * M * P * H
205 J3 = k3 * R * M * P
206 J4 = k4 * R * M * P
207 J5 = k5 * P
208 J6 = k6 * P
209 J7 = k7 * P * H
210 J8 = k8 * P * H
211 J9 = k9 * P * H * H
212 J10= k10* P * H * H
213 J11= k11* P
214 J12= k12* H
215 J13= k13* R * M * P * H

300 dP = J2 + J4 - J5 - J7 - J9 - J11
301 IF (dP/P)>.05 THEN dEP = TrJ*J1+TrJ*J3+TrP*J13-TrP*J5-TrP*J7-TrP*J9
302 IF (dP/P)<=.05 and (dP/P)>=0 THEN dEP = 0
303 IF (dP/P)<0 THEN dEP = TrP*dP

310 dH = J6 + J8 + J10 - J12 - J13
311 IF (dH/H)>.05 THEN dEH = TrP*J5+TrP*J7+TrP*J9-TrH*J13
312 IF (dH/H)<=.05 and (dH/H)>=0 THEN dEH = 0
313 IF (dH/H)<0 THEN dEH = TrH*dH

400 P = P + dP * dt
401 IF P < .01 THEN P = .01
402 EP = EP + dEP * dt

410 H = H + dH * dt
```

Appendix Table C-4 -- continued

```
411 IF H < .001 THEN H = .001
412 EH = EH + dEH * dt

500 TrP = EP/P
501 TrH = EH/H

550 Total_P = Total_P + P
551 Total_H = Total_H + H
560 Total_Power = Total_Power + J1 + J3
561 Total_EP = Total_EP + EP
562 Total_EH = Total_EH + EH
563 Trans_P = Trans_P + TrP
564 Trans_H = Trans_H + TrH

600 T = T + dt

' Plotting Simulation Result
700 PSET (T / t0 + 20, 90 - P / P0), 15
701 PSET (T / t0 + 20, 170 - H / H0), 15
702 PSET (T / t0 + 300, 90 - M / M0), 15
703 PSET (T / t0 + 300, 170 - J2/J20), 15
704 PSET (T / t0 + 300, 170 - J4/J40), 15

710 PSET (T / t0 + 20, 260 - TrP / TrP0), 15
711 PSET (T / t0 + 20, 340 - TrH / TrH0), 15
712 PSET (T / t0 + 300, 260 - J13 / .1), 15
713 PSET (T / t0 + 300, 340 - TrH*J13 / 15), 15

' Repeat the Simulation Loop
800 IF T / t0 < 250 GOTO 200

LOCATE 23
PRINT "Total Power Input          = ", Total_Power*dt, "J/m2"
'PRINT "Average storage of P       = ", Total_P/I, "J/m2"
'PRINT "Average storage of H       = ", Total_H/I, "J/m2"
PRINT "Average EMERGY storage of P = ", Total_EP/I, "sej/m2"
PRINT "Average EMERGY storage of H = ", Total_EH/I, "sej/m2"
PRINT "Average transformity of P   = ", Trans_P/I, "sej/J"
PRINT "Average transformity of H   = ", Trans_H/I, "sej/J"
```

Appendix Table C-5. Program listing of the pulse model with a detritus storage in Figure 3-36.

```
' Pulse Model with Detritus Storage
' File Name: Detritus.bas

' Plotting Frames
10 SCREEN 12
11 LINE (20, 10)-(270, 170), 15, B
12 LINE (20, 90)-(270, 90), 15
13 LINE (300, 10)-(550, 170), 15, B
14 LINE (300, 90)-(550, 90), 15
'15 LINE (20, 200)-(270, 360), 15, B
'16 LINE (20, 280)-(270, 280), 15

' Sources and Initial Values
20 MT = 50
21 J = 5000: TrJ = 1
22 P = 10: EP = 20: TrP = EP/P
23 H = 1: EH = 20: TrH = EH/H
24 D = 500: ED = 20: TrD = ED/D

' Iteration Time Step during Simulation
40 dt = .01

' Scaling Factors for Plotting
50 P0 = 20: EP0 = 8000: TrP0 = 2
51 H0 = 20: EH0 = 8000: TrH0 = 2
52 D0 = 150: ED0 = 15000: TrD0 = 2
53 t0 = 1.46

' Material Fraction of Storages
70 f1 = .02
71 f2 = .05
72 f3 = .001

' Pathway Coefficients
100 k1 = .0006
101 k2 = 3.33333E-5
102 k3 = .06
103 k4 = .02
104 k5 = .0000125
105 k6 = .000005
106 k7 = .1
```

Appendix C-5 -- continued

```
107 k8 = .05
108 k9 = .2
109 k10 = .5
110 k11 = .01
111 k12 = .004
112 k13 = .0006
113 k14 = .0000015
114 k15 = .0000004
115 k16 = .0000075

' Simulation Loop
200 M = MT - f1 * P - f2 * H - f3 * D
201 IF M < 0 THEN M = 0
202 R = J / (1 + k1 * M * P)
203 J1 = k1 * R * M * P
204 J2 = k2 * R * M * P
205 J3 = k3 * P
206 J4 = k4 * P
207 J5 = k5 * P * H * H
208 J6 = k6 * P * H * H
209 J7 = k7 * P
210 J8 = k8 * H
211 J9 = k9 * P
212 J10 = k10 * H
213 J11 = k11 * D
214 J12 = k12 * D
215 J13 = k13 * D
216 J14 = k14 * D * H * H
217 J15 = k15 * D * H * H
218 J16 = k16 * P * H * H

300 dP = J2 - J3 - J5 - J7 - J9
301 IF (dP/P)>.05 THEN dEP = TrJ*J1-TrP*J3-TrP*J5-TrPJ9
302 IF (dP/P)<=.05 and (dP/P)>=0 THEN dEP = 0
303 IF (dP/P)<0 THEN dEP = TrP*dP

310 dH = J4 + J6 + J13 + J15 - J8 - J10
311 IF (dH/H)>.05 THEN dEH = TrP*J3+TrP*J5+TrD*J12+TrD*J14-TrH*J10
312 IF (dH/H)<=.05 and (dH/H)>=0 THEN dEH = 0
313 IF (dH/H)<0 THEN dEH = TrH*dH

320 dD = J9 + J10 + J16 - J11 - J12 - J14
321 IF (dD/D)>.05 THEN dED = TrP*J9+TrH*J10+TrP*J5-TrD*J12-TrD*J14
```

Appendix C-5 -- continued

```
322 IF (dD/D)<=.05 and (dD/D)>=0 THEN dED = 0
323 IF (dD/D)<0 THEN dED = TrD*dD

400 P = P + dP * dt
401 EP = EP + dEP * dt

410 H = H + dH * dt
411 EH = EH + dEH * dt

420 D = D + dD * dt
421 ED = ED + dED * dt

450 Total_Power = Total_Power + J1

500 TrP = EP/P
501 TrH = EH/H
502 TrD = ED/D

' Plotting Simulation Result
600 PSET (T / t0 + 20, 90 - P / P0), 15
610 PSET (T / t0 + 20, 90 - H / H0), 15
620 PSET (T / t0 + 20, 170 - D /D0), 15

'621 PSET (T / t0 + 20, 280 - EP / EP0), 15
'622 PSET (T / t0 + 20, 280 - EH / EH0), 15
'623 PSET (T / t0 + 20, 360 - ED / ED0), 15

630 PSET (T / t0 + 300, 90 - TrP / TrP0), 15
640 PSET (T / t0 + 300, 90 - TrH / TrH0), 15
650 PSET (T / t0 + 300, 170 - TrD / TrD0), 15

700 T = T + dt

' Repeat the Simulation Loop
800 IF T / t0 < 250 GOTO 200

LOCATE 25
PRINT Total_Power*dt
```

Appendix Table C-6. Program listing of the layered pulse model in Figure 3-41.

```
' Layered Pulse Model
' File Name: Layered.bas

' Plotting Frames
10 SCREEN 12
11 LINE (20, 10)-(270, 130), 15, B
12 LINE (20, 70)-(270, 70), 15
13 LINE (20, 140)-(270, 260), 15, B
14 LINE (20, 200)-(270, 200), 15
15 LINE (20, 270)-(270, 390), 15, B
16 LINE (20, 330)-(270, 330), 15

17 LINE (300, 10)-(550, 130), 15, B
18 LINE (300, 70)-(550, 70), 15
19 LINE (300, 140)-(550, 260), 15, B
20 LINE (300, 200)-(550, 200), 15
21 LINE (300, 270)-(550, 390), 15, B
22 LINE (300, 330)-(550, 330), 15

' Sources and Initial Values
30 MT = 100
31 J = 5000: TrJ = 1
32 P1 = 10: EP1 = 10: TrP1 = EP1/P1
33 P2 = 10: EP2 = 10: TrP2 = EP2/P2
34 H1 = 1: EH1 = 100: TrH1 = EH1/H1
35 H2 = 1: EH2 = 100: TrH2 = EH2/H2
36 dt = .01

' Scaling Factors for Plotting
50 P10 = 120: EP10 = 2000: TrP10 = .4
51 P20 = 120: EP20 = 2000: TrP20 = .4
52 H10 = 60: EH10 = 2000: TrH10 = 5
53 H20 = 60: EH20 = 2000: TrH20 = 5
54 M0 = 1.25
55 t0 = 1.46

' Material Fraction of Storages
70 f1 = .02
71 f2 = .05
72 f3 = .02
73 f4 = .05
```

Appendix Table C-6 -- continued

```
' Pathway Coefficients
101 k1 = .0005
102 k2 = 5E-5
103 k3 = .01
104 k4 = .0015
105 k5 = .00025
106 k6 = .000075
107 k7 = .0000125
108 k8 = .000004
109 k9 = .1
110 k10= .05
111 k11= .0002
112 k12= .00003
113 k13= .005
114 k14= .0015
115 k15= .0000625
116 k16= .000025
117 k17= 1.5625E-6
118 k18= 6.875E-7
119 k19= .05
120 k20= .25
121 k21= .001
122 k22= .0001

' Simulation Loop
200 M = MT - f1 * P1 - f2 * H1 - f3 * P2 - f4 * H2
201 IF M < 0 THEN M = 0
202 R = J / (1 + k1*M*P1 + k11*M*P2)

211 J1 = k1 * R * M * P1
212 J2 = k2 * R * M * P1
213 J3 = k3 * P1
214 J4 = k4 * P1
215 J5 = k5 * P1 * H1
216 J6 = k6 * P1 * H1
217 J7 = k7 * P1 * H1 * H1
218 J8 = k8 * P1 * H1 * H1
219 J9 = k9 * P1
220 J10= k10 * H1
221 J11= k11 * R * M * P2
222 J12= k12 * R * M * P2
223 J13= k13 * P2
224 J14= k14 * P2
```

Appendix Table C-6 -- continued

```
225 J15= k15 * P2 * H2
226 J16= k16 * P2 * H2
227 J17= k17 * P2 * H2 * H2
228 J18= k18 * P2 * H2 * H2
229 J19= k19 * P2
230 J20= k20 * H2
231 J21= k21 * H1 * H2
232 J22= k22 * H1 * H2

300 dP1 = J2 - J3 - J5 - J7 - J9
301 IF (dP1/dt/P1)>.05 THEN dEP1 = TrJ*J1-TrP1*J3-TrP1*J5-TrP1*J7
302 IF (dP1/dt/P1)<=.05 and (dP1/dt/P1)>=0 THEN dEP1 = 0
303 IF (dP1/dt/P1)<0 THEN dEP1 = TrP1*dP1

310 dP2 = J12 - J13 - J15 - J17 - J19
311 IF (dP2/dt/P2)>.05 THEN dEP2 = TrJ*J11-TrP2*J13-TrP2*J15-TrP2*J17
312 IF (dP2/dt/P2)<=.05 and (dP2/dt/P2)>=0 THEN dEP2 = 0
313 IF (dP2/dt/P2)<0 THEN dEP2 = TrP2*dP2

320 dH1 = J4 + J6 + J8 - J10 - J21
321 IF (dH1/dt/H1)>.05 THEN dEH1 = TrP1*J3+TrP1*J5+TrP1*J7-TrH1*J21
322 IF (dH1/dt/H1)<=.05 and (dH1/dt/H1)>=0 THEN dEH1 = 0
323 IF (dH1/dt/H1)<0 THEN dEH1 = TrH1*dH1

330 dH2 = J14 + J16 + J18 + J22 - J20
331 IF (dH2/dt/H2)>.05 THEN dEH2 = TrP2*J13+TrP2*J15+TrP2*J17+TrH1*J21
332 IF (dH2/dt/H2)<=.05 and (dH2/dt/H2)>=0 THEN dEH2 = 0
333 IF (dH2/dt/H2)<0 THEN dEH2 = TrH2*dH2

400 P1 = P1 + dP1 * dt
401 IF P1 < .001 THEN P1 = .001
402 EP1 = EP1 + dEP1 * dt

410 P2 = P2 + dP2 * dt
411 IF P2 < .001 THEN P2 = .001
412 EP2 = EP2 + dEP2 * dt

420 H1 = H1 + dH1 * dt
421 IF H1 < .01 THEN H1 = .01
422 EH1 = EH1 + dEH1 * dt

430 H2 = H2 + dH2 * dt
431 IF H2 < .01 THEN H2 = .01
```

Appendix Table C-6 -- continued

```
432 EH2 = EH2 + dEH2 * dt

450 Total_J1 = Total_J1 + J1
451 Total_J11 = Total_J11 + J11

500 TrP1 = EP1/P1
501 TrP2 = EP2/P2
502 TrH1 = EH1/H1
503 TrH2 = EH2/H2

' Plotting Simulation Result
600 PSET (T / t0 + 20, 70 - P1 / P10), 15
601 PSET (T / t0 + 20, 130 - H1 / H10), 15
602 PSET (T / t0 + 20, 200 - P2 / P20), 15
603 PSET (T / t0 + 20, 260 - H2 / H20), 15
604 PSET (T / t0 + 20, 330 - (P1+P2)/ P20), 15
605 PSET (T / t0 + 20, 390 - (H1+H2)/ H20), 15

610 PSET (T / t0 + 300, 200 - TrP1 / TrP10), 15
611 PSET (T / t0 + 300, 260 - TrH1 / TrH10), 15
612 PSET (T / t0 + 300, 330 - TrP2 / TrP20), 15
613 PSET (T / t0 + 300, 390 - TrH2 / TrH20), 15
614 PSET (T / t0 + 300, 70 - (EP1+EP2) / EP10), 15
615 PSET (T / t0 + 300, 130 - (EH1+EH2) / EH10), 15

700 T = T + dt

' Repeat the Simulation Loop
800 IF T / t0 < 250 GOTO 200

LOCATE 29
PRINT Total_J1*dt, Total_J11*dt, (Total_J1+Total_J11)*dt
```

Appendix Table C-7. Program listing of the two module pulse model in Figure 3-50.

```
' Two Module Pulse Model
' File Name: 2Mod.bas

' Plotting Frames
10  SCREEN 12
11  LINE (20, 70)-(270, 310), 15, B
12  LINE (20, 130)-(270, 130), 15
13  LINE (20, 190)-(270, 190), 15
14  LINE (20, 250)-(270, 250), 15

16  LINE (300, 70)-(550, 310), 15, B
17  LINE (300, 130)-(550, 130), 15
18  LINE (300, 190)-(550, 190), 15
19  LINE (300, 250)-(550, 250), 15

' Sources and Intial Values
20  MT = 50
21  J = 5000: TrJ = 1
22  P = 10: EP = 1: TrP = EP/P
23  H = 1: EH = 1: TrH = EH/H
24  C = .5: EC = 10: TrC = EC/C
25  D = .1: ED = 10: TrD = ED/D

' Iteration Time Step during Simulation
40  dt = .01

' Scaling Factors for Plotting
50  P0 = 50: EP0 = 2000: TrP0 = 1
51  H0 = 15: EH0 = 2000: TrH0 = 10
52  C0 = 1.5: EC0 = 1000: TrC0 = 50
53  D0 = .5: ED0 = 1000: TrD0 = 100
54  t0 = 1.46*2

' Material Fraction of Storages
70  f1 = .02
71  f2 = .05
72  f3 = .08
73  f4 = .1

' Pathway Coefficients
100 k1 = .0006
101 k2 = 3.33333E-5
```

Appendix Table C-7 -- continued

```
102 k3 = .01
103 k4 = .0025
104 k5 = .00025
105 k6 = .00009
106 k7 = .0000125
107 k8 = .000005
108 k9 = .1
109 k10 = .005
110 k11 = .0006
111 k12 = .002
112 k13 = .0012
113 k14 = .5
114 k15 = .02
115 k16 = .0024
116 k17 = .01
117 k18 = .0012
118 k19 = .004
119 k20 = .0016
120 k21 = .02
121 k22 = .05

' Simulation Loop
200 M = MT - f1 * P - f2 * H - f3 * C - f4 * D
201 IF M < 0 THEN M = 0
203 R = J / (1 + k1 * M * P)
211 J1 = k1 * R * M * P
212 J2 = k2 * R * M * P
213 J3 = k3 * P
214 J4 = k4 * P
215 J5 = k5 * P * H
216 J6 = k6 * P * H
217 J7 = k7 * P * H * H
218 J8 = k8 * P * H * H
219 J9 = k9 * P
220 J10 = k10 * H
221 J11 = k11 * H
222 J12 = k12 * H * C
223 J13 = k13 * H * C
224 J14 = k14 * H
225 J15 = k15 * C
226 J16 = k16 * C
227 J17 = k17 * C * D
228 J18 = k18 * C * D
```

Appendix Table C-7 -- continued

```
229 J19 = k19 * C * D * D
230 J20 = k20 * C * D * D
231 J21 = k21 * C
232 J22 = k22 * D

300 dP = J2 - J3 - J5 - J7 - J9
301 IF (dP/P)>.05 THEN dEP = TrJ*J1-TrP*J3-TrP*J5-TrP*J7
302 IF (dP/P)<=.05 AND (dP/P)>=0 THEN dEP = 0
303 IF (dP/P)<0 THEN dEP = TrP*dP

310 dH = J4 + J6 + J8 - J10 - J12 - J14
311 IF (dH/H)>.05 THEN dEH = TrP*J3+TrP*J5+TrP*J7-TrH*J10-TrH*J12
312 IF (dH/H)<=.05 AND (dH/H)>=0 THEN dEH = 0
313 IF (dH/H)<0 THEN dEH = TrH*dH

320 dC = J11 + J13 - J15 - J17 - J19 - J21
321 IF (dC/C)>.05 THEN dEC = TrH*J10+TrH*J12-TrC*J15-TrC*J17-TrC*J19
322 IF (dC/C)<=.05 AND (dC/C)>=0 THEN dEC = 0
323 IF (dC/C)<0 THEN dEC = TrC*dC

330 dD = J16 + J18 + J20 - J22
331 IF (dD/D)>.05 THEN dED = TrC*J15+TrC*J17+TrC*J19
332 IF (dD/D)<=.05 AND (dD/D)>=0 THEN dED = 0
333 IF (dD/D)<0 THEN dED = TrD*dD

400 P = P + dP * dt
401 EP = EP + dEP * dt

410 H = H + dH * dt
411 EH = EH + dEH * dt

420 C = C + dC * dt
421 EC = EC + dEC * dt

430 D = D + dD * dt
431 ED = ED + dED * dt

450 Total_J1 = Total_J1 + J1

500 TrP = EP/P
501 TrH = EH/H
502 TrC = EC/C
503 TrD = ED/D
```

Appendix Table C-7 -- continued

```
' Plotting Simulation Result
600 PSET (T / t0 + 20, 310 - P / P0), 15
610 PSET (T / t0 + 20, 250 - H / H0), 15
620 PSET (T / t0 + 20, 190 - C / C0), 15
630 PSET (T / t0 + 20, 130 - D / D0), 15

640 PSET (T / t0 + 300, 310 - TrP / TrP0), 15
650 PSET (T / t0 + 300, 250 - TrH / TrH0), 15
660 PSET (T / t0 + 300, 190 - TrC / TrC0), 15
670 PSET (T / t0 + 300, 130 - TrD / TrD0), 15

700 T = T + dt

' Repeat the Simulation Loop
800 IF T / t0 < 250 GOTO 200

PRINT "Total Power Inflow = ", Total_J1*dt, "J/m2"
```

Appendix Table C-8. Program listing of the three module pulse model in Figure 3-57.

```
' Three Module Pulse Model
' File Name: 3mod.bas

' Plotting Frames
10  SCREEN 12
11  LINE (20, 20)-(270, 320), 15, B
12  LINE (20, 70)-(270, 70), 15
13  LINE (20, 120)-(270, 120), 15
14  LINE (20, 170)-(270, 170), 15
15  LINE (20, 220)-(270, 220), 15
16  LINE (20, 270)-(270, 270), 15

17  LINE (300, 20)-(550, 320), 15, B
18  LINE (300, 70)-(550, 70), 15
19  LINE (300, 120)-(550, 120), 15
20  LINE (300, 170)-(550, 170), 15
21  LINE (300, 220)-(550, 220), 15
22  LINE (300, 270)-(550, 270), 15

' Sources and Initial Values
30 MT = 50
31 J = 5000: TrJ = 1
32 P = 10: EP = 1: TrP = EP/P
33 H = 1: EH = 1: TrH = EH/H
34 C = .5: EC = 10: TrC = EC/C
35 D = .1: ED = 10: TrD = ED/D
36 K = .1: EK = 50: TrK = EK/K
37 L = .01: EL = 50: TrL = EL/L

' Iteration Time Step in Simulation
40 dt = .01

' Scaling Factors for Plotting
50 P0 = 70:  EP0 = 2500: TrP0 = 2
51 H0 = 20:  EH0 = 2500: TrH0 = 20
52 C0 = 3:   EC0 = 1600: TrC0 = 150
53 D0 = .8:  ED0 = 1600: TrD0 = 250
54 K0 = .2:  EK0 = 1600: TrK0 = 1500
55 L0 = .06: EL0 = 1600: TrL0 = 2500
56 t0 = 1.46*4
```

Appendix Table C-8 -- continued

```
' Material Fraction of Storage
70 f1 = .02
71 f2 = .05
72 f3 = .08
73 f4 = .1
74 f5 = .4
75 f6 = .5

' Pathway Coefficients
101 k1 = .00062069
102 k2 = 3.44828E-5
103 k3 = .01
104 k4 = .0025
105 k5 = .00025
106 k6 = .00009
107 k7 = .0000125
108 k8 = .000005
109 k9 = .1
110 k10 = .005
111 k11 = .0006
112 k12 = .002
113 k13 = .0012
114 k14 = .5
115 k15 = .02
116 k16 = .0024
117 k17 = .01
118 k18 = .0012
119 k19 = .004
120 k20 = .0016
121 k21 = .02
122 k22 = .002
123 k23 = .00024
124 k24 = .01
125 k25 = .006
126 k26 = .05
127 k27 = .002
128 k28 = .00028
129 k29 = .032
130 k30 = .005
131 k31 = 2
132 k32 = .4
133 k33 = .002
134 k34 = .016
```

Appendix Table C-8 -- continued

```
' Simulation Loop
200 M = MT - f1*P - f2*H - f3*C - f4*D - f5*K - f6*L
201 IF M < 0 THEN M = 0
202 R = J / (1 + k1 * M * P)
211 J1 = k1 * R * M * P
212 J2 = k2 * R * M * P
213 J3 = k3 * P
214 J4 = k4 * P
215 J5 = k5 * P * H
216 J6 = k6 * P * H
217 J7 = k7 * P * H * H
218 J8 = k8 * P * H * H
219 J9 = k9 * P
220 J10 = k10 * H
221 J11 = k11 * H
222 J12 = k12 * H * C
223 J13 = k13 * H * C
224 J14 = k14 * H
225 J15 = k15 * C
226 J16 = k16 * C
227 J17 = k17 * C * D
228 J18 = k18 * C * D
229 J19 = k19 * C * D * D
230 J20 = k20 * C * D * D
231 J21 = k21 * C
232 J22 = k22 * D
233 J23 = k23 * D
234 J24 = k24 * D * K
235 J25 = k25 * D * K
236 J26 = k26 * D
237 J27 = k27 * K
238 J28 = k28 * K
239 J29 = k29 * K * L
240 J30 = k30 * K * L
241 J31 = k31 * K * L * L
242 J32 = k32 * K * L * L
243 J33 = k33 * K
244 J34 = k34 * L

300 dP = J2 - J3 - J5 - J7 - J9
301 IF (dP/P)>.05 THEN dEP = TrJ*J1-TrP*J3-TrP*J5-TrP*J7
302 IF (dP/P)<=.05 AND (dP/P)>=0 THEN dEP = 0
303 IF (dP/P)<0 THEN dEP = TrP*dP
```

Appendix Table C-8 -- continued

```
310 dH = J4 + J6 + J8 - J10 - J12 - J14
311 IF (dH/H)>.05 THEN dEH = TrP*J3+TrP*J5+TrP*J7-TrH*J10-TrH*J12
312 IF (dH/H)<=.05 AND (dH/H)>=0 THEN dEH = 0
313 IF (dH/H)<0 THEN dEH = TrH*dH

320 dC = J11 + J13 - J15 - J17 - J19 - J21
321 IF (dC/C)>.05 THEN dEC = TrH*J10+TrH*J12-TrC*J15-TrC*J17-TrC*J19
322 IF (dC/C)<=.05 AND (dC/C)>=0 THEN dEC = 0
323 IF (dC/C)<0 THEN dEC = TrC*dC

330 dD = J16 + J18 + J20 - J22 - J24 - J26
331 IF (dD/D)>.05 THEN dED = TrC*J15+TrC*J17+TrC*J19-TrD*J22-TrD*J24
332 IF (dD/D)<=.05 AND (dD/D)>=0 THEN dED = 0
333 IF (dD/D)<0 THEN dED = TrD*dD

340 dK = J23 + J25 - J27 - J29 - J31 - J33
341 IF (dK/K)>.05 THEN dEK = TrD*J22+TrD*J24-TrK*J27-TrK*J29-TrK*J31
342 IF (dK/K)<=.05 AND (dK/K)>=0 THEN dEK = 0
343 IF (dK/K)<0 THEN dEK = TrK*dK

350 dL = J28 + J30 + J32 - J34
351 IF (dL/L)>.05 THEN dEL = TrK*J27+TrK*J29+TrK*J31
352 IF (dL/L)<=.05 AND (dL/L)>=0 THEN dEL = 0
353 IF (dL/L)<0 THEN dEL = TrL*dL

400 P = P + dP * dt
401 EP = EP + dEP * dt

410 H = H + dH * dt
411 EH = EH + dEH * dt

420 C = C + dC * dt
421 EC = EC + dEC * dt

430 D = D + dD * dt
431 ED = ED + dED * dt

440 K = K + dK * dt
441 EK = EK + dEK * dt

450 L = L + dL * dt
451 EL = EL + dEL * dt
```

Appendix Table C-8 -- continued

```
460 Total_J1 = Total_J1 + J1

500 TrP = EP/P
501 TrH = EH/H
502 TrC = EC/C
503 TrD = ED/D
504 TrK = EK/K
505 TrL = EL/L

600 T = T + dt

' Plotting Simulation Result
700 PSET (T / t0 + 20, 320 - P / P0), 15
701 PSET (T / t0 + 20, 270 - H / H0), 15
702 PSET (T / t0 + 20, 220 - C / C0), 15
703 PSET (T / t0 + 20, 170 - D / D0), 15
704 PSET (T / t0 + 20, 120 - K / K0), 15
705 PSET (T / t0 + 20, 70 - L / L0), 15

710 PSET (T / t0 + 300, 320 - TrP / TrP0), 15
711 PSET (T / t0 + 300, 270 - TrH / TrH0), 15
712 PSET (T / t0 + 300, 220 - TrC / TrC0), 15
713 PSET (T / t0 + 300, 170 - TrD / TrD0), 15
714 PSET (T / t0 + 300, 120 - TrK / TrK0), 15
715 PSET (T / t0 + 300, 70 - TrL / TrL0), 15

' Repeat the Simulation Loop
800 IF T / t0 < 250 GOTO 200

LOCATE 25
PRINT "Total Power Inflow = ", Total_J1*dt, "J/m2"
```

LIST OF REFERENCES

Abel, A.B. and B.S. Bernanke. 1995. Macroeconomics. Addison-Wesley, Reading. 641pp.

Abrams, P.A. and J.D. Roth. 1994. The effects of enrichment of three-species food chains with nonlinear functional responses. Ecology, 75:1118-1130.

Alexander, J.F. 1978. Energy basis of disasters and the cycles of order and disorder. Ph.D. dissertation, Environmental Engineering Sciences, University of Florida, Gainesville. 232pp.

Allen, J.C., W.M. Schaffer, and D. Rosko. 1993. Chaos reduces species extinction by amplifying local population noise. Nature, 364:229-232.

Alvarez, L.W., W. Alvarez, F. Asaro, H.V. Michel. 1980. Extraterrestrial cause for the Cretaceous-Tertiary extinction. Science, 208:1095-1108.

Ascioti, F.A., E. Beltrami, T.O. Carroll, and C. Wirick. 1993. Is there chaos in plankton dynamics? J. plank. Res., 15:603-617.

Azam, F. and B.C. Cho. 1987. Bacterial utilization of organic matter in the sea. In: M. Fletcher, T.R.G. Gray, and J.G. Jones (eds.), Ecology of microbial communities. Cambridge University Press, Cambridge. pp.261-281

Azam, F., T. Fenchel, J.G. Field, J.S. Gray, L.A. Meyer-Reil, and F. Thingstad. 1983. The ecological role of water-column microbes in the sea. Mar. Ecol. Prog. Ser., 10:257-263.

Balch, W.M. 1981. An apparent lunar tidal cycle of phytoplankton blooming and community succession in the Gulf of Maine. J. exp. Mar. Biol. Ecol., 55:65-77.

Baumgartner, T.R., A. Soutar, and V. Ferreira-Bartrina. 1992. Reconstruction of the history of Pacific sardine and northern anchovy populations over the past two millenia from sediments of the Santa Barbara basin, California. CalCOFI Rep., 33:24-40.

Beckerman, M. 1997. Adaptive Cooperative Systems. John Wiley & Sons, New York. 427pp.

Behl, R.J. and J.P. Kennett. 1996. Brief interstadial events in the Santa Barbara basin, NE Pacific, during the past 60 kyr. Nature, 379:243-246.

Berger, A. 1988. Milankovitch theory and climate. Reviews of geophysics, 26:624-657.

Berman, T., L. Stone, Y.Z. Yacobi, B. Kaplan, M. Schlichter, A. Nishri, and U. Pollingher. 1995. Primary production and phytoplankton in Lake Kinneret: A long-term record (1972-1993). Limonol. Oceanogr., 40:1064-1076.

Berry, B.J.L. 1991. Long-Wave Rhythms in Economic Development and Political Behavior. Johns Hopkins University Press, Baltimore. 241pp.

Beyers, R.J. and H.T. Odum. 1993. Ecological Microcosms. Springer-Verlag, New York. 557pp.

Bigger, M. 1976. Oscillations of tropical insect populations. Nature, 259:207-209.

Boltzmann, L. 1905. The second law of thermodynamics. Populare Schriften, Essay No. 3 (address to Imperial Academy of Science in 1886). Reprinted in English in Theoretical Physics and Philosophical Problems, Selected Writings of L. Boltzmann. D. Reidel, Dordrecht.

Bond, G., W. Showers, M. Cheseby, R. Lotti, P. Almasi, P. de Menocal, P. Priore, H. Cullen, I. Hajdas, and G. Bonani. 1997. A pervasive millennial-scale cycle in North Atlantic Holocene and glacial cycles. Science, 278:1257-1266.

Brett, C.E. and G.C. Baird. 1992. Coordinated stasis and evolutionary ecology of Silurian-Devonian marine biota in the Appalachian basin. Geol. Soc. Am. Abstr. Programs, 24:139.

Brett, C.E., L.C. Ivany, and K.M. Schopf. 1996. Coordinated stasis: An overview. Palaeogeography, Palaeoclimatology, Palaeoecology, 127:1-20.

Brockmann, U.H., K. Eberlein, P. Hosumbek, H. Trageser, E. Maier-Reimer, H.K. Schone, and H.D. Junge. 1977. The development of a natural plankton population in an outdoor tank with nutrient-poor sea water. I. Phytoplankton succession. Marine Biology, 43:1-17.

Broecker, W.S. 1997. Thermohaline circulation, the Achilles heel of our climate system: Will man-made CO2 upset the current balance? Science, 278:1582-1588.

Broecker, W.S., G. Bond, M. Klas, G. Bonani, and W. Wolfli. 1990. A salt oscillator in the glacial Atlantic? 1. The concept. Paleoceanography, 5:469-477.

Brokaw, N.V.L. 1982. Treefalls: Frequency, timing, and consequences. In: E.G. Leigh, Jr., A.S. Rand, and D.M. Windsor (eds.), The ecology of a tropical forest: seasonal rhythms and long-term changes. Smithsonian Institution Press, Washington DC. pp.101-108.

Camilo, G.R. and M.R. Willig. 1995. Dynamics of a food chain model from an arthropod-dominated lotic community. Ecological Modelling, 79:121-129.

Campbell, D.E. 1984. Energy filter properties of ecosystems. Ph.D. dissertation, Environmental Engineering Sciences, University of Florida, Gainesville. 478pp.

Carson, H.L. 1975. The genetics of speciation at the diploid level. Am. Nat., 109:83-92.

Carson, H.L. 1982. Speciation as a major reorganization of polygenic balances. In: C. Barigozzi (ed.), Mechanisms of speciation. Alan R. Liss, New York. pp.411-433.

Clark, W.C. 1985. Scales of climate impacts. Climatic Change, 7:5-27.

Clark, W.C., D.D. Jones, and C.S. Holling. 1978. Patches, movements, and population dynamics in ecological systems: A terrestrial perspective. In: J.H. Steele (ed.), Spatial pattern in plankton communities. Plenum Press, New York. pp.385-432.

Connell, J.H. 1978. Diversity in Tropical Rain Forests and Coral Reefs. Science, 199:1302-1310.

Conner, W.H. and J.W. Day, Jr. 1982. The ecology of forested wetlands in the southeastern United States. In: B. Gopal, R.E. Turner, R.G. Wetzel, and D.F. Whigham (eds.), Wetlands: Ecology and Management. National Institute of Ecology and International Scientific Publications, Jaipur, India. pp.69-87.

Crowley, T.J. and G.R. North. 1988. Abrupt climate change and extinction events in earth history. Science, 240:996-1002.

Cullen, J.J., E. Stewart, E. Renger, R.W. Eppley, and C.D. Winant. 1983. Vertical motion of the thermocline, nitracline and chlorophyll maximum layers in relation to currents on the Southern California Shelf. J. Mar. Res., 41:239-262.

Cushing, D.H. 1981. Fisheries biology: A study in population dynamics. University of Wisconsin Press, Madison. 295pp.

Cushing, D.H. 1982. Climate and Fisheries. Academic Press, London. 373pp.

Dansgaard, W., H.B. Clausen, N. Gundestrup, C.U. Hammer, S.J. Johnson, P. Kristinsdottir, and N. Reeh. 1982. A new Greenland deep ice core. Science, 218:1273-1277.

Day, J.W., Jr., D. Pont, P.F. Hensel, and C. Ibanez. 1995. Impacts of sea-level rise on deltas in the Gulf of Mexico and the Mediterranean: The importance of pulsing events to sustainability. Estuaries, 18:636-647.

de Bernadi, R., G. Giussani, M. Manca, and D. Ruggiu. 1988. Trophic status and the pelagic system in Lago Maggiore. Hydrobiologia, 191:1-8.

Delcourt, H.R., P.A. Delcourt, and T. Webb III. 1983. Dynamic plant ecology: The spectrum of vegetational change in space and time. Quaternary Science Reviews, 1:153-175.

Demers, S. and L. Legendre. 1981. Melange vertical et capacite photosynthetique du phytoplancton estuarien (estuarie du Saint-Laurent). Marine Biology, 64:243-250.

Denham, D. 1979. Earthquake hazard in Australia. In: R.L. Heathcote and B.G. Thom (eds.), Natural Hazards in Australia. Australian Academy of Science, Canberra. pp.94-118.

Denman, K.L. and A.E. Gargett. 1983. Time and space scales of vertical mixing and advection of phytoplankton in the upper oceans. Limnol. Oceanogr., 28:801-815.

Doyle, T.W. 1981. Chapter 6. The role of disturbance in the gap dynamics of a montane rain forest: An application of a tropical forest succession model. In: D.C. West, H.H. Shugart, and D.B. Botkin (eds.), Forest succession: Concepts and application. Springer-Verlag, New York. pp.56-73.

Dubois, D.M. 1975. A model of patchiness for prey-predator plankton populations. Ecological Modelling, 1:67-80.

Ebenhoh, W. 1988. Coexistence of an unlimited number of algal species in a model system. Theoret. Pop. Biol., 34:130-144.

Eldredge, N. and S.J. Gould. 1972. Punctuated equilibria: An alternative to phyletic gradualism. In: T.J.M. Schopf (ed.), Models in Paleobiology. Freeman, Cooper & Company, San Francisco. pp.82-115.

Eldridge, P.M. and M.E. Sieracki. 1993. Biological and hydrodynamic regulation of the microbial food web in a periodically mixed estuary. Limnol. Oceanogr., 38:1666-1679.

Elena, S.F., V.S. Cooper, and R.E. Lenski. 1996. Punctuated evolution caused by selection of rare beneficial mutations. Science, 272:1802-1804.

Elton, C. 1942. Voles, Mice and Lemmings: Problems in Population Dynamics. Oxford University Press, London. 496pp.

Elton, C. and M. Nicholson. 1942. The ten-year cycle in numbers of the lynx in Canada. Journal of Animal Ecology, 11:215-244.

Falkowski, P.G., D. Ziedmann, Z. Kolber, and P.K. Bienfang. 1991. Role of eddy pumping in enhancing primary production in the ocean. Nature, 352:55-58.

Fenchel, T. 1988. Marine plankton food chains. Ann. Rev. Ecol. Syst., 19:19-38.

Field, R.J. 1975. Limit cycle oscillations in the reversible Oregonator. J. Chem. Phys., 63:2289-2296.

Field, R.J., E. Koros, and R.M. Noyes. 1972. Oscillations in chemical systems. II. Through analysis of temporal oscillation in the bromate-cerium-malonic acid system. J. Am. Chem. Soc., 94:8649-8664.

Field, R.J. and R.M. Noyes. 1974. Oscillations in chemical systems. IV. Limit cycle behavior in a model of a real chemical reaction. J. Chem. Phys., 60:1877-1884.

Field, R.J. and F.W. Schneider. 1989. Oscillating chemical reactions and nonlinear dynamics. Journal of Chemical Education, 66:195-204.

Franses, P.H. 1996. Periodicity and Stochastic Trends In Economic Time Series. Oxford University Press, Oxford. 230pp.

Gaedeke, A. and U. Sommer. 1986. The influence of the frequency of periodic disturbances on the maintenance of phytoplankton diversity. Oecologia, 71:25-28.

Gardner, W.D. and L.G. Sullivan. 1981. Benthic storms: Temporal variability in a deep-ocean nepheloid layer. Science, 213:329-331.

Garnier, J. and D. Benest. 1991. Influence of light attenuation on primary production in a shallow sand-pit lake. Verh. Internat. Verein. Limnol., 24:1536-1542.

Getz, L.L., L.E. Simms, B. McGuire, and M.E. Snarski. 1997. Factors affecting life expectancy of the prairie vole, *Microtus ochrogaster*. Oikos, 80:362-370.

Glansdorff, P. and I. Prigogine. 1971. Structure, stability, and fluctuations. Wiley-Interscience, Chichester, UK. 306pp.

Glantz, H.M. 1992. Climate variability, climate change, and fisheries. Cambridge Univ. Press. 450pp.

Glover, H.E., B.B. Prezelin, L. Campbell, M. Wyman, and C. Garside. 1988. A nitrate-dependent *Synechococcus* bloom in surface Sargasso Sea water. Nature, 331:161-163.

Goldman, J.C. 1984a. Oceanic nutrient cycles. In: M.J.R. Fasham (ed.), Flows of energy and materials in marine ecosystems. Plenum Press, New York. pp.137-170.

Goldman, J.C. 1984b. Conceptual role for microaggregates in pelagic waters. Bull. Mar. Sci., 35:462-476.

Goldstein, J.S. 1988. Long Cycles: Prosperity and war in the modern age. Yale University Press, New Haven. 433pp.

Gooday, A.J., B.J. Bett, and D.N. Pratt. 1993. Direct observation of episodic growth in an abyssal xenophyophore (Protista). Deep-Sea Res., 40:2131-2143.

Gould, S.J. and N. Eldridge. 1977. Punctuated equilibria: The tempo and mode of evolution reconsidered. Paleobiology, 3:115-151.

Gray, P. and S.K. Scott. 1990. Chemical Oscillations and Instabilities: Non-linear Chemical Kinetics. Oxford University Press, New York. 453pp.

Gulland, J.A. 1977. Fish population dynamics. John Wiley & Sons, London. 372pp.

Hallam, A. 1987a. Radiations and extinctions in relation to environmental change in the marine Lower Jurassic of northwest Europe. Paleobiology, 13:152-168.

Hallam, A. 1987b. End-Cretaceous mass extinction event: Argument for terrestrial causation. Science, 238:1237-1242.

Hanski, I, P. Turchin, E. Korpimaki, and H. Henttonen. 1993. Population oscillations of boreal rodents: regulation by mustelid predators leads to chaos. Nature, 364:232-235.

Hanski, I. and E. Korpimaki. 1995. Microtine rodent dynamics in northern Europe: Parameterized models for the predator-prey interactions. Ecology, 76:840-850.

Harris, G.P. 1980. Temporal and spatial scales in phytoplankton ecology. Mechanisms, methods, models, and management. Can. J. Fish. Aqaut. Sci., 37:877-900.

Hastings, A. and T. Powell. 1991. Chaos in a three-species food chain. Ecology, 72:896-903.

Hays, J.D., J. Imbrie, and N.J. Shackleton. 1976. Variations in the Earth's orbit: Pacemaker of the Ice Ages. Science, 194:1121-1132.

Heusser, L.E. and F. Sirocko. 1997. Millennial pulsing of environmental change in southern California from the past 24 k.y.: A record of Indo-Pacific ENSO events? Geology, 25:243-246.

Holland, A.F. 1985. Long-term variation of macrobenthos in a mesohaline region of Chesapeake Bay. Estuaries, 8:93-113.

Holligan, P.M., R.D. Pingree, and G.T. Mardell. 1985. Oceanic solitons, nutrient pulses and phytoplankton growth. Nature, 314:348-350.

Horne, E.P. and T. Platt. 1984. The dominant space and time scales of variability in the physical and biological fields on continental shelves. Rapp. P.v. Reun. Cons. int. Explor. Mer, 183:8-19.

Huston, M. 1979. A general hypothesis of species diversity. Am. Nat., 113:81-101.

Imbrie, J., A.C. Mix, and D.G. Martinson. 1993. Milankovitch theory viewed from Devils Hole. Nature, 363:531-533.

Inman, D. 1992. Learning BASIC. Sams, Indianapolis. 601pp.

Ivany, L.C. 1996. Coordinated stasis or coordinated turnover? Exploring intrinsic vs. extrinsic controls on pattern. Palaeogeography, Palaeoclimatology, Palaeoecology, 127:239-256.

Jenkins, W.J. 1988. Nitrate flux into the euphotic zone near Bermuda. Nature, 331:521-523.

Johnston, A.C. 1981. On the use of the frequency-magnitude relation in earthquake risk assessment. In: J.E. Beavers (ed.), Proceedings of earthquakes and earthquake engineering: the eastern United States. Ann Arbor Science, Ann Arbor. pp.161-181.

Jorgensen, S.E. 1992. Integration of ecosystem theories: A pattern. Kluwer Academic Publishers, Dordrecht. 383pp.

Jorgensen, S.E. 1994. Review and comparison of goal functions in system ecology. Vie Milieu, 44:11-20.

Jury, M.R. and G.B. Brundrit. 1992. Temporal organization of upwelling in the southern Benguela ecosystem by resonant coastal trapped waves in the ocean and atmosphere. S. Afr. J. mar. Sci., 12:219-224.

Kang, D. and V. Engel. 1996. Diurnal graphs of carbon dioxide and oxygen and spreadsheets used to evaluate metabolism. Data report to Biosphere 2, Center for Environmental Policy, Environmental Engineering Sciences, University of Florida, Gainesville. 75pp.

Kauffman, S.A. 1993. The Origins of Order. Oxford University Press, New York. 709pp.

Kemp, W.M. and W.J. Mitsch. 1979. Turbulence and phytoplankton diversity: A general model of the “Paradox of Plankton”. Ecological Modelling, 7:201-222.

Kersting, K. 1985. Properties of an aquatic micro-ecosystem: V. Ten years of observations of the prototype. Verh. Internat. Verein. Limnol., 22:3040-6045.

Kierstead, H. and L.B. Slobodkin. 1953. The size of water masses containing plankton blooms. Journal of Marine Research, 12:141-147.

Kotliar, N.B. and J.A. Wiens. 1990. Multiple scales of patchiness and patch structure: a hierarchical framework for the study of heterogeneity. Oikos, 59:253-260.

Lathrop, R.C. and S.R. Carpenter. 1992a. Phytoplankton and their relationship to nutrients. In: J.F. Kitchell (ed.), Food Web Management. Springer-Verlag, New York. pp.97-126.

Lathrop, R.C. and S.R. Carpenter. 1992b. Zooplankton and their relationship to phytoplankton. In: J.F. Kitchell (ed.), Food Web Management. Springer-Verlag, New York. pp.127-150.

Leach, M.K. and T.J. Givnish. 1996. Ecological determinants of species loss in remnant prairies. Science, 273:1555-1558.

Leichter, J.J., S.R. Wing, S.L. Miller, and M.W. Denny. 1996. Pulsed delivery of subthermocline water to Conch Reef (Florida Keys) by internal tidal bores. Limnol. Oceanogr., 41:1490-1501.

Lewin, R. 1986. In ecology, change brings stability. Science, 234:1071-1073.

Lohrenz, S.E., R.A. Arnone, D.A. Wiesenburg, and I.P. DePalma. 1988. Satellite detection of transient enhanced primary production in the western Mediterranean Sea. Nature, 335:245-247.

Lotka, A.J. 1922. Contribution to the energetics of evolution. Proc. Natl. Acad. Sci. USA, 8:147-151.

Ludwig, D., D.D. Jones, adn C.S. Holling. 1978. Qualitative analysis of insect outbreak systems: The spruce budworm and forest. Journal of Animal Ecology, 47:315-332.

MacLulich, D.A. 1937. Fluctuations in the numbers of the varying hare (*Lepus americanus*). Univ. Toronto Studies, Biol. Ser., No. 43. 136pp.

Marchand, P.J. 1995. Waves in the Forest. Natural History, 104(2):26-32.

Margalef, R. 1958. Temporal succession and spatial heterogeneity in phytoplankton. In: A.A. Buzzati-Traverso (ed.), Perspectives in marine biology. University of California Press, Berkeley. pp.323-349.

Margalef, R. 1958. Perspectives in ecological theory. Chicago Univ. Press. 122pp.

Marra, J. 1978. Phytoplankton photosynthetic response to vertical movement in a mixed layer. Marine Biology, 46:203-208.

McCauley, E. 1993. Internal versus external causes of dynamics in a freshwater plant-herbivore system. Am. Nat., 141:428-439.

McClelland, L., T. Simkin, M. Summers, E. Nielsen, and T.C. Stein. 1989. Global volcanism 1975-1985. Prentice Hall, Englewood Cliffs. 655pp.

McGowan, J.A. and T.L. Hayward. 1978. Mixing and oceanic productivity. Deep-Sea Research, 25:771-793.

McGrane, G. 1998. Simulating whole-earth cycles using hierarchies and other general systems concepts. Ph.D. dissertation, Environmental Engineering Sciences, University of Florida, Gainesville, 372pp.

Mejer, H.F. and S.E. Jorgensen. 1979. Energy and ecological buffer capacity. In: S.E. Jorgensen (ed.), State-of-the-art of Ecological Modelling. Environmental Sciences and Applications, 7. Proc. Conf. Ecological Modelling, 28th August-2nd September 1978, Copenhagen. International Society for Ecological Modelling, Copenhagen. pp.829-846.

Miron, J.A. 1996. The Economics of Seasonal Cycles. MIT Press, Cambridge. 225pp.

Mitsch, W.J. and K.C. Ewel. 1979. Comparative biomass and growth of cypress in Florida. American Midland Naturalist, 101:417-426.

Mitsch, W.J. and J.G. Gosselink. 1993. Wetlands. Van Nostrand Reinhold, New York. 722pp.

Mitsch, W.J., J.R. Taylor, and K.B. Benson. 1991. Estimating primary productivity of forested wetland communities in different hydrologic landscapes. Landscape Ecology, 5:75-92.

Modelski, G. 1987. Long Cycles in World Politics. University of Washington Press, Seattle. 244pp.

Moloney, C.L. 1992. Simulation studies of trophic flows and nutrient cycles in Benguela upwelling foodwebs. S. Afr. J. mar. Sci., 12:457-476.

Moloney, C.L. and J.G. Field. 1991. Modelling carbon and nitrogen flows in a microbial plankton community. In: P.C. Reid, C.M. Turley, and P.H. Burkill (eds.), Protozoa and their role in marine processes, Springer-Verlag, Berlin. pp.443-474

Moloney, C.L., J.G. Field, and M.I. Lucas. 1991. The size-based dynamics of plankton food webs. II. Simulations of three contrasting southern Benguela food webs. J. Plankton Res., 13:1039-1092.

Morris, R.F. 1963. The dynamics of epidemic spruce budworm populations. Memoirs of the Entomological Society of Canada, 31:1-332.

Moselkilde, E., E.R. Larson, J.D. Sterman, and J.S. Thompson. 1992. Nonlinear mode-interaction in the macroeconomy. Annals of Operations Research, 37:185-215.

Odum, E.P. 1971. Fundamentals of Ecology. Saunders, Philadelphia. 574pp.

Odum, H.T. 1971. Environment, Power and Society. Wiley, New York. 331pp.

Odum, H.T. 1982. Pulsing, power and hierarchy. In: W.J. Mitsch (ed.), Energetics and systems. Ann Arbor Science, Ann Arbor. pp.33-59.

Odum, H.T. 1983. Systems Ecology. Wiley, New York. 644pp.

Odum, H.T. 1987. Chapter 13. Models for national, international, and global systems policy. In L.C. Braat and W.F.J. van Lierop (eds.), Economic-ecological modeling. Elsevier Science, New York. pp.203-251.

Odum, H.T. 1988. Self organization, transformity, and information. Science, 242:1132-1139.

Odum, H.T. 1994. Ecological and general systems, An introduction to systems ecology. University Press of Colorado, Niwot. 644pp.

Odum, H.T. 1995. Chapter 28. Self-organization and maximum empower. In: C.A.S. Hall (ed.), Maximum power. University Press of Colorado, Niwot. pp.311-330.

Odum, H.T. 1996. Environmental Accounting: EMERGY and Decision Making. John Wiley, New York. 370pp.

Odum, H.T. 1997. The limits of information and biodiversity in the future. Proceedings of the conference on Social Politics and Problems of Ecology in the Future, Austrian Academy of Science, Vienna, Austria (in press).

Odum, H.T. and M. Munroe. 1993. Simulation of the Laguna Joyuda ecosystem in western Puerto Rico. Acta Cientifica, 7:189-227.

Odum, H.T. and E.C. Odum. 1996a. A Prosperous Way Down. In press, University Press of Colorado, Niwot. 235pp.

Odum, H.T. and E.C. Odum. 1996b. Modeling for All Scales. In press, Academic Press, New York. 396pp.

Odum, W.E., E.P. Odum, and H.T. Odum. 1995. Nature's Pulsing Paradigm. Estuaries, 18:547-555.

Odum, H.T. and R.C. Pinkerton. 1955. Time's speed regulator: The optimum efficiency for maximum power output in physical and biological systems. Am. Scientist, 43:331-343.

Okamoto, S. 1984. Introduction to Earthquake Engineering. University of Tokyo Press, Tokyo. 629pp.

O'Neill, R.V., W.F. Hanes, B.S. Ausmus, and D.E. Reichle. 1975. A theoretical basis for ecosystem analysis with particular reference to element cycling. In: F.G. Howell, J.B. Bentry, and M.H. Smith (eds.), Mineral Cycling in Southeastern Ecosystems. NTIS pub. CONF-750513.

Pages, F. 1992. Mesoscale coupling between planktonic cnidarian distribution and water masses during a temporal transition between active upwelling and abatement in the Northern Benguela system. S. Afr. J. mar. Sci., 12:41-52.

Parsons, T.R., M. Takahashi, and B. Hargrave. 1984. Biological Oceanographic Processes. Pergamon Press, Oxford. 330pp.

Philips, E.J., P.V. Zimba, M.S. Hopson, and T.L. Crisman. 1993. Dynamics of the plankton community in submerged plant dominated regions of Lake Okeechobee, Florida, USA. Verh. Internat. Verein. Limnol., 25:423-426.

Pierce, P.S. 1991. The Dow Jones averages, 1885-1990. Business One Irwin, Homewood.

Pikovsky, A.S. 1981. A dynamical model for periodic and chaotic oscillations in the Belousov-Zhabotinsky reaction. Physics Letters, 85A:13-16.

Platt, T. 1972. Local phytoplankton abundance and turbulence. Deep-Sea Res., 19:183-187.

Platt, T. 1978. Spectral analysis of spatial structure in phytoplankton populations. In: J.H. Steele (ed.), Spatial Pattern in Plankton Communities. Plenum Press, New York. pp.73-84.

Platt, T. and K.L. Denman. 1975. Spectral analysis in ecology. Ann. Rev. Ecol. Syst., 6:189-210.

Platt, T. and W.G. Harrison. 1985. Biogenic fluxes of carbon and oxygen in the ocean. Nature, 318:55-58.

Press, F. 1975. Earthquake prediction. Scientific American, 232:14-23.

Press, F. and R. Siever. 1994. Understanding Earth. W.H. Freeman, New York. 593pp.

Radach, G. 1992. Ecosystem functioning in the German Bight under continental nutrient inputs by rivers. Estuaries, 15:477-496.

Raleigh, C.B., K. Sieh, L.R. Sykes, D.L. Anderson. 1982. Forecasting southern California earthquakes. Science, 217:1097-1104.

Raup, D.M. 1986. Biological extinction in earth history. Science, 231:1528-1533.

Raup, D.M. 1991. Extinction: Bad genes or bad luck? Norton, New York. 210pp.

Raup, D.M. 1994. The role of extinction in evolution. Proc. Natl. Acad. Sci. USA, 91:6758-6763.

Raup, D.M. and J.J. Sepkoski, Jr. 1984. Periodicity of extinctions in the geologic past. Proc. Natl. Acad. Sci. USA, 81:801-85.

Raup, D.M. and J.J. Sepkoski, Jr. 1986. Periodic extinction of families and genera. Science, 231:833-836.

Richardson, J.R. 1988. Spatial patterns and maximum power in ecosystems. Ph.D. dissertation, Environmental Engineering Sciences, University of Florida, Gainesville. 254pp.

Richardson, J.R. and H.T. Odum. 1981. Power and a pulsing production model. In: W.J. Mitsch (ed.), Energy and ecological modeling. Elsevier, Amsterdam, pp.641-648.

Ricklefs, R.E. 1992. Chapter 13. Scaling pattern and process in marine ecosystems. In: K. Sherman, L.M. Alexander, and B.D. Gold (eds.), Large marine ecosystems:

Patterns, processes, and yields. American Association for the Advancement of Science, Washington, D.C. pp.169-178.

Ringelberg, J. 1977. Properties of an aquatic micro-ecosystem: II. Steady-state phenomena in the autotrophic subsystem. Helgolander wiss. Meeresunters, 30:134-143.

Robinson, J.V. and C.D. Sandgren. 1983. The effect of temporal environmental heterogeneity on community structure: a replicated experimental study. Oecologia, 57:98-102.

Rothschild, B.J. 1986. Dynamics of marine fish populations. Harvard Univ. Press, Cambridge. 277pp.

Rowe, G.T. 1996. The cycling of organic matter in food-limited environments. In: F. Uiblein, J. Ott, and M. Stachowitsch (eds.), Deep-sea and extreme shallow water habitats: affinities and adaptations. Biosystematics and Ecology Series, 11:233-260.

Russell, F.S. 1973. A summary of the observations on the occurrence of planktonic stages of fish off Plymouth 1924-1972. J. Mar. Biol. Ass. U.K., 53:347-355.

Sastre, A.V., N.H. Santinelli, S.H. Otano, M.E. Ivanissevich, and M.G. Ayestaran. 1994. Diatom blooms and their relation to water supply. Verh. Internat. Verein. Limnol., 25:1974-1978.

Scott, S.K. 1991. Chemical Chaos. Oxford University Press, New York. 454pp.

Sepkoski, J.J., Jr. 1984. A kinetic model of Phanerozoic taxonomic diversity III. Post-Paleozoic families and mass extinctions. Paleobiology, 10:246-267.

Simpson, G.G. 1952. How many species? Evolution, 6:342.

Simpson, R.H. and H. Riehl. 1981. The Hurricane and Its Impact. Louisiana State University Press, Baton Rouge. 398pp.

Sommer, U. 1985. Comparison between steady and non-steady state competition: Experiments with natural phytoplankton. Limnol. Oceanogr., 30:335-346.

Sousa, W.P. 1979. Disturbance in marine intertidal boulder fields: The nonequilibrium maintenance of species diversity. Ecology, 60:1225-1239.

Sprugel, D.G. and F.H. Bormann. 1981. Natural Disturbance and the Steady State in High-Altitude Balsam Fir Forests. Science, 211:390-393.

Steven, D.M. and R. Glombitza. 1972. Oscillatory variation of a phytoplankton population in a tropical ocean. Nature, 237:105-107.

Stocker, T.F. and L.A. Mysak. 1992. Climatic fluctuations on the century time scale: A review of high-resolution proxy data and possible mechanisms. Climatic Change, 20:227-250.

Stokey, N.L. and R.E. Lucas, Jr. 1989. Recursive Methods in Economic Dynamics. Harvard University Press, Cambridge. 588pp.

Stone, L. and T. Berman. 1993. Lake Kinneret: A seasonal model for carbon flux through the planktonic biota. Limnol. Oceanogr., 38:1680-1695.

Straskraba, M. 1979. Natural control mechanisms in models of aquatic ecosystems. Ecological Modelling, 6:305-322.

Strizhak, P. and M. Menzinger. 1996. Nonlinear dynamics of the BZ reaction: A simple experiment that illustrates limit cycles, chaos, bifurcations, and noise. Journal of Chemical Education, 73:868-873.

Suttle, C.A., J.G. Stockner, and P.J. Harrison. 1987. Effects of nutrient pulses on community structure and cell size of a freshwater phytoplankton assemblage in culture. Can. J. Fish. Aquat. Sci., 44:1768-1774.

Swetnam, T.W. and J.L. Betancourt. 1990. Fire-Southern Oscillation Relations in the Southwestern United States. Science, 249:1017-1020.

Swetnam, T.W. and M. Lynch. 1993. Multiplicity, regional-scale patterns of western spruce budworm outbreaks. Ecological Monographs, 63:399-424.

Tester, J.R. 1989. Effects of fire frequency on oak savanna in east-central Minnesota. Bull. Torrey Bot. Club, 116:134-144.

Thompson, L.G., T. Yao, M.E. Davis, K.A. Henderson, E. Mosley-Thompson, P.-N. Lin, J. Beer, H.-A. Synal, J. Cole-Dai, and J.F. Bolzan. 1997. Tropical climate instability: The last glacial cycle from a Qinghai-Tibetan ice core. Science, 276:1821-1825.

Thresher, R.E., G.P. Harris, J.S. Gunn, and L.A. Clementson. 1989. Phytoplankton production pulses and episodic settlement of a temperate marine fish. Nature, 341:641-643.

Townsend, C.R. and M.R. Scarsbrook. 1997. The intermediate disturbance hypothesis, refugia, and biodiversity in streams. Limnol. Oceanogr., 42:938-949.

Travers, M. 1971. Diversite du microplancton du Golfe de Marseille en 1964. Marine Biology, 8:308-343.

Turner, J.S., J.-C. Roux, W.D. Mccormick, and H.L. Swinney. 1981. Alternating periodic and chaotic regimes in a chemical reaction- experiment and theory. Physics Letters, 85A:9-12.

Tyler, P.A. 1988. Seasonality in the deep sea. Oceanogr. Mar. Biol. Ann. Rev., 26:227-258.

Tyler, P.A. 1996. Faunal responses to temporal disequilibrium in the deep sea. In: F. Uiblein, J. Ott, and M. Stachowitsch (eds.), Deep-sea and extreme shallow water habitats: affinities and adaptations. Biosystematics and Ecology Series, 11:261-270.

Ulanowicz, R.E. 1980. An hypothesis on the development of natural communities. J. Theor. Biol., 85:223-245.

Valiela, I. 1995. Marine Ecological Processes. Springer, New York. 686pp.

Verheye, H.M., L. Hutchings, J.A. Huggett, and S.J. Painting. 1992. Mesozooplankton dynamics in the Benguela ecosystem, with emphasis on the herbivorous copepods. S. Afr. J. mar. Sci., 12:561-584.

Vrba, E.S. 1985. Environment and evolution: alternative causes of the temporal distribution of evolutionary events. South African Journal of Science, 81:229-236.

Vrba, E.S. 1993. Turnover-pulses, the Red Queen, and related topics. American Journal of Science, 293A:418-452.

Vrba, E.S. 1995. Chapter 3. On the connections between paleoclimate and evolution. In: E.S. Vrba, G.H. Denton, T.C. Patridge, and L.H. Burckle (eds.), Paleoclimate and evolution with emphasis on human origins. Yale University Press, New Haven. pp.25-45.

Vrba, E.S. and N. Eldredge. 1984. Individuals, hierarchies and processes: towards a more complete evolutionary theory. Paleobiology, 10:146-171.

Walsh, J.J. 1983. Death in the sea: Enigmatic phytoplankton losses. Prog. Oceanog. 12:1-86.

Watt, K.E.F. 1989. Evidence for the role of energy resources in producing long waves in the United States economy. Ecological Economics, 1:181-195.

Wheeler, P.A., D.L. Kirchman, M.R. Landry, and S.A. Kokkinakis. 1989. Diel periodicity in a ammonium uptake and regeneration in the oceanic subarctic Pacific: Implications for interactions in microbial food webs. Limnol. Oceanogr., 34:1025-1033.

Whittaker, R.H. and G.M. Woodwell. 1971. Evolution of natural communities. In: J.A. Weins (ed.), Ecosystem Structure and Function. Oregon State Univ. Press, Corvallis. pp.137-159.

Wiegel, R.L. 1964. Oceanographical Engineering. Prentice Hall, Englewood Cliffs. 532pp.

Witman, J.D., J.J. Leichter, S.J. Genovese, and D.A. Brooks. 1993. Pulses phytoplankton supply to the rocky subtidal zone: Influence of internal waves. Proc. Natl. Acad. Sci. USA, 90:1686-1690.

Wootton, J.T., M.S. Parker, and M.E. Power. 1996. Effects of disturbance on river food webs. Science, 273:1558-1561.

Wu, J. and O.L. Loucks. 1995. From balance of nature to hierarchical patch dynamics: A paradigm shift in ecology. Q. Rev. Biol., 70:439-466.

Yoshida, R., T. Takahashi, T. Yamaguchi, and H. Ichijo. 1996. Self-oscillating gel. J. Am. Chem. Soc., 118:5134-5135.

Yoshikawa, K., S. Nakata, M. Yamanaka, and T. Waki. 1989. Amusement with a salt-water oscillator. J. Chem. Educ., 66:205-207.

Zimmerman, R.C. and J.N. Kremer. 1984. Episodic nutrient supply to a kelp forest ecosystem in Southern California. J. Mar. Res., 42:591-604.

Zwick, P.D. 1985. Energy systems and inertial oscillation. Ph.D. dissertation, Environmental Engineering Sciences, University of Florida, Gainesville. 240pp.

BIOGRAPHICAL SKETCH

Daeseok Kang was born on October 26, 1964, in Suncheon, Korea. He received his Bachelor of Science degree in oceanography from Seoul National University in Korea, in 1987. He continued his study toward a Master of Science in biological oceanography in Seoul National University and studied zooplankton ecology. He received his Master of Science degree in 1989. After completing his military service from 1989 to 1991, he worked as a research assistant in the Department of Environmental Engineering at Ajou University in Korea from 1991 to 1993. During this time, he participated in a project on oil extraction from waste sludge. In August 1994, he began graduate studies in the systems ecology program in the Department of Environmental Engineering Sciences, University of Florida. During his study, he worked as a graduate research assistant. He graduated with a Doctor of Philosophy degree in 1998.

I certify that I have read this study and that in my opinion it conforms to acceptable standards of scholarly presentation and is fully adequate, in scope and quality, as a dissertation for the degree of Doctor of Philosophy.

H T Odum

Howard T. Odum, Chair
Graduate Research Professor
Emeritus of Environmental
Engineering Sciences

I certify that I have read this study and that in my opinion it conforms to acceptable standards of scholarly presentation and is fully adequate, in scope and quality, as a dissertation for the degree of Doctor of Philosophy.

MT Brown

Mark T. Brown
Assistant Professor of Environmental
Engineering Sciences

I certify that I have read this study and that in my opinion it conforms to acceptable standards of scholarly presentation and is fully adequate, in scope and quality, as a dissertation for the degree of Doctor of Philosophy.

Clay L. Montague

Clay L. Montague
Associate Professor of Environmental
Engineering Sciences

I certify that I have read this study and that in my opinion it conforms to acceptable standards of scholarly presentation and is fully adequate, in scope and quality, as a dissertation for the degree of Doctor of Philosophy.

Paul A Mueller

Paul A. Mueller
Professor of Geology

I certify that I have read this study and that in my opinion it conforms to acceptable standards of scholarly presentation and is fully adequate, in scope and quality, as a dissertation for the degree of Doctor of Philosophy.

David A. Denslow

David A. Denslow
Distinguished Service Professor
of Economics

This dissertation was submitted to the Graduate Faculty of the College of Engineering and to the Graduate School and was accepted as partial fulfillment of the requirements for the degree of Doctor of Philosophy.

December, 1998

Winfred M. Phillips
Dean, College of Engineering

M. J. Ohanian
Dean, Graduate School